MOLECULAR MECHANISM UNDERLYING THE EFFECT OF miRNA EXPRESSION ON MEDULLOBLASTOMA CELL BEHAVIOR

By

Harish Shrikrishna Bharambe

LIFE09201404008

Tata Memorial Centre

Kharghar, Navi Mumbai-410210

A thesis submitted to the
Board of Studies in Life Sciences
In partial fulfillment of requirements
For the Degree of

DOCTOR OF PHILOSOPHY

of

HOMI BHABHA NATIONAL INSTITUTE

March 2021

Homi Bhabha National Institute

Recommendations of the Viva Voce Committee

As members of the Viva Voce Committee, we certify that we have read the dissertation prepared by Mr. Harish Shrikrishna Bharambe entitled *"Molecular mechanism underlying the effect of miRNA expression on medulloblastoma cell behavior"* and recommend that it may be accepted as fulfilling the thesis requirement for the award of Degree of Doctor of Philosophy.

S. N Dalal 09/3/2021

Chairperson – Dr. Sorab N. Dalal Date:

9.3.2021

Guide/Convener – Prof. Neelam V. Shirsat Date:

External Examiner – Prof. Kumaravel Somasundaram Date: 09/03/2021

Pritha Ray 13/03/2021

Member – Dr. Pritha Ray Date:

09/03/2021

Member - Dr. Rukmini Govekar Date:

Final approval and acceptance of this thesis is contingent upon the candidate's submission of the final copies of the thesis to HBNI.

I hereby certify that I have read this thesis prepared under my direction and recommend that it may be accepted as fulfilling the thesis requirement.

Date: 9.3.2021
Place: Navi Mumbai

Prof. Neelam V. Shirsat
Guide

STATEMENT BY AUTHOR

This dissertation has been submitted in partial fulfillment of requirements for an advanced degree at Homi Bhabha National Institute (HBNI) and is deposited in the Library to be made available to borrowers under rules of the HBNI.

Brief quotations from this dissertation are allowable without special permission, provided that accurate acknowledgement of source is made. Requests for permission for extended quotation from or reproduction of this manuscript in whole or in part may be granted by the competent authority of HBNI when in his or her judgment the proposed use of the material is in the interests of scholarship. In all other instances, however, permission must be obtained from the author.

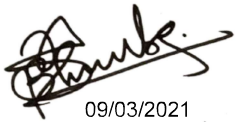

Harish Shrikrishna Bharambe

DECLARATION

I, hereby declare that the investigation presented in the thesis has been carried out by me. The work is original and has not been submitted earlier as a whole or in part for a degree / diploma at this or any other Institution / University.

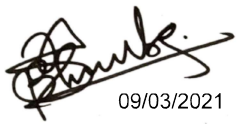

09/03/2021

Harish Shrikrishna Bharambe

Publications in peer reviewed Journals

1. **Restoration of MiR-193a expression is tumor-suppressive in MYC amplified Group 3 medulloblastoma**
   Harish Shrikrishna Bharambe, Annada Joshi, Kedar Yogi, Sadaf Kazi and Neelam Vishwanath Shirsat. **Acta Neuropathologica Communications** 8, 70 (2020). https://doi.org/10.1186/s40478-020-00942-5

2. **Downregulation of miR-204 expression defines a highly aggressive subset of Group 3/Group 4 medulloblastomas**
   Harish Shrikrishna Bharambe*, Raikamal Paul*, Pooja Panwalkar*, Rakesh Jalali, Epari Sridhar, Tejpal Gupta, Aliasgar Moiyadi, Prakash Shetty, Sadaf Kazi, Akash Deogharkar, Shalaka Masurkar, Kedar Yogi, Ratika Kunder, Nikhil Gadewal, Atul Goel, Naina Goel, Girish Chinnaswamy, Vijay Ramaswamy and Neelam Vishwanath Shirsat. **Acta Neuropathologica Communications** 7, 52 (2019). https://doi.org/10.1186/s40478-019-0697-3. *First co-authors

3. **Autophagy inhibition impairs the invasion potential of medulloblastoma cells**
   Raikamal Paul, **Harish Shrikrishna Bharambe** and Neelam Vishwanath Shirsat. **Molecular Biology Reports** (2020). https://doi.org/10.1007/s11033-020-05603-3

Conference/Symposium

1. 75th TMC Platinum Jubilee "A Conference of New Ideas in Cancer: Challenging Dogmas" held in Mumbai, 26th-28th February 2016.
2. Attended workshop on **"**Mass Spectrometry based Quantitative Proteomics for Beginners"**,** 26th-29th September 2016, organized by Institute of Bioinformatics, Bengaluru.
3. International Congress of Cell Biology - "The Dynamic Cell- From Molecules and Networks to Form and Function", 27th-31st January 2018, Hyderabad. **Presented poster**-"Role of microRNAs in medulloblastoma pathogenesis"

4. 38th Annual Convention of Indian Association for Cancer Research, 1st – 3rd March 2019, PGIMER, Chandigarh. Received First Prize – "**Roche Scholar in Training Award for Best Oral Presentation"** on "MiR-204 acts as tumor suppressor and risk stratification marker in medulloblastomas"

Dedicated to Aai, Baba, Bhagyashree……and Surbhi

ACKNOWLEDGEMENT

"Experience is the Best Teacher"

Indeed the learning of any person would be incomplete without learning from one's own experiences. The enormous knowledge which I have gathered through my experiences during Ph. D. research work will be my life-long companion when I will be wandering through the streets of science. Completing any task successfully imparts a great sense of mirth in me which is my Ph.D. project here. And really, this to happen needs the help and support of many people. The joy of successful completion of any task would be incomplete without mentioning the people who actually made it possible.

At this moment of accomplishment, I would like to pay my gratitude to my esteemed research guide Dr. Neelam V. Shirsat for giving me an opportunity to work with her. This work would not have been possible without her guidance, support and constant encouragement. Her comprehensive understanding of the field, timely review of my project progress, involvement in scientific discussions, valuable suggestions always kept me on track. Her extreme enthusiasm of exploring science has imparted the same sense in me too which helped me grow as a researcher. I appreciate her caring nature as my guardian during the difficult times when I experienced health issues within my tenure.

I sincerely thank Dr. Sudeep Gupta (Director, ACTREC), Dr. Shubhada V. Chiplunkar (Ex-Director, ACTREC) for providing us excellent research facilities and academic infrastructure. I would also like to thank Dr. Prasanna Venkatraman (Deputy-Director, CRI) for her pro-student and pro-research nature which ensures the welfare of researchers in ACTREC.

I am indebted to my Doctoral committee members, Dr. Sorab N. Dalal (Chairperson), Dr. Pritha Ray and Dr. Rukmini Govekar for their patience, keen review of my research and timely suggestions throughout the tenure. They always encouraged my ideas and helped me giving them a right shape.

This research would not have been possible without the helping hands of various expertise. I wish to record my sincere and heartily thanks to Dr. Arvind Ingle, (In-Charge, Laboratory Animal Facility), for maintaining an excellent laboratory animal facility. I thank Dr. Rahul Thorat for teaching me to handle laboratory animals and conduct the experiments in proper way. I also thank Mahesh dada, Shashi dada, Pravin and Pawar dada from animal facility for their timely technical help. I specially thank Dr. Abhijeet De and Snehal for the In vivo Imaging facility. I will always remember the crucial help from Dr. Prasanna Venkataraman, Dr. Abhijeet De and Dr. Arvind Inglle for completing the revisions of my manuscript during the difficult time of COVID-2019 Pandemic. I extend my heartful thanks to Mr. Uday Dandekar, He truly is the lifeline of all the laboratory instruments and the common instrument facility, always maintaining them in a proper state. A great thanks to Shymal ma'am, Prashant and Ravi from Flow cytometry facility, Vaishali ma'am, Tnauja ma'am and Jayraj sir from the Microscopy facility and Dr. Vinita Sawant and Siddhi ma'am from the electron microscopy facility for their help during my experiments. I highy appreciate the efforts of Maya Ma'am, Sharwari Ma'am, Chitra Ma'am, Lisa Ma'am from admin department because of whom the official documentation work was always up-to-date.

This journey will be always remembered as I was blessed to have a bunch of nice, kind and beautiful individuals around me. They always created a cheerful and conducive environment which helped me remain active and energetic. The Shirsat Lab was an excellent place to receive rigorous training to be proficient in this filed. Sadaf, helped me to learn the technique of tissue culture and provided assistance with real-time RT-PCR assays and DNA methylation analysis. Umeshji ensured availability of the resources and proper functioning of the tissue culture facility. Anandji was always a fatherly figure for me. He taught me the disciplined way of working in the molecular biology lab. He was always there to coax me during the frustrated situations and stood behind me firmly. With pride and pleasure, I extend my deepest thank to these caring and lovely people. It is great a pleasure to acknowledge the hearty cooperation of my beloved seniors in the lab Dr. Kedar, Dr. Pooja, Dr. Vijay and Dr. Satish who always guided me for conducting scientific experiments and keenly helped whenever required. I specially thanks Dr. Kedar for teaching me an organized manner of working in the lab. His help for the luciferase reporter assays and animal experiments is commendable. I thank Dr. Pooja for helping me during the miR-204 study. I extend my thanks to the Postdocs in the lab Dr. Aditi and Dr. Annada for maintaining cheerful environment in the lab.

And finally to my best buddies in the lab, Raikamal, Shalaka, Akash, Purna and Shweta, I thank you from the core of my heart, for always being there with me during every moment in this tenure. Raikamal, has a significant contribution in this journey being my project partner in miR-204 study. She is “always happy” person and tries to inculcate the same in others too. Her help during the time of presentation made them easy for me. I can never forget enumerate regular never ending tantrums with her which always entertained us and others too. The funny souvenirs and the ever incomplete balance sheet of samosa’s, plea requests and bike pickup and drops are one of the unforgettable things of this tenure. Shalaka was co-ordinator of the NGS related work in the lab and assisted me in preparing the NGS libraries. She was my financial advisor and guided me to use money in a conserved way. Her efforts in making me understand the importance and the necessity of the situation are adorable. I will always cherish Akash’s perfectly timed mischievous comments, supposedly funny jokes which always made the time funny. With his assistance, the animal experiments became simple and smooth. He was there with me throughout the hospital visits when I was sick during this tenure. No matter who instigates me, my rage always landed on him. I thank him for bearing me so much. Purna and Shweta are happy to go individuals. It was difficult to win an argument with Purna. She always took extreme efforts in explaining me issues of day to day life and finding out ways resolving them. Photography and camera tech related disscussions with Shweta helped me follow my hobby. Her skills in bird photography were amazing. I will always remember the mind blowing personality development sessions from Shalaka, Purna and Raikamal. The good time enjoyed with the lab members during the lab trips to Sikkim and Kaas plateau were one of the memorable moments of my PhD tenure. I cannot forget the great help from the trainees in the lab. Harshika, Sahana, Roshni, Shivali, Shruti, Yona, Sailee, Rohan, Akash. U, Lekha, Shreya, Kasturi and Uma, I thank you all.

I will always cherish the love, affection, encouragement and support of my ACTREC friends Ajay, Rahul, Burhan, Prathamesh, Raghav and Shalini D whose continuous encouragement rendered throughout this work. My Ph. D. batchmates (Batch 2014) Ajit, Mukund, Saim, Jyoti, Usha, Trupti, Arijit, Maitreyi and Shalini S were always there happy to help whenever required.

Being my best buddy, Ajit was a great moral, scientific and technical support throughout this tenure. The scientific as well as funny discussions with Mukund and Saim are one to be always remembered.

I am indebted to Department of Atomic Energy, Government of India and Indian Council of Medical Research for awarding me Fellowship for the PhD tenure.

I owe this project to my beloved parents Mr. Shrikrishna and Mrs. Sharada and especially to my lovely younger sister Miss. Bhagyashree. Their continuous encouragement, support blessings, dedication and much more has helped me to acquire the zeal to achieve this task. I cannot forget the blessings and support from my elder parents Mr. Janardan and Mrs. Indu without whom I am incomplete. I am happy to mention the names of my dear buddies Rahul K., Vaibhav, Prasad, Sachin, Sudhir and Pavan for being with me at every moment during this task. I will always be grateful to my lovely and caring wife Surbhi for her dedication and constant support from the moment she became the part of my life. She is a wonderful person of genuine character who spared the most important thing in this world for me, i.e the 'time'. She always understood my needs without even said and acted accordingly especially during the last few months of this tenure. She holds a worthy contribution in the successful completion of my Ph. D.

Finally I express my most sincere thanks to **God** who had given me the best till now, and without whose support it would have been impossible for me to achieve this success.

Harish Shrikrishna Bharambe

Table of Content

List of Figures

List of tables

Chapter 6

6. Summary and Conclusions

WNT subgroup medulloblastomas have excellent survival among the four molecular subgroups of medulloblastomas. The molecular mechanism underlying this high survival rate of the WNT subgroup is largely not understood. WNT subgroup has the most distinctive microRNA profile, which could play a crucial role in its biology. The functional role of two WNT subgroup microRNAs, miR-193a and miR-204, was studied in detail. The molecular mechanism underlying the WNT subgroup enriched expression of the two microRNAs was investigated. The microRNA was expressed in a doxycycline-inducible manner in established medulloblastoma cell lines. The effect of restoration of microRNA expression on the growth and malignant characteristics of medulloblastoma cells was investigated by studying their anchorage-independent growth, invasion potential, and tumorigenicity. The underlying molecular mechanism was deciphered by transcriptome sequencing and by identifying direct targets of the microRNAs.

The salient findings of the present study are as follows.

6.1. MiR-193a

- The expression of miR-193a is restricted to the WNT subgroup medulloblastomas, as analyzed in two independent cohorts of molecularly classified medulloblastomas.
- The miR-193a expression is upregulated by MYC, a downstream target of WNT signaling. Therefore, the expression of miR-193a in the WNT subgroup medulloblastomas appears to be upregulated by the constitutively activated WNT signaling pathway.
- The CpG island in the miR-193a promoter region was found to be hypermethylated in the three non-WNT subgroups of medulloblastomas. The expression of miR-193a could be restored upon the treatment of medulloblastoma cell lines with a DNA methylation

inhibitor, 5-aza-2'-deoxycytidine. Thus, miR-193a expression appears to be downregulated in non-WNT medulloblastomas due to promoter hypermethylation.

- Restoration of miR-193a expression in MYC amplified/overexpressing Group 3 medulloblastoma cells inhibited their growth, tumorigenic potential, and increased their sensitivity to radiation, indicating a tumor-suppressive role of miR-193a in medulloblastoma pathogenesis.
- *MAX*, *DCAF7*, and *STMN1* were identified as novel targets of miR-193a that are likely to contribute to its tumor-suppressive effect.
- MAX is an obligate heterodimerization partner of MYC required for the transcriptional activity of MYC. The expression of miR-193a in MYC overexpressing/amplified Group 3 medulloblastoma cells resulted in the downregulation of MAX and destabilization of MYC as indicated by the reduction in the half-life of MYC. Thus, miR-193a appears to act as a feedback inhibitor of the MYC signaling.

- MAX has been reported to suppress the expression of miR-193a by directly interacting with the miR-193a promoter [10]. Therefore, miR-193a and MAX appear to negatively regulate each other's expression, thereby modulating the activity of the MYC transcription factor family.
- MiR-193a expression in the medulloblastoma cells brought about widespread repression of gene expression that included genes involved in the WNT signaling, NOTCH signaling, cell cycle regulators, DNA replication as well as chromatin organization and modification. The miR-193a mediated widespread repression of gene expression was found to be accompanied by a substantial decrease in the global levels of H3K4me3,

H3K27ac, the histone marks of active chromatin, and an increase in H3K27me3, a mark of repressed chromatin, indicating genome-wide chromatin remodeling.

- In cancer cells having high MYC expression, MYC accumulates at the promoters of actively transcribed genes bringing about their transcriptional amplification. Therefore, miR-193a mediated inhibition of MYC activity is likely to contribute to the widespread repression of gene expression in Group 3 medulloblastoma cells.
- MiR-193a expression led to a tumor-suppressive effect in MYC overexpressing Group 3 cells mediated by a decrease in the activity of MYC and reduction in the levels of several oncogenic targets and global epigenomic repression of gene expression. Hence miR-193a has a therapeutic potential in MYC overexpressing aggressive Group 3 medulloblastomas.

6.2. MiR-204

- MiR-204 is differentially expressed in the four molecular subgroups of medulloblastomas. However, the miR-204 promoter region was not found to be hypermethylated in medulloblastoma tumor tissues MiR-204 expression could be partially restored in medulloblastoma cells upon treatment with HDAC inhibitors.
- Restoration of miR-204 inhibited tumorigenicity of Group 3 medulloblastoma cell lines, with an increase in the survival duration of the tumor-bearing mice by 25-34 %. This indicates the tumor-suppressive effect of miR-204 in medulloblastomas, which is consistent with its role in several other cancers.
- The transcriptome analysis of miR-204 expressing cells has identified downregulation of several known validated target genes of miR-204 like RAB22A, M6PR, AP1S2, and EZR.

- IGF2R and LAMP1, which were downregulated upon miR-204 expression were identified as novel target genes of miR-204.
- The protein-protein interaction network analysis of the genes significantly downregulated upon miR-204 expression identified downregulation of several genes involved in the extracellular matrix organization and degradation. The downregulation of these genes is consistent with the inhibition of tumorigenicity and invasion potential of medulloblastoma cells upon miR-204 expression.
- Lysosomal degradation pathway is one of the major pathways identified to be affected by miR-204 expression in medulloblastoma cells as indicated by downregulation of key genes involved in this pathway which includes IGF2R, M6PR, LAMP1, and AP1S2.
- IGF2R, M6PR, and AP1S2 are known to be involved in the transportation of lysosomal proteases from the trans-Golgi network to the lysosomal compartment. MiR-204 expression significantly reduced the levels of mature lysosomal proteases cathepsin B and cathepsin D in medulloblastoma cells.
- The miR-204 expression increased the levels of SQSTM1/p62, an adaptor protein involved in the pathway of autophagy, which gets degraded by lysosomal activity upon fusion of autophagosomes with lysosomes. This suggests the reduction in the lysosomal degradation and autophagy pathway upon miR-204 expression medulloblastoma cells.
- The expression miR-204 in medulloblastoma cells brings about inhibition of autophagy (Ph.D. thesis, Raikamal Paul). Lysosomal degradation pathway is known to play a pivotal role in autophagy. Hence, downregulation of key genes involved in the lysosomal pathway accompanied by reduced levels of lysosomal proteases are likely to contribute to autophagy inhibition upon miR-204 expression,

- Autophagy inhibition upon ATG5 knockdown in medulloblastoma cells led to inhibition of their invasion potential (Ph. D. thesis, Raikamal Paul) [156]. Therefore, the inhibition of the autophagy-lysosomal degradation pathway is likely to contribute to the decrease in the invasion potential of medulloblastoma cells upon miR-204 expression.
- Upregulation of miR-204 expression upon treatment with HDAC inhibitors, although modest, suggests a role of these inhibitors in the treatment of medulloblastomas.

6.3. Contribution of microRNAs in excellent survival rates of WNT subgroup medulloblastomas

The WNT subgroup tumors have the most distinctive microRNA expression profile with overexpression of several microRNAs, including miR-193a, miR-204, miR-148a, miR-224 [9, 151]. Previously in our lab, miR-204 and miR-148a have been shown to inhibit the anchorage-independent growth, tumorigenicity, and invasion potential of medulloblastoma cells. Interestingly, miR-148a was also found to be induced by MYC (Ph.D. thesis, Kedar Yogi). The tumor-suppressive activity of miR-148a in medulloblastoma cells was found to be contributed by a reduction in the levels of its direct target NRP1, a co-receptor of several growth factors including VEGF, EGF, PDGF, TGF-β1, and HGF. MiR-204 is another microRNA overexpressed in the WNT subgroup and downregulated in almost all SHH and several Group 3 and Group 4 tumors. The higher expression of miR-204 correlates with the better overall survival in Group 3/Group 4 medulloblastomas. Restoration of miR-204 expression inhibited anchorage-independent growth, invasion potential, tumorigenicity and increased the radiation sensitivity of medulloblastoma cells (Ph. D. Thesis- Raikamal Paul) accompanied by inhibition of autophagy indicating a tumor-suppressive role of miR-204 in medulloblastoma pathogenesis [11]. Exogenous expression of miR-224 was found

to inhibit growth and increase the radiation sensitivity of medulloblastoma cells. MiR-224 was also reported to be downregulated in glioma tumor tissues and cell lines and its expression was shown to increase the radiation sensitivity of glioma cells by targeting API5 [246]. Therefore, the higher expression of several tumor-suppressive microRNAs is likely to contribute to the excellent survival of WNT subgroup medulloblastomas by decreasing the malignant potential and increasing response to radiation therapy.

6.4. MicroRNAs: the evolving therapeutic agents

Despite the tremendous progress in understanding the cancer biology, there is a paucity of effective therapies due to inadequate targeting of the oncogenic pathways, the emergence of drug resistance, and drug-induced toxicity [247, 248]. Cancer is caused by multiple genetic alterations. Targeting a single oncogene, therefore, has limited efficacy both due to lack of complete dependence of cancer cells on a single alteration and due to the development of resistance. Each microRNA targets multiple genes in a biologically relevant manner. MicroRNAs are evolutionarily conserved natural endogenous small RNAs that cells use for controlling cellular mechanisms like proliferation, stem cell maintenance, differentiation. MicroRNAs, therefore, offer a novel natural therapeutic modality for cancer treatment. Numerous studies have proved the oncogenic and tumor-suppressive role of microRNAs in cancer [8, 248]. The microRNAs can be used for the treatment provided they are exclusively tumor-suppressive or oncogenic. Although microRNA-based drugs have not yet entered the clinics, the safety of microRNA-based therapeutics has been demonstrated in several phase I clinical trials [249, 250]. Restoration of tumor suppressor microRNA expression or inhibition of oncomiR function is the current strategy for the microRNA-based therapeutics for the treatment of cancer. MiR-34 is a

validated tumor-suppressor microRNA known to target over 30 oncogenes involved in various cellular pathways in multiple tumor types. MiR-16 mimic, encapsulated in bacterially derived minicells conjugated to anti-EGFR antibody, has entered phase II clinical trial for the treatment of lung cancer cells having a high expression of EGFR [250, 251]. Several clinical trials are ongoing like the miR-10b inhibitor in glioblastoma and miR-155 inhibitor in T-cell lymphoma. These trials using formulations of the lock nucleic acids for the inhibition of microRNAs have yielded promising results [252]. Rapid advances are being made in designing and optimizing various approaches for targeted microRNA delivery that include use of liposomes, nanoparticles, exosomes, as well as viral vectors like adeno-associated vectors [253, 254]. In the case of brain tumors, the blood-brain barrier also needs to be overcome. Non-invasive focused ultrasound treatment that disrupts the blood-brain barrier in a targeted area is one of the potential approaches for targeted delivery into brain tumors [255]. In the present study, the tumor-suppressive role of miR-193a and miR-204 was experimentally demonstrated in highly aggressive MYC overexpressing Group 3 medulloblastoma cell lines, making them promising molecules for the treatment of medulloblastomas. The therapeutic efficacy and safety of these microRNAs in combination with other treatment modalities like radiation therapy could be evaluated in patient-derived xenograft models by delivering these microRNAs systemically or by directly injecting into the tumor.

6.5. Significance of the study

- Both miR-193a and miR-204 are WNT subgroup enriched microRNAs, which exhibited a significant tumor-suppressive effect in MYC overexpressing/amplified Group

3 medulloblastoma cells. Thus, both microRNAs hold a therapeutic potential in the treatment of the highly aggressive Group 3 medulloblastomas.

- The WNT subgroup has an excellent long-term survival of over 90 %, even though WNT signaling is expected to impart a highly malignant nature to the tumors. MiR-193a and miR-204, two microRNAs expressed in the WNT subgroup were found to be tumor-suppressive in medulloblastoma cells. MiR-193a was found to decrease the activity of MYC, a crucial downstream target of WNT signaling. MiR-193a increases the radiation sensitivity of medulloblastoma cells. MiR-204 was found to inhibit invasion potential of medulloblastoma cells by inhibiting autophagy-lysosomal degradation pathway. Thus, the microRNAs are likely to contribute to the better overall survival of the WNT subgroup medulloblastomas.
- MYC is overexpressed in more than 50 % of malignancies and is a known marker of poor prognosis [82]. MiR-193a, on the other hand, was shown to destabilize MYC by downregulation of MAX. Thus, miR-193a is likely to be a promising therapeutic microRNA for other MYC overexpressing malignancies as well.

6.6. Future directions

- The tumor-suppressive effect of miR-193a and miR-204 on the highly aggressive MYC overexpressing/amplified Group 3 medulloblastoma cell lines suggests the therapeutic potential of the two microRNAs in the treatment of Group 3 medulloblastomas. The therapeutic efficacy of these microRNAs either alone or in combination, could be evaluated in pre-clinical models, including PDX models and transgenic mouse models of medulloblastomas. The microRNAs can be delivered as lipid encapsulated mimics, using adenoviral vectors or encapsulated in exosomes.

- MiR-204 expression is downregulated in almost all SHH subgroup medulloblastomas. The role of miR-204 in the pathogenesis of SHH subgroup tumors and possibly on the SHH signaling pathway could be explored using SHH medulloblastoma cell lines, PDX models, and transgenic mouse models of SHH subgroup medulloblastomas. MiR-204 may have therapeutic potential in the treatment of SHH subgroup medulloblastomas as well.

Thesis Summary

Name: Mr. Harish Shrikrishna Bharambe

Enrollment Number: LIFE09201404008

Thesis Title: Molecular mechanism underlying the effect of miRNA expression on medulloblastoma cell behavior

Medulloblastoma is the single most common malignant brain tumor in children consisting of four distinct molecular subgroups: WNT, SHH, Group 3 and Group 4. WNT subgroup medulloblastomas have a distinct microRNA expression profile with upregulation of several microRNAs that can contribute to their excellent overall survival of over 90 %. MiR-193a, a WNT subgroup specific microRNA was found to be induced by MYC, a downstream target of WNT signaling. It was demonstrated to be silenced as a result of promoter hypermethylation in non-WNT medulloblastomas. Restoration of miR-193a expression inhibited proliferation, anchorage independence, *in vivo* tumorigenicity and increased radiation sensitivity of MYC overexpressing Group 3 medulloblastoma cell lines. The inhibition of tumorigenic properties was accompanied by widespread repression of gene expression in these cell lines including downregulation of its novel targets DCAF7, SMTN1 and MAX. Furthermore, miR-193a mediated downregulation of MAX, an obligate heterodimerization partner of MYC, was found to destabilize MYC which can contribute to the widespread repression of gene expression. Thus, miR-193a appears to be a feedback inhibitor of MYC signaling, thereby acting as a tumor suppressor in the MYC amplified Group 3 medulloblastoma cell lines. The strong tumor suppressive role of miR-193a in MYC overexpressing Group 3 medulloblastoma cell lines suggest its therapeutic potential not only in the treatment of medulloblastomas but also for other MYC addicted cancers.

Restoration of miR-204 expression inhibited tumorigenic potential of Group 3 medulloblastoma cell lines and resulted in downregulation of several genes involved in extracellular matrix organization and degradation and lysosomal pathway. IGF2R and LAMP1were identified as novel miR-204 targets. MiR-204 was found to decrease expression levels of mature lysosomal proteases cathepsin D and cathepsin B thereby affecting lysosomal degradation pathway. Furthermore, treatment with HDAC inhibitors resulted in upregulation of miR-204 expression in medulloblastoma cells, suggesting therapeutic role for these inhibitors in the treatment of medulloblastomas.

Chapter 1

1. Introduction

Medulloblastoma is the most frequently occurring malignant brain tumor in children and is the leading cause of cancer-related mortality and morbidity in this age group [1]. It occurs in the posterior fossa region of the brain and has a tendency to metastasize to the craniospinal axis, with about one-third of patients having metastasis at the time of diagnosis. Medulloblastomas are classified as grade IV, the highest grade of malignancy. The current multimodal treatment of medulloblastomas includes surgical resection followed by craniospinal irradiation and chemotherapy. The risk stratification is based on the clinicopathological variables like age of the patient, presence of metastasis at the diagnosis, and the extent of tumor resection. The overall survival rate of average-risk patients is over 70%, but the survival of high-risk patients is less than 50 %. Besides, the patients suffer from secondary effects of the therapy like neurocognitive and neuroendocrine deficits, and at times secondary malignancies. Therefore, an in-depth understanding of the molecular mechanism of pathogenesis of medulloblastoma is necessary for better risk stratification and the development of novel treatment strategies with the least side effects.

Medulloblastoma is not a single disease but comprises four distinct molecular subgroups WNT, SHH, Group 3, and Group 4 [2, 3]. WNT and SHH subgroup medulloblastomas are characterized by the activation of the canonical WNT signaling pathway and the SHH signaling pathway, respectively. Group 3 and Group 4 medulloblastomas have overlapping gene expression profiles. Group 3 tumors are distinguished by the expression of retina-specific genes, whereas the expression of genes associated with neuronal differentiation is enriched in Group 4 medulloblastomas. The four subgroups differ not only in their gene expression profiles, underlying genetic alterations but also differ in their clinical

characteristics like age and gender-related incidence, incidence of metastasis at diagnosis and overall survival [2, 4]. WNT subgroup medulloblastomas have an excellent long-term overall survival of over 95 %, whereas Group 3 has the worst five-year survival rate of ~50 %. SHH subgroup and Group 4 medulloblastomas have intermediate survival of 60 - 70 %. WNT subgroup medulloblastomas harbor activating mutations in the *CTNNB1* gene encoding beta-catenin in over 90 % of tumors, which result in the constitutive activation of the canonical WNT signaling pathway. The canonical WNT signaling is known to bring about the epithelial-mesenchymal transition, stem cell self-renewal, and maintenance. It is also involved in immune evasion. All these characteristics are known to be associated with aggressive cancers. Moreover, *MYC* oncogene is expressed in WNT subgroup medulloblastomas, *MYC* being the direct target of the WNT signaling. Nonetheless, the WNT subgroup medulloblastomas have the best survival rates among the four medulloblastoma subgroups. *MYC* oncogene is also overexpressed in Group 3 medulloblastomas, with 10 – 17 % of these tumors carrying amplification of the *MYC* locus. Furthermore, overexpression of *MYC* is a marker of poor prognosis in Group 3 medulloblastomas, which has the worst survival rate among the four medulloblastoma subgroups.

MicroRNAs are small non-coding RNAs of about 20-22 bp in length, which regulate gene expression at the post-transcriptional level [5, 6]. MicroRNAs are known to control vital cellular processes like proliferation, growth, apoptosis, and differentiation. MicroRNAs are often deregulated in cancer and play a crucial role in pathogenesis [7, 8]. MicroRNA expression profiling study identified differential microRNA expression across the four molecular subgroups of medulloblastomas [9]. The WNT subgroup medulloblastoma has

the most distinctive microRNA profile with the expression of several microRNAs, including miR-193a, miR-204, miR-148a, and miR-224. MiR-193a is one of the most WNT subgroup-specific microRNAs, which is downregulated in non-WNT medulloblastomas. In an isogenic model of cellular transformation of breast epithelial cells and fibroblasts, the expression of miR-193a was found to be downregulated upon malignant transformation [10]. MiR-193a is known to act as a tumor suppressor in various cancers, including lung cancer, AML, and oral cancer. The fact that miR-193a acts as a tumor suppressor in several cancers and its expression is restricted to the WNT subgroup, which has the best overall survival rate, intrigued us to investigate its role in the pathogenesis of medulloblastoma.

MiR-204 is one of the microRNAs that is highly expressed in all the WNT subgroup tumors. Almost all SHH subgroup, 60 % Group 3 and 15 % Group 4 medulloblastomas have low miR-204 expression as compared to normal cerebellar tissues [11]. MiR-204 is an intragenic microRNA located in the sixth intron of the host gene *TRPM3*, and is abundantly expressed in brain and kidney. MiR-204 is located at 9q21.1–q22.3, a cancer-associated genomic region that is frequently deleted in various cancers [12]. In a large-scale study on 3312 tumors, 1107 non-malignant tissues, the miR-204-211 family was found to be the top deleted miRNA family [13]. Furthermore, the expression of miR-204 was found to correlate with overall survival in Group 3/Group 4 medulloblastomas, where lower expression levels of miR-204 identified a highly aggressive subset of these tumors [11]. Restoration of miR-204 expression inhibited the anchorage-independent growth and invasion potential of medulloblastoma cells. In the present study, the effect of restoration of miR-204 expression on the tumorigenic potential of group 3 cell lines was studied, and

the molecular mechanism underlying the tumor-suppressive effect of miR-204 expression was delineated.

Objectives

1. To investigate the effect of miR-193a expression on the growth and malignant behavior of medulloblastoma cells and delineate the underlying molecular mechanism.
2. To study the molecular mechanism underlying the effect of miR-204 expression on medulloblastoma cell behavior.

The molecular mechanism underlying the differential expression of miR-193a in molecular subgroups of medulloblastomas was investigated by studying the methylation status of the CpG island in the miR-193a promoter region. MiR-193a expression was found to be upregulated by MYC, a downstream target of WNT signaling. The effect of restoration of miR-193a and miR-204 expression on the malignant potential of MYC amplified/overexpressing Group 3 medulloblastoma cell lines was studied. The effect of the miRNA expression on the proliferation, anchorage-independent growth, cell-cycle profile, radiation sensitivity, and tumorigenic potential of medulloblastoma cells was investigated. The molecular mechanism underlying the tumor-suppressive effect of miR-193a and miR-204 expression was investigated by transcriptome analysis. The genes and molecular pathways affected upon the restoration of miR-193a and miR-204 expression in Group 3 medulloblastoma cell lines were identified by the protein-protein interaction network analysis and further validated.

Chapter 2

2. Review of Literature

2.1. Medulloblastoma: A historical perspective

During the investigation on 400 gliomas at the Peter Bent Bingham Hospital, Dr. Harvey Cushing and Dr. Percival Bailey identified a group of 29 'very cellular of a peculiar kind' tumors. These tumors occurring mainly in children initially named s*pongioblastoma cerebelli* were identified to be originating from the roof of the fourth ventricle, further extending to the center of the cerebellum. In a parallel study by Dr. Globus and Dr. Strauss, the term *spongioblastoma multiforme* was used to describe a group of cerebral tumors showing marked cellular differentiation, a feature, which was distinct from the tumors of cerebellar origin described by Bailey and Cushing. After a discussion with Strauss and Globus and analysis of their specimens, Bailey and Cushing adopted the term '**Medulloblastoma'** to describe a set of cerebellar tumors with an unmistakable microscopic appearance, which distinguishes them from gliomas. These tumors were thought to originate from hypothetical cells then referred to as *medulloblasts,* which correspond to the undifferentiated cells of the ectodermal origin in the developing cerebellum, capable of differentiating in both neuronal and glial lineages [14]. Thus the adoption of the term medulloblastoma aided in the uniform classification of the tumors of the posterior fossa made up of undifferentiated cells. However, the existence of the cell type *medulloblast* has never been proven, the term medulloblastoma was continued to be used to describe small round blue cells containing undifferentiated tumors of the posterior fossa. Years later, based on the findings of Hart and Earle [15], L. B. Rorke proposed a method of classification of the central nervous system (CNS) tumors occurring in infancy composed of an undifferentiated mass of cells. The classification was based on the concept of malignant transformation of the early neuroepithelial cells giving rise to the tumors

which were typed based upon their appearance under a light microscope, immunocytochemical analysis, and ultra-structural characteristics, irrespective of the site of origin of the tumor. These neoplasms of CNS histologically similar in nature were referred to as primitive neuroectodermal tumors (PNETs). Being a tumor composed mostly of undifferentiated cells, medulloblastoma was also included in this category [16]. Further in 1993, based on the gene expression profiling using microarrays, it was revealed that medulloblastomas are a molecularly distinct set of tumors as compared to other PNETs, atypical teratoid and rhabdoid tumors (AT/RTs)s and malignant gliomas [17].

Out of his extensive experience with medulloblastoma, Cushing described the clinical, pathological and epidemiological salient features of the disease which include increased intracranial pressure, young age at presentation, predominance in males, a short history of symptoms, the precise location in midline/vermis, and the easily suckable nature of the tumors. He also reported the tendency of medulloblastomas to invade the floor of the fourth ventricle and metastasize to the locations in the craniospinal axis away from their primary location.

Medulloblastomas were primarily classified based on their histopathological characteristics as judged by the appearance of the tumors under the light microscope. By far, five histological variants of medulloblastomas are known. Classic medulloblastomas are the most common and characterized by a group of small identical cells with high nuclear to cytoplasmic ratio. These cells are typically identified by a large round blue nucleus surrounded by a fine ring of pink cytoplasm, which resembles the medulloblastomas described by Bailey and Cushing. In contrast to classic histology, desmoplastic medulloblastomas show nodules of slow multiplying differentiated

neurocytic cells demarcated by internodular zones comprised of rapidly multiplying pleomorphic desmoplastic cells. The medulloblastomas with extensive nodularity (MBEN) are closely related to desmoplastic nodular medulloblastomas with relatively larger nodules and advanced neuronal differentiation. Usually occurring in children, MBENs are reported to be associated with favorable prognosis [18]. The large cell variant of the disease consists of cells with large pleomorphic nuclei with prominent nucleoli and abundant cytoplasm. This variant shows a high mitotic index and apoptotic rates. The anaplastic medulloblastomas are described as tumors with highly variable nuclear structures, mitotic index and especially, cell-cell wrapping. Owing to their morphological and phenotypic similarity and co-occurrence, these variants are together termed as large cell and anaplastic tumors (LC/A), and are known to be associated with poor prognosis. In all, the desmoplastic medulloblastomas have a favorable outcome followed by classic medulloblastomas with LC/A medulloblastomas being the most aggressive of all with poor prognosis [19].

2.2. Epidemiology

Tumors of the central nervous system are the second most common cancers and the leading cause of cancer-related deaths in children [1]. Medulloblastoma is the single most common pediatric malignant brain tumor, which accounts for 20 % of all pediatric intracranial tumors [20, 21]. Its reported incidence in the United States of America is 1.5-5 cases per million per year and is thought to be similar worldwide [22]. The disease is prevalent in early age with 80 % of the cases reported during the first 15 years of age with the median age of diagnosis between 5 - 9 years. About 10-15 % cases occur in infants [20]. The

disease is much less common in adults (age > 16 years, 1 % of all CNS tumors) with the incidence of 0.05 cases per million per year, which decreases with an increase in age [23-25]. Medulloblastomas occur more frequently in males with 1.2-2 times higher incidence than females [20]. Medulloblastomas are classified as the grade IV tumors, which is the highest grade of malignancy [26].

2.3. Treatment and clinical outcome

At the outset, when medulloblastomas were identified by Bailey and Cushing, surgical removal of the tumor was the only available treatment for medulloblastomas. Initially, with the limited success of the surgical extirpation of the tumor, the patient survival was only six months, with all cases rapidly succumbing to the recurrences, thus making the disease incurable. The first attempted radical removal of the tumor by Cushing showed extended survival of 17 months. Cushing's experience with the only one case where the patient received three regimens of cranial irradiation and additional surgeries for the recurrence made him suggest the possible benefits of the posterior fossa irradiation in the treatment of medulloblastomas [27, 28]. The concept of craniospinal irradiation for the treatment of medulloblastomas emerged as a result of post-mortem findings of the presence of disease lesions in the cerebellum as well as at distant locations in the craniospinal axis. A report published by Ingrahm in 1948 indicated that the irradiation of the craniospinal axis led to an improvement in survival. However, the patients eventually succumbed to the disease as they received suboptimal doses of radiation [29]. A breakthrough came from the study published by Patterson and Farr, which included irradiation of the posterior fossa and the rest of the craniospinal axis following partial or complete surgical resection significantly

improved the 3-year survival to 65 % [30]. The study, however, shed very less light on the sequelae associated with the therapy. Later, Dennis Maureen and colleagues presented a comprehensive report over the neuropsychological sequelae associated with the radiation therapy and concluded that the children less than 7 - 8 years of age are vulnerable to the harmful effects of irradiation [31]. All these observations lead to the conclusion that the combination of surgery and radiation therapy can potentially cure the disease, and medulloblastomas are not necessary the fatal disease. However, the improvement in survival, especially in younger children, has come at the expense of poor quality of life. Several attempts were made to further improve the clinical outcome using the improved methods of craniospinal irradiation; however, the efforts did not meet success owing to the sequelae associated with the therapy. This led to the search for other therapies used instead of or adjunct to the craniospinal irradiation. In this quest, the chemotherapy proved as an efficient adjunct to the available modalities for the treatment of medulloblastomas. The combination of craniospinal irradiation and chemotherapy as an adjunct to the surgery was shown to further improve the 5-year progression-free survival of the patients to 79 % with the reduction in the dose of irradiation [32]. Moreover, the advent of imaging modalities and the introduction of magnetic resonance imaging (MRI) for the staging of medulloblastomas have dramatically improved the ability to detect metastases and helped in more robust identification of high risk-individuals with metastatic dissemination.

The surgery followed by chemotherapy and craniospinal irradiation is the current gold standard treatment for medulloblastomas. The recent advances in the multimodal treatment and the risk stratification criteria based on clinical characteristics and molecular characteristics like *TP53* mutations and *MYC/MYCN* amplifications have yielded the

survivorship of about 80 %. Although the clinical outcome has greatly improved, most long-term survivors suffer from neurocognitive, neuroendocrine deficits, and in some cases secondary malignancies [32]. Therefore, the understanding of the molecular mechanism involved in the pathogenesis of the disease is of prime importance for the development of novel molecularly targeted treatment strategies with the least side effects.

2.4. Molecular genetics of medulloblastomas

Genetic alterations in common oncogenes/tumor suppressor genes, like *TP53, EGFR*, $p16^{INK4A}$, *PTEN* are relatively rare in medulloblastomas [33, 34]. The most common genetic alteration is isochromosome 17q, which involves the loss of p arm of chromosome 17 with the simultaneous gain of q arm occurring in about 40-50 % of medulloblastomas [35]. The tumor cells resembling neural stem cell-like cells, the prevalence of the disease in children, and occurrence in the region that develops postnatal suggested that the deregulation of development may underlie the origin of medulloblastomas [36]. The direct evidence of the involvement of the deregulated developmental pathways in the pathogenesis of medulloblastomas initially came forth from the study of two familial syndromes: Gorlin's syndrome and Turcot's syndrome. The patients with Gorlin's syndrome who primarily develop naevoid basal cell carcinoma harbor germline mutations in the *PTCH1* gene, which encodes a transmembrane receptor involved in the Sonic Hedgehog (SHH) signaling pathway. Germline mutations in the *APC* (adenomatous polyposis coli) gene, the negative regulator of β-catenin in the canonical WNT signaling pathway are frequently reported in the patients with Turcot's syndrome in which patients are predisposed to develop colorectal cancer. About 5 % of the patients with Gorlin's syndrome and 79 % of the patients with

Turcot's syndrome with germline *APC* mutations were found to have a predisposition to medulloblastomas [37, 38]. Moreover, 25-30 % of sporadic medulloblastomas also show mutations in the genes (*PTCH1*, *SMO,* and *SUFU*) involved in the SHH signaling and WNT signaling pathway (*CTNNB1*, *APC*, *AXIN1*) [4].

2.4.1. Sonic Hedgehog Signaling Pathway

Attempts to answer the very fundamental question in the developmental biology that how a single cell egg develops into a complex organism led to the discovery of the Sonic Hedgehog signaling pathway. In 1970's, Christiane Nusslein-Volhard and Eric Wieschaus studied mutations in genes that control segment polarity and formation of the anterio-posterior body axis in the development of fruit fly *Drosophila melanogaster*. Among those genes, Drosophila hedgehog [39] gene was found to govern the formation of anterior and posterior parts of individual body segments. The mutations in the hedgehog gene gave rise to short spiny larvae having an abnormal arrangement of cuticular denticles making the larvae appear like a hedgehog [40]. Thus, the name of the hedgehog gene is inspired by the appearance of the larvae like hedgehog due to the mutation in the key signaling molecule involved in this pathway. So far, three homologs of the *hh* protein have been identified in the mammals, which are Sonic hedgehog (SHH), Indian hedgehog (IHH) and Desert hedgehog (DHH). Among these, the Sonic hedgehog is the most studied ligand. Various studies have established the role of the SHH pathway in early embryonic development, body axis formation, cell proliferation, and organogenesis in a concentration-dependent manner [41]. The pathway was also shown to be involved in the regulation of adult stem cells from various tissue types [42-44]. The SHH pathway controls the development of the cerebellum, where the SHH ligand secreted by the Purkinje cells activates SHH signaling

in the cerebellar granule neural precursors (CGNPs) leading to the formation of the external granular layer [45, 46].

The binding of the SHH ligand to its receptor patched (PTCH) on the cell membrane results in the internalization of the ligand-bound PTCH by endocytosis. As a result of this, its inhibitory effect on the effector protein smoothened [22] is relieved, which is usually sequestered inside the vesicles [22]. SMO is further translocated from the intracellular vesicles to the membrane of the primary cilium where it activates the GLI family of transcription factors. The activated GLI proteins then move to the nucleus and initiate the transcription of the hedgehog target genes like *CCND1*, *MYCN,* and *PTCH1*. In the absence of the hedgehog ligands, the PTCH inhibits the activity of SMO and suppressor of fused (SUFU), which sequesters the GLI transcription factor in the cytoplasm keeping the signaling inactive [41, 46, 47].

The loss of function mutations in the genes *PTCH1* and *SUFU* and activating mutations in the *SMO* gene have been identified in about 25 % cases of sporadic medulloblastomas [4]. The mechanism by which SHH drives the tumorigenesis of the medulloblastoma has been well studied by generating murine models. One of the most characterized SHH mouse model was generated by deleting the *Ptch1* gene. The homozygous deletion of *Ptch1* (*Ptch1*$^{-/-}$) is embryonic lethal whereas, the mice harboring heterozygous deletion of *Ptch1* (*Ptch1*$^{+/-}$) were found to be larger in size, and about 10-15 % of mice gave rise to medulloblastoma of the cerebellum with high expression of *Gli1* which indicates the activation of the Shh pathway [48]. Another model was generated by expressing an activating mutant of the *Smo* gene under the NeuroD2 promoter, a promoter known to be active in CGNPs. This murine model has about 94 % incidence of medulloblastomas by

two months of age and was the first mouse model to show leptomeningeal spread [49]. These models have been instrumental in the development of SHH pathway inhibitors for the treatment of medulloblastomas that have entered into clinical trials. However, the efforts were subverted due to the emergence of drug-resistant mutations [50]. `

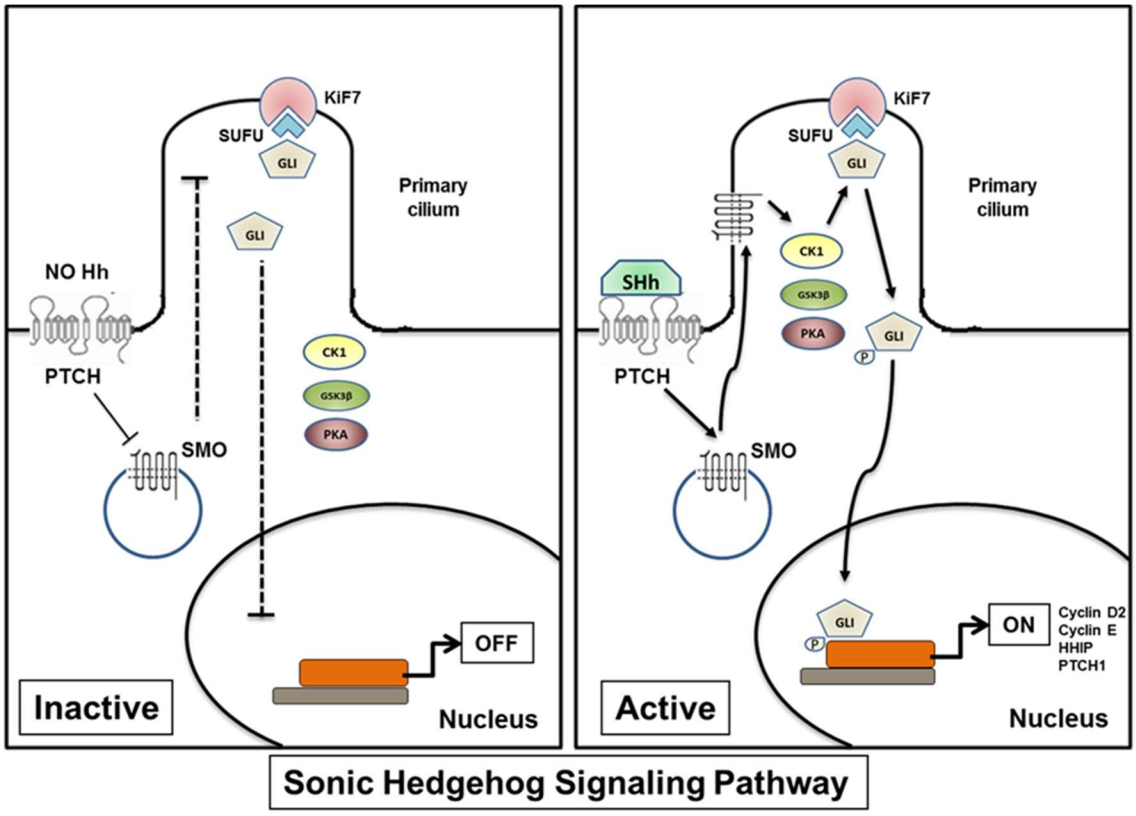

Fig 2.1: Pictorial representation of the Sonic Hedgehog signaling pathway.

2.4.2. WNT signaling pathway

In an attempt to identify the role of oncogenic retroviruses in the pathogenesis of breast cancer, Roel Nusse and Harold Varmus discovered the gene *integration1* (*int1*) as a gene activated upon the integration of viral DNA of mouse mammary tumor virus. The activation of the *int1* gene could cause breast cancer. The *int1* gene was later found to be highly conserved among the species and was identified as the homolog of the Drosophila

melanogaster gene *Wg* (wingless), a segment polarity gene, which regulates the formation of body axis during the embryonic development [51]. This led to the conclusion that the gene int1 discovered in mice has role in embryonic development. The name WNT was thus coined by the fusion of the terms Wingless and *int1*. Later studies in various models like Xenopus and Drosophila led to the identification of various key components of the WNT signaling pathway. There are three variants of the WNT signaling pathway: the canonical WNT pathway and the non-canonical planar cell polarity and WNT/Calcium pathway. All three pathways are activated by binding of several WNT family ligands to the frizzled family of receptors, which regulate the signaling through various signal relay proteins and downstream effectors.

The activation of the canonical WNT signaling pathway leads to the regulation of transcription of the genes involved in embryonic development, cell fate decision, cell growth, proliferation, and stem cell renewal [52]. β-catenin encoded by the *CTNNB1* gene is the key signaling intermediate in the cascade of the canonical WNT signaling pathway. In the absence of the WNT ligands, β-catenin is sequestered in the cytoplasm by a destruction complex composed of proteins AXIN1, APC, glycogen synthase kinase 3β (GSK3β), casein kinase 1α (CK1α) and protein phosphatase 2A (PP2A). AXIN1 acts as a scaffold protein for other components of the destruction complex. In the destruction complex, β-catenin is phosphorylated at serine 33 and serine 37 residues by GSK3β and is subjected to ubiquitination by an E3 ubiquitin ligase, β-TrCP (β-transducin repeat-containing protein) [53]. The ubiquitination of β-catenin results in its proteasomal degradation thus maintaining its low cytoplasmic pool. The Dickkopf family of proteins (DKKs), SFRP, and WNT inhibitory factor 1 (WIF1) attenuate the WNT signaling by

interacting with the frizzled receptor and WNT ligands, respectively. The binding of the WNT ligands to the frizzled receptors triggers the formation of their complex with another transmembrane protein low-density lipoprotein receptor-related protein 5/6 (LRP5/6). This leads to the recruitment of the negative regulator AXIN1 mediated by the protein disheveled (DVL) at the cytoplasmic tail of the LRP5/6 on the inner side of the cell membrane leading to the disruption of the destruction complex. The cytoplasmic β-catenin, thus stabilized, translocated to the nucleus and upregulates the transcription of the WNT signaling target genes like *CCND1*, *MYC* by acting as a transcriptional co-activator for the T-cell factor/Lymphoid enhancer factor (TCF/LEF) family of transcription factors. In the absence of β-catenin, the transcriptional activity of TCF/LEF is repressed by the interaction with Groucho family proteins which prevents the binding of activator CBFβ/p300 complex [54]. About 10 % of medulloblastomas carry a mutation in the *CTNNB1*, *AXIN1,* or *APC*, gene leading to the activation of the WNT signaling [4].

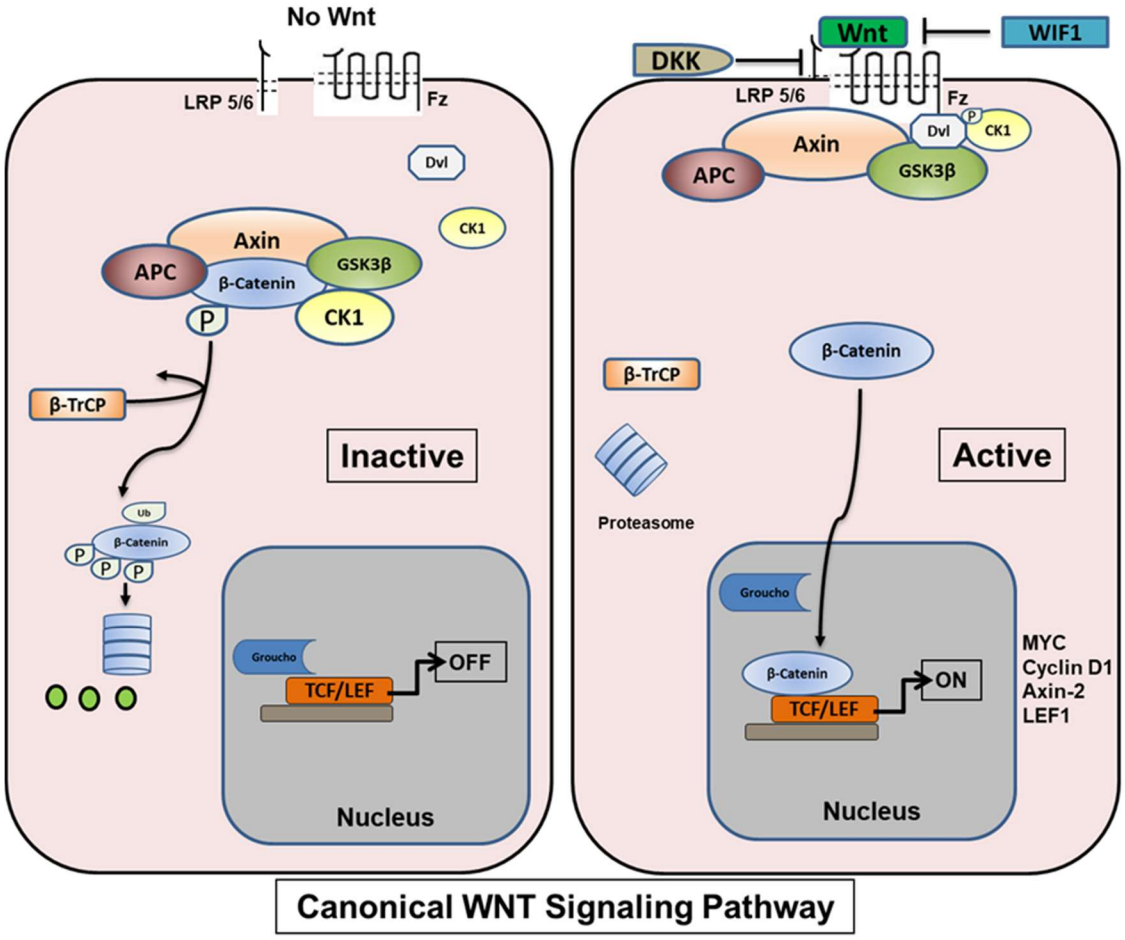

Fig 2.2: Pictorial representation of the canonical WNT signaling pathway.

2.5. Molecular classification of medullolastoma

The invention of the expression profiling and sequencing technologies has revolutionized the understanding of biological systems and also helped in deciphering the underlying biology of various diseases. In 2006, Thompson *et al*. conducted genome-wide expression profiling of 46 medulloblastoma tumor tissues using the Affymetrix gene chip HG-U133A and identified five subgroups of medulloblastomas characterized by specific genetic alterations like monosomy of chromosome 6, isochromosome 17q. [55]. The expression

profiling of 62 medulloblastomas by Kool et al. using the Affymetrix gene chip HG-U133A v2.0 arrays segregated medulloblastomas associated with the WNT and SHH signaling pathway and demonstrated correlation of the molecular subgroups with age at diagnosis, gender, and histology [56]. In 2011, a study published by Northcott *et al*. classified medulloblastomas into four subgroups based on the gene expression profiling data that not only segregated WNT and SHH signaling tumors but also showed subgroup-specific chromosomal level alterations. The study also showed a correlation of molecular subgroups with the survival outcome, demographics, and metastasis at diagnosis [57]. Another study by Cho *et al*. identified six subgroups based upon expression profiling data that segregated non-WNT, non-SHH medulloblastomas into four subgroups. This study showed a subgroup associated with *MYC* amplification and expression of photoreceptor-specific genes having poor survival as compared to a related subgroup. The existence of subtypes within the subgroups was postulated in this study [58]. The gene expression profiling study carried out in our lab using the Affymetrix Gene 1 ST array identified four molecular subgroups similar to those reported by Northcott *et al*. [9].

The findings of all these studies indicated that medulloblastoma is not a single disease but comprises distinct molecular subgroups which not only differ in their expression profiles but are also distinct in their clinical behavior. Considering the variation in the numbers and composition of molecular subgroups among the aforementioned studies, a conference was held in 2011 at Boston, which came to a consensus of the existence of four evidence supported molecular subgroups of medulloblastomas, which were named as WNT, SHH, Group 3 and Group 4. The transcriptional, genetic, demographic, and clinical differences between the four subgroups were listed in this consensus [3].

2.5.1. WNT subgroup

The WNT subgroup medulloblastomas are characterized by the constitutive activation of the canonical WNT signaling pathway. WNT subgroup is the least common subgroup accounting for about 10 % of total medulloblastoma cases. The subgroup is prevalent in older children and adults with a peak incidence at 10-12 years of age with an equal gender distribution. The metastasis at the time of presentation is detected in about 10 % cases [59]. With the current treatment modalities, the WNT subgroup has an overall long-term survival of about 90 % regardless of the metastatic status at the time of presentation [4, 34]. The majority of the cases belonging to this subgroup are known to have classic histology, with very few cases having LC/A variant.

About 90 % of the WNT subgroup medulloblastomas carry an activating mutation in the exon 3 of the gene *CTNNB1* encoding for β-catenin, the key regulator of the canonical WNT signaling pathway. Theses mutations render β-catenin phosphorylation resistance preventing it from proteasomal degradation. The stabilization of β-catenin leads to its accumulation inside the nucleus keeping the WNT signaling constitutively active. The activation of the WNT signaling pathway is evident from the higher expression of WNT signaling related genes like *WIF1*, *DKK1, LEF1, CCND1,* and *MYC* in this subgroup tumors [2, 9, 57]. Apart from *CTNNB1*, mutations in the genes encoding proteins of the destruction complex like *APC* [60] and *AXIN1* are also reported in a mutually exclusive manner in the WNT subgroup tumors [2, 60]. Recurrent alterations in *DDX3X* (36 %), *CSNK2B* (14 %), *TP53* (14 %), *ATM* (6 %) and epigenetic modifier genes *SMARCA4* (19 %), *KMT2D* (14 %), *PIK3CA* (11 %), *ARID1A* (8 %), *ARID2* (8 %) are also reported to occur in the WNT subgroup medulloblastomas [2]. The genome of the WNT subgroup

tumors is stable as compared to other subgroups with the monosomy of chromosome 6 (76-85 %) being the most common chromosomal level aberration in these tumors, which often co-occurs with the *CTNNB1* mutation [39, 55, 60].

A mouse model generated by Gibson *et al*. by expressing an activating mutant of the *CTNNB1* gene under the Blbp promoter in a p53 null background showed tumors, although at lower frequency of 15 % resembling the human WNT medulloblastomas. The tumors recapitulated the expression profiles and the anatomic location of the human WNT subgroup medulloblastomas. Interestingly, the activating mutations in the *CTNNB1* gene does not affect the proliferation of the cerebellar CGNPs, thus reducing their probability of being the cell of origin for the WNT subgroup tumors. Further, it was shown that the mossy fiber neuron precursors in the lower rhombic lip/dorsal brain stem could be the cell of origin for this subtype [61]. The human WNT subgroup tumors are located in the fourth ventricle infiltrating in the dorsal brain stem, whereas the SHH medulloblastomas are located well within the cerebellar hemispheres away from the brain stem [34, 61]. Thus consistent with the difference in the probable cells of origin, the anatomical locations of the WNT and SHH tumors was found to be distinct in the mouse models as well, indicating distinct cell of origin for these two medulloblastoma subgroups.

2.5.2. SHH subgroup

The SHH medulloblastomas constitute 28-30 % of all sporadic medulloblastomas and are characterized by the activation of the SHH signaling pathway. This subgroup has the bimodal distribution for the age of incidence where the incidence peaks at 2-3 years and 16-18 years of age. The subgroup shows marginally higher prevalence in males with the male to female ratio of 1.5:1. About 15-20 % of the cases are presented with metastasis at

diagnosis. The SHH subgroup has long-term survival of 60-70 %. Almost all histological variants are found within the SHH subgroup with classic histology in 40-45 %, desmoplastic nodular in 30-35 %, MBEN in 10 %, and LC/A in 15-20 % of the cases [2].

The majority of the SHH tumors harbor somatic mutation or copy number alteration in one of the genes of the SHH signaling pathway. Loss of function mutations or deletions in *PTCH1* or *SUFU* genes are found in about 43 % and 10 % patients, respectively whereas, activating mutations in the *SMO* gene are found in 9 % patients. Amplifications of *GLI1/GLI2* or *MYCN* gene are present in 9 % and 7 % SHH tumors, respectively [2]. The alterations in any of these genes bring about activation of the SHH signaling pathway in a ligand-independent manner leading to the increased expression of SHH target genes that drive cell growth and proliferation. Recurrent somatic copy number alterations (SCNAs) in the genes involved in the p53 pathway and receptor tyrosine kinase (RTK) signaling mediated by phosphatidylinositol-3-kinase (PI3K) pathways are also known to occur in the SHH subgroup medulloblastomas. The alterations in the p53 pathway include amplification of *MDM4* (9 %), *PPM1D* gene (8.3 %), and focal deletion of *TP53* gene (29 %). Amplifications of the IGF signaling genes viz. *IGF1R* (6 %), *IRS2* (9.4 %), *PIK3C2G* (2.6 %) and *PIK3C2B* (9 %), and deletion of PTEN (9.8 %) affecting RTK-PI3K pathway are also known to occur in SHH subgroup tumors [2, 60]. Apart from this, recurrent mutations in *DDX3X* (21 %), *KMT2D* (13 %), *CREBBP* (10 %), *TCF4* (8 %), *KMT2C* (7 %), *FBXW7* (7 %) and *BCOR* (5 %) are observed in SHH tumors. Mutations in the promoter of the gene encoding telomerase reverse transcriptase (*TERT*) are found in about 39 % of SHH tumors and are more common in this subgroup as compared to other subgroups. The most common chromosomal aberrations are loss of chromosome 9q and 10q chromosome

arms in 47 % and 26 % tumors, respectively leading to the loss of heterozygosity of the negative regulators of the SHH pathway *PTCH1* (9q22) and *SUFU* (10q24) [57, 58]. *TP53* mutation status has been recently included in the risk stratification criteria as SHH tumors with *TP53* loss of function mutations have poor prognosis [62].

Several mouse models of the SHH subgroup medulloblastomas have been developed. The homozygous germline deletion of *Ptch1* gene in mice is embryonic lethal. Heterozygous deletion of *Ptch1* leads to the development of cerebellar tumors resembling human SHH medulloblastomas by the age of 6 months in 15-20 % mice [48]. Furthermore, heterozygous deletion of *Ptch1* gene in *TP53* null background caused SHH like tumors at an incidence of 100 % by the latency of 3 months [63]. Several other models including constitutive expression of mutant *Smo* gene under the *NeuroD2* promoter [49], *Mycn* overexpression [64] and heterozygous *Sufu* deletion in p53 null background [65] also gave rise to spontaneous human SHH like medulloblastomas.. The extensive cellular and molecular characterization of the tumors from these mouse models identified cerebellar granule neuron progenitors (CGNPs) as the probable cell of origin for the SHH subgroup medulloblastomas [66, 67]. These models are still playing a crucial role in understanding the biology of SHH medulloblastomas and for the development of novel targeted treatment strategies.

2.5.3. Group 3

Group 3 medulloblastomas constitute 25-28 % of all medulloblastoma cases and are known to occur mostly in infants and younger children. Their occurrence in adolescents and adults is rare. Group 3 tumors predominantly occur in male children with the male:female ratio of 2:1. The majority of group 3 tumors have classic histology with few

having LC/A histology [2, 60]. The incidence of metastasis at diagnosis is 45 % which is highest among the four subgroups of medulloblastomas thus stratifying these tumors as high risk. Moreover, the disease recurs in most of the cases with metastatic dissemination with the primary location of the tumor remaining free of the disease [59]. Group 3 tumors are known to be frequently associated with multiple markers of poor outcome including a higher incidence of metastasis and amplification of the MYC oncogene. The subgroup has five-year overall survival rate of about 50 %, which is the worst among the medulloblastoma subgroups.

Group 3 and Group 4 medulloblastomas have overlapping gene expression profiles characterized by expression of transcription factors involved in brain development like *EOMES*, *FOXG1B, and* a testes specific gene *LEMD1*, [9, 57]. The Group 3 tumors are characterized by overexpression of transcription factors involved in retinal development, proliferation-related genes (*MYC*, *CCND2*), genes involved in ribosomal biosynthesis, RNA processing, nucleotide metabolism and several components of the TGFβ and NOTCH signaling pathway [4, 39, 56, 58, 68].

The recurrent single nucleotide variants (SNVs) are less common in Group 3 as compared to other subgroups. The genes commonly mutated include epigenetic modifiers like *SMARCA4* (9 %), *KMT2D* (5 %), and *KBTBD4* (6 %), a component of ubiquitin-proteasome system [39]. On the other hand, the chromosomal level aberrations are frequently detected in this subgroup indicating that the genome of Group 3 medulloblastomas is highly unstable. The frequent chromosomal alterations include gain of 1q (35 %), 7 (55 %), deletions of chromosome 11, 16q (50 %), isochromosome 17q (26 %), and 12q (17 %). Group 3 tumors often overexpress *MYC* oncogene with 17 % tumors

having amplification of the MYC locus. Amplification of the *MYCN* (2-4 %) and *OTX2* (3 %) loci are also found in Group 3 tumors in a mutually exclusive manner with that of the MYC oncogene [60]. Irrespective of the amplification status, *OTX2*, a gene encoding a pioneer transcription factor is highly expressed in Group 3 and Group 4 medulloblastomas. It has been shown to maintains medulloblastoma tumor cells in a stem and/or progenitor-like state by repressing neuronal differentiation and promoting cell-cycle [69-72]. The presence of isochromosome 17q and *MYC*/*OTX2* amplifications have been earlier associated with poor outcome in poor-risk childhood medulloblastomas [4, 73, 74]. Recently, other structural variants resulting fromrearrangement of far distant active enhancers/superenhancers to the proximity of the coding sequences (enhancer hijacking) are reported to occur in Group 3 and Group 4 medulloblastomas. About 15-20 % of Group 3 medulloblastomas express oncogenes *GFI1*/*GFI1B* due to enhancer hijacking in a mutually exclusive manner [39, 75]. Recurrent structural rearrangements generating *PVT1*-*MYC* fusions formed as a result of chromothripsis are seen in ~50 % of *MYC* amplified group 3 tumors. The region of the *PVT1* gene undergoing the amplification carries a cluster of four microRNAs which have been shown to enhance the MYC driven oncogenesis in this subgroup [60].

2.5.4. Group 4

Group 4 medulloblastomas make the largest subgroup of medulloblastoma accounting for 40-45 % of total cases of medulloblastomas. These tumors occur across all age groups with the peak incidence in the older children (median age of incidence- 9-10 years). Group 4 medulloblastomas occur 2.5-3 times more frequently in males than in females. Most tumors are presented with classic histology with few cases of LC/A histology. About 35-40 %

cases of Group 4 medulloblastomas are presented with metastasis at the time of diagnosis. Group 4 has a five-year overall survival of 60-70 %.

Gene expression profiling studies have shown an enrichment of genes involved in neuronal differentiation (*UNC5D*, *KCNA1*) and glutamatergic signaling (*GRM8*) [4, 9] in these tumors. Similar to Group 3 medulloblastomas, SNVs are rare in Group 4 medulloblastoma with no single gene mutation existing in more than 10 % cases [39]. Of note, the mutations in the epigenetic modifier genes are prevalent in this subgroup suggesting the critical role of epigenetic mechanisms in the biology of Group 4 tumors. Mutations in the epigenetic modifier gene *KDM6A* (9 %*)*), *KMT2C* (6 %), and *ZMYM3* (6 %) are reported in Group 4 tumors [2, 60]. Chromosome level aberrations are common in Group 4 medulloblastomas which include gains of chromosome 7 (40-50 %) and 17q (80 %) and deletions of chromosomes 8 (40-50 %), 11 (30 %) and 17p (75 Amplification of *MYCN* (6 %), *CDK6* (6 %), and *OTX2* (6 %) are also reported in Group 4 tumors. Cyclin-dependent kinase 6 (*CDK6*) is an important regulator of cell cycle governing the G1-S transition along with the kinase *CDK4*. Abrogation of *CDK4*/*CDK6* function using small molecule inhibitors has shown encouraging results in preclinical studies. The *CDK4*/*CDK6* inhibitors are in clinical trials of patients with relapsed medulloblastomas [76, 77]. The enhancer-hijacking mediated overexpression of *GFI1*/*GFI1B* is reported to occurin 5-10 % of Group 4 tumors [60]. Recently, the whole genome sequencing study identified a tandem duplication of *SNCAIP*, a gene associated with the Parkinson's disease and neurodegeneration in these tumors. *SNCAIP* is among the most highly expressed genes in group 4 medulloblastomas, however, its role in the pathogenesis remains to be understood [60].

The integrated analysis of genome-wide methylation, expression profiles, and SCNAs have shown the exsistence of multiple subtypes within Group 3/Group 4 subgroups that are characterized by subtype specific driver genetic alterations and copy number variations [39, 78, 79]. A meta-analysis of the three studies have came to the consensus of eight subtypes of Group 3/Group 4 medulloblastomas with some subtypes consisting of both Group 3 and Group 4 tumors, indicating a broad continuum of the subtypes. Subtypes II, III, and V often harbor amplifications of the *MYC* and *MYC*/*MYCN* gene, respectively and have the worst five-year overall survival [80].

Table 2.1: The salient features of the four molecular subgroups of medulloblastomas.

Subgroup	WNT	SHH	Group 3	Group 4
Incidence	10 %	28-30 %	25-28 %	40-45%
Age of incidence	Older children, adults	Infants, children, adults	Infants, younger children	Older children, adults
Histology	Classic, rarely LC/A	Classic, rarely LC/A	Classic, LC/A	Cassic, rarely LC/A
Anatomic location	Central, frequently near the brainstem	Cerebellar hemisphere, rarely in midline vermis	Midline (filling fourth ventricle), rarely hemispheric	Midline (filling fourth ventricle)
Potential cell of origin	Progenitors in the lower rhombic lip/ dorsal midbrain	Cerebellar granule neural progenitors in the EGL	CGNPs in the cerebellar analage arising from upper rhombic lip (prominin	Not defined

			1+/lineage–neural stem cells)	
Metastatic disease at diagnosis	10 %	18-20 %	35-40 %	40-45 %
Male:female ratio	1:1	1-1.2:1	2:1	2.3-3:1
Five-year overall survival	~90 %	~60-70 %	~60-70 %	~50 %
Expression signature	WNT signaling	SHH signaling	Retina-specific genes, MYC	Neuronal differentiation, glutamatergic neuronal genes
Chromosomal aberrations (Gain +, Loss -)		3q+, 9p+	1q+, 7+, 17q+, 18+	4+, 7+, 17q+, 18+
	6-	9q-, 10q-, 14q-, 17p-	8-, 10q-, 11-, 16q-, 17p-	8-, 10-, 11-, 17p-, X-
Gene mutations	*CTNNB1*, *DDX3X*, *SMARCA4*, *MLL2*, *TP53*	*PTCH1*, SUFU, *TP53*, *MLL2*, *DDX3X*, *BCOR*	*SMARCA4*, *CTDNEP1*, *MLL2*	*KDM6A*, *KMT2C*, *ZMYM3*, *KDM1A*, *KDM4C*
Focal amplification		*MYCN*, *GLI2*	*MYC*, *MYCN*, *AVCRA1*, *AVCRA2*	*MYCN*, *OTX2*, *CDK6*
Gene fusion			*MYC-PVT1*, *MYC-NDRG1*	
Rearrangement (enhancer hijacking)			*GFI1*/*GFI1B*	*GFI1*/*GFI1B* and *SNCAIP-PRDM6*

2.6. Role of MYC family transcription factors in medulloblastoma

The MYC oncogene, was first identified upon as a homolog of the viral oncogene carried by the avian acute leukemia virus MC29 in myelocytomatosis. The MYC family of transcription factors consists of *MYC*, *MYCN,* and *MYCL* [81]. The overexpression of these transcription factors is associated with more than 50 % cancers and is an indicator of aggressive phenotype with poor outcome [82]. The MYC transcription factors contain a basic-helix-loop-helix (bHLH) motif, which allows the DNA binding to E-box sequences, whereas the leucine zipper structural motif allows the heterodimerization with MAX [83]. The expression of *MYC* transcription factors is upregulated upon various mitogenic signals including growth factor signaling and activation of WNT, SHH or EGF signaling via mitogen activated protein kinase (MAPK)/ERK pathway [84]. The activation of MYC transcription factors drives various cellular processes like cell proliferation, cell growth, apoptosis, stem cell renewal, differentiation via upregulation of its target genes.The targets of *MYC* includes genes involved in cell cycle regulation, nucleotide metabolism, ribosome biogenesis, and cellular metabolism [84-86]. Apart from this, the cells having high *MYC* overexpression show higher occupancy of MYC at the promoter regions of actively transcribed genes leading to their transcriptional amplification [85].

Deregulation of *MYC* family transcription factors has been well established in medulloblastomas by several expression profiling studies [4, 56, 58, 60, 78]. The amplification of the MYC transcription factors are one of the prevalent amplified loci in medulloblastoma genomes [60]. *MYC* is known to be overexpressed in the WNT subgroup as a result of constitutively active WNT signaling. The *MYCN* and *MYCL1* are also moderately overexpressed in the WNT subgroup as compared to Group 3 and Group 4

tumors [87]. The activation of the SHH signaling in CGNPs is known to upregulate the expression of *MYCN* [88]. Furthermore, the constitutive activation of SHH signaling by expression of mutant *PTCH1* gene in CGNPs has been shown to promote MYCN protein stabilization [88, 89]. The expression profiling studies have identified higher expression of *MYCN* and *MYCL1* in SHH subgroup medulloblastomas as compared to other subgroups [60, 87]. Moreover, *MYCN* and *MYCL1* amplifications are found in 8 % and 2-4 % SHH medulloblastomas, respectively in a mutually exclusive manner with *MYCN* amplification acting as an indicator of poor prognosis [34, 60]. The enforced expression of MYCN in CGNPs collaborates with the heterozygous deletion of *Ptch1* or with loss of *Tp53* and Cdkn2c and gives rise to aggressive, invasive, and resistant human SHH like tumors with an increased penetrance in mouse models [63, 64, 90, 91]. Thus, *MYCN* overexpression plays an important role in the induction and maintenance of SHH tumors.

MYC is overexpressed in Group 3 medulloblastomas as compared to SHH and Group 4 tumors, whereas the expression is comparable to that found in WNT subgroup medulloblastomas [60]. *MYC* amplifications occur frequently (10-17 %) in this subgroup with 2-4 % tumors harboring *MYCN* amplification [60]. These amplifications occur in a mutually exclusive manner in Group 3 medulloblastomas suggesting their overlapping function in the biology of this subgroup. Two different mouse models have been described for the Group 3 medulloblastomas. The first model was generated by overexpression of *MYC* oncogene in CGNPs obtained from the p53 null mice [92] whereas the second model was established by concurrent expression of stable (phosphorylation resistant, T58A) form of *MYC* oncogene and dominant-negative p53 in *CD133*/prominin-1 positive neural stem cells of the cerebellum [93]. The orthotropic implantation of these cells in the cerebellum

of mice gave rise to the tumors that transcriptionally resembled the Group 3 medulloblastomas. Furthermore, the Cre-mediated withdrawal of the expression of *MYC* oncogene resulted in complete regression of the tumors [93] indicating the essential role of *MYC* in the initiation and maintenance of the tumors [94]. Interestingly, the mouse models of Group 3 medulloblastomas are based on the loss of function of tumor suppressor p53, yet the *TP53* somatic mutations are majorly restricted to the WNT (16 %) and SHH (21 %) medulloblastomas [95]. The expression profiling analysis has shown significant enrichment of *MYC* expression in the *GF1*/*GFI1B* activated tumors as compared to Group 3 tumors lacking *GFI* activation. Significant enrichment of MYC target genes in the *GFI*-activated Group 3 medulloblastomas is also reported. Furthermore, activation of *GFI* oncogenes and *MYC* amplifications were found to co-occur in several Group 3 tumors suggesting that *GFI*-activation and *MYC* expression may collaborate in the tumorigenesis of Group 3 tumors. Indeed the co-expression of either of the *GFI* genes with *MYC* in the neural stem cells resulted in the generation of Group 3 like tumors whereas expression of *GFI* genes alone was insufficient for tumorigenesis [75].

Group 4 medulloblastomas are known to have lower expression *MYC* an *MYCN* as compared to other medulloblastoma subgroups, however the expression levels are higher than those in the normal adult cerebellum and are comparable to that found in the embryonic cerebellum [96]. There are no definitive mouse models for group 4 medulloblastomas. One of the described model is based on the enforced expression of stable phosphorylation resistant MYCN in the neural stem cells from postnatal day 1 through adulthood, which results in the development of Group 4 like tumors [68]. Intriguingly Group 4 medulloblastomas also prevalently occur in older children. This is

consistent with the mouse model as Group 4 like tumors arise in the neural cells after conditional expression of stable *MYCN* in post-natal cerebellum. This observation indicates that there may be finite duration during which a specific population of cells within the cerebellum are vulnerable for Group 4 related tumorigenesis.

2.7. MicroRNA: Small molecules with a big impact

MicroRNAs are endogenous, evolutionarily conserved small non-coding RNAs of about 20-22 bp in length and are known to regulate gene expression at the post-transcriptional level in metazoan eukaryotes. These small RNA molecules function by directly interacting with complementary binding sequences in the target messenger RNA (mRNA) thereby hindering the translation or leading to the mRNA destabilization [5, 6]. Computational and bioinformatic analysis has revealed that one miRNA can target several genes, and about 50 % of protein-coding genes are regulated by microRNAs [97]. MicroRNAs are known to regulate vital cellular processes including proliferation, growth, apoptosis, and differentiation [5, 6, 98, 99]. MicroRNAs are known to be deregulated in various cancers and play a crucial role in their pathogenesis [99, 100].

2.7.1. Regulation of microRNA expression

MicroRNAs are either known to exist as discrete genes (intergenic microRNAs) or they lie within the intronic regions of the protein-coding host genes (intragenic/intronic microRNAs) [5]. The microarray profiling of microRNAs and whole-genome sequencing studies have shown that microRNA genes are dispersed over the entire genome, and those that are located in clusters are often coexpressed as polycistronic units that may have

similar functions [101]. The regulation of expression of these small non-coding however remains less understood. Recently, the understanding of the basic gene regulation mechanism and the epigenome profiling have greatly helped in understanding the transcriptional regulation of microRNA genes. The chromatin immunoprecipitation-sequencing (CHIP-seq) of the RNA-Polymerse II (RNA Pol II), other transcription factors and the epigenetic marks H3K27Ac, H3K9Ac, H3K4me3, the markers present at the actively transcribed loci have further aided in marking the usptream regulatory regions of the microRNA genes [102, 103]. Various studies have shown that majority of microRNAs are transcribed in RNA pol II dependent transcription where long transcripts are generated which are subsequently capped, spliced and polyadenylated [5, 103]. A small proportion of microRNAs are also transcribed by RNA pol III especially those located in the regions of genome enriched with the Alu repeats [104]. The microRNAs within the polycistronic microRNA clusters are usually expressed through a single regulatory element whereas the intronic microRNAs either gets expressed using the promoters of the host genes or some of them have their own regulatory elements which are atypical in nature. Employing the recently developed techniques like expressed sequence tag analysis, capped analysis of gene expression (CAGE) and analysis of DNAse I sensitive regions have further helped in identifying the transcription start sites (TSS) and upstream regulatory sequences of the microRNA genes [105-107]. About 45 % of microRNAs are derived from ncRNA transcripts, while the rest are transcribed from protein-coding loci [108]. Recently, various studies have been conducted using the various experimental and bioinformatics approaches including the above mentioned techniques to accurately predict the TSS for microRNAs. The findings of these studies are publically available as the databases [105-107].

Epigenetic regulation of the microRNA expression have also been demonstrated especially in the diseased states including cancers. The presence of CpG islands at the genomic loci of more than half of the total number of miRNAs suggests the involvement of DNA methylation as one of the mechanisms governing transcriptional regulation of the microRNAs [109]. The first evidence of an involvement of epigenetic regulation of microRNAs in cancer was presented from the study of Saito and colleagues which included the analysis microRNA expression profiles of bladder cancer cells treated with DNMT inhibitor 5-Aza-2‟-deoxycytidine (5‟-Aza-CdR) and HDAC inhibitor 4-Phenyl-butyric acid (4-PBA). In this study, miR-127 and miR-34 family of microRNAs were the miRNAs whose expression was linked to first for which aberrant DNA methylation and histone deacetylation at their promoters [110]. CpG DNA methylation and histone modification are known to be interlinked to each other, where presence of DNA methylation can target repressive histone modifications, which in turn further enhances DNA methylation at that locus [111]. The tissue specific regulation of microRNA expression is suggested to be governed by histone modifications [112].

2.7.2. Biogenesis of microRNAs and their gene silencing mechanism

The microRNA biogenesis starts with the RNA polymerase II/polymerase III dependent transcription of microRNAs or intron splicing in case of intragenic microRNAs leading to the formation of a primary microRNA (pri-miR), a hairpin containing primary transcript with single stranded extensions at both the ends [5, 113]. If the pri-miR is transcribed from a ploycistronic locus, the pri-miR consists of multiple hairpin structures of 60-80 bp length interspersed by the length of sequences necessary for the processing of individual hairpin by the microprocessor complex [114, 115]. Inside the nucleus, the pri-miR is further

processed by multi-protein complex called as the microprocessor. The microprocessor consists of the two major components which are Drosha (RNASEN in humans), an RNAse III family protein and its associate protein Pasha (DGCR8 in humans) [116]. The pri-miR is cleaved by the microprocessor complex at an approximate distance of one helical turn from the hairpin base or two helical turns from the terminal loop to generate a hairpin structure having imperfect complementarity called as pre-microRNA (pre-miR) [117]. The pre-miR is further exported outside of the nucleus by an Exportin 5 (XPO5) / RAN GTP complex [118]. Once in the cytoplasm, the pre-miR is recognized and processed by another RNAse III family protein Dicer in conjunction with a RNA binding protein TRBP. As a result of the cleavage of the terminal-loop, a small RNA duplex of 20-22 bp with overhangs on both the ends is generated [119]. Most of the times, one of the strands (guide strand) of the small RNA duplex gets incorporated into the microRNA induced silencing complex (miRISC) majorly formed by the Argonaut family proteins [120, 121]. The other strand called as the passenger strand is released and further degraded. However, in some cases, the passenger strand can also be loaded in the miRISC and functions as the mature miRNA [5]. The microRNAs are designated as -3p or -5p depending upon which arm of the small miRNA duplex gets incorporated in the miRISC, the exact mechanism of the strand selection however remains unknown [122].

Upon formation of the miRISC, it recognizes complementary binding sequences in the target mRNA molecules. The extent of the complementary binding of the microRNA seed sequence with the MRE dictates if there is translational repression or mRNA degradation. A perfect complementarity of the microRNA to the mRNA induces the AGO2 mediated endonucleolytic cleavage of the mRNA leading to its destabilization [123]. In case of

imperfect complementary, the microRNA in the miRISC interacts with the target gene through the seed sequence and leads to the translational repression. The binding of the miRISC to the target mRNA mediates the recruitment of the GW182 family protein which in turn provides a scaffold for the binding of the effector proteins like the poly(A-deadenylase complexes PAN2-PAN3 and CCR4-NOT [124]. The deadenylation makes the mRNA susceptible for the exonucleolytic degradation and also causes decapping of the mRNA inhibiting its translation.

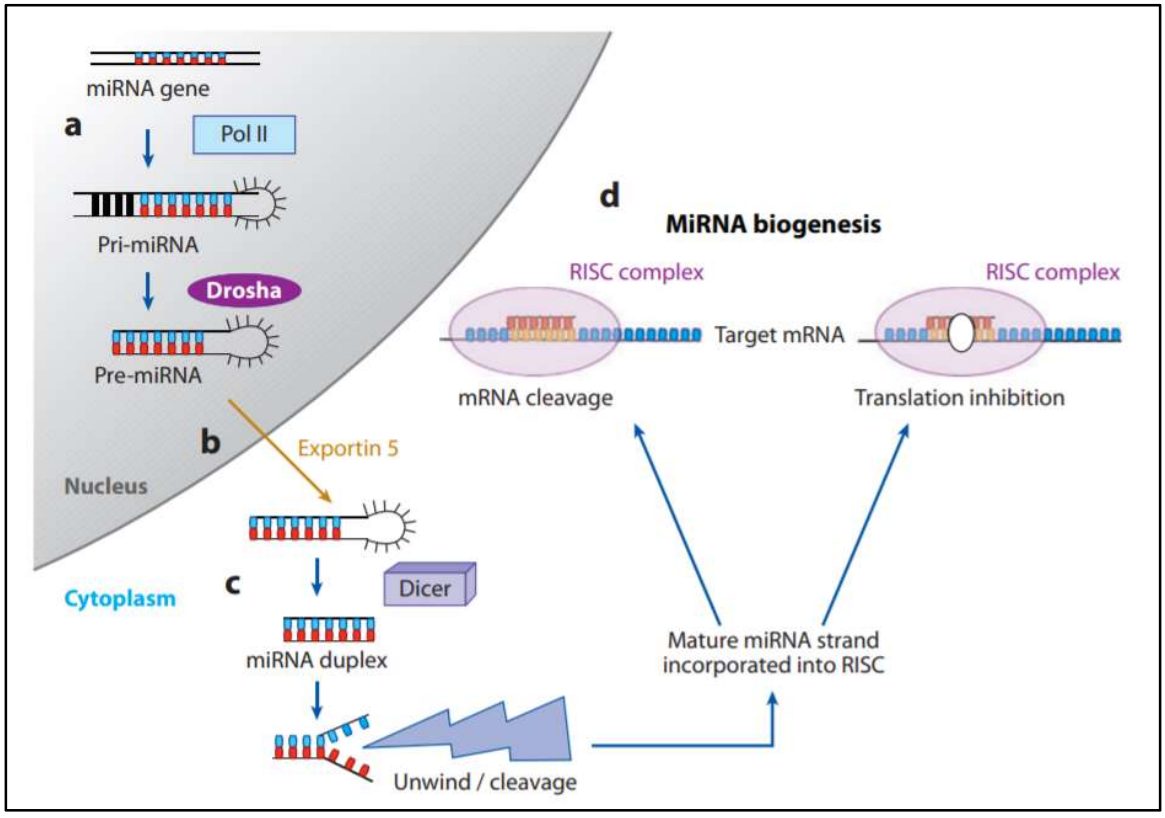

Fig 2.3: MicroRNA biogenesis and mechanism of action.

a) RNA pol II dependent transcription of microRNA to from pri-miRNA. b) Clevage of pri-miRNA by Drosha to form pre-miRNA and its export outside the nucleus. c) Processing by Dicer to form microRNA duplex. d) Formation of miRISC and bind of the miRISC to the target mRNA (Figure adopted from Garzon, R. et al. 2009, 2014) [7, 8].

2.7.3. Identification of microRNA target genes

The discovery of thousands of microRNAs in variety of organisms have driven the researchers to scrutinize the functional role of microRNAs. The key answers to these question were presented by the discoveries about the mechanism of microRNA action and the development novel of methods for the identification of microRNA targets. The initial idea for the microRNA target recognition came from the finding that lin-4 microRNA targets lin-14 mRNA by binding at multiple complementary sequences within the lin-14 mRNA [125]. The microRNAs bind the target mRNA to a motif called microRNA response element (MRE) through a seed sequences usually located between nucleotides 2-8 of the mature microRNA [6]. The microRNA binding sites were initially thought to be present in the 3'UTR of the mRNA targets, however, recent studies have shown the presence of the microRNA binding sites located outside the 3'UTR region and even the lack of pairing of the seed sequence compensated by center pairing or 3' complementarity may still enable microRNA regulatory function [126, 127].

Since the discovery of microRNAs, several bioinformatic approaches have been developed for microRNA target identification. These approaches are based on observations like seed complementarity to the target and the evolutionary conserved nature of the seed sequence which improves the prediction specificity, and the site context which considers the type of site (8-mer, 7-mer m8, 7 mer A1, 6 mer), the position of the site within the mRNA and the accessibility of the site due to the presence of secondary sturctures [6, 128]. As far, computational and bioinformatic analysis has revealed that one miRNA can target several genes and about 50 % of protein coding genes are regulated by microRNAs [97]. The bioinformatic prediction although ensued thousands of targets for microRNA, however,

included high number of false-positives and negatives [129]. Several computational target prediction programs namely TargetScan (v6), Pictar, RNA22, miRanda, DIANA-microT, microInspector and RNAhybrid are recently developed considering the above mentioned criteria's and are helpful in atleast in part prediction of microRNA target genes. Considering the underlying complexity and difficulty in specific and accurate identification of microRNA targets, a wide variety of experimental methods have recently been developed which includes gene expression profiling, polysome profiling (ribosome profiling), proteomic profiling after enforced expression or by antagonizing the microRNA function in cells, pull-down of members of RISC and tagged microRNA pull-down [6, 130, 131]. The target prediction is usually followed by the experimental validation of the microRNA targets by luciferase reporter assay, real-time RT-PCR assay, and western blotting [130].

2.7.4. Role of microRNAs in cancer

Extensive research has taken place in unraveling the functional role of microRNAs in the various aspects of biology. Given their overwhelming impact on the gene expression, it is not surprising that they play a pivotal role in the diseased states, including cancer. Numerous microRNA profiling studies have been conducted over the past decade for the quantitative and qualitative assessment of micorRNA expression in normal tissues and cancers. These studies have shown remarkable changes in miRNA expression profiles in cancers. MicroRNAs are thought to have an instrumental role in cancer pathogenesis owing to the two significant observations a) microRNA genes coincide with fragile sites and hot spots that are found to be frequently deleted in cancers which correlate with tumorigenesis

and b) the expression of microRNAs was frequently observed to be deregulated in various types of cancers [7, 100, 132].

The first report portraying the role of miRNAs in human cancers was presented in the study on chronic lymphocytic leukemia (CLL). In this study, it was shown that a 30 kb region at the chromosome 13q14 was often deleted in CLL. The detailed analysis of this region has demonstrated the presence of two clustered microRNAs, miR-15a and miR-16-1 in this region. Subsequently, frequent deletion or downregulation of these miRNAs was detected in greater than 60 % of CLL cases [133]. Later, it was shown that miR-15a and miR-16-1 function as tumor suppressors, and their expression have an inverse correlation with the expression of an anti-apoptotic gene *BCL2* [134]. Let-7, a microRNA downregulated in lung cancer, has been reported to target the proto-oncogene *RAS* [135]. MiR-34, another microRNA deregulated in non-small cell lung cancer been reported to act as a tumor suppressor by targeting *MYC*, *MET* and *HMGA2* [136, 137]. Moreover, recent studies have identified a number of microRNAs downregulated in a variety of cancers playing a tumor-suppressive function by regulating the expression of oncogenes.

In contrast to this, there are few microRNAs that are known to act as oncogenes. MiR-21 was the first miRNA to be coined an oncomiR due to the universal overexpression of this miRNA in several cancers, including AML, CLL, breast cancer, glioblastoma, and medulloblastoma, with PTEN and PDCD4 identified as its targets [7, 8]. MiR-155 is one of the well-characterized oncogenic microRNAs that is overexpressed in several malignancies like breast cancer, lung cancer, CLL, and diffuse large B-cell lymphoma (DLBCL) [138-140]. MiR-17 / 92 polycistron, also known as oncomiR-1 has also been found to play an oncogenic role in several tumor types including medulloblastoma [7, 141,

142]. Indeed, the oncomiR addicted tumors are utterly reliant upon the oncomiRs and are vulnerable to their loss showing rapid tumor regression upon the abrogation/removal of oncomiR. This is best exemplified by the observation that overexpression of miR-155 in B-cells leads to the formation of very aggressive DLBCLs and the depletion of miR-155 results in rapid tumor regression [143].

Various transgenic mouse models have been described in the literature, which experimentally demonstrated the causative roles of many microRNAs deregulated in cancer. Transgenic mice overexpressing miR-155 in early B-cells have exhibited a pre-leukemic expansion of the pre-B-cell population, ultimately resulting in full-blown B cell tumors [138, 139, 143]. In another study, the conditional expression of miR-21in K-ras^{LA2} model of lung cancer resulted in increase in number of lesions whereas, the knockout of miR-21 in the same model caused delayed tumorigenesis with relatively less number of tumor nodules [144]. In a transgenic model having the conditional expression of miR-21 at ROSA26A locus, the development of pre-B malignant lymphoid-like phenotype was observed, thus demonstrating its oncogenic potential. Similar to the miR-155 model, the tumors were oncomiR addicted, and removal of miR-21 led to rapid tumor regression [145]. MiR-17-92 polycistron was found to be overexpressed in B-cell lymphomas. The retrovirus-mediated enforced expression of the miR-17/92 cluster in the Eμ-Myc model of B-cell lymphoma shows accelerated lymphoma formation in collaboration with MYC [146]. All these evidence clearly suggested that the deregulation of a single miRNA can potentially lead to malignancy and highlights the significance of microRNAs in cancer biology.

Since the cellular transformation is usually associated with the deregulated microRNA expression, the profiling of microRNA expression can be an essential tool for diagnostics, prognostics, and treatment of disease. Apart from the tumor milieu, aberrant levels of microRNAs can also be detected in the body fluids. The profiling of the microRNAs from the body fluids can thus be an efficient non-invasive way for the early detection, staging, prognosis of the disease, and the treatement response [147].

2.7.5. The role of microRNAs in medulloblastoma biology

In the past decade, several studies have spotted the role of microRNAs in medulloblastoma biology. The first report of deregulation of microRNA in medulloblasstoma showed that miR-124 a brain enriched microRNA, is downregulated in medulloblastomas and its overexpression in medulloblastoma cells decreases cell growth by directly targeting *CDK6*, a marker of poor prognosis in medulloblastomas [148]. Later on, it was shown that miR-124 regulates glycolysis by modulating the expression of a solute carrier protein *SLC16A1* further answering the growth inhibition of medulloblastoma cells upon miR-124 expreesion [149]. Both these studies indicated the tumor-suppressive role of miR-124 in medulloblastomas. In the same year, the first microRNA profiling study for medulloblastomas was reported by Ferretti et al. The study included the profiling 248 human microRNAs in the cohort of 14 primary medulloblastomas using Taqman real-time PCR based assay. Specific expression patterns of microRNAs that differentiate medulloblastomas with respect to their histology, molecular characteristics like *ErbB2* or *MYC* expression and prognosis were identified in this study. Of the 86 microRNAs selected for analysis based on their native expression in neuronal cell types or previous association with cancers, the majority of them were found to be downregulated in medulloblastomas,

indicating their tumor-suppressive roles. Expression of only four miRNAs (miR-19a, miR-191 miR-106b, and miR-let7g) was sufficient to distinguish the histological variants of medulloblastomas. The *ErbB2* overexpressing tumors were found to have expression of six microRNAs (miR-10b, miR-135a, miR-135b, miR-125b, miR-153, miR-199b), whereas *MYC* overexpressing tumors have high expression of miR-181b, miR-128a, and miR-128b. Higher expression miR-31 and miR-153 was identified as an indicator of poor prognosis. MiR-9 and miR-125a were among the downregulated microRNAs, and their enforced expression in medulloblastomas cells inhibited growth and induced apoptosis by targeting a pro-proliferative truncated form of neurotrophin receptor *TrKc* [150].

The MicroRNA expression profiling of 19 medulloblastoma tumor tissues was also carried out in our lab using the Taqman Low-density Arrays v1.0, having a panel of 365 unique microRNAs. Out of the 365 microRNAs studied, 216 microRNAs were differentially expressed among the four subgroups of medulloblastomas. The unsupervised hierarchical clustering of the differentially expressed microRNAs could classify medulloblastomas into the subgroups similar to those based on gene expression data. WNT subgroup medulloblastomas have the most distinctive microRNA profile with overexpression of 16 microRNAs. These microRNAs have 3-100 fold higher expression as compared to their expression in other subtypes and normal cerebellar tissues and include microRNAs like miR-193a, miR-204, miR-148a, miR-365, miR-135a, miR-335, and miR-328, miR-146b, miR-224/miR-452 cluster, miR-182/miR-183/miR-96 cluster, miR-23b/miR-24/miR-27b cluster, miR-449/miR-449b cluster. MiR224/miR-452 cluster is an intragenic cluster located within the intron of the *GABRE* gene whose expression is high in the WNT subgroup tumors indicating that this cluster is co-expressed along with the *GABRE* gene.

The SHH signaling associated tumors have high expression of miR-199a, miR-92 and miR-565, whereas miR-135b, miR-204, and miR-153 were found to be downregulated in these tumors. Expression of miR-135b was found to be high in Group 3 and Group 4 tumors and was found to correlate with the higher expression of its host gene *LEMD1* in these subgroups. Another microRNA mir-204, was found to be significantly downregulated in almost all SHH tumors and a majority of Group 3 tumors and downregulation correlated with lower expression of its host gene *TRPM3* in these subgroups. Group 4 meulloblastomas had higher expression of miR-204, and a let family microRNA let-7c. Expression of polycistron miR17/92 cluster was found to be upregulated in WNT, SHH, and Group 3 tumors and was consistent with its regulation by *MYC*, *MYCN* and *E2F* family of transcription factors [9]. Based on the differential expression of protein-coding genes and microRNAs, a 21 marker real time-RT PCR assay was developed that included nine miRNAs and 12 genes. This assay could classify medulloblastomas into four subgroups with 97 % accuracy. This study highlighted the robustness of the use of miRNAs as markers for molecular classification of medulloblastomas, especially for classification of archived formalin-fixed paraffin-embedded (FFPE)tissues as miRNAs being very small in size are less susceptible to degradation during formalin fixation [151].

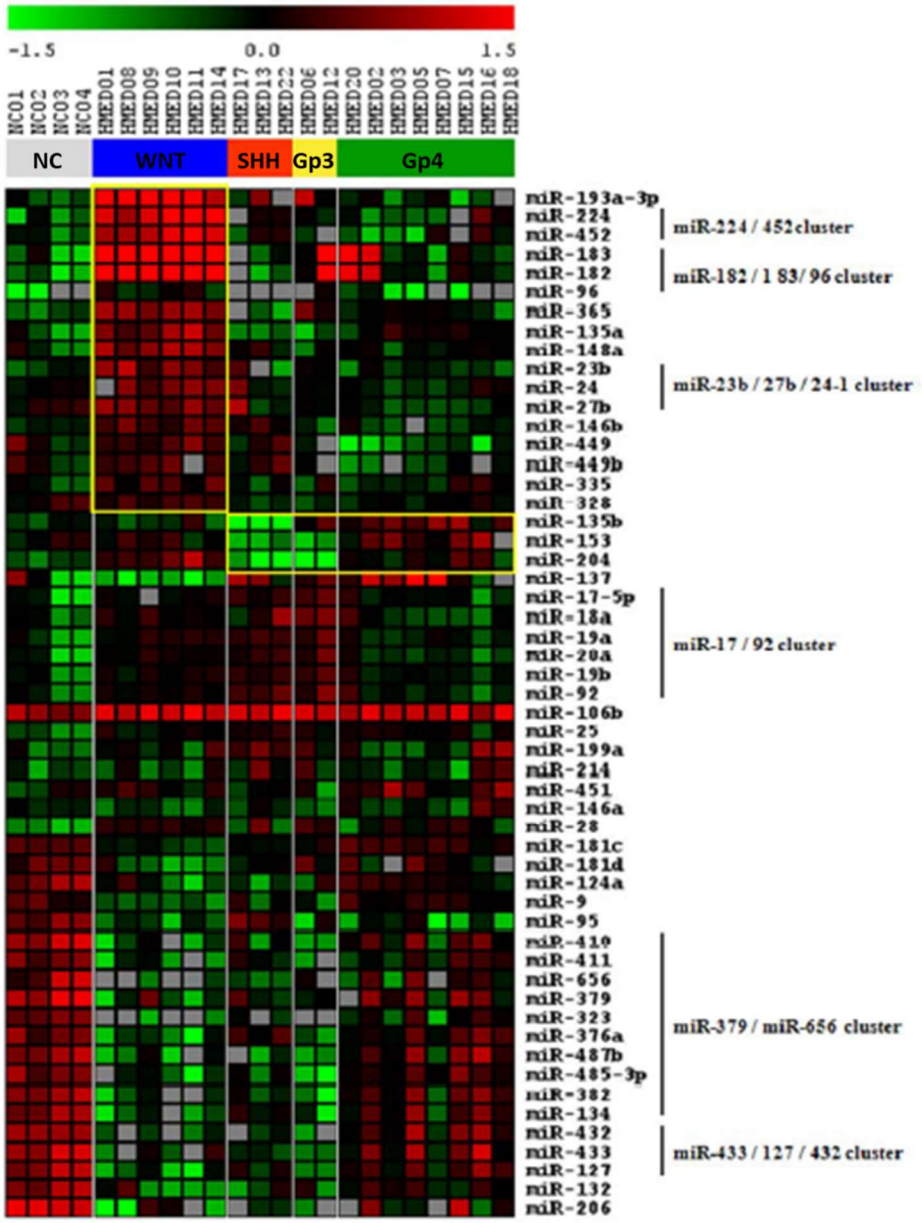

Fig 2.4: Heat map representing differential expression of miRNAs in four molecular subgroups of medulloblastoma and normal cerebellar tissues

Grey: normal cerebellum, blue: WNT, red: SHH, yellow: Group 3 and green: Group 4 [9].

The miR-17/92 is also known to be aberrantly expressed in various malignancies and was shown to play an oncogenic role [152]. It is also one of the well-characterized oncogenic microRNA cluster in medulloblastomas. The polycistron was found to be amplified in 6 % of medulloblastomas with the highest expression in the SHH signaling associated medulloblastomas. It was frequently upregulted in tumors having elevated levels of *NMYC*/*MYC*. Its expression was found to be induced by SHH ligand treatment to CGNPs. The enforced expression of miR-17/92 cluster in CGNPs collaborated with SHH ligand treatment to induce proliferation and also enabled the CGNPs to multiply in the absence of SHH [142]. The silencing of miR-17/92 cluster using locked nucleic acid, LNA targeting miR-17 and miR-19 inhibited cell growth *in vitro* an progression of the allograft tumors derieved from spontaneous models of medulloblatomas *in vivo*, indicating the oncogenic role of these microRNAs in medulloblastomas [141]. MiR-1204 is one of the microRNAs located at the *PVT1* locus and is found to be frequently upregulated in Group 3 medulloblastomas as a result of *PVT1-MYC* fusion. The upstream region of *PVTI* has two E-box sequences resulting in MYC mediated expression of the MYC and miR-1204. Inhibition of miR-1204 using the LNA based approach led to the proliferation inhibition of medullobastoma cells having *PVT1-MYC* fusion. Interestingly, cell lines without *PVT1-MYC* fusion were neutral to the effect of the miR-1204 inhibition. Thus, miR-1204 regulated by the positive feedforward loop of *PVT1-MYC* fusion seems to play an oncogenic role in Group 3 medulloblastomas [2, 60].

Previously in our lab, it was shown that exogenous expression of miR-193a and miR-224 by transfection of synthetic microRNA mimics in Daoy medulloblastoma cells inhibited proliferation, anchorage-independent growth and increased the radiation sensitivity of

Daoy cells [9]. Stable expression of WNT subgroup enriched microRNA miR-148a in medulloblastoma cells inhibited their tumorigenicity and invasion potential by directly targeting NRP1 [153]. Exogenous expression of miR-30a, a microRNA downregulated in all four subgroups, decreased proliferation, anchorage-independent growth, and tumorigenic potential of medulloblastoma cells, which was accompanied by inhibition of autophagy [154]. MiR-206, a cerebellum enriched microRNA was observed to be downregulated across medulloblastoma subgroups and its overexpression inhibited medulloblastoma cell growth and anchorage independence by directly targeting *OTX2* [155]. Expression of miR-204 is high in all the WNT subgroup tumors. Almost all SHH subgroup, 60 % Group 3 and 15 % Group 4 medulloblastomas have low miR-204 expression as compared to the normal cerebellar tissues. Expression of miR-204 was found to correlate with overall survival in the Group 3/Group 4 medulloblastomas where lower expression levels of miR-204 identified a highly aggressive subset of these tumors. Restoration of miR-204 expression inhibited the anchorage-independent growth and invasion potential of medulloblastoma cells. The expression of miR-204 was further found to inhibit autophagy in medulloblastoma cells (Ph.D. Thesis-Raikamal Paul) [11]. Blockade of autophagy by knockdown of *ATG5*, a key regulator of autophagy, resulted in decreased invasion potential but did not affect the proliferation and anchorage-independent growth of medulloblastoma cells [156]. Thus, the miR-204 expression seems to reduce the invasion potential of medulloblastoma cells by inhibiting autophagy in medulloblastoma cells.

Various studies depicting the role of microRNAs in the pathogenesis of medulloblastomas have been published in the past decade [157-159]. All these studies indicate the critical role

microRNAs in medulloblastoma biology and demands for the detailed investigation to identify the function of various deregulated microRNAs in medulloblastomas and for the further development of the microRNA based diagnostics and therapeutics.

Chapter 3

3. Materials and Methods

3.1. Materials

The following reagents were obtained from Applied Biosystems, Life technologies, Carlsbad, CA, USA: 2X TaqMan Universal PCR Master Mix (Cat No. 4304437); 2X Power SYBR Green PCR Master Mix (Cat No. 4367659), TaqMan MicroRNA Asays (Cat No. 4427975) - Assay IDs for each miRNA assays are: hsa-miR-193a (000492), hsa- has-miR-204 (000508), and RNU48 (001006); MicroAmp optical 384-well Reaction Plate with Barcode (Cat No. 4309849) and MicroAmp Optical Adhesive Film Kit (Cat No.4313663).

The following reagents were obtained from Invitrogen, Life technologies, Carlsbad, CA, USA: MMLV-RT 200 U/ul, Dulbecco's modified Eagle medium, DMEM/ Nutrient mixture F12, DNAse I, amplification grade, Fetal bovine serum, LMP (low melting point) agarose, Trypsin, L-Glutamine, Formamide, etc.

The following molecular biology grade/cell culture grade chemicals and reagents were obtained from Sigma-Aldrich, St Louis, MO, USA: Agarose, Proteinase K, Guanidium Isothiocyanate (GITC), Diethyl pyrocarbonate (DEPC), DMSO, EDTA, Ethidium bromide, BES, Puromycin, 5-Aza-2'-deoxyctidine, Trichostatin A, Ammonium persulphate, Tris base, Sodium dodecyl sulphate, Sodium chloride, Potassium chloride, Calcium chloride, Sodium hydrogen carbonate, Manganese chloride, N-Lauryl sarcosine, Glucose, etc.

The following chemicals were obtained from Amersham Lifesciences, GE Healthcare Life Sciences, Pittsburgh, PA, USA: Deoxynucleotide triphosphate set containing dATP, dGTP, dTTP, dCTP (100 mM each) (Cat. No.27-2035-01), Random hexamers pd(N)6 Sodium salt.

The following molecular biology reagents were obtained from Thermo Scientific, Life technologies, Carlsbad, CA, USA: Taq DNA polymerase (1U/ µl), Conventional and Fast digest restriction enzymes (AgeI, EcoRI, HindIII, BamHI, XhoI, XbaI, SalI, KpnI, NheI, NdeI, NcoI, SmaI, Bsu15I, BsaI, TaqI, DpnI etc), DNA modifying enzymes like , Shrimp Alkaline Phosphatase (SAP), T4-Polynucleotide kinase, Exonuclease I, Gene Ruler 1 Kb DNA ladder, 100 bp ladder, T4-DNA ligase.

The following molecular biology reagents reagents were obtained from New England Biosciences (NEB), Ipswich, MA, USA: Standard Taq DNA polymerase, T4-PNK, Phusion High fidelity DNA polymerase, Q5 High fidelity DNA polymerase, Rstriction enzymes and DNA modifying enzymes etc.

The following molecular biology grade reagents, general grade laboratory reagents and analytical grade chemicals were obtained from Merck-Millipore, Dermstadt, Germany; Qualigens, Thermo Fischer Scientific India Pvt Ltd, Mumbai, India or Sd Fine-chem limited, Mumbai, India, HIMEDIA Laboratories Ltd, India: Xylene, Methanol, Glacial Acetic Acid, Potassium Acetate, Sodium Acetate, Sulfuric Acid (LR), Potassium dichromate (LR), Tri-Sodium citrate (LR), Citric Acid (LR), Hydrogen peroxide, Tryptone, Yeast extract, NaCl, Sodium hydrogen orthophosphate, disodium hydrogen phosphate, potassium hydrogen orthophosphate, dipotassium hydrogen phosphate, sodium carbonate, etc.

The following kits were used:

QiaAmp DNA mini kit (Qiagen, Limburg, Netherlands; Cat No.51304)

Qiagen Plasmid Midi kit (Qiagen, Limburg, Netherlands ; Cat No.12143)

QIAquick Gel Extraction Kit (Qiagen, Limburg, Netherlands; Cat No.28704)

EZ DNA Methylation-Gold Kit (Zymo-Research, Irvine, CA, USA; Cat No.D5005)

TruSeq RNA Library Preparation Kit v2, Set A/Set B (48 samples, 12 indexes) (Illumina, San Diego, CA, USA, Cat. No. RS-122-2001/RS-122-2002)

HiSeq Rapid SBS Kit v2 (50 cycles) (Illumina, San Diego, CA, USA, Cat. No. FC-402-4022)

Plasticware: Disposable plasticware certified as DNase, RNase, and protease-free including microcentrifuge tubes and tips for micropipettes was obtained from Axygen, California, USA.

Disposable sterile plasticware used for tissue culture was obtained from Nunc, Rochester, NY, USA and BD Falcon, NJ, USA.

Primers: All PCR primers and oligonucleotide sequences were synthesized and obtained from Merck-Sigma Aldrich in the lyophilized form.

Ultrapure water: The water used for the preparation of all solutions and reagents was Ultrapure water (Resistivity = 18 MΩ cm) obtained from a Milli-Q water plant (Millipore, Billerica, MA,USA).

Cell lines: The human medulloblastoma cell lines Daoy (RRID:CVCL_1167), D283 Med (RRID:CVCL_1155), D341 Med (RRID:CVCL_0018), D425 Med (RRID:CVCL_1275), HD-MB03 (RRID:CVCL_S506) and HEK293FT (RRID:CVCL_6911) were used in this study. The cell lines Daoy and D283 Med (henceforth referred as D238) were procured from the American Type Culture Collection (ATCC), Manassas, VA, USA. The cell lines

D341 Med and D425 Med (henceforth referred as D341 and D425) were kind gift from Dr. Darell Bigner, Duke University Medical Centre, Durham, NC, USA. Dr. Till Milde, German Cancer Research Center (DKFZ), Heidelberg, Germany, gifted the recently established cell line HD-MB03. The Human Embryonal Kidney cell line HEK293FT was procured from the Thermo Fisher Scientific, Waltham, MA, United States.

The cell lines were characterized for the subgroup-specific gene expression using a real-time RT-PCR assay as described earlier [151]. The cell line Daoy has high expression of gene *HHIP* and low expression *OTX2*. Moreover, the tumor from which the cell line was established was found to have desmoplastic histology. All these characteristics are known to be associated with SHH subgroup medulloblastoma. Thus the cell line Daoy belongs to the SHH subgroup medulloblastoma. The cell lines D283 overexpress MYC without amplification of MYC locus, whereas the cell line D341, D425 and HD-MB03 have MYC overexpression due to *MYC* locus amplification. These cell lines harbor isochromosome 17q (*i17q*) chromosomal aberration which is known to be associated with Group 3 and Group 4 medulloblastomas. Also, the genes specific to Group 3 medulloblastomas, like *IMPG2*, *CRX* and *NPR3* are expressed in these cell lines. Thus, the cell lines D283, D341, D425 and HD-MB03 belongs to the Group 3 medulloblastomas (Thesis- Pooja Panwalkar). HD-MB03 is the relatively recently established cell line characterized as Group 3 cell line by transcriptome analysis [160].

3.2. Methods

3.2.1. Cell culture

Reagents

1) *Tissue culture media*: The Dulbecco's Modified Eagle Medium (DMEM) and DMEM:Nutrient Mixture F12 (DMEM/F12) media were used for the routine maintenance of the cell lines. The DMEM medium contains glucose, high levels of amino acids, vitamins and sodium pyruvate. The DMEM/F12 is 1:1 mixture of DMEM and Ham's F12 medium. The media were prepared as per the manufacturer's instructions.

Method:

1. The powder from 1 packet of the either medium were dissolved in around 800 ml of sterile ultrapure water in sterile glass volumetric flask (1 lit capacity). Required quantity of anhydrous sodium bicarbonate (3.7 g/lit for DMEM and 2.438 g/lit for DMEM/F12) was added and dissolved in the medium.
2. The pH of the medium was adjusted to 7.5 with 1N hydrochloric acid (HCl) and the final volume of the medium was adjusted to 1 lit with sterile ultrapure water.
3. The medium was further filtered through a 0.22 µ membrane filter using a vacuum-assisted filter assembly and stored in sterile glass bottles at 4^{o}C until further use.
4. Both media are supplied by the manufacturer devoid of the growth factors. Thus, for the maintenance of the cell lines, the media were supplemented with 10 % Fetal Bovine Serum (FBS). Penicillin (50-100 I.U./ml), streptomycin (50-100 µg/ml) and amphotericin-B (0.25 µg/ml) were added to the culture medium to reduce the chances

of bacterial and fungal contamination in cell cultures (1 ml of 100X antibiotic antimycotic solution per 100 ml of complete medium).

2) *10X phosphate buffered saline (PBS)*: (1.4 M NaCl, 27 mM KCl, 100 mM, Na_2HPO_4, 17.7 mM KH_2PO_4 and 1 % Glucose)

80.81 g NaCl, 2.01 g KCl, 17.8 g Na_2HPO_4. 2 H2O, 2 g KH_2PO_4, and 10 g glucose were dissolved in sterile ultrapure water in a volumetric flask. The pH of the solution was adjusted to 7.4 using conc. HCl and the final volume was adjusted to 1 lit using ultrapure water. The solution was filtered through a 0.22 µ membrane filter and stored in sterile glass bottle at 4°C. For working stock, the 10 ml of 10X stock PBS solution was diluted to 100 ml with sterile ultrapure water.

3) *10X Trypsin solution (2.5 % w/v)*: 2.5 g of Trypsin powder was dissolved in 90 ml of ultrapure water in sterile volumetric flask and the final volume was adjusted to 1 lit. The solution was filter sterilized by passing through a 0.22 µ membrane filter. The filtered solution was stored as 10 ml aliquots at -20^{o}C. The working stock of trypsin solution was prepared by diluting 10 ml of 10x trypsin to 100 ml with 1X PBS. The working stock was stored at 4^{o}C.

3.2.1.1. Routine maintenance of cell lines

Sterile cell culture grade glassware and plastic ware was used for cell culture. All the cell culture operations were performed inside the laminar flow cabinets in the designated area. All the working reagents were brought to room temperature prior to their use.

The cell lines Daoy and HEK293FT grow in adherent manner and were cultured in DMEM medium supplemented with 10 % FBS. The cell lines D283 and HD-MB03 grow in semi-

adherent manner whereas the cell lines D341 and D425 grow in suspension manner and form clumps. These cell lines were cultured in DMEM/F12 medium supplemented with 10 % FBS. The cell were maintained at 37ºC, in a humidified chamber with 5 % carbon dioxide (CO_2). For routine maintenance, the cells were passaged at 70-80 % confluence and were replated at 1:2 to 1:5 split ratios depending upon the need of the experiments. The cells were passaged at least twice a week and all the experiments were carried out within 10-12 passages after revival of the cells from the frozen stocks.

Passaging of adherent cell lines (Daoy and HEK293FT):

5. At 70-80 % confluence, the spent medium was aspirated from the culture dish/flask using a sterile Pasteur pipette and the cells were rinsed twice with sterile 1X PBS to remove the traces of the medium.
6. The quantity of 1X trypsin sufficient to cover the surface of cell layer was added to the plate (2 ml for 60 mm dish or 4 ml for 100 mm dish). About 80 % of the added trypsin volume was aspirated from the plate leaving behind a thin layer of trypsin. The plate was transferred to the incubator until the cells become spherical in shape/detatched from the surface.
7. The trypsinized cells were collected in complete medium and transferred to a centrifuge tube using a sterile pipette. The cell suspension was centrifuged at 600g/1000 rpm in a moving angle centrifuge for 3-5 min.
8. The supernatant medium was gently aspirated using a Pasteur pipette without disturbing the cell pellet.

9. The cell pellet was dislodged by gently tapping the tube and the cells were suspended in fresh complete medium. The suspended cells were then transferred to the new culture dish and were seeded at desired confluence.

Passaging of semi-adherent and non-adherent cell lines (D283, D341, D425 and HD-MB03):

1. After attaining 70-80 % confluence, the cells are dislodged from the surface and the cell suspension was transferred to the centrifuge tube with the help of a Pasteur pipette.
2. The cell suspension was centrifuged at 600g/1000 rpm in a moving angle centrifuge for 3-5 min.
3. The supernatant medium was gently aspirated using a Pasteur pipette without disturbing the cell pellet.
4. The cell pellet was dislodged by gently tapping the tube and the cells were suspended in fresh complete medium. The suspended cells were then transferred to the new culture dish and were seeded at desired confluence.

3.2.2. Estimation of the cell count and cell viability

The cell counting of the single cell suspension was done using a Neubauer's Haemocytometer. The cell viability was assessed by Trypan blue exclusion method. The assay works on the principle of exclusion of certain dyes like trypan blue, eosin, propidium etc. from the living cells owing to their intact cell membranes [161].

Trypan blue solution (0.4 % w/v): 0.04 g of trypan blue powder was dissolved in 10 ml of 1X PBS. The solution was passed through 0.45 µ membrane filter to avoid any particulate matter. The solution was stored in dark at 4ºC.

1. After trypsinization, the cells were harvested and the cell pellet was resuspended in fresh complete medium. A single cell suspension was achieved by gently passing the suspension several times through a glass pipette. A small aliquot of the cell suspension was taken out in 1.5 ml centrifuge tube for cell counting.
2. 100 µl of cell suspension was mixed with 100 µl of 0.4 % trypan blue solution and mixed well with gentle pipetting. About 10 µl of the mixture was carefully loaded at the loading notch of the haemocytometer. Care was taken not to overload the chamber or incorporate any air bubble while loading the cell suspension.
3. The unstained (viable) stained (non-viable) cells were counted and the cell count and cell viability was calculated using the following equations.

Total cell count = [(total no. of cell from four corner squares/4)] X 2 X 104 cells/ml

Percentage cell viability = (Total no. of viable cells per ml of aliquot/ Total no. of cell per ml of aliquot) x 100

3.2.3. Cryopreservation and revival of cell cultures

Cryopreservation is a method by which the cells are preserved by cooling them to very low temperature in presence of a preservative for their long term storage. This minimizes the genetic changes which occur during the course of the continuous cultures and also helps avoiding loss of precious cultures due to contamination. The cells could be revived from the frozen stocks whenever required. For the optimal revival of the cell culture, usually healthy cells in log phase of growth are frozen.

Freezing medium: Complete medium supplemented with 10 % Dimethyl sulfoxide (DMSO) was used as a freezing medium. The prechilled freezing medium was used for cryopreservation.

Method for cryopreservation:

1. For cryopreservation, cells are harvested by above mentioned method upon attaining 70-80 % confluence.
2. The cell suspension was centrifuged at *600g/1000 rpm* in a moving angle centrifuge for 3-5 min.
3. The supernatant medium was aspirated using a Pasteur pipette without disturbing the cell pellet. The cell pellet was dislodged by gently tapping the tube and the cells were kept on ice.
4. The cells were immediately suspended in chilled cell freezing medium to form a single cell suspension. The suspended cells were then transferred to labelled and pre-chilled cryopreservation tubes. The cryotubes were then allowed to cool gradually by keeping them in 0ºC cooler at -80ºC overnight. The tubes were further transferred in vapor phase of liquid nitrogen for long term storage. The cryotubes were properly labelled mentioning the cell type, passage number, date and the name of the handling personnel and position of tube storage in the cryo-container was documented.

Method for revival of frozen cell stocks:

1. The cryovial containing the an appropriate cell stock was taken out from the cryo-container and the content of the tube was rapidly thawed by immediately placing the tube in water bath maintained at 37ºC. As soon as the cell suspension was thawed, the

tubes was removed from the water bath, wiped with 70 % ethanol solution and was then brought inside the laminar flow cabinet.

2. The cell suspension was the immediately transferred to the centrifuge tube containing 4 ml of the complete medium using a Pasteur pipette and mixed well by gentle pipetting.
3. The cell suspension was centrifuged at *600g/1000 rpm* in a moving angle centrifuge for 3-5 min.
4. The supernatant medium was gently aspirated using a Pasteur pipette without disturbing the cell pellet. The cell pellet was dislodged by gently tapping the tube and the cells were suspended in fresh complete medium. The suspended cells were then transferred to the new culture dish. 24 h after plating, the spent medium was replenished with fresh complete medium and the cells were further passaged after attaining 70-80 % confluence.

3.2.4. Treatment of medulloblastoma cells with DNA methylation inhibitor and Histone deacetylase (HDAC) inhibitors

The medulloblastoma cell lines D283, D425, HD-MB03 and Daoy were treated with varying concentrations of DNA methylation inhibitor, 5-Aza-2'-deoxycytidine and HDAC inhibitors sodium valproate and Trichostatin A.

Treatment with 5-Aza-2'-deoxycytidine

1) *10 mM 5-Aza-2'-deoxycytidine solution*: 5 mg powder of 5-Aza-2'-deoxycytidine (M.W. 228.21) was dissolved in 2.19 ml of sterile dimethyl sulfoxide (DMSO). 25 µl of 10 mM stock solution was diluted to 500 µl with sterile DMSO to make 0.5 mM

solution. 100 µl of 0.5 mM 5-Aza solution was further diluted to 500 µl with sterile DMSO to make 0.1 mM solution.

Method:

1. 2-4 X 10^5 D283, D425, HD-MB03 or Daoy medulloblastoma cells were seeded in 35 mm culture dish.
2. The cells were treated with varying concentrations of 5-Aza-2'-deoxycytidine ranging from 50 nM to 500 nM for a period of 5 days. Cells only treated with DMSO was kept as a control.
3. The medium was replaced every 24 h and fresh 5-Aza-2'-deoxycytidine was added.
4. RNA was extracted after 5 days of treatment and the expression of miR-193a was estimated by real-time RT-PCR assay.

Treatment with HDAC inhibitors Sodium valproate and Trichostatin A

1. 2-4 X 10^5 D283, D425, HD-MB03 or Daoy medulloblastoma cells were seeded in 35 mm culture dish.
2. The cells were treated with 6 mM of sodium valproate and 200 nM of Trichostatin A for a period of 3 days and 24 h, respectively. Cells only treated with DMSO was kept as a control.
3. The medium was replaced every 24 h and fresh 5-Aza-2'-deoxycytidine was added.
4. RNA was extracted after 5 days of treatment and the expression of miR-204 was estimated by real-time RT-PCR assay. Protein lysates were prepared from control and HDAC inhibitor treated cells and the levels of acetylated histone H3 at lysine 9 was assessed by western blot analysis.

3.2.5. Authentication of cell lines by short tandem repeat (STR) profiling

The short tandem repeat (STR) loci are the sequences in the genome that are typically formed by multiple repeats of 4-6 bp in length. The number of repeats for each STR loci varies within the population. This variability in the number of repeats makes STR profiling a valuable versatile tool for confirming the identity of the individual. STR profiling of the cell lines is a simple way to confirm the identity of the cell lines routinely used in research. Using this technique, the cross-contaminated, genetically drifted cell populations could be easily identified, which might lead to erroneous results. Recently, several databases were generated which contain detailed information and reference STR profiles of the widely used cell lines. Studies have shown that at least 8 markers are required for positive identification of the sample. The commonly used loci are D5S818, D13S317, D7S820, D16S539, vWA, Th01, TPOX, CSF1PO and, amelogenin for the identification of the gender [162]. The STR profiles for the cell lines Daoy, D283, D341, and HD-MB03 were obtained from the ATCC STR database (https://www.atcc.org/str_database.aspx) or the Cellosaurus database (https://web.expasy.org/cellosaurus/). The STR profile for the cell line D425 is not available.

Markers	D283 Med	D341 Med	HD-MB03	Daoy
Amelogenin (Gender)	X, Y	X	X, Y	X
D5S818	11	11, 12	11	11, 13
D7S820	10	9, 13	9, 10	8, 10
D13S317	8, 10	11, 13	11, 12	13, 14
D16S539	11	12, 14	9, 11	10
CSF1PO	9, 12	10, 11	10, 12	11
TH01	7	6, 9.3	6, 9.3	9
TPOX	8, 11	8, 11	8, 11	8, 10
vWA	16, 18	17, 18	18, 19	14, 20

Isolation of genomic DNA:

The genomic DNA was extracted from the medulloblastoma cell lines using QIAmp DNA mini kit (Cat No. 51304), QIAGEN, Heidelberg, Germany according to the manufactures' protocol.

Polymerase Chain Reaction (PCR) amplification of selected STR markers:

The primers used for STR profiling were obtained from Sigma-Aldrich. At least one of the primer from each primer pair was fluorescently labelled at the 5' end.

Table 3.1: The sequences of the primers used for the STR profiling.

Marker	Forward primer (5'- 3')	Reverse Primer (5'- 3')	Label
Amelogenin (Gender)	ACCTCATCCTGGGCACCCTGG	ACCTCATCCTGGGCACCCTGG	PET:Red
D5S818	GGTGATTTTCCTCTTTGGTATCC	AGCCACAGTTTACAACATTTGTATCT	NED: Yellow
D7S820	ATGTTGGTCAGGCTGACTATG	GATTCCACATTTATCCTCATTGAC	NED: Yellow
D13S317	ACAGAAGTCTGGGATGTGGA	GCCCAAAAAGACAGACAGAA	VIC:Green
D16S539	GGGGGTCTAAGAGCTTGTAAAAAG	GTTTGTGTGTGCATCTGTAAGCATGTATC	VIC:Green
CSF1PO	AACCTGAGTCTGCCAAGGACTAGC	TTCCACACACCACTGGCCATCTTC	6FAM: Blue
TH01	GTGGGCTGAAAAGCTCCCGATTAT	ATTCAAAGGGTATCTGGGCTCTGG	6FAM: Blue
TPOX	ACTGGCACAGAACAGGCACTTAGG	GGAGGAACTGGGAACCACACAGGT	6FAM: Blue
vWA	CCCTAGTGGATAAGAATAATC	GGACAGATGATAAATACATAGGATGGATGG	6FAM: Blue

1. The STR loci were PCR amplified using the Phusion high fidelity DNA polymerase, New England Biolabs, using genomic DNA extracted from the cell lines as template.
2. The PCR reaction was assembled as follows:

Component	Volume	Final concentration
5X Phusion HF Buffer	4 µl	1X
10 mM dNTP mix	0.4 µl	0.2 mM
Forward primer (2 pmol/µl)	1 µl	0.2 µM
Reverse primer (2 pmol/µl)	1 µl	0.2 µM
Template DNA (25 ng / µl)	2 µl	50 ng
Phusion High Fidelity DNA Polymerase 1U/µl	0.2 µl	0.2 U
Nuclease Free Water	11.4 µl	To make up total volume to 20 µl

The reaction volume was scaled up with respect to the number of samples.

3. Following program was set in the thermal cycler.

PCR conditions for STR marker Amelogenin				
Step	**Temperature**	**Time**	**Condition**	**No. of cycles**
Initial denaturation	95ºC	5 min		1
Denaturation	95ºC	45 sec	0.5ºC reduction per cycle in annealing temperature (Autoreduce- 0.5ºC)	13
Annealing	60ºC	45 sec		
Extension	72ºC	45 sec		
Denaturation	94ºC	45 sec		18
Annealing	53ºC	45 sec		
Extension	72ºC	45 sec		
Final extension	72ºC	5 min		1
Hold	4ºC	∞		

PCR conditions for remaining STR markers				
Step	**Temperature**	**Time**	**Condition**	**No. of cycles**
Initial denaturation	95ºC	5 min		1
Denaturation	95ºC	45 sec	0.5ºC reduction per cycle in annealing temperature (Autoreduce- 0.5ºC)	13
Annealing	60ºC	45 sec		
Extension	72ºC	45 sec		
Denaturation	94ºC	45 sec		25
Annealing	56ºC	45 sec		
Extension	72ºC	45 sec		
Final extension	72ºC	5 min		1
Hold	4ºC	∞		

4. The PCR products were electrophoresed on 2 % Agarose gel.
5. The STR markers were segregated into two groups according to their molecular size and the fluorescent tags and 2 µl of each PCR product was pooled. Pool 1 consisted of amelogenin, D5S818, D13S317, TPOX, and CSF1PO. Pool 2 consisted of vWA, TH01, D7S820, and D16S539.
6. The fragment analysis was done by capillary electrophoresis on the ABI 3500 Genetic Analyzer, Applied Biosystems, Waltham, MA, USA. The Gene Scan 500 LIZ size standards (Applied Biosystems, Waltham, MA, USA) were used as markers.
7. The size of the PCR products was identified with respect to the molecular size standards. The STR profile of the sample cell lines was generated.
8. The profile was matched with the available STR profiles in the Cellosaurus or ATCC STR database and the identity of the cell lines was confirmed.

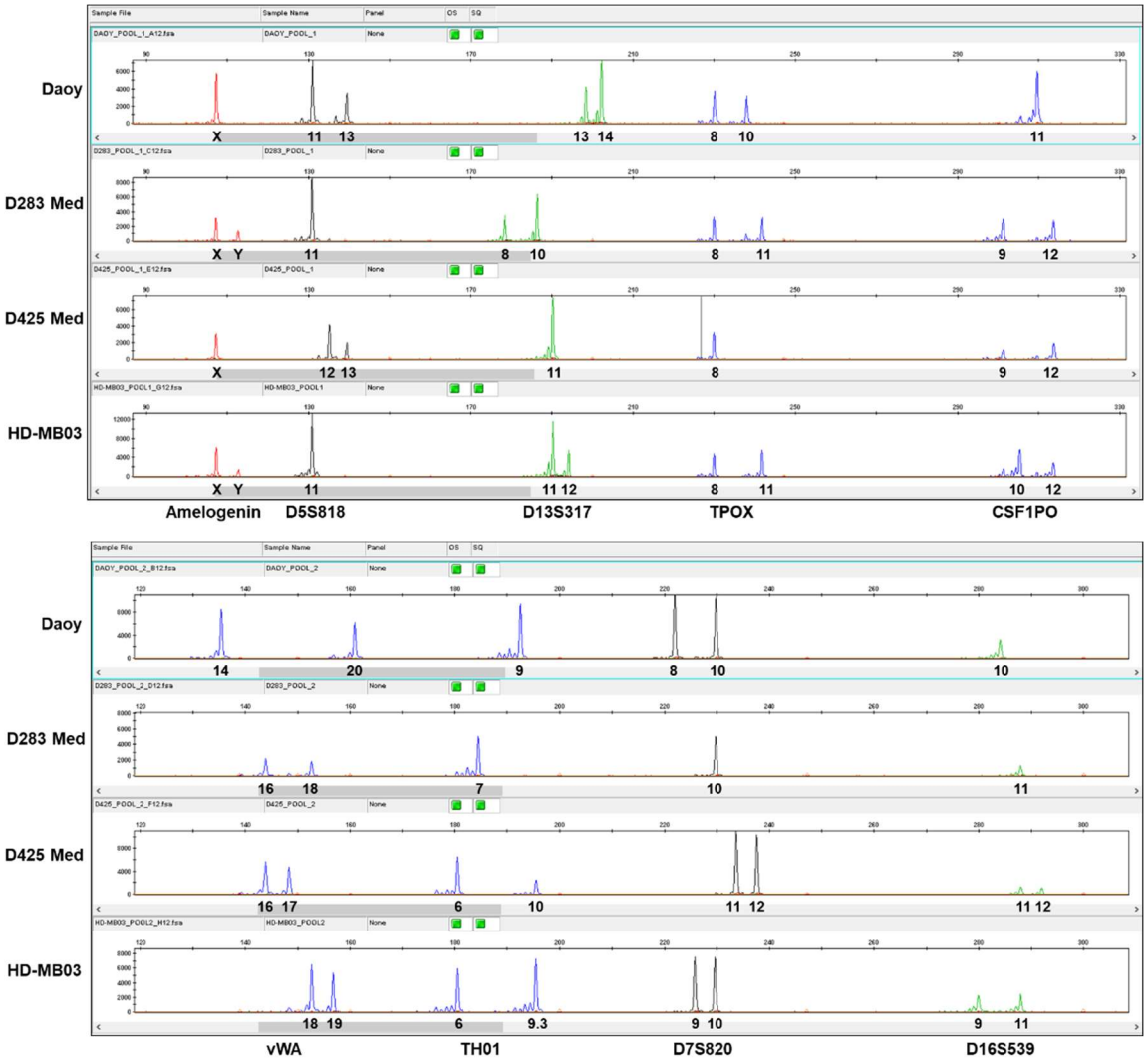

Fig 3.1: Electropherograms of DNA fragment analysis of PCR amplified STR loci.

The STR profiles obtained from the analysis showed 100 % identity for cell lines Daoy, D283, D341, and HD-MB03 with the published profiles on the Cellosaurus/ATCC web site. The STR profile is not available for the D425 cell line (Fig. 3.1). The cell line was obtained from Dr. Darell Bigner, Duke University, Durham NC, USA. Nonetheless, the cell line does not show 100 % identity with any other known cell line on the Cellosaurus web site (Table 3.1). The peak positions are marked with respect to the size of LIZ size standards.

Table 3.2: STR profiles of the medulloblastoma cell lines obtained after fragment analysis.

Markers	Daoy	D283 Med	D425 Med	HD-MB03
Amelogenin	X	X, Y	X	X, Y
D5S818	11, 13	11	12, 13	11
D13S317	13, 14	8, 10	11	11, 12
TPOX	8, 10	8, 11	8	8, 11
CSF1PO	11	9, 12	9, 12	10, 12
vWA	14, 20	16, 18	16, 17	18, 19
TH01	9	7	6, 10	6, 9.3
D7S820	8, 10	10	11, 12	9, 10
D16S539	10	11	11, 12	9, 11

3.2.6. Assessment of mycoplasma contamination status of the cell lines and polyclonal populations of the medulloblastoma cell lines

Mycoplasma has been known since decades as the most common contaminant found in cell cultures throughout the academic laboratories and laboratories of biopharmaceutical industries. Depending on the laboratory, it is estimated that around 15-85 % of the cultures are contaminated with mycoplasma. Nevertheless, mycoplasmas can have deleterious effects on eukaryotic cells, as they can alter every cellular function (proliferation, protein synthesis, susceptibility to viral infection, etc.). Thus, such alterations can lead to improper behavior of the cells during the conducted experiments and consequently to the improper results and conclusions from any experiment.

The cell populations used in this study were periodically checked for the mycoplasma free status to ensure true reproducible results. The mycoplasma status was assessed by PCR based assay described earlier [163, 164].

Rapid isolation of genomic DNA from cultured cells

Reagents

1) *Solution A (Genomic DNA Extraction Buffer)*:

Stock solution	For 50 ml	For 10 ml	For 5 ml	For 2 ml	Final conc.
1 M Tris-Cl, pH 9.0	5 ml	1 ml	500 µl	200 µl	100 mM
0.5 M EDTA, ph 8.0	10 ml	2 ml	1 ml	100 µl	100 mM
20 % SDS w/v	2.5 ml	0.5 ml	250 µl	100 µl	1 % w/v
Sterile ultrapure water	32.5 ml	6.5 ml	3.25 ml	1.6 ml	

2) *8 M Potassium acetate*: 39.26 g of potassium acetate was dissolved in 10 ml of ultrapure water and the final volume of the solution was adjusted to 50 ml with ultrapure water. The solution was sterilized by autoclaving and stored at room temperature. (Note: Potassium acetate is highly deliquescent substance, thus weighing should be carried out quickly. The weighed potassium acetate should not be exposed to air for long and must be quickly dissolved in the solvent.)

All centrifugation steps were carried out at room temperature (RT) unless specific temperature required in certain steps is mentioned.

1. After harvesting, the cells were collected in 1.5 ml centrifuge tube. The cells were washed with 1X PBS and centrifuged at *800g/2000 rpm* in a table top centrifuge. The supernatant was discarded and the cell pellet was loosen by gently tapping the tube.
2. 500-1000 µl of solution A (1 ml buffer per 1-5 X 10^6 cells) was added to the cells and mixed gently by inverting the tubes several times.

3. The lysate was then incubated at 72ºC for 30 min with intermittent mixing of the contents every 10 min.
4. 140 µl of 8 M potassium acetate solution was added per 1 ml of the cell lysate, mixed rapidly and incubated on ice for 30 min.
5. The samples were then centrifuged for 10 min at *12000 rpm*.
6. The supernatant was transferred to a fresh 1.5 ml centrifuge tube using a cut pipette tip. The samples were centrifuged for 10 min at *12000 rpm*.
7. The gDNA was precipitated by adding 0.7 volume of isopropanol and centrifugation at *12000 rpm* for 15 min.
8. The DNA pellet was washed twice with 70 % ethanol. The pellet was air-dried and dissolved in 50-100 µl of TE buffer containing 1 µg/ml of RNase A. The samples were incubated at 37ºC for 1 h to degrade the RNA. The DNA was further used for restriction digestion or as a template in PCR reactions.

PCR for the detection of mycoplasma

For the detection of mycoplasma contamination, PCR reactions were set up using the gDNA extracted from the cells as template. The primers for detection of commonly found strains of mycoplasma and acholeplasma were adopted from [163, 164]. A pool of six forward primers and three reverse primers each added at the concentration of 10 pmol/µl was prepared and used in PCR reactions. Genomic DNA isolated from the cell line previously known to be contaminated with mycoplasma was used as a positive control. Also, to show whether the extracted gDNA was of PCR quality, a PCR reaction was set up for each sample gDNA using a separate known set of primers routinely used in lab.

Table 3.3: List of primer sequences used for detection of Mycoplasma contamination.

Primers	Sequence	
Forward (5'- 3')	CGCCTGAGTAGTACGTTCGC	Used as primer pool of all forward primers in 10 pmol/µl concentration each
	CGCCTGAGTAGTACGTACGC	
	TGCCTGAGTAGTACATTCGC	
	TGCCTGGGTAGTACATTCGC	
	CGCCTGGGTAGTACATTCGC	
	CGCCTGAGTAGTATGCTCGC	
Reverse (5'- 3')	GCGGTGTGTACAAGACCCGA	Used as primer pool of all reverse primers in 10 pmol/µl concentration each
	GCGGTGTGTACAAAACCCGA	
	GCGGTGTGTACAAACCCCGA	

1. All the reagents including 10X Standard Taq Buffer without $MgCl_2$, 10 mM dNTP mix, forward and reverse primer pools, and Taq DNA polymerase were thawed and kept on ice.
2. The PCR reaction was assembled as below:

Component	Volume	Final concentration
10X Taq DNA Polymerase Buffer	2 µl	1X
25 mM $MgCl_2$	1.2 µl	1.5 mM
10 mM dNTP mix	0.4 µl	0.2 mM
Forward primer pool	1 µl	0.2 µM each
Reverse primer pool	1 µl	0.2 µM each
Template DNA (25 ng/µl)	2 µl	50 ng
Taq DNA Polymerase 1U/µl	0.5 µl	0.25 U
Nuclease Free Water	11.9 µl	To make up total volume to 20 µl

Depending upon the number of samples, a master mix was prepared by scaling up the reaction.

3. The PCR cycling parameters were set in the Thermal cycler as follows:

Step	Temperature	Time	No. of cycles
Initial denaturation	95ºC	5 min	1
Denaturation	95ºC	45 sec	35
Annealing	65ºC	30 sec	
Extension	72ºC	1 min	
Final extension	72ºC	10 min	1
Hold	4ºC	∞	

4. 10 µl of each PCR product was electrophoresed on 1 % Agarose gel and the results were assessed based on the presence or absence of the band around 500-520 bp in the samples.

3.2.7. Analysis of miR-193a and miR-204 expression and DNA methylation status of promoter region of miR-193a and miR-204 in medulloblastoma

Analysis of miR-193a and miR-204 expression

The expression of miR-193a and miR-204 was studied from fresh frozen tumor and Formalin fixed paraffin embedded medulloblastoma tumor samples by Real-Time Reverse Transcription Polymerase Chain Reaction assay (Real-Time RT-PCR assay) as described earlier [151]. The expression of these microRNAs was also studied from the recently published expression dataset (GEO: GSE85218) for an independent large cohort of 763 medulloblastoma tumor tissues from Medulloblastoma Advanced Genomics International Consortium (MAGIC) [78]. The expression data was retrieved from the Gene Expression Ominbus (GEO) Pubmed as a text file in tab delimited format. The tab delimited file was accessed through Microsoft Excel software. The expression data was sorted with respect to the four molecular subgroups of medulloblastoma and the expression of miR-193a and

miR-204 was plotted in Graphpad Prism v6.0 software. The significance of the differential expression was interpreted by One-way Analysis of Variance (ANNOVA) in Graphpad Prism v6.0 software.

Analysis of DNA methylation status of miR-193a and miR-204 (TRPM3) promoter region using the genome wide methylation data of 763 tumor samples from MAGIC cohort

1. The genome wide methylation data of 763 tumor samples from MAGIC cohort analyzed on the Illumina Infinium HumanMethylation450 BeadChips was retrieved from the Gene Expression Ominbus (GEO), Pubmed as a text file in tab delimited format (GEO: GSE85218) [78]. The information regarding the position of the probes across the genome was obtained from the Illumina technical support service. https://support.illumina.com/downloads/infinium_humanmethylation450_product_files.html.
2. The probes corresponding to the miR-193a locus on chromosome 17 and miR-204 locus (TRPM3 gene promoter as miR-204 is an intragenic microRNA) on chromosome 9 were identified.
3. Due to the large size of the downloaded methylation data file, the Global regular expression print (Grep) command in the LINUX was used to sort the specific data. The Grep command scans the file for particular pattern of characters. Upon identification of the related characters, the lines containing the characters are printed in a separate file in designated format.

   Syntax: grep -w -F -f (from search file name) -e Sample (extract data from this file) > (new file name)

4. The sorted β-values were further arranged with respect to the subgroup affiliation of the samples and the data for each probe was plotted in Graphpad Prism v6.0 software. The significance of the differential β-value distribution was interpreted by One-way Analysis of Variance (ANNOVA) in Graphpad Prism v6.0 software.

3.2.8. Analysis of DNA methylation status of the miR-193a promoter in medulloblastoma cell lines by methylation specific PCR

DNA methylation status of the miR-193a promoter in medulloblastoma cell lines D425, HD-MB03 and Daoy was studied by methylation specific PCR. The miR-193a locus on chromosome 17 was analyzed in University of California, Santa Cruz (UCSC) Genome browser (https://genome.ucsc.edu/). The sequence of the region 4 kb upstream and 1 kb downstream of the pre-miR-193a was retrieved. The sequence was used for designing primers for methylation-specific PCR using the MethPrimer software (https://www.urogene.org/methprimer/).

Table 3.4: List of primer sequences used for analysis of DNA methylation status of miR-193a promoter by methylation specific PCR.

Primer name	Forward (5'- 3')	Reverse (5'- 3')
MiR-193a_MSP Meth	GGGGACGTATTTCGAATTTC	TAAAAAACAACCTAACCGAAACG
MiR-193a_MSP UM	GGGGATGTATTTTGAATTTTGA	ACACACACCAACCCAAAAA
Meth ACTB_1	TATATAGGTTGGGGAAGTTTG	TATAAAAACATAAAACCTATAACC
Meth ACTB_2	TGGTGATGGAGGAGGTTTAGTAAGT	AACCAATAAAACCTACTCCTCCCTTAA

For methylation specific PCR, the genomic DNA extracted from the medulloblastoma cell lines was subjected for bisulphite conversion. The bisulphite converted gDNA was used as template for the methylation specific PCR.

Isolation of the genomic DNA:

The genomic DNA was isolated from the medulloblastoma cell lines using QIAmp DNA mini kit (Cat No. 51304), QIAGEN, Heidelberg, Germany according to the manufactures' protocol.

Bisulphite conversion of the genomic DNA:

The bisulphite conversion of the genomic DNA is a process in which the DNA is denatured followed by the treatment with sodium bisulphite leading to the deamination of the unmodified cytosine residues into uracil. The methylated cytosine residues remain unchanged in this process. The amplification of this DNA by PCR results in the conversion of uracils to thiamines. Thus, the bisulphite converted DNA can be used for studying the DNA methylation pattern of the gene and various regulatory sequences.

In this study, the bisulphite conversion of the genomic DNA was achieved by using the EZ DNA Methylation-Gold Kit (Zymo Research, Irvine, CA, USA) following manufacturer's instructions. The CT conversion reagent was dissolved by adding 900 µl of nuclease free ultrapure water, 300 µl of M-Dilution Buffer, and 50 µl M-Dissolving Buffer to a tube of CT Conversion Reagent. The content were mixed at RT for 10 min with intermittent vortexing. Use of freshly prepared CT conversion reagent was preferred. Once diluted, the CT conversion reagent was stored at -20^{o}C and used within 15 days. The final volume of M-Wash Buffer was adjusted by addition of 24 ml of 100 % ethanol prior to use. All

centrifugation steps were carried out at room temperature (RT) unless specific temperature required in certain steps is mentioned.

1. A total of 500 ng of gDNA was diluted upto 20 µl with nuclease free ultrapure water and 130 µl of the CT conversion reagent was added to it. The reagent as mixed properly.
2. The samples were incubated at 98^{o}C for 10 min followed by 64^{o}C for 150 min in a thermal cycler.
3. 600 µl of M-Binding buffer was added to the Zymo spin IC column kept in a collection tube. The sampe was loaded to the Zymo spin column containing M-binding buffer.
4. The column was capped and the content was mixed by inverting the column several times.
5. The samples were centrifuged at 14000 rpm for 30 sec. The flow-through was discarded.
6. The column was washed with 100 µl of M-Wash buffer and the samples were centrifuged at 14000 rpm for 30 sec. The flow-through was discarded.
7. 200 µl of M-Desulphonation buffer was added to the column and it was allowed to rest at room temperature for 15-20 min. The samples were centrifuged at 14000 rpm for 30 sec. The flow-through was discarded.
8. The column was washed twice with 200 µl M-Wash buffer. The column was dry-spun to remove traces of ethanol.
9. The bisulphite converted DNA was eluted from the column in 10 µl of M-Elution buffer.
10. The eluted DNA was quantified by using NanoDrop spectrophotometer and was further used for methylation specific PCR.

Methylation-specific PCR of bisulphite converted gDNA of medulloblastoma cell lines

1. All the reagents including 10X Standard Taq Buffer without $MgCl_2$, 10 mM dNTP mix, forward and reverse primer, and Taq DNA polymerase were thawed and kept on ice.
2. The PCR reaction was assembled as below:

Component	Volume	Final concentration
10X Taq DNA Polymerase Buffer	2 µl	1 X
25 mM $MgCl_2$	1.2 µl	1.5 mM
10 mM dNTP mix	0.4 µl	0.2 mM
Forward primer (10 pmol/µl)	0.5 µl	0.2 µM
Reverse primer (10 pmol/µl)	0.5 µl	0.2 µM
Template DNA (25 ng/µl)	2 µl	50 ng
Taq DNA polymerase (5U/µl)	0.5 µl	2.5 units
Nuclease free water	12.9 µl	To make up total volume to 20 µl

Depending upon the number of samples, a master mix was prepared by scaling up the reaction.

3. The designed primers yield a PCR product ranging from 200-220 bp. Thus, the PCR cycling parameters were set in the Thermal cycler as follows:

Step	Temperature	Time	No. of cycles
Initial denaturation	95ºC	5 min	1
Denaturation	95ºC	45 sec	30
Annealing	65ºC	30 sec	
Extension	72ºC	1 min	
Final extension	72ºC	10 min	1
Hold	4ºC	∞	

4. 10 µl of each PCR product was electrophoresed on 1 % Agarose gel and the results were assessed based on the presence or absence of the band around 200 bp in the methylated or unmethylated samples.

Agarose Gel Electrophoresis

Agarose gel electrophoresis is a technique that separates DNA based on its size or configuration using an electric field in a matrix of porous agarose.

Reagents:

1) *50X Tris-Acetate-EDTA Buffer*: The concentration of salts in 1X buffer is 40 mM Tris, 20 mM acetate and 50 mM EDTA. The buffer has a pH around 8.6-8.8

   242.28 g of Tris base and 18.61 g of Disodium-EDTA were dissolved in 800 ml of ultrapure water. 57.1 ml of glacial acetic acid was added and the final volume of the solution was adjusted to 1 lit with ultrapure water. The solution was sterilized by autoclaving and stored at RT. The solution was diluted to 1X using ultrapure water as per the requirement.
2) *Ethidium bromide solution (10 mg/ml)*: 100 mg of ethidium bromide powder was dissolved in 10 ml of ultrapure water. The solution was stored at RT protected from light.
3) *6X DNA gel loading dye 0.25 % (w/v) bromophenol blue. 0.25 % (w/v) xylene cyanol FF*: 25 mg of bromophenol blue and 25 mg of Xylene cyanol FF dyes were dissolved in 40 % Glycerol. The dye was stored at RT.

Method:

1. The amount of low electroendosmotic (EEO) agarose to make desired percentage was weighed and added to required volume of 1X TAE buffer. The mixture was heated in a microwave oven to dissolve the agarose completely. The solution was allowed to cool.
2. Meanwhile, the agarose gel casting tray was cleaned, secured on the sides using paper tape and the comb of desired size was inserted in the notch provided for the comb.
3. Required volume of 10 mg/ml of ethidium bromide solution was added to the agarose solution to a final concentration of 0.5 µg/ml when the temperature of the agarose solution was below 50ºC and mixed thoroughly.
4. The slurry was poured in the gel casting tray without forming bubbles. The agarose was allowed to solidify at RT.
5. The side tapes were removed and the solidified gel was placed submerged in a electrophoresis chamber containing an appropriate volume of 1X TAE buffer. The comb was removed without damaging the wells.
6. The DNA samples were mixed with 6X DNA gel loading dye and loaded to the wells along with the molecular size markers. The electrophoresis was conducted using the potential of 10-15 V per cm of gel length until the lower dye reaches at least 2/3rd of the gel length.
7. The DNA bands in the gel were visualized using UV-transilluminator. The sizes of the bands were determined by comparing the position with the bands in the molecular weight markers and the results were interpreted.

3.2.9. RNA extraction from tissue culture cells by acid guanidinium thiocyanate-phenol chloroform extraction method

Total RNA was isolatied from cells using the protocol described by Chomoczynski and Sacchi [165]. The method involves the use Guanidinium salts and water saturated acidic phenol. The Guanidinium salts acts as protein denaturant and inhibitor of ribonuleases thus, enabling cell lysis and maintaining RNA stability. The gDNA partitions in the acidic phenol leaving the RNA fraction in the aqueous phase. The RNA could then be precipitated by using isopropanol.

Nuclease free plasticware was used for RNA isolation procedure. Reagents used for RNA extraction were prepared using certified nuclease free molecular biology grade chemicals. A separate set of micropippetes meant only to be used for RNA work was used. The extraction procedure was performed in clean dust free environment and the surface of the working place was cleaned by RNAse elimination agents like RNase Zap.

Reagents:

1) *Diethyl pyrocarbonate (DEPC) treated ultrapure water*: 50 µl of DEPC was added to 50 ml of ultrapure water taken in nuclease free centrifuge tube. The tubes were shaken vigorously to ensure proper mixing of DEPC in water. The tubes were wrapped in aluminium foil with the cap kept slightly loose and left at 37ºC overnight. The DEPC treated water in 50 ml tubes was autoclaved and stored at RT until used.

   All the reagents required for RNA isolation were prepared in DEPC treated ultrapure water.

2) *1 M citric acid solution*: 9.60 g of citric acid was dissolved in 40 ml ultrapure water and the final volume was adjusted to 50 ml using ultrapure water. 50 µl of DEPC was

added to the citric acid solution, mixed vigorously and incubated at 37ºC overnight in dark. The solution was sterilized by autoclaving and stored at RT.

3) *1 M sodium citrate solution pH 7.0*: 14.7 g of sodium citrate, dehydrate was dissolved in 40 ml DEPC treated ultrapure water. The pH of the solution was adjusted to 7.0 using 1M citric acid solution. The final volume of the solution was adjusted to 50 ml using ultrapure water. 50 µl of DEPC was added to the sodium citrate solution, mixed vigorously and incubated at 37ºC overnight in dark. The solution was sterilized by autoclaving and stored at RT.
4) *10 % N-Lauryl sarcosine solution*: 5 g of N-Lauroyl sarcosine sodium salt was dissolved in 40 ml of DEPC treated ultrapure water. The final volume of the solution was adjusted to 50 ml using DEPC treated ultrapure water. The solution was stored at RT.
5) *4 M Guanidinium isothiocyanate (GITC) solution*: The solution of GITC was prepared in a buffered solution of sodium citrate containing 25 mM of sodium citrate and 0.5 % N-lauryl sarcosine. 23.6 g of guanidinium isothiocyanate was dissolved in 20 ml of DEPC treated ultrapure water. 1.25 ml of 1M sodium citrate pH 7.0 and 2.5 ml of 10 % N-lauryl sarcosine solution was added and the final volume of the solution was adjusted to 50 ml with DEPC treated ultrapure water. The solution was stored at RT. The working reagent, solution D was prepared freshly before use by adding β-mercaptomethanol to the final concentration of 0.1M.
6) *DEPC treated water saturated Phenol*: Molecular biology grade liquid phenol and DEPC treated ultrapure water were mixed in equal proportions in 50 ml nuclease free tube. The mixture was shaken vigorously and allowed to stand at 4ºC until the two

phases separate out. The upper aqueous layer was replaced with fresh DEPC treated ultrapure water, mixed vigorously and the two phases were allowed to separate. The water saturated phenol was stored at 4°C until further use.

7) *2 M Sodium acetate pH 4.0*: 13.6 g of sodium acetate trihydrate was dissolved in 15 ml DEPC treated ultrapure water. The pH of the solution was adjusted to 4.0 using glacial acetic acid. The final volume of the solution was adjusted to 50 ml using ultrapure water. 50 µl of DEPC was added to the sodium acetate solution, mixed vigorously and incubated overnight at 37°C overnight in dark. The solution was sterilized by autoclaving and stored at RT.
8) *Chloroform*
9) *Isopropanol*
10) *70 % ethanol*

Method:

1. 1-5 X 10^6 cells were harvested and washed with sterile 1X PBS. For adherent cells, the spent medium was poured off form the 70-80 % confluent plate and the cells were rinsed once with sterile 1X PBS.
2. 500 µl - 1 ml of solution D was added to the tube. For adherent cells, the solution D was added to plate directly, the plate was swirled to spread solution D over the entire surface. The cell lysate was collected in 1.5 ml nuclease-free centrifuge tube.
3. The lysate was then passed through syringe fixed with 26 gauge needle at least 10-12 times. This ensures the shearing of the gDNA as judged by the loss of viscosity of the solution. At this step, the lysates were either processed directly to the next step or stored at -80°C until further use.

4. 50 µl of 2 M sodium acetate solution, pH 4.0 was added per 500 µl of the lysate and mixed properly.
5. 500 µl of phenol saturated with DEPC treated water was added per 500 µl of the lysate followed by the addition of 250 µl of chloroform. The tubes were then vortexed vigorously for at least 1 min. The pressure inside the tubes was loosened by opening the tubes and the tubes were further vortexed for another 30 sec.
6. The tubes were then incubated on ice for 15 min.
7. The tubes were centrifuged at *10,000 rpm* for 10 min at 4ºC. The upper aqueous layer was transferred to fresh 1.5 ml centrifuge tube and again centrifuged at *10,000 rpm* for 5 min at 4ºC.
8. The upper aqueous solution was transferred to fresh 1.5 ml centrifuge tube leaving behind lower volume in the tube. Equal volume of isopropanol was added for the precipitation of RNA, mixed properly and the tubes were kept at -20ºC for at least 1 h to overnight.
9. The tubes were centrifuged at *10,000 rpm* for 10 min at 4ºC to obtain a pellet of RNA.
10. The supernatant was discarded and the RNA pellet was washed with 500 µl 70 % ethanol. The tubes were centrifuged at *10,000 rpm* for 10 min at 4ºC.
11. The 70 % ethanol was discarded and the pellet was air-dried and dissolved in 10-100 µl of DEPC treated ultrapure water. The RNA was allowed to dissolve by keeping the tubes on ice for at least 1 h. During air-drying the caps of the tubes were left open and the mouths of the tubes were covered with a tissue paper.
12. The secondary structure of the RNA was denatured by incubating the dissolved RNA at 65ºC for 5 min followed by quickly chilling the tubes on ice.

13. The RNA was quantified using NanoDrop spectrophotometer and the integrity of the RNA was assessed by electrophoresing the samples on 1.8 % denaturing agarose gel.
14. For long term storage, the samples were stored at -80ºC. Repeated freeze thawing of the samples was avoided to prevent degradation of RNA. When required, the frozen RNA was strictly allowed to thaw completely on ice before use.
15. For ensuring the isolated RNA samples are free from gDNA, the RNA was treated with RNase free DNase1 in a DNase1 reaction buffer. 1U of DNase1 per ug of RNA was used. The DNase1 treatment was carried out at 37ºC for 10 min.
16. The activity of DNase1 in the reaction was attenuated by addition of 0.5 M EDTA, pH 8.0, upto the concentration of 5 mM and the enzyme was heat inactivated for 10 min at 70ºC. The DNA free RNA was further used for complementary DNA (cDNA) synthesis.

3.2.10. Estimation of microRNA expression by Real-time Reverse Transcription Polymerase Chain Reaction (RT-PCR) assay

The small size of microRNAs makes their detection a challenging task. The real-time RT-PCR assay enables accurate and sensitive detection of microRNAs in RNA samples isolated from cultured mammalian cells and tissues. The method involves the reverse transcription of these small RNA molecules using stem-loop primers which hybridize to their 3'-end. The expression of microRNAs could be quantified using both Taqman and SYBR Green based methods of quantitation. The PCR consists of a microRNA specific forward primer, and the reverse primer complementary to the stem and loop region. If, Taqman method is used, the Taqman probe binds the region between forward and reverse primer [166, 167].

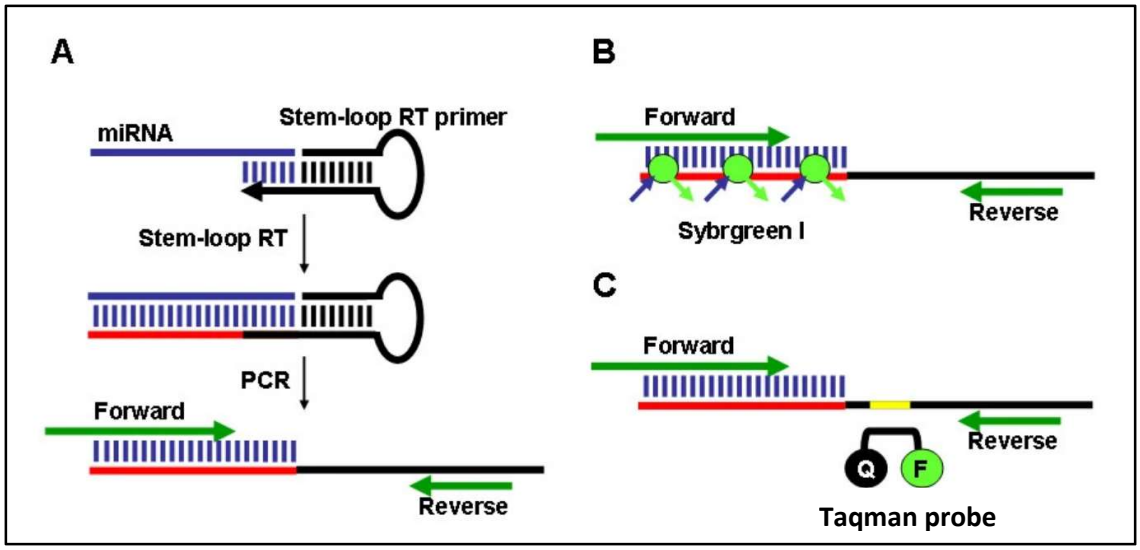

Fig 3.2: Schematic representation of stem-loop RT-PCR based detection of microRNAs.

(Figure adopted from Varkonyi-Gasic, E. *et. al., Plant Methods*, 2007 [167]). **A**. Reverse transcription of mature microRNAs using stem-loop primers. **B. & C**. Detection of microRNAs using SYBR Green based method and Taqman probe method, respectively.

For microRNA detection in total RNA extracted from medulloblastoma cell lines, 50 ng of total RNA was reverse transcribed using Moloney-Murine Leukemia Virus Reverse Transcriptase (M-MLV RT) following the manufacturer's instructions. A pool of stem-loop primers for miR-193a/ miR-204 and RNU48, a small endogenous non-coding RNA was used for Reverse transcription for Taqman based detection whereas custom designed stem-loop primers for miR-193a, miR-204 and RNU48 were used separately for the reverse transcription reaction for SYBR Green method based detection.

Stem-loop reverse transcription of microRNAs

Materials:

1) 5X First Strand Buffer

2) *100 mM dNTP mix*
3) *0.1 M Dithiothritol (DTT) solution*
4) *RNase inhibitor (20 U/µl)*
5) *M-MLV RT (200 U/µl)*
6) *DEPC treated ultrapure water*
7) *Multiplex RT primer pool containing 5X RT primers for miR-193a/miR-204 and RNU48 in 1X TE buffer, pH 8.0) for Taqman RT*

Table 3.5: Assay ID's of Taqman assays used for quantitation of microRNAs by real-time RT-PCR assays.

Name of assay	Catalogue no.	Assay id
hsa-miR-193a-3p	4427975	002250
hsa-miR-204-5p		000508
RNU48		001006

8) *Custom designed reverse transcription (RT) primers for miR-193a, miR-204 and RNU48 as 10 pmol/µl stock for SYBR Green method*

Table 3.6: List of stem-loop primers used for reverse transcription of microRNAs to be quantitated by real-time RT-PCR assays using SYBR Green method.

Name of RT primer	Sequence (5'- 3')
MiR-193a RT primer	GTCGTATCCAGTGCAGGGTCCGAGGTATTCGCAC TGGATACGACCTGGGA
MiR-204 RT primer	GTCGTATCCAGTGCAGGGTCCGAGGTATTCGCAC TGGATACGACAGGCAT
RNU48 RT primer	GTCGTATCCAGTGCAGGGTCCGAGGTATTCGCAC TGGATACGAGGTCAGAGCG

Method:

1. The RNA samples were thawed on ice and diluted to 50 ng/µl concentration using DEPC treated ultrapure water. All the reagents were thawed on ice, tap mixed, and the tubes were spun to gather the content of the tubes to the bottom.
2. A 5 µl reverse transcription reaction was assembled as follows:

RT reaction for Taqman based detection		
Component	**Volume**	**Final concentration**
5X First Strand Buffer	1 µl	1X
0.1 M DTT solution	0.5 µl	10 mM
100 mM dNTP mix	0.1 µl	0.5 mM
Multiplex RT primer pool	2 µl	1X
RNase inhibitor (20 U/µl)	0.1 µl	2 units
M-MLV RT (200 U/µl)	0.25 µl	50 units
RNA (50 ng/µl)	1 µl	50 ng
DEPC treated ultrapure water	0.05 µl	To make up total volume to 5 µl

RT reaction for SYBR Green based detection		
Component	**Volume**	**Final concentration**
5X First Strand Buffer	1 µl	1X
0.1 M DTT solution	0.5 µl	10 mM
100 mM dNTP mix	0.1 µl	0.5 mM
RT primer (10 pmol/µl)	0.5 µl	1X
RNase inhibitor (20 U/µl)	0.1 µl	2 units
M-MLV RT (200 U/µl)	0.25 µl	50 units
RNA (50 ng/µl)	1 µl	50 ng
DEPC treated ultrapure water	1.55 µl	To make up total volume to 5 µl

3. The reaction was scaled up depending upon the number of samples and master mix was prepared except the addition of RNA. 4 µl of master mix was aliquot in 0.2 ml thin-walled PCR tubes and 1 µl of RNA (50 ng/µl) was added separately. The content of the tubes were tap mixed, and the tubes were pulse spun and placed in a master cycler previously set at 16ºC.

   (Note: It is essential that the reaction should be assembled on ice and the thermal cycler should be preset at 16ºC before placing the tubes to prevent denaturation of the stem-loop RT primers.)

   The below mentioned program was set in the thermal cycler:

Temperature	Time
16ºC	30 min
42ºC	30 min
85ºC	5 min
4ºC	∞

4. The RT reactions were either used for setting real-time RT-PCR assay or stored at -20ºC until further used. The RTs were used within 2 weeks.

Real-time PCR for microRNA expression analysis

Materials for Taqman based detection

1) *2X Universal Taqman PCR master mix*
2) *20X microRNA primer-probe*
3) *DEPC treated ultrapure water*

Materials for SYBR Green based detection

1) *2X PowerUp SYBR Green PCR master mix*
2) *MiR-193a, miR-204 and RNU48 specific real time forward primer (10 pmol/µl)*
3) *Common miR-10b reverse primer (10 pmol/µl)*

Method:

1. The 20X microRNA primer-probe or specific primers were removed for the storage and strictly thawed on ice.

Table 3.7: List of primer sequences used for quantitation of microRNA expression by real-time RT-PCR using SYBR Green method.

Name of real time RT-PCR primer	Sequence (5'- 3')
MiR-193a forward primer	GAAGCGAACTGGCCTACAAAG
MiR-204 forward primer	GCACGCTTCCCTTTGTCATCCT
RNU48 forward primer	TTGAGTGTGTCGCTGATGCC
MiR-10b reverse primer (common)	GTGCAGGGTCCGAGGT

2. The RT reactions were diluted in equal ratio with DEPC treated ultrapure water.
3. The master mix for 5 µl real-time RT-PCR reaction was set up as mentioned below:

Reaction for Taqman based detection		
Component	**Volume**	**Final concentration**
2X Universal Taqman master mix	2.5 µl	1X
20X microRNA primer probe	0.25 µl	1X
DEPC treated ultrapure water	0.25 µl	To make up total volume to 3 µl
Diluted RT reaction (5ng/µl)	2 µl	10 ng

Reaction for SYBR Green based detection		
Component	**Volume**	**Final concentration**
2X PowerUP SYBR Green master mix	2.5 µl	1X
Forward primer (10 pmol/µl)	0.25 µl	1X
Reverse primer (10 pmol/µl)	0.25 µl	To make up total volume to 3 µl
Diluted RT reaction (5ng/µl)	2 µl	10 ng

Each real-time reaction was at least set up in duplicate. Master mix for each microRNA to be detected was prepared by scaling up the volumes depending upon the number of reaction to set. No template control (NTC) reaction was set up for each master mix prepared and DEPC treated ultrapure water was added instead of cDNA to rule out the chances of erroneous measurement of gene expression due to accidental cross contamination.

4. 3 µl master mix was aliquot in separate tubes and 2 µl of diluted cDNA was added to the tubes. The contents were mixed and pulse spun.
5. The prepared reactions were loaded in 384 well plate and the position of each sample in the plate was documented.
6. The wells were sealed with optical adhesive sheet with the help of plastic applicator. The sealing of the wells was ensured by evenly moving the applicator through horizontal and vertical groves between the wells.
7. The bubbles in the wells were removed by gentle tapping and the plate was spun in a moving angle rotor at 2000 rpm for 2 min at RT to gather the contents of the wells to the bottom.

8. An appropriate program for Taqman or SYBR Green method was selected and parameters were set in the QuntStudio 12K Flex/QuantStudio 5 real-time RT-PCR thermal cycler instruments, Applied Biosystems, Waltham, MA, USA using the QuantStudio software. The 384 well plate was kept in the heating block and the program was run.

   The PCR cycling condition were set as follows:

Stage	Temperature	Time	Condition	No. of cycles
Hold	50°C	2 min		1
	95°C	10 min		1
PCR	95°C	15 sec		40
	60°C	1 min	Fluorescence data acquisition	

   The rampage rate was set at 1.6°C per sec.

9. The data was analysed using QuantStudio software by comparative Delta Delta Ct method and the expression of miR-193a and miR-204 relative to the expression of endogenous small RNA control (RNU48) was calculated in terms of Relative quantity.

   $RQ=2^{\wedge(Ct\ miRNA - Ct\ RNU48)} * 100$

10. The data was exported in Microsoft Excel format. Both raw data file and the analysed data file were preserved for record.

3.2.11. Gene expression analysis by real-time RT-PCR assay

***Primer designing*:**

Primers were designed using Oligo explorer software v1.4 (http://www.genelink.com/tools/gl-oe.asp) to amplify a fragment less than 200 bp of the coding sequence of the target gene to be analyzed by real-time RT-PCR assay. The 18-25 bp primer sequences were selected such that they correspond to two adjacent exons of the gene with at least one sequence spanning the boundary of the exons to avoid amplification of genomic fragent. The melting temperature for both primers was kept between 54-60ºC and the GC content between 40-60 %. The presence of pyrimidine base was preferred at the 3' position of the primers. The specificity of the primers was ensured using the e-PCR-Priemr search option in the Bisearch software (http://bisearch.enzim.hu/). The primers were obtained in the form of lyophilized powder which was reconstituted to the concentration of 100 µM using nuclease free 1X TE buffer, pH 8.0. The working stock of 10 pmol/µl was prepared by diluting the 100 µM stock as 1:10 using 1X TE buffer. The diluted primers were stored at -20ºC.

Table 3.8: List of primer sequences used for estimation of gene expression by real-time RT-PCR assay using SYBR Green method.

Name of primer	Forward (5'- 3')	Reverse (5'- 3')
GAPDH_RT-PCR	GAAGGTCGGAGTCAACGGATT	GAGTTAAAAGCAGCCCTGGTG
MYC_RT-PCR	GTAGTGGAAAACCAGCAGCC	CGAGTCGTAGTCGAGGTCAT
WIF1_RT-PCR	GGAGACCTCTGTTCAAAGCCT	ATTTGTTGGGTTCATGGCAGG
DCAF7_RT-PCR	CCCATACCCCACCACAA	TTCACCAACCCTCCACAC

KMT2A_RT-PCR	GCGGAGAGGATGAGCAAT	TTTCGGTCAGAGCCACTTC
STMN1_RT-PCR	ATTCTCAGCCCTCGGTCA	ACTTGCGTCTTTCTTCTGC
RAB22A_RT-PCR	TGTAAGAGAAGTCATGGAGAGAGAT	CAGGTTGGCGTCAGTGGAT
M6PR_RT-PCR	CAGTTTCCCACGACACGATG	GCCAGGAGTAGTAGTAGCA
IGF2R_RT-PCR	GAAAACCCTGGGAACTCCTG	CATAGCATGGCACCTCCTTA
LAMP1_RT-PCR	CAGATGTGTTAGTGGCACCC	TGTTCACAGCGTGTCTCTCC

First strand cDNA synthesis using M-MLV RT

Materials:

1) 5X First Strand Buffer

2) 100 mM dNTP mix

3) 0.1M Dithiothritol (DTT) solution

4) pdN(6) Random hexamer peimers (100 ng/µl) or OligodT primers

5) RNase inhibitor (20 U/µl)

6) M-MLV RT (200 U/µl)

7) *DEPC treated ultrapure water*

Method:

For gene expression analysis by real-time RT-PCR analysis, 500 ng of total RNA was reverse transcribed in a 10 µl reaction as follows.

1. The RNA samples were thawed on ice and diluted to a concentration of 250 ng/µl with DEPC treated ultrapure water.

2. The following components were mixed in 0.5 ml centrifuge tube as follows:

Component	Volume	Final concentration
Total RNA (250 ng/µl)	2 µl	500 ng
10 mM dNTP mix	0.5 µl	0.2 mM
pdN(6) Random hexamer peimers (100 ng/µl)	0.5 µl	5 ng
DEPC treated ultrapure water	3 µl	
Total volume	6 µl	

The reaction volume was scaled up depending upon the number of samples.

3. The contents were mixed, the tube was pulse spun. The sample was then heated at 65°C for 5 min to denature the secondary structures in RNA and quickly chilled on ice for 2 min.
4. The reaction mix was preared as follows:

Component	Volume	Final concentration
5X First Strand Buffer	2 µl	1X
0.1 M DTT	1 µl	10 mM
RNase inhibitor (20 U/µl)	0.25 µl	5 units
DEPC treated ultrapure water	0.25 µl	
Total volume	3.5 µl	

5. 3.5 µl of the above reaction mix was added to the denatured RNA, the contents were mixed and the tube was incubated at 37°C for 5 min to allow annealing of the random hexamer primers.
6. 0.5 µl of M-MLV RT was added to the reaction, the contents were mixed properly and the tube was further transferred to the thermal cycler set at below mentioned parameters.

Temperature	Time
25°C	10 min
37°C	60 min
70°C	10 min
4°C	∞

7. The synthesized cDNA was either immediately used for gene expression analysis or stored at -20°C until further used.

Real time PCR for gene expression analysis

Materials:

1) 2X PowerUP SYBR Green master mix

2) Gene specific forward primer

3) Gene specific reverse primer

4) DEPC treated ultrapure water

Method:

1. The primers were thawed on ice and tap mixed. The cDNA was diluted to 5 ng/µl (1:10) with DEPC treated ultrapure water. 10 ng of cDNA was used per reaction.
2. The master mix for 5 µl real-time RT-PCR reaction was set up as mentioned below:

Component	Volume	Final concentration
2X PowerUp SYBR Green master mix	2.5 µl	1X
Forward primer (10 pmol/µl)	0.25 µl	0.5 pmol
Reverse primer (10 pmol/µl)	0.25 µl	0.5 pmol
Total volume	3 µl	

Each real-time reaction was set up at least in duplicate. Master mix for each gene to be detected was prepared by scaling up the volumes depending upon the number of reactions

to set. No template control (NTC) reaction was set up for each master mix prepared and DEPC treated ultrapure water was added instead of cDNA to rule out the chances of erroneous measurement of gene expression due to accidental cross contamination.

3. 3 µl master mix was aliquot in separate tubes and 2 µl of diluted cDNA was added to the tubes. The contents were mixed and pulse spun.
4. The prepared reactions were loaded in 384 well plate and the position of each sample in the plate was documented.
5. The wells were sealed with optical adhesive sheet with the help of plastic applicator. The sealing of the wells was ensured by evenly moving the applicator through horizontal and vertical groves between the wells.
6. The bubbles in the wells were removed by gentle tapping and the plate was spun in a moving angle rotor at 2000 rpm for 2 min at RT to gather the contents of the wells to the bottom.
7. An appropriate program for SYBR Green method was selected and parameters were set in the QuntStudio 12K Flex/QuantStudio 5 real-time RT-PCR thermal cycler instruments, Applied Biosystems, Waltham, MA, USA using the QuantStudio software. The 384 well plate was kept in the heating block and the program was run. The PCR cycling parameters were as mentioned below:

Stage	Temperature	Time	Condition	No. of cycles
Hold	50ºC	2 min		1
	95ºC	10 min		1
PCR	95ºC	15 sec		40
	60ºC	1 min	Fluorescence data acquisition	
Melt curve	95ºC	15 sec		1

	60ºC	1 min	Fluorescence data acquisition	
	95ºC	15 sec		

The rampage rate was set at 1.6ºC/sec.

8. The data was analysed using QuantStudio software by comparative Delta Delta Ct method and the expression of target genes relative to the expression of GAPDH was expressed in terms of Relative quantity.

   $RQ=2^{\wedge(Ct\ Gene\ -\ Ct\ GAPDH)}*100$

9. The data was exported in Microsoft Excel format. Both raw data file and the analysed data file were preserved for record.

3.2.12. Stable expression of microRNAs in medulloblastoma cell lines in a doxycycline inducible manner using lentiviral vector pTRIPz

The transfection efficiency of available medulloblastoma cell line D283, D341, D425, HD-MB03 and Daoy is poor. Thus, the microRNAs miR-193a and miR-204 were stably expressed in a doxycycline inducible manner using a lentiviral pTRIPz vector. The genomic region encoding miR-193a (564 bp) and miR-204 (604 bp) was cloned earlier by restriction cloning method in the pTRIPz vector (Ph. D. Thesis-Pratibha Boga).

Stable polyclonal populations (P1 and P2) of D283, D425, D341, HD-MB03 and Daoy medulloblastoma cells expressing mir-193a and miR-204 were established by transducing lentiviral particles generated using pTRIPz constructs. A polyclonal population of each cell line expressing an empty pTRIPz vector was established as a control population.

Generation of lentiviral particles of empty and microRNA expressing pTRIPz constructs:

All the procedures involving the use of lentiviral particles were approved by institutional biosafety committee of ACTREC-TMC. All the procedures were performed in certified biosafety level 2 laminar flow cabinet (Esco Technologies, Hatboro, PA, USA). The infected cell cultures/contaminated plasticware and fluids were decontaminated using 10 % sodium hypochlorite solution and autoclaved in biohazard bags prior to disposal.

For generation of lentiviral particles, HEK93FT was used as packaging host cell line and the second generation packaging plasmids psPAX2 (coat), and pMD2.G (envelope) were used (psPAX2, Addgene plasmid # 12260 and pMD2.G, Addgene plasmid # 12259, were gift from Dr. Didier Trono). pAdvantage vector (Promega, Madison, WI, USA) was used for enhancing the efficiency of transient protein expression in host cells.

Method:

1. 6-7 X 10^5 HEK293FT cells were seeded in 60 mm culture dish form a 70-80 % confluent plate one day prior to the transfection. The plate should be 50-60 % confluent at the time of transfection.
2. The spent medium was replaced with the fresh complete medium 4 h prior to the transfection.
5. The cells were transfected with a total 12 µg of plasmid mixture consisting of transfer plasmid, coat plasmid and envelope plasmid in the ratio of 4:3:1. (6 µg of Transfer plasmid-pTRIPz-miR-193a/pTRIPz-miR-204/pTRIPz empty, 4.5 µg coat plasmid psPAX2 and 1.5 µg of envelope plasmid pMD2.G)

3. An appropriate volumes of the plasmids were mixed in a sterile 1.5 ml centrifuge tube and the plasmid DNA mixture was diluted up to 100 µl using sterile ultrapure water.
4. 100 µl of 0.5 M $CaCl_2$ solution was added dropwise to the plasmid mixture. (The contents of the tube were not mixed at this step.)
5. 200 µl of 2X BES Buffered Saline (2X BBS) solution was added to the tube dropwise to form a total of 400 µl of the transfection mixture. The content of the tube was mixed gently 2-3 times by pipetting.
6. The mixture was incubated for at least 20 min at room temperature (not more than 40 min).
7. The DNA-calcium phosphate complexes were then added dropwise to the HEK293FT cells, mixed gently by swirling the content of the plate and then the cells were incubated at 37ºC in a CO_2 incubator.
8. The medium was replaced with fresh complete medium 16-18 h after transfection.
9. The lentivirus containing cell culture supernatant was collected at 48 h and 72 h post transfection, centrifuged at 600g/1000 rpm at RT for 5 min in a moving angle centrifuge and filtered through 0.45 µ syringe filters.
10. The filtered supernatant was either directly used for transduction or subjected for concentration in the ratios of 5:1 – 10:1 by ultracentrifugation at 26500 rpm at 4ºC for 90 min.
11. For long term storage, the virus containing supernatant was made in to aliquots and stored at -80ºC until further use.

***Transduction with lentiviral particles for stable expression of miR-193a and miR-204 in medulloblastoma cell lines*:**

After generation of lentiviral particles, the viral titer in the harvested supernatant was assessed by transducing 5 X 10^4 HEK293FT cell with the serial dilutions of the viral supernatant. 24 h after transduction, the cells were induced with doxycycline for transgene expression and the number of RFP positive cells was estimated by flow cytometer 48 h after doxycycline induction. The viral titer in the supernatant was determined using the formula [(N X C/V) X D], where, N is the number of RFP positive cells, C is the number of cells at the time of seeding, V is the volume of viral supernatant used for transduction in ml and D is the dilution factor for the viral supernatant used for transduction. The titre was expressed as TU/ml of supernatant (TU-transducing units). MiR-193a was stably expressed in Group 3 medulloblastoma cell lines D283, D425 and HD-MB03 whereas, miR-204 was stably expressed in cell lines D283, D341, D425, HD-MB03 and Daoy.

1. One day prior to transfection, 1 X 10^5 cells of cell line D283, D341, D425, HD-MB03 and 5 X 10^4 cells of Daoy or HEK293FT cells were seeded in 35 mm culture dish.
2. 1 ml of neat, diluted or concentrated viral supernatant was added to the cells culture dish for transduction. 4 µg/ml of Polybrene (Hexadimethrine bromide) was added to the viral supernatant to neutralize the charge repulsion between the viral particles and the cell membrane.
3. The medium was replaced 18-24 h after transduction and the cells were further allowed to grow for 24 h.
4. The transduced cells were selected in presence of puromycin. (200 ng/ml for D283, D341 and D425 cells and 250 ng/ml for HD-MB03 and Daoy cells).

5. For the stable expression of transgene, the cells were treated with 2-4 µg/ml of Doxycycline. The expression of miR-193a and mir-204 in the polyclonal populations was assessed by real-time RT-PCR assay as described earlier.

3.2.13. MTT assay

The MTT assay is a colorimetric assay which measures the conversion of the tetrazolium dye to insoluble formazan crystals by living cells. Thus, this assay could be used for the assessment of cytotoxicity, cell growth and proliferation [168].

Reagents:

1) *MTT solution (5 mg/ml)*: 50 mg of MTT powder (3-(4,5-dimethylthiazol-2-yl)-2,5-diphenyltetrazolium bromide) was dissolved in 10 ml of 1X PBS. The solution was stored at 4ºC protected from light in 1 ml aliquots.
2) *Acidified 10 % Sodium dodecyl sulfate (SDS) solution*: 10 g of SDS powder was dissolved in 75 m of sterile ultrapure water. The dissolution was assisted by keeping the bottle at 60ºC for 1 h. 86.4 µl of concentrated HCl was added to the solution (final concentration of HCl-0.01N). The final volume of the solution was adjusted to 100 ml with sterile ultrapure water. The solution was stored at RT.

The effect of miR-193a expression on growth of medulloblastoma cell lines D283, D425 and HD-MB03 was studied by MTT assay for the period of 8-10 days as described below.

Method:

1. The vector control and P1, P2 polyclonal populations of Group 3 medulloblastoma expressing miR-193a were treated with 4 µg/ml of doxycycline for 48 h.

2. 1000 cells of each polyclonal population treated with doxycycline were seeded per well of 96 well plate in 100 µl of complete medium. The cells were seeded at least in triplicate for each time interval.
3. 50 µl of doxycycline containing medium was replenished at 48 h time interval.
4. 20 µl of MTT solution was added to the wells at the intervals of 48/72 h and the plate was incubated for 4 h at 37^{o}C in CO_2 incubator to allow the formation of formazan crystals.
5. The formazan crystals were dissolved by the addition of 100 µl of acidified 10 % SDS solution to each well with overnight incubation in CO_2 incubator.
6. The optical density of the wells was measured using ELISA plate reader at 540 nm wavelength against the reference wavelength of 690 nm.
7. The growth of the cells was calculated as follows:

   Percent Growth = {(O.D. Day 8/10 – O.D. Day 0)/ O.D. Day 0}*100
8. The Growth curves of the cell populations were plotted as line charts in GraphPad Prism v6.0 software.

3.2.14. Radiation sensitivity assay

The Group 3 cell lines grow in non-adherent manner. Therefore, the effect of miR-193a expression on radiation sensitivity of medulloblastoma cells was studied by MTT assay.

Method:

1. The vector control and P1, P2 polyclonal populations of Group 3 medulloblastoma expressing miR-193a were treated with 4 µg/ml of doxycycline.

2. 2000-2500 cells of each polyclonal population treated with doxycycline were seeded per well of 96 well plate in 100 µl of complete medium. The cells were seeded at least in triplicate for each time interval.
3. The cells in 96 well plates were irradiated at the doses of 2 Gy, 4 Gy and 6 Gy using Bhabhatron, an indigenously developed telecobalt machine developed by Bhabha Atomic Resarch Center, Mumbai, India. An untreated plate was kept as control.
4. 50 µl of doxycycline containing medium was replenished 24 h post irradiation and 48 h time interval henceforth.
5. 20 µl of MTT solution was added to the wells at 0 day (Immediately after irradiation), 3 day and 6 day time points. After the addition of MTT, the plates were incubated for 4 h at 37^{o}C in CO_2 incubator to allow the formation of formazan crystals.
6. The formazan crystals were dissolved by the addition of 100 µl of acidified 10 % SDS solution to each well with overnight incubation in CO_2 incubator.
7. The optical density of the wells was measured using ELISA plate reader at 540 nm wavelength against the reference wavelength of 690 nm.
8. The growth of the cells was calculated

   Percent Growth = {(O.D. Day 8/10 – O.D. Day 0)/ O.D. Day 0}*100
9. The effect of irradiation was calculated by normalizing the growth of irradiated cells with that of the untreated cells. The data was represented as line charts in GraphPad Prism v6.0 software.
10. The D_0 dose of radiation (the dose of radiation required to reduce the surviving population to 37 %) was calculated from the Graph [169].

3.2.15. Analysis of cell cycle and apoptosis by flow cytometry

The total DNA content of the cells varies depending upon the phase of the cell cycle. The fragentation of the cellular DNA is the hallmark of apoptosis. The DNA content within the cells could be efficiently quantitated by staining with variety of DNA binding dyes like propidium iodide, 7-amino actinomycin D (7-AAD) and zombie aqua etc. which bind the DNA in a stoichiometric ratio. The staining procedure includes fixation step followed by permeabilization which enables the entry of these dyes inside the cells. As the DNA in the apoptotic cells is fragented, the smaller fragents of the DNA are lost during fixation and permeabilization steps, reducing the cellular DNA content. The stained cells could be then analyzed by flow cytometry and depending upon the cellular DNA content, the cell cycle phase or apoptotic fraction of cells could be identified [170, 171].

The effect of miR-193a expression on cell cycle and apoptosis of Group 3 medulloblastoma cells was studied propidium iodide staining followed by flow cytometric analysis of the stained cells.

Materials:

1) *1X PBS(cold)*
2) *70 % Ethanol (chilled)*
3) *Popidium iodide solution (50 µg/ml): 5 mg of propidium iodide was dissolved in nuclease free ultrapure water to form 500 µg/ml solution. The resultant solution was further diluted 10 time using nuclease free ultrapure water to obtain 50 µg/ml solution of propidium iodide. The solution was stored at 4°C in 1 ml aliquots protected from light.*
4) *RNase A solution (100 µg/ml)*

Method:

1. Vector control and miR-193a expressing polyclonal populations of Group 3 medulloblastoma cell lines were induced with 4 µg/ml of doxycycline for 96 h before fixation.
2. The cells were harvested including the cells in the supernatant in 15 ml centrifuge tube and pelleted by centrifugation at 600g for 5 min at 4ºC in a moving angle centrifuge. (At least 0.5-1 X 10^6 cells are required for cell cycle analysis.)
3. The supernatant was discarded and the pellet was loosened by gentle tapping. The cells were suspended in 4 ml cold 1X PBS.
4. The cells were again pelleted by centrifugation at 600g for 5 min at 4ºC in a moving angle centrifuge.
5. The supernatant was discarded carefully without disturbing the pellet. The pellet was loosened by gentle tapping.
6. The cells were then fixed by dropwise addition of 1 ml chilled 70 % ethanol with constantly vortexing the tube. Vortexing helps avoiding cell clumping during fixation and ensures the single cell suspension. The cells tend to become sticky after fixation and were not handled using micropippete tips henceforth to avoid cell loss.
7. The cells were then kept at 4ºC for 24 h to ensure complete fixation. (The fixed cells could be stored at 4ºC for 3-4 weeks.)
8. Next day, the fixed cells were taken out and pelleted by centrifugation at 600g for 5 min at 4ºC in a moving angle centrifuge.
9. The 70 % ethanol was discarded. The pellet was loosened by gentle tapping and suspended in 1X PBS.

10. The cells were again pelleted by centrifugation the supernatant was discarded and the cells were suspended in 500 µl of 1X PBS. The cell suspension was then poured in polycarbonate flow tube.
11. 20 µl of 50 µg/ml of propidium iodide solution and 5 µl of 100 µg/ml RNaseA solution were added to the cell suspension. The tubes were then incubated at 37ºC in dark for 30 min.
12. The cells were then subjected to analysis using AttuneNxt Acousting Focusing Flow Cytometer. The fluorescence was read at 605 nm using an appropriate band pass filter.
13. The data was analysed using ModFit software. The pulse processing was performed by gating the single cell population considering the forward and side scatters of the individual pulse. The gated data was plotted in terms of histogram having fluorescence intensity on X-axis and number of acquired events on Y-axis.

3.2.16. Soft Agar colony formation assay

The effect of miR-193a expression on anchorage independent growth potential of Group 3 medulloblastoma cell lines was studied by soft agar colony formation assay. The cells were seeded in suspension manner in semi-solid matrix 0f 0.3-0.4 % agarose over a basal layer of 1 % agarose in complete medium.

Materials:

1) *2 % Low melting point (LMP) agarose solution*: 1 g of low melting point agarose was added to 50 ml of ultrapure water and dissolved by microwaving. The solution was further sterilized by autoclaving. The solution was taken out from the autoclave before solidifying and stored in water bath set at 42ºC with constant shaking.

2) *2X Complete DMEM/F12 medium*: To 80 ml 2X DMEM/F12 medium, 20 ml of FBS and 1 ml of 100X antibiotic-antimycotic solution was added.
3) *1X complete medium supplemented with 10 % FBS*

Method:

1. The vector control and miR-193a expressing polyclonal populations of Group 3 medulloblastoma cell lines D283, D425 and HD-MB03 were treated with doxycycline 48 h before seeding for soft agar colony formation assay.
2. 2X Complete medium and 2 % LMP agarose solution were mixed in equal proportions to make 1X complete medium containing 1 % agarose. The basal layer was prepared by pouring 1 ml of this mixture in a 35 mm dish. The medium was uniformly spread by swirling the dish and the basal layer was allowed to solidify at RT for at least 1 h.
3. The cells of each uninduced and doxycycline induced polyclonal population were harvested. The cell suspension were serially diluted with complete medium to obtain 1 X 10^4 viable cells per ml of medium.
4. 1000 cells per plate of each uninduced and doxycycline induced polyclonal population were seeded in a layer containing 0.4 % agarose in 1X complete medium. Cells of each polyclonal population were seeded in triplicate.
5. For cell seeding in triplicate, the components were mixed thoroughly as follows:

   400 µl of the cell suspension (1 X 10^4 cell per ml) + 2 ml of 1X complete medium + 800 µl of 2X complete medium + 800 µl of 2 % LMP agarose solution. (4 µg/ ml doxycycline containing medium was used for seeding induced polyclonal populations.)

6. 1 ml of the above mixture was immediately poured and spread over the previously prepared basal layer.
7. The upper layer was allowed to solidify at RT for at least 30 min before transferring the plates to CO_2 incubator.
8. The cells were fed with 100-200 µl of 1X complete medium (containing doxycycline for induced populations) after every 48 h.
9. The colonies containing at least 20 cells were counted from each plate after 10-15 days of seeding. The average colony count for each polyclonal population from three sets of experiment was plotted as a bar chart in GraphPad Prism v6.0 software. The significance of the differences was assessed by student's t-test.

3.2.17. Generation of orthotopic medulloblastoma xenograft in immunodeficient mice using stereotactic method of intracranial injection

The assessment of in vivo tumorigenic potential of miR-193a and miR-204 expressing polyclonal populations of Group 3 medullobastoma cell lines. The experiments were conducted as per the ethical guidelines approved by the Institutional Animal Ethics Committee of Tata Memorial Centre, ACTREC.

Reagents:

1) *Anaesthetic agents (Ketamine hydrochloride injection and Xylazine hydrochloride injection)*
2) *Analgesic agents (Buprenorphine, Neon Laboratories, India, Meloxicam, Intas Pharmaceuticals, India)*
3) *Sterile ocular lubricant (Neosporin ointment, Neon Laboratories, India)*

4) *1X PBS, sterile*
5) *70 % ethanol*
6) *Bone cement (Cat. No. W810, Ethicon Inc, Johnson & Johnson Ltd)*
7) *Tissue adhesive- VetBondTM (n-butyl cyanoacrylate) Cat. No. 1469SB, 3M Animal care*
8) *products, St Paul, MN, USA)*
9) *Doxycycline capsules (Biodoxi 100 mg capsules, Biochem Pharmaceuticals, India)*
10) *5 % Sucrose solution (w/v)*

Equipment:

1) *Small animal stereotaxic frame, Ultra Precise Just for Mouse Stereotaxic Instrument, 51730U, Stoelting, Wood Dale, IL, USA*
2) *Syringe needle 30G*
3) *Hamilton Glass syringe, Model 710 SN, 80868, 100uL Customized Syringe Fixed Needle, Needle length: 2 inches, Needle diameter: 26 Gauge, Point style: 4, Angle of Bevel: 45º*
4) *Sterile cotton buds*
5) *Surgical instruments including Fine forceps, Iris Scissors, Blunt forceps, sterile scalpel blades.*
6) *Electric microdrill and non-corrosive surgical grade steel drill bits (Ideal Micro Drill Kit, Cat. No.67-1000, Cell Point Scientific, Gaithersburg, MD, USA)*
7) *Regulated heating pad/chamber (with thermometer)*
8) *Electric clippers*

Animal type and strain used:

Immunodeficient mice: *NOD/SCID (NOD/NcrCrl-Prkdcscid)* received from The Jackson Laboratory, Charles River, USA.

Age and gender of animal:

6-8 weeks old both male and female animals were used.

Stable expression of Firefly luciferase 2 (Fluc2) gene in control vector and mir-193a/miR-204 expressing polyclonal populations of Group 3 medulloblastoma cell lines

The Fluc2 gene was stably expressed in polyclonal populations of medulloblastoma cell lines by lentivirus mediated gene transfer using the vector pCS-CG-CMV-FL2-Neo, in inhouse generated vector. The DNA fragent consisting of FLuc2 cDNA followed by an SV40 promoter and aminoglycoside 3'-phosphotransferase cDNA which confers resistance against aminoglycoside antibiotics (G418 Geniticin sulfate, Neomycin), was PCR amplified using pCAG-Luciferase vector (pCAG-luciferase was a gift from Prof. Snorri Thorgeirsson, Addgene plasmid # 55764) as template [172]. The restriction sites for the enzymes NheI and KpnI were introduced in forward and reverse primer, respectively. The amplified DNA fragent was cloned in pCS-CG vector (pCS-CG was a gift from Prof. Inder Verma, Addgene plasmid # 12154) [173] replacing the eGFP cDNA sequence by restriction cloning method. Thus, the vector pCS-CG-CMV-FL2-Neo was built for the high expression of FLuc2 gene and selection of the cells using G418. Lentiviral particles generated using this vector were transduced to vector control and miR-193a and miR-204 expressing polyclonal populations of Group 3 medulloblastoma cell lines. The cells expressing the FLuc2 were selected in presence of 750 µg/ml of G418. The

bioluminescence intensity of luciferase was confirmed by measuring the luciferase activity of the cells after addition of D-luciferin.

Method:

Preparation of cells for implantation:

1. The cells to be implanted were expanded in 100 mm culture dish and induced with doxycycline for 48 h.
2. The cells were harvested by centrifugation and suspended in an appropriate volume of fresh complete medium.
3. The cells were counted using haemocytometer and the number of viable cells per ml of cell suspension was determined by Trypan blue staining.
4. The volume of cell suspension containing 4 X 10^5 cells was aliquot in non-stick sterile 1.5 ml centrifuge tube.
5. The cells were spun and the medium was discarded. The cell pellet was loosened by tapping and the cells were suspended in 10 µl of sterile 1X PBS. The cells suspension was then kept on ice till the time of implantation.

Setup of equipment and requirements for surgery:

1. The surgical procedure was carried out in the sterile environment inside the laminar air flow cabinet. Thus, before starting the work, the surface area and side walls were sanitized by spraying 70 % ethanol. The stereotaxic frame and the heating plate was sprayed with 70 % ethanol, wiped properly with paper towel and placed inside the laminar air flow cabinet. The air flow was started and the cabinet was sterilized by ultraviolet light for 10 min.

2. The box containing the sterile surgical instruments, micro drill fit with sterile drill-bit, heating plate and Vetbond tissue adhesive were placed on right hand side of the stereotaxic frame whereas rest of the requirements were placed on left hand side of the stereotaxic frame.
3. The heating plate was switched-on and set at 37^{o}C. The bone cement was placed on the heating plate and was allowed to soften.

Induction of surgical anesthesia in mice for surgery:

1. The 6-8 weeks animals were used for the study. The mice were weighed and the dose of Ketamine hydrochloride (90-120 mg/kg body weight) and Xylazine hydrochloride (20 mg/kg body weight) was calculated.
2. The anesthesia was induced by injecting the required volumes of anesthetic agents through intraperitonial route using a syringe fixed with 30 gauge needle.
3. The animal was then placed in empty cage and was allowed to get immobilized. The induction of anesthesia was checked by pressing the paw of the hind legs.
4. The animals were then taken for the surgery once they were completely immobilized.

Surgical implantation of cells in the cerebellar region of mice:

1. Ophthalmic lubrication ointment was applied to the eyes of the anesthetized animal with the help of sterile cotton bud to prevent corneal drying.
2. Hair form the surgical site (area of skull between ears) were trimmed using the clippers.
3. The surgical site was disinfected by wiping with 70 % ethanol.
4. The animal was then placed dorso-ventrally on the stereotaxic frame and the incisors were hooked in the mouth fixture of the frame.

5. The ear bars were gently adjusted in the occiput of the skull and were sufficiently tightened. The height of the mouth fixture and ear bars was adjusted such that the skull remains in absolutely steady and flat position. The surgical site was again disinfected by wiping with 70 % ethanol.

Surgical opening of the skull:

6. About 1 cm long midline sagittal incision was made along the superior aspect of the cranium from intra-aural line towards the anterior aspect of head with the help of sterile surgical blade or iris-scissor.
7. The positions of the Brega (intersection of coronal and sagittal sutures) anteriorly and the lambda (conjunction of sagittal and lambdoidal sutures) posteriorly were identified.
8. The fascial membrane was cut away with the aid of pointed forceps and scissor.
9. A guiding needle was attached to the holder attached to dorso-ventral [106] axis of stereotactic apparatus and was adjusted to 2.5 mm posterior to lambda at midline by using vernier scale on anterio-posterior (AP) axis. The position was precisely marked with marker pen. The DV and AP coordinates required for precise implantation of cells in the cerebellum were determined by referring The Mouse Brain in Stereotaxic Coordinates: An Atlas of the sterotaxic coordinates of mouse brain [174].
10. A small hole was burr at the marked position precisely using the micro drill. The drilling was performed with utmost care not to cause accidental injury to the mouse brain.

Injection of cell suspension in cerebellar region:

11. The earlier prepared cell suspension was mixed by tapping the tube gently or with the help of micropipette. 5 µl volume of the cell suspension containing 2 X 10^5 cells was carefully drawn into the Hamilton syringe avoiding the aspiration of the bubbles.
12. The Hamilton syringe was attached in a perpendicular position to the syringe holder and positioned over the burr hole in the skull. The needle was slowly inserted through the whole 3 mm deep in cerebellum with the help of vernier scale by rotating the guidance screw in clock wise manner.
13. After waiting for 1 min, the syringe was gently pulled back by 0.5 mm. 5 µl of cell suspension was injected slowly over the time period of 3-5 min.
14. The syringe was allowed to rest in position for 1-2 min after injecting the cell suspension and then pulled out slowly by rotating the guidance screw in reverse direction.
15. The burr hole in the skull was sealed by applying softened bone cement with the help of blunt forceps. The incision was then closed by application of Vetbond tissue adhesive.
16. The ear bars were loosened and gently taken out. The incisors were removed from the mouth fixture.
17. The animal was placed on the heating pad maintained at 37ºC till it recovered from the anesthesia.
18. After the animal turned conscious, it was placed back in the housing cage and supplied with food.

19. The animals were fed with 1 g/lit of doxycycline in 5 % sucrose solution throughout the course of experiment. The doxycycline containing 5 % solution was replaced every 48 h with fresh solution. 3-5 drops of Malonex oral suspension (analgesic agent) were added for three days after surgery as a post-operative care for animals.
20. The tumor growth was monitored at 7 day interval by *in vivo* bioluminescence imaging.
21. The mice were sacrificed upon more than 15 % loss of body weight or on development of clinical signs like vertigo, hunched posture and abnormal gait.
22. Kaplan Meier survival analysis was done based on the survival duration of the mice. Log Rank test was used to determine the statistical significance of the difference in the survival of the vector control and miR-193a/miR-204 expressing tumor bearing mice.

3.2.18. *In vivo* Bioluminescence imaging

Instrument:

1) IVIS Spectrum In Vivo Imaging System, (Caliper Life Sciences) Perkin Elmer, Waltham, MA, USA.

2) Small animal Veterinary Isoflurane Vaporizer

3) *Anesthesia induction chamber*

Anesthetic agent:

1) Isoflurane (Forane injection, Abbott Laboratories, India or Aerrane injection, Baxter International, IL, USA)

Reagents:

1) D-luciferin, potassium salt (Cat. No.L8220 Biosynth AG, Switzerland): 3 mg/100 µl solution in 1X sterile PBS. 30 mg of D-luciferin, potassium salt was dissolved in 1 ml

of sterile 1X PBS. The solution was stored on ice protected from light until used for injection. The solution was prepared fresh before use.

2) *Sterile 1X PBS*
3) *70 % Ethanol*

Method:

Induction of anesthesia

1. The small animal Veterinary Isoflurane Vaporizer system was switched on. The oxygen supply switch and the exhaust valve was set at on position. The isoflurane supply was set at 3 % for the induction of anesthesia.
2. The animal was placed in the anesthesia induction chamber, the lid of the chamber was closed and the 3 % mixture of isoflurane in oxygen was allowed to flow in the induction chamber.
3. Once the animal was immobilized, the gas supply to the induction chamber was shut off.
4. The abdominal region of the animal was disinfected with 70 % ethanol. The animal was injected with 100 µl of the D-luciferin solution through the intraperitoneal route using the insulin syringe with 30 G needle. The animal was again placed back in the anesthesia induction chamber.
5. The isofulrane supply was reduced to 2 % and the supply valve was turned on. The animal was kept in the anesthesia induction chamber for 5 min after injecting with D-luciferin.
6. After 5 min, the isoflurane supply valve for the IVIS Spectrum instrument was turned on and the anesthetized animal was transferred to the IVIS Spectrum instrument.

In vivo bioluminescence imaging

7. After the animal was injected with D-luciferin, the Living Image 4.0 software provided with the IVIS spectrum system instrument was opened. Using the software, the IVIS Spectrum was initialized by clicking the initialize tab in the control window of the software.
8. Once the instrument was initialized, the animal position grid was opted for the size 'C'. The anesthesia supply was aligned to the upper border of the grid. For mice imaging, the image size was set at medium and the height of the object was set at 1.5 cm.
9. The animal was placed inserting the snout of the animal inside the nozzle of the isoflurane supply in the imaging system. The isoflurane supply was maintained at 2 % throughout the procedure.
10. The initial image was acquired at auto settings to determine the optimal exposure time. The exposure time was then set as determined and a series of 8-10 images was captured at 2 min interval. Images were always captured so that count of photons was detected in the recommended detectable range for the instrument i.e. 600 to 60000. Exposure time and camera aperture (f/Stop) settings were adjusted in case required.

Imaging data analysis:

11. All animals for the set of experiment were imaged at day 2 post implantation and later 7 day time interval. The last time point of imaging before euthanizing the control animals was considered as end-point for the experiment.
12. For data analysis, the image showing the highest count number from each series of images for all animals at every time point was identified and loaded in the software as a group.

13. A precise region of interest (R was drawn manually around the site of luminescence in any one of the image in the group. The ROI was copied and pasted in remaining images. The position in each image was precisely adjusted over the site of luminescence in each image.
14. The photon output was set to radiance and the luminescence intensity was measured for every image. The data was exported to the Microsoft Excel sheet and the data was sorted with respect to the animal.
15. The fold difference in the average radiance was calculated for Day 2 and Day 21/28 and was plotted as scatter chart for vector control and microRNA expressing group in Graphpad Prism v6.0 software. The average radiance for each time point for vector control and microRNA expressing group was also represented as a line chart. The student's t-test was used to calculate the significance of differences at the endpoint of the experiment.

3.2.19. Transcriptome profiling by RNA-Seq analysis

RNA-seq analysis was carried out to study the differential gene expression upon miR-193a and miR-204 expression in HD-MB03 and Daoy Medulloblastoma cells. The expression profiles of doxycycline treated miR-193a or miR-204 expressing P1, P2 populations were compared the expression profiles of doxycycline-induced parental and the vector control expressing HD-MB03 or Daoy cells.

1. The libraries were prepared from the total RNA using the Illumina TruSeq RNA library preparation kit. A unique index adaptor was used for library preparation for each sample.

2. The prepared libraries were quantified for the molar concentration using the real-time RT-PCR based approach. Parallely, the quality of the prepared libraries was assessed on the Agilent Bioanalyzer.
3. The libraries were pooled and the at the concentration of 100 nM each.
4. 10-12 pM pf the pooled libraries were subjected to 100 nucleotides single-read deep sequencing using the Illumina HiSeq 2500 (San Diego, USA) system to get a minimum of 10 million reads per library.
5. After sequencing, the data was demultiplexed based on the unique index sequences using the BaseSpace module to generate the Fastq files.
6. The sequence data for each sample was aligned to the reference human genome hg19 with the help of HISAT2 aligner software using the default parameters (https://ccb.jhu.edu/software/hisat2).
7. The count of the number of reads per gene was derived using the HTSeq-count algorithm (www.bioinformatics.babraham.ac.uk) using the default parameters.
8. The genes significantly differentially expressed upon miR-193a or miR-204 expression were identified using the DESeq2 module in the R-Bioconductor package (https://bioconductor.org/packages/release/bioc/html/DESeq2.html).
9. The data was normalized by variance stabilizing transformation using the DESeq2 software.
10. A heat map of the top 60 significantly (padj < 0.05) downregulated genes (in the decreasing order of $\log_2$ Fold Change) was plotted using the Multiple Experiment Viewer (http://mev.tm4.org) after median centering the data.

11. The Gene set enrichment analysis of the data was performed using the microRNA motif database, the KEGG reactome database and the hallmarks of cancer database using the GSEA software of the Broad institute to identify the networks and pathways affected by the microRNA expression. (https://www.gsea-msigdb.org/gsea/index.jsp)

3.2.20. Protein interaction network analysis

In order to identify the biological pathways enriched upon miR-193a or miR-204 expression, the set of genes significantly differentially expressed were analyzed using the ClueGO version 2.5.5 (http://apps.cytoscape.org/apps/cluego), a Cytoscape plug-in software. This software not only identifies enriched biological pathways but also builds a protein-protein interaction network among the differentially expressed genes that could help to identify the hub proteins. The GO biological processes database, Reactome pathway database and the KEGG database were used for the analysis. The genes significantly (padj < 0.1) upregulated ($\log_2$ Fold Change ≥ 0.8) upon miR-193a or miR-204 expression were analyzed by the ClueGO software. No additional interacting genes were added to build the network. Two-sided hypergeometric test was used for evaluating the statistical significance of enriched pathways. The p-value corrected using the Bonferroni step down correction method was considered significant at the cut-off of 0.01. For the inclusion in the protein-protein interaction network, a minimum of 2 % interacting genes and the Kappa score threshold of 0.47 was used [175].

3.2.21. Generation of luciferase reporter, mir-193a/miR-204 expression constructs and cMYC expression constructs.

Constructs required for the miR-193a promoter luciferase reporter assay

a) **MiR-193a promoter construct:** The putative miR-193a promoter (− 1292 bp to − 158 bp upstream of pre-miR-193a) was amplified by PCR using human lymphocyte DNA as a template. The promoter amplicon was cloned upstream to firefly luciferase cDNA in a promoter-less pGL3-basic luciferase reporter vector (Promega Corporation, Madison, WI, USA) (Thesis-Kedar Yogi). The E-box sequence in the promoter construct was mutated by site directed mutagenesis using the Q5 High fidelity DNA polymerase.

b) **pcDNA 3.0-cMYC:** The MYC expression vector was generated by cloning cMYC cDNA in pcDNA3.0 expression vector from the pBS-cMYC parent vector. (The pBS-MYC expression vector was (kindly provided by Dr. Joan Massague, Memorial Sloan Kettering Cancer Centre, NY, USA).

Constructs required for the 3'UTR luciferase reporter assay

a) **pcDNA 3.0 luciferase reporter construct:** The 3'UTR reporter vector was generated by cloning the luciferase cDNA from pGL3-basic vector in a pcDNA 3.0 plasmid vector in KpnI and BamHI sites. The firefly luciferase cDNA was amplified by PCR using the pGL3-basic vector as a template using Phusion high fidelity DNA polymerase. The restriction sites for the enzymes KpnI and BamHI were added to the forward and reverse primer, respectively which were used for the amplification of the firefly luciferase cDNA.

b) **3'UTR luciferase reporter constructs:** The microRNA binding sites in the putative target genes was identified by Targetscan software. The 3'UTR regions of the genes *ERBB4*, *KMT2A*, known miR-193a targets and *DCAF7*, *STMN1*, *MAX*, and *MAP3K3*, the putative miR-193a targets as well as 3'UTR of *EZR*, a known miR-204 target and *IGF2R* and *LAMP1*, the putative mir-204 targets were amplified by PCR using human lymphocyte DNA as template using Phusion high fidelity DNA polymerase. The BamHI and XhoI restriction sites were added to the forward and reverse primers, respectively used for the PCR amplification. The 3'UTR sequences were further ligated bewteen the BamHI and XhoI sites of the pCDNA 3.0 luciferase reporter vector. The microRNA biding sites in the 3'UTR constructs were mutated by site directed mutagenesis.

c) **MiR-193a and miR-204 expression construct in pcDNA 4.0 Myc His B vector:** The 564 bp genomic region encoding miR-193a and 632 bp genomic region encoding miR-204 were amplified by PCR using human lymphocyte DNA as template using Phusion high fidelity DNA polymerase. The EcoRI and XbaI restriction sites were added to the forward primer and reverse primer, respectively. The amplified fragents were cloned into pcDNA 4.0 Myc-His B plasmid vector between the EcoRI and XbaI restriction sites.

Reagents:

1) *Plasmids*: pGL3 bsaic, pcDNA 3.0, pcDNA 4 Myc His B, and pcDNA3 Luc
2) *DNA polymerases*: Taq DNA polymerase (Thermo Fisher scientific and NEB), Pusion high fidelity DNA polymerase (NEB), and Q5 high fidelity DNA polymerase NEB

3) *Template DNA for the amplification of the sequence of interest*: Human lymphocyte DNA
4) *Restrction enzymes*: Commonly used restriction from Thermo Fisher scientific and NEB
5) *DNA end modifying enzymes*: Fast Alkaline phosphatase (FastAP, Thermo Fisher scientific), Recombinant Shrimp Alkaline phosphatase (rSAP, NEB) and T4 DNA ligase (Thermo Fisher scientific and NEB)
6) QIAamp DNA mini Kit, QIAquick PCR Purification Kit, QIAquick Gel Extraction Kit, QIAGEN Plasmid Maxi kit, QIAGEN, GmBH, Hieledbrg, Germany
7) *Ultracompetent cells*: The E.coli DH5α and E. coli Stbl3 ultracompetent cells were prepared following Inoue's protocol for ultracompetent cell preparation.
8) *Bacteriological media*: Luria-Bertani broth, Luria-Bertani Agar supplemented with an appropriate antibiotics like Ampicillin or Kanamycin.

Method for cloning:

Primer designing for the amplification of sequence of interest:

The primer sequences of 18-20 nucleotide length were designed to amplify genomic regions encoding miR-193a and miR-204, promoter region of miR-193a, 3'UTR regions of the known and putative direct target genes of miR-193a and miR-204 using normal human lymphocyte DNA as template. The primer sequences were also designed to amplify Firefly luciferase cDNA using pGL3 basic vector as template. An appropriate restriction sites were added to the 5'end of the primer sequences with three extra nucleotide before the restriction sites to facilitate the bind of restriction enzyme to the DNA.

Table 3.9: List of primer sequences used for amplification of genomic sequences for generation of plasmid constructs.

Name of primer	Forward (5'- 3')	Reverse (5'- 3')
MiR-193a_Gen	GAGGAATTCGAGCGTCGTGTAACCCTTGG	GGTATCTAGAGTCCCGTCTGTCCACTCAAC
MiR-193a_Prom	TATGGTACCCGGTACTATGCTTGGCACT	CCAGATATCCAAGGGTTACACGACGCTC
ERBB4 _3'UTR	GTGGATCCGCCTCCACCTTACAGAC	TCTCTCGAGCCCTTCTCCTGCTCTACC
KMT2A_3'UTR	ATAGGATCCATGGCAGAGACTTCCTTGT	ATACTCGAGCAATGACCCGCTTTTCCTT
MAX_ 3'UTR	CTATCTAGACCCAAAGCAGGAAGAAG	TAATCTAGAGCAAATGCCAGGAACGG
DCAF7_3'UTR	ATAGGATCCGCAGGGGCTTTGTATTTCC	ATACTCGAGCAGTGGTGCTTCAGGGTAA
STMN1_3'UTR	ATAGGATCCTTTCTCCCCATCCCCTTC	ATACTCGAGCGTGCGGTCATTTGTGCGTT
MAP3K3_3'UTR	TAAGGATCCTGTTTTTCCTTCCAATGTCTG	TAACTCGAGTAATGCGCAACACTGG
EZR_3'UTR	CTCGAATTCTAGGAACTCCCTCAGATCCC	ATTTCTAGACTGCGGCATGGAATCCACCT
IGF2R_3'UTR	GACGGATCCGCACCTCCAACCAAATAAGACT	GTCCTCGAGCCTATCGGGACTAAAGCAGC
LAMP1_3'UTR	TTAGGATCCTTTCTCTGGGCTTAGGGTCC	CATCTCGAGAACGCACCGATCTCACATTG

PCR amplification:

1. The PCR reaction for the amplification of desired sequence of interest was set as follows:

Component	Volume	Final concentration
5X Phusion HF/GC Buffer	10 µl	1X
10 mM dNTP mix	1 µl	0.2 mM
Forward primer 10 pmol/µl	1 µl	0.2 µM each

Reverse primer 10 pmol/µl	1 µl	0.2 µM each
Template DNA (25 ng/µl)	5 µl	50 ng
Phusion DNA Polymerase 1U/µl	0.5 µl	0.25 U
Nuclease Free Water	31.5 µl	To make up total volume to 50 µl

The PCR cycling parameters were set in the Thermal cycler as follows:

Step	Temperature	Time	No. of cycles
Initial denaturation	95ºC	5 min	1
Denaturation	95ºC	45 sec	35
Annealing	56-66ºC	30 sec	
Extension	72ºC	1 min	
Final extension	72ºC	10 min	1
Hold	4ºC	∞	

2. 2 µl of each PCR product was electrophoresed on 1 % Agarose gel and the remaining PCR product was purified using the QIAquick PCR purification kit/ QIAquick Gel extraction kit according to manufacturer's instruction. The purified PCR product was further disgeted with resyriction enzyme and used for ligation in vector.

Restriction digestion of vector and insert and dephosphorylation of the digested vector

1. About 5 µg of plasmid vector DNA and 500 ng of purified PCR product was subjected for restriction enzyme digestion. The reaction was set up as follows:

Components	For Vector DNA	For PCR product	Final concentration
10X RE digestion buffer	5 µl	2 µl	1X
Restriction Enzyme 1 (10 U/µl)	1 µl	0.5 µl	1-5 U/µg of DNA
Restriction Enzyme 2 (10 U/µl)	1 µl	0.5 µl	

DNA	10 µl of 500 ng/ µl	10 µl of 500 ng/ µl	
Nuclease free water	33 µl	12 µl	
Total volume	50 µl	25 µl	

2. The reaction were incubated for 2 h to overnight at 37ºC in water bath.
3. For dephosphorylation of the free ends of the vector DNA, 10 µl of dephosphorylation mix was prepared and added to the RE digestion of the vector DNA. The mix was prepared as follows:

Components	Volume	Final concentration
RE digestion reaction of vector DNA from previous step	50 µl	
10X RE digestion buffer	5 µl	1X
Alkaline phosphatase enzyme (1U/µl)	5 µl	1 unit of enzyme per µg of DNA
Nuclease free water	40 µl	
Total volume	100 µl	

4. The reaction was further incubated for 1 h at 37ºC in water bath.
5. The restriction enzymes and alkaline phosphatase were inactivated by incubating the reaction at 80ºC for 10 min.
6. The RE digestion reaction for vector backbone was purified using QIAquick PCR purification kit according to manufacturer's instruction. The purified vector was diluted to the concentration of 25 ng/µl. The digested purified vector backbone was stored at -20ºC until further use.

Ligation of vector backbone and the insert and transformation of the ligation mix

The vector and the insert DNA were ligated in the ration of 1:6. Amount of insert (ng) = 6 X $\frac{Leng\quad of\ insert\ in\ bp}{leng\quad of\ vector\ in\ bp}$ X Amount of vector used

The ligation reaction was set up as follows:

Components	Volume	Final concentration
10X T4 DNA Ligase buffer	2 µl	
Digested vector DNA (25 ng/µl)	4 µl	100 ng
Digested insert DNA	- µl	Amount required to obtain vector : insert ratio of 1:6
T4 DNA Ligase (5 U/ µl)	1 µl	
Nuclease free water	- µl	Quantity sufficient to make 20 µl
Total volume	20 µl	

1. The ligation reaction was incubated at 22ºC for 2h to overnight. 10 µl of the ligation reaction was transformed to 100 µl ultracompetent *E. coli* cells.
2. The transformed cells were plated on the surface of the sterile Luria-Bertani agar plates supplemented with an appropriate antibiotic and the plate was incubated at 37ºC overnight.
3. On next day, the plates were observed for the presence of colonies formed by the transformed cells. The plates containing transformants were stored at 4ºC in refrigerator after securing the lid of the plate with a strip of parafilm.

Isolation of plasmid DNA from transformants by alkaline lysis method

Reagents:

1) *Solution I: Glucose Tris EDTA solution*

Components	Volume	Final concentration
2M Glucose	1.25 ml	50 mM
2 M Tris, pH 8.0	1 ml	10 mM
0.5 M EDTA, pH 8.0	0.625 ml	25 mM
Nuclease free water	47.05 ml	
Final volume	50 ml	

2) *Solution II: Alkaline lysis buffer* (Prepared fresh before use)

Components	Volume	Final concentration
5M NaOH	0.2 ml	0.2 N
20 % SDS	0.25 ml	1 %
Nuclease free water	4.55 ml	
Final Volume	5 ml	

3) *Solution III/ (3 M Potassium 5 M acetate, pH 4.8)*: 14.7 g of Potassium acetate was dissolved in 20 ml Milli Q water and the pH of the solution was adjusted to 4.8 using glacial acetic acid. The final volume was adjusted to 50 ml with nuclease free water. The solution was sterilized by autoclaving and stored at RT until further use.

Method:

1. Single colonies of the transformants were inoculated in 1-5 ml of the sterile Luria-Bertani broth supplemented with an appropriate antibiotic. The culture was incubated at 37ºC overnight with constant shaking at 150-180 rpm.

2. Next day, the bacterial cultures were centrifuged at 3000 rpm for 5 min at room temperature in 1.5 ml microcentrifuge tube. The cell pellet was suspended in ice cold 100 µl solution I by vortexing and incubated for 5 min at room temperature.
3. 200 µl freshly prepared solution II was added and mixed by gentle inverting the tubes for 8-10 times followed by incubation for 5 min on ice.
4. 150 µl solution III was added and immediately mixed by vortexing for 10 sec, followed by incubation for 5 min on ice.
5. The tubes were centrifuged at 12000 rpm for 10 min and clear supernatant was transferred to a fresh tube without disturbing the pellet.
6. To this supernatant, equal volume of phenol-chloroform (1:1) (for example, 250 µl of Tris saturated phenol and 250 µl of chloroform) was added per 500 µl of supernatant.
7. The content of the tubes was mixed thoroughly by vortexing and centrifuged at 12000 rpm for 5 min. The upper aqueous layer was removed carefully ad transferred to fresh tube.
8. Equal volume of chloroform was added to the aqueous layer and tubes were vortexed to thoroughly mix the contents. Step 6 was repeated.
9. 1 ml (or 2X volume) of absolute ethanol was added to the supernatant, mixed and the plasmid DNA allowed to precipitate at room temperature for 5 min.
10. The tubes were centrifuged at 12000 rpm at room temperature for 5 min. The supernatant was decanted carefully without losing the DNA pellet.
11. The DNA pellet was washed with 1 ml of 70 % ethanol. The tubes were centrifuged at 12000 rpm at room temperature for 5 min rpm for 5 min. The ethanol was aspirated and the DNA pellet was air dried.

12. The plasmid pellet was dissolved in 10-25 µl TE containing RNase (1 µg/ml) and further screened for insert and orientation by Restriction digestion analysis.
13. The presence of the insert was also confirmed by Sanger sequencing of the plasmid DNA using an appropriate sequencing primer.
14. The positive constructs were further retransformed and the plasmid DNA constructs were purified on a large scale using QIAGEN Plasmid Maxi kit following manufacturer's instructions. The purified plasmids were then used for downstream applications including the luciferase reporter assays.

Site directed mutagenesis for mutating E-box sequence in miR-193a promoter luciferase reporter construct and microRNA binding sites in the 3'UTR luciferase reporter constructs

The site directed mutagenesis was performed based on the principle of overlap extension PCR. High fidelity DNA polymerase capable of amplifying long DNA sequence was used for this purpose.

Primer designing: Primers were designed to have (a) 25 to 45 bases long primers were designed with the desired mutation kept at the center of the primer (b) reverse primer sequence should be complimentary to forward primer sequence, (c) the Tm was kept more than or equal to 78ºC and the GC content of more than 40 % with G or C preferred at 3' end. The E-box and microRNA binding sites were mutated to create new restriction site which aided in screening of the sequences carrying desired mutations.

Table 3.10: List of primer sequences used for site directed mutagenesis.

Name of primer	Forward (5'- 3')	Reverse (5'- 3')
MiR-193a_Prom_Mut1	GATGTGTCACCAGCGGGTGGAGCCAGGTCGG	CCGACCTGGCTCCACCCGCTGGTGACACATC
MiR-193a Prom_Mut2	GTGTCACCAGCACGGGGAGCCAGGTCGGGC	GCCCGACCTGGCTCCCCGTGCTGGTGACAC
MAX_3'UTR_Mut	AATTCTTTGGGTGGCATAGAGGTTTTGTATTGAGGATATCTGATGATGTT	GAAACCCACCGTATCTCCAAAACATAACTCCTATAGACTACTACAAAGCT
DCAF7_ 3'UTR_Mut	GAAACATGTTTCCAGTGGCCCGGGTGTCTTTCATTGCTTTGC	GCAAAGCAATGAAAGACACCCGGGCCACTGGAAACATGTTTC
STMN1_3'UTR_Mut	ATATCCAAAGACTGTACTGGCATATGTCATTTTATTTTTTCCC	GGGAAAAAATAAAATGACATATGCCAGTACAGTCTTTGGATAT
LAMP1_3'UTR_Mut	CTCAGATTTAAGCCTTACAATATAAAAGCCTCTGGCCGTCACACG	CGTGTGACGGCCAGAGGCTTTTATATTGTAAGGCTTAAATCTGAG
IGF2R_3'UTR_Mut	CTTTAACAGAAACTTTCAAATATAAAGAGTTTTTGTGATGGGGGAG	CTCCCCCATCACAAAAACTCTTTATATTTGAAAGTTTCTGTTAAAG

Method:

1. The PCR reaction for site directed mutagenesis was set up as follows:

Component	Volume	Final concentration
5X Phusion HF/GC Buffer or Q5 buffer	10 µl	1X
10 mM dNTP mix	1 µl	0.2 mM
Forward primer 10 pmol/µl	1 µl	0.2 µM each
Reverse primer 10 pmol/µl	1 µl	0.2 µM each
Template DNA (25 ng/µl)	2 µl	50 ng
DMSO	1.5 µl	3 %
Phusion/Q5 DNA Polymerase 1U/µl	1 µl	0.25 U

Nuclease Free Water	32.5 µl	To make up total volume to 50 µl
Total volume	50 µl	

2. Following conditions were set in the thermal cycler and the reaction was conducted.

Step	Temperature	Time	No. of cycles
Initial denaturation	98ºC	3 min	1
Denaturation	98ºC	45 sec	25
Annealing	56-66ºC	30 sec	
Extension	72ºC	30 sec per kb of DNA	
Final extension	72ºC	10 min	1
Hold	4ºC	∞	

3. 10 µl of the SDM PCR reaction was electrophoresed on 1 % Agarose gel to check the efficiency and specificity of the amplification.
4. To the remaining 40 µl reaction, 1 µl of restriction enzyme DpnI was added to the reaction and the reaction was incubated at 37ºC for overnight in water bath. The DpnI is a Dam methylation sensitive restriction enzyme and can digest the DNA only when Dam methylation marks are present. Thus, the DpnI treatment to the PCR reaction leads to the digestion of the template DNA which harbors the Dam methylation marks leaving the in vitro synthesized DNA intact. The DpnI enzyme from NEB is compatible with the Phusion and Q5 PCR buffers with 50-100 % enzymatic activity. Thus, the enzyme was directly added to the PCR reaction for the digestion of the template DNA.
5. The DpnI enzyme was inactivated by incubating the reaction at 85ºC for 10 min.
4. 10 µl of the DpnI digested PCR reaction was transformed to ultracompetent *E. coli* DH5α cells by heat-shock method. The transformed cells were plated on the surface of

the sterile Luria-Bertani agar plates supplemented with an appropriate antibiotic and the plate was incubated at 37^{o}C overnight.

6. On next day, the plates were observed for the presence of colonies formed by the transformed cells. The plates containing transformants were stored at 4^{o}C in refrigerator after securing the lid of the plate with a strip of parafilm.
7. The plasmid was isolated from the transformants by alkaline lysis method and screened with restriction enzyme digestion. The incorporation of desired mutations in the E-box sequence in the miR-193a promoter luciferase reporter construct and microRNA binding sites in the 3'UTR luciferase reporter constructs was confirmed by restriction enzyme digestion and Sanger sequencing using an appropriate sequencing primer.

3.2.22. Luciferase reporter assay

The luciferase reporter assay was used for assessment of the promoter activity and screening of the microRNA target genes. The assays were performed in HEK293FT cells with the transient transfection of reporter constructs, MYC/microRNA expreesion construct along with an EGFP expression plasmid using calcium phosphate DNA precipitation method of transfection as describe in section 3.2.12.

Reagents:

1) *Plasmids*: Luciferase reporter constructs, MYC expression construct, microRNA exprrression constructs and an EGFP expression construct pCS-CG-EGFP as mentioned in section 3.2.20.

2) *1 M Gly-Gly solution, pH 7.8*: 6.60 g of Gly-Gly was dissolved in 40 ml of ultrapure water. The pH of the solution was adjusted to 7.8 using concentrated HCl and the final

volume of the solution was adjusted to 50 ml witth ultrapure water. The solution was sterilized by filteration through 0.45 µ syringe ffilter and stored at RT until further use.

3) *1 M $MgSO_4$ solution*: 6.018 g of anhydrous $MgSO_4$ was dissolved in 40 ml of ultrapure water and the final volume of the solution was adjusted to 50 ml witth ultrapure water. The solution was sterilized by autoclaving and stored at RT until further use.
4) *0.25 M EGTA, pH 8.0*: pH 7.8: 4.754 g of EGTA was dissolved in 40 ml of ultrapure water. The pH of the solution was adjusted to 8 using 5N NaOH solution and the final volume of the solution was adjusted to 50 ml witth ultrapure water. The solution was sterilized by filteration through 0.45 µ syringe ffilter and stored at RT until further use.
5) *20 mM D-Luciferin solution*: 63.68 mg of potassium salt of D-luciferin was dissolved in 10 ml of strile ultrapure water. The solution was stored in aliquots at -20ºC until further use.
6) *1 M Potasium phosphate buffer, pH 7.8*:
7) *100 mM ATP solution*
8) *100 mM DTT solution (Sigma Aldrich, Cat. No. 43816)*
9) *2X BBS*
10) *0.5 M $CaCl_2$ solution*
11) *Triton X-100*

Working reagents:

1) *Cell lysis buffer*:

Components	Volume	Final concentration
1 M Gly-Gly, pH 7.8	1.25 ml	25 mM
1 M $MgSO_4$ solution	0.75 ml	15 mM
0.25 M EGTA, pH 8.0	0.8 ml	4 mM

Triton X-100	0.5 ml	1 % (v/v)
100 mM DTT	*	1 mM
Ultrapure water	46.7 ml	
Total volume	50 ml	

2) Luciferase assay buffer:

Components	Volume	Final concentration
1 M Potassium phosphate buffer pH 7.8	0.75 ml	15 mM
1 M Gly-Gly, pH 7.8	1.25 ml	25 mM
1 M $MgSO_4$ solution	0.75 ml	15 mM
0.25 M EGTA, pH 8.0	0.8 ml	4 mM
100 mM ATP	*	2 mM
100 mM DTT	*	1 mM
Ultrapure water	45.95 ml	
Total volume	50 ml	

3) Luciferin solution:

Components	Volume	Final concentration
1 M Gly-Gly, pH 7.8	1.25 ml	25 mM
1 M $MgSO_4$ solution	0.75 ml	15 mM
0.25 M EGTA, pH 8.0	0.8 ml	4 mM
20 mM D-Luciferin solution	*	0.2 mM
100 mM DTT	*	1 mM
Ultrapure water	45.95 ml	
Total volume	50 ml	

*- ATP, DTT and –luciferin were added prior to use.

Method:

1. $5x10^4$ HEK293FT cells were seeded per well of 24 well plate.
2. 1.5 µg DNA per well of 24 well dish was transfected using calcium-phoshate DNA precipitation method of 16-24 h post seeding of cells.
3. DNA mixture was prepared in autoclaved Milli-Q as given below.

For promoter luciferase reporter assay:

Components	Amount/Volume
pGL3 basic/pGL3b-Promoter	750 ng
pcDNA3/pcDNA3-MYC	500 ng
pCS-CG-EGFP	250 ng
Sterile ultrapure water	To make final volume of 12.5 µl
0.5M $CaCl_2$ solution	12.5 µl
2X BBS	25 µl

For 3'UTR luciferase reporter assay:

Components	Amount/Volume
pLuc/pLuc-3'UTR	100 ng
pcDNA3.0	250 ng
pcDNA4/pcDNA4-miR-193a/pcDNA4-miR-204	1000 ng
pCS-CG-EGFP	150 ng
Sterile ultrapure water	To make final volume of 12.5 µl
0.5M $CaCl_2$ solution	12.5 µl
2X BBS	25 µl

4. After addition of 0.5M $CaCl_2$ and 2X BBS solution, tubes were incubated for 20 min at RT. The transfection mix was added to the respective wells.
5. The cultre medium was changed after 16 h from transfection.
6. 72 h after transfection, the culture medium was removed and cells were washed twice with ice cold 1X PBS. 100 µl of cell lysis buffer was added per well of a 24 well plate and the cells were scraped from the surface of the well.
7. The cell clumps were disrupted by gently pipetting the volume several times and the cell suspension was transferred to a microcentrifuge tube.
8. The tube were allowed to stand on ice for 10 min and then centrifuged at 12000 rpm, 4^{o}C for 5 min. The supernatant was transferred in fresh microcentrifuge tubes.
9. The fluorescence and luminescence using Cytation Hybrid multimode reader, BIOTEK.
10. 10 µl of sample was added per well of 384 well Optiplate (Cat No. 6007290, Perkin Elmer), and fluorescence was measured at excitation and emission wavelengths of 485 nm and 515 nm. was measured Each sample was assayed in triplicates.
11. 20 µl of luciferase assay buffer and 10 µl of luciferin solution were added to sample and mixed by swirling the plate several times. The luminiscence was read immediately at exposure time of 0.1 sec.
12. The luciferase readings were normalized by dividing with the fluorescence values of the respective samples to compensate the variations in transfection efficiency among the wells.

3.2.23. Preparation of whole cell lysate and protein estimation

The total proteins were extracted from the vector control and microRNA expressing P1, P2 polyclonal of the medulloblastoma cell lines after 72 h of doxycycline treatment using the SDS cell lysis buffer. The doxycycline containing medium was replenished after 48 h.

For HDAC treatment experiments, the parental medulloblastoma cells were treated with DMSO or HDAC inhibitors sodium valproate or Trichostatin A, and the cells were lysed after the treatment in SDS cell lysis buffer. For, cycloheximide pulse chase experiment, the doxycycline treated vector control population and P2 polyclonal population expressing miR-193a were treated with CHX and the cell were lysed at 0 min, 30 min 60 min and 90 min after CHX treatment. For MG132 treatment experiments, the doxycycline treated vector control population and P2 polyclonal population expressing miR-193a were treated with MG132 and the cell were lysed at 0 min and 6 h after CHX treatment.

Reagents:

1) *1X PBS*
2) *1X SDS cell lysis buffer:* 62.5 mM Tris pH 6.8, 2 % w/v SDS, 1 % v/v Glycerol

   To prepare 10 ml of the SDS cell lysis buffer, 625 µl of 1 mM Tris-Cl pH 6.8, 1 ml of 20 % w/v SDS solution and 1 ml Glycerol was mixed with 7.325 ml of water. The buffer was stored at room temperature.

Method:

1. At the endpoint of each experiment, the cells were collected in the centrifuge tube and centrifuged at RT at 600 g.

2. The cell pellet was washed wit 1X PBS and the cell suspension was centrifuged at RT at 600 g.
3. The PBS was discarded without disturbing the cell pellet. The cell pellet was gently dislodged by tapping the tube.
4. An appropriate volume of the 1X SDS cell lysis buffer was added to the cells and mixed by pulse vortexing. (400-500 µl of 1X SDS lysis buffer was used to lyse cell harvested from 80-90 % confluent 600 mm culture dish).
5. The samples were denatured by incubating the tubes at 95-100ºC in water bath for 10 min.
6. The lysate was transferred to the 1.5 ml centrifuge tube and centrifuged at maximum speed for 90 min at 20ºC.
7. The supernatant was transferred to the fresh 1.5 ml centrifuge tube. The amount of total proteins in the prepared lysate was estimated using the Folin-Lowry method of protein estimation.
8. The samples were stored in aliquots at -20ºC until further use. Repeated freeze thawing was avoided to prevent degradation of the lysates.

3.2.24. Folin-Lowry's method of protein estimation

The protocol is adjusted for performing protein estimation in a 96-well plate.

Reagents:

1) 0.2 % Cupric sulphate solution: 0.1 g of cupric sulphate anhydrous (0.1917 g for penthydrate salt was dissolved in 40 ml ultrapure water and the final volume was

adjusted to 50 ml with ultrapure water. The solution was stored at RT protected from light until further use.

2) *0.4 % Sodium potassium tartarate*: 0.2 g of Sodium potassium tartarate was dissolved in 40 ml ultrapure water and the final volume was adjusted to 50 ml with ultrapure water. The solution was stored at RT until further use.
3) *20 % Sodium carbonate*: 10 g of anhydrous Na_2CO_3 was dissolved in 40 ml of ultrapure water and the final volume was adjusted to 50 ml with ultrapure water. The solution was stored at RT until further use.
4) *10 % Sodium dodecyl sulphate solution (10 % SDS)*: 10 g of Sodium dodecyl sulphate was dissolved in 60 ml of ultrapure water and keep at 60ºC until SDS dissolved completely. The final volume of the solution was adjusted to 100 ml with ultrapure water. The solution was stored at RT until further use.
5) *0.8 N Sodium hydroxide solution*: 1.6 g of Sodium hydroxide pellets were dissolved in 40 ml ultrapure water and the final volume was adjusted to 50 ml with ultrapure water. The solution was stored at RT until further use.
6) *Bovine serum albumin 10 mg/ml solution*: 10 mg of BSA was weighed approximately and dissolved in an appropriate volume of ultrapure water. The solution was filter sterilized by passing through 0.45 µ membrane filter and stored at -20ºC in small aliquots until further use.
7) *Bovine serum albumin 1 mg/ml solution*: 10 mg/ml BSA was diluted 1: 10 in ultrapure water to get 1 mg/ml solution.

Cu-tartarate carbonate solution (CTC): This solution was always prepared fresh from the stock solutions.

	For 10 ml CTC	For 5 ml CTC	For 2.5 ml CTC
0.2 % Cupric sulphate solution	2 ml	1 ml	0.5 ml
0.4 % Sodium potassium tartarate	2 ml	1 ml	0.5 ml
Ultrapure water	1 ml	0.5 ml	0.25 ml
Mixed well and added 20 % Sodium carbonate solution dropwise with constant vortexing at medium speed			
20 % Sodium carbonate	5 ml	2.5 ml	1.25 ml

Working Reagent A:

CTC : 10 % SDS : 0.8 N NaOH : Ultrapure water

1 : 1 : 1 : 1

Working Reagent B: Diluted Folin Ciocalteaues reagent in ultrapure water (1:6)

Method:

The reactions were prepared at least in duplicates in a transparent bottom 96 well plate according to the following table

Standards/ samples	Ultrapure water	1X Sample buffer	1 mg/ml BSA or Sample	Working Reagent A		Working Reagent B	
Blank	96 µl	4 µl	-	100 µl	**Mix well and incubate in dark for 10 min at RT**	50 µl	**Mix well and incubate in dark for 30 min at RT**
1 µg	95 µl	4 µl	1 µl	100 µl		50 µl	
2 µg	94 µl	4 µl	2 µl	100 µl		50 µl	
3 µg	93 µl	4 µl	3 µl	100 µl		50 µl	
4 µg	92 µl	4 µl	4 µl	100 µl		50 µl	
5 µg	91 µl	4 µl	5 µl	100 µl		50 µl	
7.5 µg	88.5 µl	4 µl	7.5 µl	100 µl		50 µl	
10 µg	86 µl	4 µl	10 µl	100 µl		50 µl	
15 µg	81 µl	4 µl	15 µl	100 µl		50 µl	
Sample	96 µl	-	4 µl	100 µl		50 µl	

The absorbance was read using the Elisa plate reader at 750 nm wavelength. The averaged reading of the blank wells was subtracted from each reading. A standard curve was prepared by plotting the absorbance of the standard concentrations of BSA on Y-axis against respective concentration on X-axis. The slope of the line was calculated and the concentration of the samples was determined using the standard equation of the regression line $y = mx + c$.

3.2.25. Sodium Dodecyl Sulfate-Polyacrylamide Gel Electrophoresis (SDS-PAGE)

The Tris-Glycine chemistry was used for separation and detection of proteins above 30 kDa for western blot analysis. For the analysis of proteins smaller than 30 kDa, histones and histone modifications, the total protein extracted from the cultured cells were resolved using the Tris-tricine gels.

The electrophoresis was carried out using the Mini-PROTEAN® Electrophoresis System from BIORAD, Hercules, CA, USA.

Reagents for Tris-Glycine chemistry:

1) *1.5 M Tris-Cl pH 8.8*: 90.855 g of Tris base was dissolved in 400 ml of ultrapure water. The pH of the solution was adjusted to 8.8 using concentrated hydrochloric acid and the final volume was adjusted to 500 ml with ultrapure water. The solution was sterilized by autoclaving and stored at 4ºC until further use.
2) *1 M Tris-Cl pH 6.8*: 60.57 g of Tris base was dissolved in 400 ml of ultrapure water. The pH of the solution was adjusted to 6.8 using concentrated hydrochloric acid and the final volume was adjusted to 500 ml with ultrapure water. The solution was sterilized by autoclaving and stored at 4ºC until further use.

3) *30 % Acrylamide/bis-acrylamide solution (29 % acrylamide w/v and 1 % bis-acrylamide w/v)*: 290 g of acyralamide and 10 g of N-N'-methylenebisacrylamide were dissolved in 800 ml of ultrapure water and the final volume of the solution was adjusted to 1 lit using ultrapure water. The solution was filtered through 1 no. Whatman filter paper. The solution was stored in amber colured wide mouth glass bottle at RT until further use.
4) *10 % SDS*
5) *10 % Ammonium persulfate (APS) solution*: 1 g of ammonium persulfate was dissolved in 5 ml ultrapure and the final volume was adjusted to 10 ml to make the 10 % solution of APS. The solution was store in dark at 4ºC until further use.
6) *TEMED (N,N,N',N'-tetramethylethanediamine)*
7) *10 X Tris-Glycine electrophoresis buffer (250 mM Tris base, 2.5 M glycine (pH ~ 8.3) and 1 % w/v SDS)*: 30.3 g of Tris base, 144 g of electrophoresis grade glycine and 10 g of SDS were dissolved in 800 ml ultrapure water and the final volume of the solution was adjusted to 1 lit with ultrapure. The solution was stored in glass bottle at RT until further use. When required, the 10X stock solution was diluted to 1X with ultrapure water.
8) *1X Gel loading dye solution (0.025 % w/v Bromophenol blue in 1X sample buffer)*: 2.5 mg of Bromophenol blue were added and dissolved in 10 ml of 1 X sample buffer. β-mercaptoethanol at the final concentration of 0.05 % was added to the protein solution before loading the samples.

Reagents for Tris-Tricine chemistry:

1) *3X Gel buffer (3 M Tris-HCl pH-8.45. 0.3 % w/v SDS)*: 36.34 g of Tris base was dissolved in 80 ml of ultrapure water and the pH of the solution was adjusted to 8.45 with concentrated HCl. 0.3 g of SDS was dissolved in this solution and the final volume was adjusted to 100 ml with ultrapure water. The solution was stored in glass bottle at RT until further use.
2) *AB-3 solution (49.5 % T and 3 % C mixture)*: 48 g of acyralamide and 1.5 g of N-N'-methylenebisacrylamide were dissolved in 80 ml of ultrapure water and the final volume of the solution was adjusted to 100 ml with ultrapure water. The solution was stored in amber colored wide mouth glass bottle at 7-8^{o}C until further use.
3) *Glycerol*
4) *10X Anode buffer (1 M Tris-HCl, pH 8.9)*: 60.57 g of Tris base was dissolved in 400 ml of ultrapure water. The pH of the solution was adjusted to 8.9 using concentrated hydrochloric acid and the final volume was adjusted to 500 ml with ultrapure water. The solution was sterilized by autoclaving and stored at 4^{o}C until further use.
5) *10X Cathode Buffer (1 M Tris, 1 M Tricine (pH ~ 8.25) and 1 % SDS w/v)*: 60.57 g of Tris base and 17.92 g of Tricine salt was dissolved in 400 ml of ultrapure water. The pH of the resultant solution remains ~ 8.25. 1 g of SDS was dissolved in this solution final volume was adjusted to 500 ml with ultrapure water. The solution was sterilized by autoclaving and stored at 4^{o}C until further use.

   10X stock solution of both anode and cathode buffers were diluted to 1X using ultrapure water at the time of use.

6) *1X Gel loading dye solution (0.025 % w/v Coomassie Brilliant blue G-250 in 1X sample buffer)*: 2.5 mg of Coomassie Brilliant blue G-250 were added and dissolved in 10 ml of 1 X sample buffer. β-mercaptoethanol at the final concentration of 0.05 % was added to the protein solution before loading the samples.

Method:

1. The Glass plates with 1mm or 1.5 mm spacers and short plates were washed thoroughly and dried. The spacer pate and short plate were arranged over each other, clamped together and mounted on gel casting stand.
2. The percentage of the resolving gel to be prepared was determined according to the size of the proteins detected in the western blotting and the resolving gel mixture was prepared as follows:

Tris-Glycine gel				
Ingredients	**Final concentration of acrylamide**			
	8 %	**10 %**	**12 %**	**15 %**
Ultrapure water	6.9 ml	5.9 ml	4.9 ml	3.4 ml
30 % acrylamide mix	4 ml	5 ml	6 ml	7.5 ml
1.5 M Tris (pH 8.8)	3.8 ml	3.8 ml	3.8 ml	3.8 ml
10 % SDS	150 µl	150 µl	150 µl	150 µl
10 % APS	150 µl	150 µl	150 µl	150 µl
TEMED	9 µl	6 µl	6 µl	6 µl
Total volume	15 ml	15 ml	15 ml	15 ml

Tris-Tricine gel	
Ingredients	**For 10 % final concentration of acrylamide**
Glycerol	1.5 g
Ultrapure water	~ 6.8 ml
AB-3	3 ml
3X Gel Buffer	5 ml
10 % APS	75 µl
TEMED	7.5 µl
Total volume	15 ml

3. The resolving gel mixture was poured between the plates without incorporating air bubbles leaving sufficient space for stacking gel. The upper layer of the resolving gel mixture was covered with ultrapure water to cut off its contact with air and enhance the polymerization.
4. After the resolving gel was polymerized, the water layer was blotted out and the stacking gel mixture was overlaid on the surface. The stacking gel mixture was prepared as follows.

Tris-Glycine gel 5 % stacking gel			**Tris-Tricine gel** 4 % stacking gel	
Ultrapure water	3.4 ml			
30 % acrylamide mix	830 µl		**Ultrapure water**	3.95 ml
1.5 M Tris (pH 8.8)	630 µl		**AB-3**	500 µl
10 % SDS	50 µl		**3X Gel Buffer**	1.5 ml
10 % APS	50 µl		**10 % APS**	45 µl
TEMED	5 µl		**TEMED**	5 µl
Total volume	5 ml		**Total volume**	6 ml

5. After pouring stacking gel, a comb of 1 mm or 1.5 mm thickness having desired number of teeth was inserted on the top of the plates inside the stacking gel.
6. After complete polymerization of the stacking gel, the comb was properly removed and the wells were flushed clean with the help of syringe fixed with 24 gauge needle for removal of gel debris. The casted gels were immediately used for separation of proteins or stored at RT in electrophoresis buffer until further use.
7. For resolving the proteins, the casted gels were mounted in the electrode assembly which was then placed in buffer tank. For Tris-Glycine gels, both the anode and cathode compartments were filled with 1X Tris-Glycine electrophoresis buffer whereas for Tris-Tricine gels, 1X anode and cathode buffers were filled in the respective compartments.
8. The equal amount of whole cell lysate proteins were taken, the tracking dye and 0.05 % β-mercaptoethanol was added as reducing agent. The samples were cracked at 95^{o}C for 3 min for Tris-Glycine gels and at 40^{o}C for 60 min for Tris-Tricine gels.
9. The cracked samples were loaded in wells along with the molecular weight marker and resolved by applying constant voltage. The constant voltage of 100-120 V was used for Tris-Glycine gels. The voltage was gradually increased for Tris-Tricine gels from 100 to 180 V during the course of electrophoresis. The gel was removed carefully and either stained with Coomassie blue to check for equal loading of the proteins or processed further for western blotting.

3.2.26. Western Blotting

The whole cell lysates prepared from medulloblastoma cells separated by SDS-PAGE were electrophoretically transferred to PVDF or nitrocellulose membrane. The desired proteins

of interest were detected by probing the blots with the specific antibodies. The blots were further probed with secondary antibodies conjugated to Horse Radish Peroxidase (HRP) to recognize the protein bound primary antibody. The final signals were obtained using chemiluminescent substrate for the HRP. The results were documented using Chemidoc and the data was analyzed by densitometric analysis.

Electrophoretic transfer of proteins from gel on membrane

The separated proteins were transferred on membrane using the Mini Trans-Blot® Cell from BIORAD.

The 0.45 or 0.2 µ pore size PVDF or nitrocellulose membranes were used for transfer. The 0.2 µ pore size membranes were used for the detection of proteins below 30 kDa size.

Reagents:

1) *Methanol*
2) 1X Transfer buffer *(25 mM Tris base, 250 mM glycine, 20 % v/v methanol)*: 3.03 g of Tris base and 14.4 g of electrophoresis grade glycine were dissolved in 600 ml ultrapure water and the final volume of the solution was adjusted to 800 ml with ultrapure. 200 ml of methanol was added and mixed properly. The solution was prepared fresh, and chilled before used for setting transfer.

Method:

1. The 3 MM Whatman filter paper, and PVDF or nitrocellulose membrane were cut according to the size of the gel. The cut PVDF or nitrocellulose membranes were activated by immersing them in methanol or ultrapure water respectively for 30 sec to

2 min. The activated membrane, filter papers and sponges were then kept in transfer buffer.

2. After the proteins are separated, the gels were removed from the plates and equilibrated for 5-10 min in transfer buffer.
3. The transfer sandwich was assembled in a tray containing transfer buffer. The black side of the transfer cassette was placed on lower side in the tray. The wet sponge was first placed on the surface of transfer cassette, wet 3 mm filter paper was placed over the sponge pad. The equilibrated gel was laid in reverse orientation of the loading sequence was laid on the surface of the filter paper. The activated membrane was then placed on the surface of the gel without trapping any air bubbles between the gel and the membrane. At this step, the sandwich was rolled with the help of roller to remove any trapped air bubbles. After this, another piece of filter paper and sponge pad was placed over the membrane. The cassette was carefully closed and secured in position by sliding the lock in position.
4. The assembled transfer sandwich was then placed between the transfer electrodes with the black side of the cassette facing the black (negative) electrode. The transfer chamber was filled completely with chilled transfer buffer.
5. The transfer was carried out at 20V-40V constant overnight in cold room. After the transfer the bolts were removed from the sandwich, the orientation of the bolt was marked by giving a cut to one of its corners and processed further.

Staining of proteins after transfer to membrane

After transferring the proteins on the membrane, the proteins were stained with the reversible stain Ponceaue S for assessing the efficiency of transfer. The images of the

Ponceaue S stained blots were documented and used for quantitation of total proteins per lane by densitometric analysis, which was later used as a loading control.

Reagents:

1) *Ponceaue S staining solution (0.25 % w/v in 1 % glacial acetic acid)*: 0.25 g of Ponceaue S dye was dissolved in 100 ml of 1 % glacial acetic acid. The solution was stored at RT protected from light.
2) *Destaining solution (5:4:1 mixture of methanol, water and glacial acetic acid respectively)*: 1 liter of destaining solution was prepared by mixing 500 ml of methanol, 400 ml ultrapure water and 100 ml of glacial acetic acid. The solution was stored in glass bottle at RT protected from light.

Method:

1. After removing the blots from the transfer sandwich, they were rinsed with 1X TBST.
2. The blots were then immersed in the Ponceaue S staining solution for 3-5 min.
3. The stained background from the blots was removed by rinsing the blots with destaining solution. The extra margins of the blots were cut off using sharp blade.
4. The images of the Ponceaue S stained blots were documented using the Chemidoc.
5. The Ponceaue stained blots were analyzed for total protein content per lane by densitometric analysis using Image lab software, BIORAD.
6. The Ponceaue S staining was removed by washing the blots with 1X TBST until the stain was removed.

Blocking, probing and detection:

Reagents:

1) *10X TBS (1.5 N NaCl, 1 M Tris-Cl pH 7.5)*: 121.14 g of Tris base and 87.7 g of NaCl was dissolved in 800 ml of ultrapure water. The pH of the solution was adjusted to 7.5 using concentrated HCl. The final volume of the solution was adjusted to 1 lit with ultrapure water. The solution was sterilized by autoclaving and stored at RT until further used. The 10X stock solution was diluted to 1X whenever required.
2) *1X TBS with 0.1 % Tween-20 (TBST)*: 1 ml of Tween-20 detergent was added to 1 lit of 1X TBS and mixed well.
3) *Blocking buffer (1-5 % milk or BSA in 1X TBST)*: 1 to 5 g of non-fat dry milk powder or bovine serum albumin was dissolved in 100 ml of 1X TBST. The blocking buffer containing milk needs to be freshly prepared. The BSA containing blocking buffer could be prepared in advance and stored at -20^{o}C until further used.
4) *Chemiluminescent substrate*: Westar ETA C 2.0 Ultra, Cynagen, Italy for detection of proteins in picogram range and Advansta Western Bright ECL substrate, Advansta, USA for detection in femto-lower femto range.

Method:

1. After removing the Ponceaue S stain, blocking was performed to block empty space on the surface of the membrane so as to prevent non-specific binding of the antibody to the membrane. The blots were kept immersed in the blocking solution for 1 h with gentle shaking at RT. The milk or BSA was used as blocking agent as suggested by the

manufacturer of the primary antibody used in the experiment or was determined by conducting pilot experiments.

2. The blocking buffer was discarded and the blots were washed with 1X TBST 3 times for 5 min each with gentle shaking.
3. The blots were then probed with an appropriate primary antibody diluted in blocking buffer.

Table 3.11: The working conditions for all antibodies used in this study are mentioned in the following table:

Name of Antibody	Description	Blocking buffer	Dilution	Duration of incubation
Anti-PARP	Cell Signaling Technology #9542, Rabbit polyclonal	5 % milk in 1X TBST	1:1000 in 5 % BSA	4ºC O/N
anti-p16 (CDKN2A) (C-20)	Santa Cruz Biotechnology (sc-468), Rabbit polyclonal	5 % milk in 1X TBST	1:500 in 2 % BSA	4ºC O/N
Anti-MAX (S-20)	Cell Signaling Technology #4739, Rabbit polyclonal	5 % milk in 1X TBST	1:500 in 5 % BSA	4ºC O/N
Anti-MAX (C-17)	Santa Cruz Biotechnology (sc-197), Rabbit polyclonal	5 % milk in 1X TBST	1:200 in 2 % BSA	4ºC O/N
Anti-CCND1 antibody (72-13G)	Santa Cruz Biotechnology (sc-450), Mouse monoclonal	1 % BSA in 1X TBST	1:3000 in 2 % BSA	4ºC O/N
Anti-MCL1	Cloud Clone Corporation (PAC615Hu01), Rabbit polyclonal	5 % milk in 1X TBST	1:1000 in 2 % BSA	4ºC O/N
Anti-Histone H3 (trimethyl K4) (C42D8)	Cell Signaling Technology #9751, Rabbit monoclonal	5 % milk in 1X TBST	1:1000 in 5 % BSA	4ºC O/N
Anti-Histone H3 (acetyl K27) (D5E4)	Cell Signaling Technology #8173, Rabbit monoclonal	5 % milk in 1X TBST	1:1000 in 5 % BSA	4ºC O/N

Anti-H3 (trimethyl K27)	Abcam (ab6002), Mouse monoclonal	3 % BSA in 1X TBST	1:1000 in 2 % BSA	4ºC O/N
Anti-Histone H3	Abcam (ab10799), Mouse monoclonal	3 % BSA in 1X TBST	1:2000 in 2 % BSA	4ºC O/N
Anti-MYC (N-262)	Santa Cruz Biotechnology (sc-764), Rabbit polyclonal	5 % milk in 1X TBST	1:2000 in 5 % BSA	4ºC O/N
Anti-MYC (D84C12)	Cell Signaling Technology #5605, Rabbit monoclonal	5 % milk in 1X TBST	1:1000 in 5 % BSA	4ºC O/N
Anti-Histone H3 (acetyl K9)	Abcam (ab10812), Rabbit polyclonal	3 % BSA in 1X TBST	1:3000 in 2 % BSA	4ºC O/N
Anti-IGF2R/CI-M6PR (D3V8C)	Cell Signaling Technology #14364, Rabbit monoclonal	5 % milk in 1X TBST	1:1000 in 5 % milk	4ºC O/N
Anti-LAMP1 (H4A3)	Developmental Studies Hybridoma Bank, Mouse monoclonal	5 % milk in 1X TBST	1:5000 in 2 % BSA	4ºC O/N
Anti-CTSB (D1C7Y)	Cell Signaling Technology #31718, Rabbit monoclonal	5 % milk in 1X TBST	1:1000 in 5 % BSA	4ºC O/N
Anti-CTSD	Cell Signaling Technology #2284, Rabbit polyclonal	5 % milk in 1X TBST	1:1000 in 5 % BSA	4ºC O/N
Anti-p62/SQSTM1 (D5E2)	Cell Signaling Technology #8025, Rabbit monoclonal	5 % milk in 1X TBST	1:1000 in 5 % BSA	4ºC O/N
Anti-GAPDH (6C5)	Santa Cruz Biotechnology (sc-32233), Mouse monoclonal	5 % milk in 1X TBST	1:3000 in 2 % BSA	4ºC O/N
Anti-γ-Tubulin	Siga (Merck) T3559, Rabbit polyclonal	5 % milk in 1X TBST	1:3000 in 2 % BSA	4ºC O/N
Anti-Vinculin (E1E9V)	Cell Signaling Technology #13901, Rabbit monoclonal	5 % milk in 1X TBST	1:5000 in 5 % BSA	4ºC O/N
Secondary antibodies				
Goat anti-Rabbit IgG (H+L) Cross-Adsorbed Secondary Antibody, HRP	Thermo Fisher Scientific (Pierce) G-21234		1:2000-1:10000 in 2 % milk	Room temperature for 1-2 h
Goat anti-Mouse IgG (H+L) Cross-Adsorbed Secondary Antibody, HRP	Thermo Fisher Scientific (Pierce) G-21040		1:2000-1:10000 in 2 % milk	Room temperature for 1-2 h

4. The primary antibody solution was drained off and the membrane was washed six times for 5 min each with 1X TBST, on the rocker with vigorous shaking.
5. Then the membrane was then incubated with an appropriately diluted horseradish peroxidase (HRP) conjugated secondary antibody (anti-IgG) for 1 h at RT on the rocker with gentle shaking.
6. The secondary antibody solution was drained off and the membrane was washed six times for 5 min each with 1X TBST and then three times with 1X TBS with vigorous shaking.
7. The proteins of interest wer detected on antibody probed blots using the enhanced chemiluminescent substrates. The images of the blots were captured using Chemidoc instrument, BIORAD using optimal settings.
8. The blots were reprobed with the antibody for GAPDH, γ-tubulin or vinculin which served as an endogenus loading controls.

Reprobing blots earlier probed with different antibody

After detection of one protein of interest, the blots were reprobed to either detect the expression of another protein of interest in the same set of protein samples or for detection of the endogenous control proteins.

Reagent:

1) Stripping buffer: Restore™ PLUS Western Blot Stripping Buffer, Thermo Fisher Scientific, Carlsbad, USA

Method:

1. After finishing detection of the first protein of interest, the blots were washed 3 times for 5 min each with gentle shaking.
2. The blots were then immersed in the stripping buffer and kept on gentle shaking for 5-15 min at RT.
3. The stripping buffer was drained off and the blots were washed 3 times for 5 min each with vigorous shaking to remove the traces of stripping buffer.
4. The blots were further processed for the detection of another protein of interest following the same steps from blocking to detection.

Densitometric analysis of western blots

The densitometric analysis of western blots or Ponceaue S stained blots was performed using the Image Lab software, BIORAD or using Image J following the steps mentioned by the software designers.

The band intensities of the proteins of interest for each sample were normalized to the intensity of the band for endogenous loading control for the same lane. The normalised band intensities of the protein of interest in test samples were represented as fold change in expression with respect to the expression of protein of interest in control sample. For CHX chase experiments, the normalization for MYC expression levels was done using the measured total intensity of the respective lane from the Ponceaue S stained blot.

3.2.27. Statistical analysis

The GraphPad Prism version 6.0 was used for statistical analysis of the data.

Chapter 4

To investigate the effect of miR-193a expression on the growth and malignant behavior of medulloblastoma cells and delineate the underlying molecular mechanism.

4. Objetive 1- Results and Discussion

4.1. Results

MicroRNA expression profiling of medulloblastoma tumor tissues has shown that WNT subgroup medulloblastomas have the most distinctive microRNA profile with overexpression of several microRNAs. MiR-193a is one of the most WNT subgroup-specific microRNA, which is downregulated in non-WNT medulloblastoma tumors [9, 151]. It is known to be downregulated in various malignancies and is an experimentally proven tumor suppressor microRNA [176, 177]. The fact that miR-193a acts as a tumor suppressor in several cancers and its expression is restricted to the WNT subgroup, which has the best overall survival, intrigued us to investigate its role in the pathogenesis of medulloblastoma. In this section, the role of miR-193a in the biology of medulloblastoma is described.

4.1.1. Regulation of miR-193a promoter activity and expression by MYC

The expression of miR-193a is primarily restricted to the WNT subgroup as evaluated by the real-time RT-PCR analysis in a cohort of 103 medulloblastomas [151]. The median expression level in the WNT subgroup medulloblastomas was RQ = 7.5 (CI 3.3 to 19.5). The median expression levels of miR-193a in the SHH, Group 3, and Group 4 tumors, on the other hand, were 0.13, 0.4, and 0.09, respectively (Fig. 4.1A) [151]. A recently published microarray expression data of an independent large cohort consisting of 763 medulloblastomas (MAGIC cohort) was retrieved from the Gene Expression Omnibus (GEO85217) [78]. Analysis of miR-193a expression in the MAGIC cohort also showed that the expression of miR-193a to be restricted to the WNT subgroup medulloblastomas (Fig. 4.1B). The miR-193a expression in the medulloblastoma cell lines D283, D425, HD-

MB03 and Daoy was also found to be low as studied by the real-time RT-PCR assay (Fig. 4.1A).

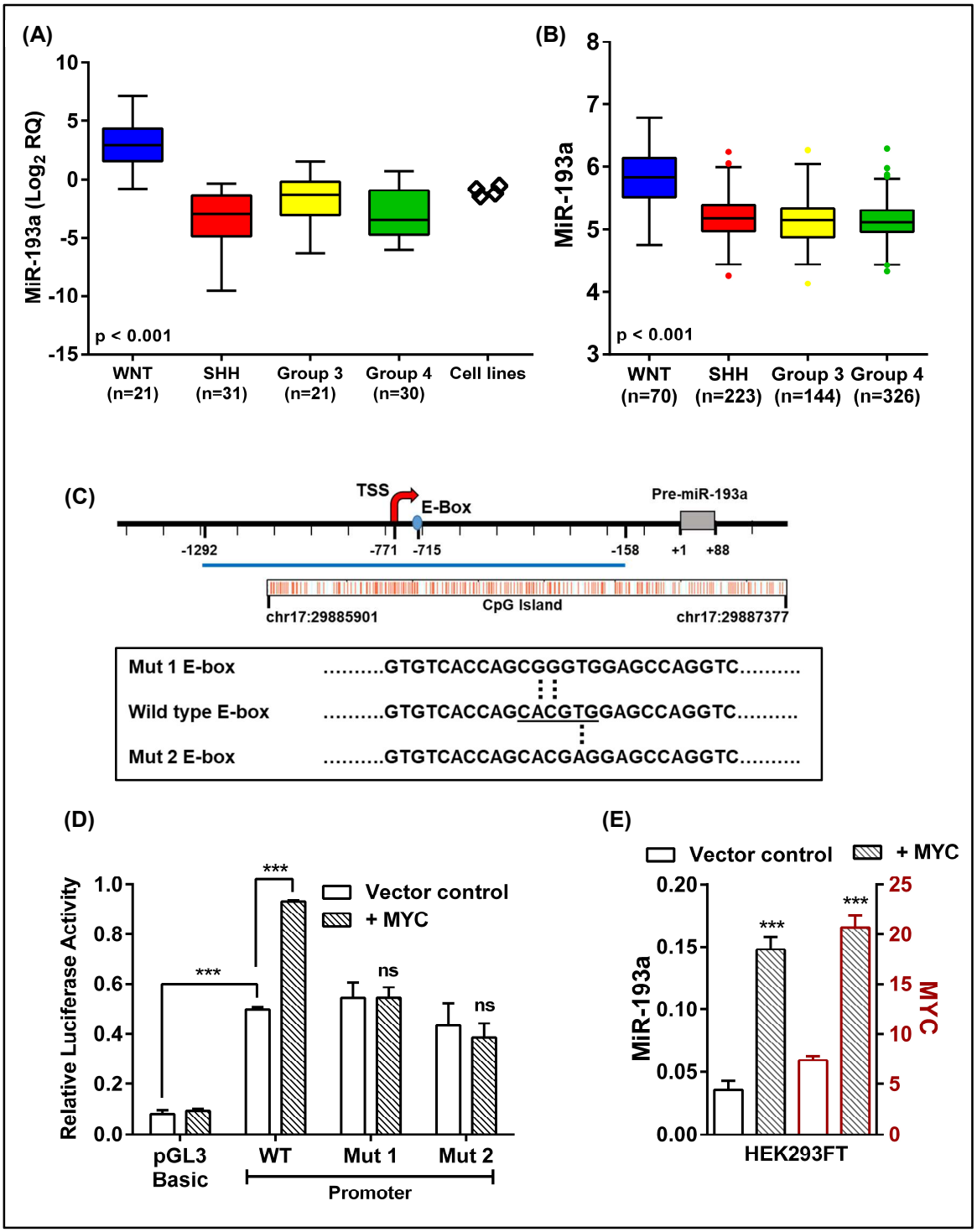

Fig 4.1: Expression of miR-193a in the four molecular subgroups of medulloblastomas. Regulation of miR-193a promoter activity by MYC and induction of miR-193a expression by MYC in HEK293FT cells.

(**A) and (B)** MiR-193a expression in the four molecular subgroups of 103 medulloblastomas from an Indian cohort and 763 medulloblastomas from the MAGIC cohort, respectively. **(C)** A schematic showing location of the CpG island, E-box, the transcription start site (TSS) relative to the pre-miR-193a start site (+ 1) on chromosome 17, and the mutations introduced in the E-box sequence by the site-directed mutagenesis. **(D)** Bar chart depicting the relative luciferase reporter activity of the miR-193a promoter wild-type (WT) construct or the mutant construct (Mut 1, Mut 2) upon cotransfection with the MYC expression construct or vector control into the HEK293FT cells. **(E)** Bar chart depicting the expression of miR-193a and MYC upon transient transfection of MYC expressing construct or the vector control in the HEK293FT cells as evaluated by the real-time RT-PCR analysis. *** and ns indicates $p < 0.0001$ and non-significant, respectively.

To unravel the molecular mechanism underlying the WNT subgroup-specific expression of miR-193a, the miR-193a promoter region was analyzed for the presence of a binding site for the WNT signaling transcription factors. MYC is a bHLH leucine zipper transcription factor and is one of the downstream targets of the WNT signaling pathway. The UCSC genome browser showed the MYC-binding motif (E-box) near the validated transcription start site [106] of the miR-193a gene. The binding of MYC to this E-box sequence has been earlier demonstrated experimentally by CHIP-Seq in multiple cell lines, including the K562 and A549 cells in the 'ENCODE' project (www.encodeproject.org). Therefore, the miR-193a promoter region (1134 bp DNA fragment corresponding to -158 to -1292 with respect to the pre-miR-193a +1 harboring the miR-193a TSS and the E-box) was cloned upstream of the luciferase cDNA in a promoter-less pGL3-Basic vector (Ph. D. thesis: Kedar Yogi). Luciferase reporter assay showed a basal promoter activity of this construct upon transient transfection into the HEK293FT cells. Co-transfection with MYC-expressing plasmid construct resulted in a 1.7 to 2 fold induction of the basal activity of the miR-193a promoter. Further, the E-box sequence in the miR-193a promoter was altered by the site-directed mutagenesis. The mutation in the E-box nucleotide sequence abrogated the induction of the miR-193a promoter activity by MYC (Fig. 1C and 1D).

To further validate MYC induction of the miR-193a promoter, a construct expressing MYC (pcDNA3-cMYC) or an empty pcDNA 3.0 vector as control was transiently transfected in the HEK293FT cells. The total RNA from the transfected populations was isolated 72 h post-transfection, and the expression of miR-193a and *MYC* was analyzed by real-time RT-PCR assay. The transient transfection of MYC expressing construct in the HEK293FT cells resulted in around 2.5 fold increase in the expression of *MYC*. Further, the endogenous expression levels of miR-193a increased by ~ 3 fold upon *MYC* expression (Fig. 2E). Thus, the MYC-driven induction of the promoter activity and the expression levels of miR-193a suggests that MYC could induce miR-193a expression in the WNT subgroup medulloblastomas.

4.1.2. CpG methylation status of the miR-193a promoter region across medulloblastoma subgroups and in medulloblastoma cell lines

WNT subgroup medulloblastomas overexpress MYC as a result of the constitutively activated WNT signaling pathway. MYC is known to be overexpressed in Group 3 medulloblastomas whereas 10-17 % of these tumors harbor MYC amplification. The expression of MYC was isis high in almost all tumors belonging to the WNT and Group 3 medulloblastomas in an Indian cohort of 103 medulloblastomas (Fig. 4.2A) [151]. The Group 3 medulloblastoma cell lines D425 and HD-MB03 overexpress MYC with an amplification of the MYC oncogene, whereas D283, another Group 3 cell line has MYC overexpression without amplification of the MYC locus [178]. The expression of MYC in Group 3 medulloblastoma cell lines is comparable to that observed in the Group 3 medulloblastomas.

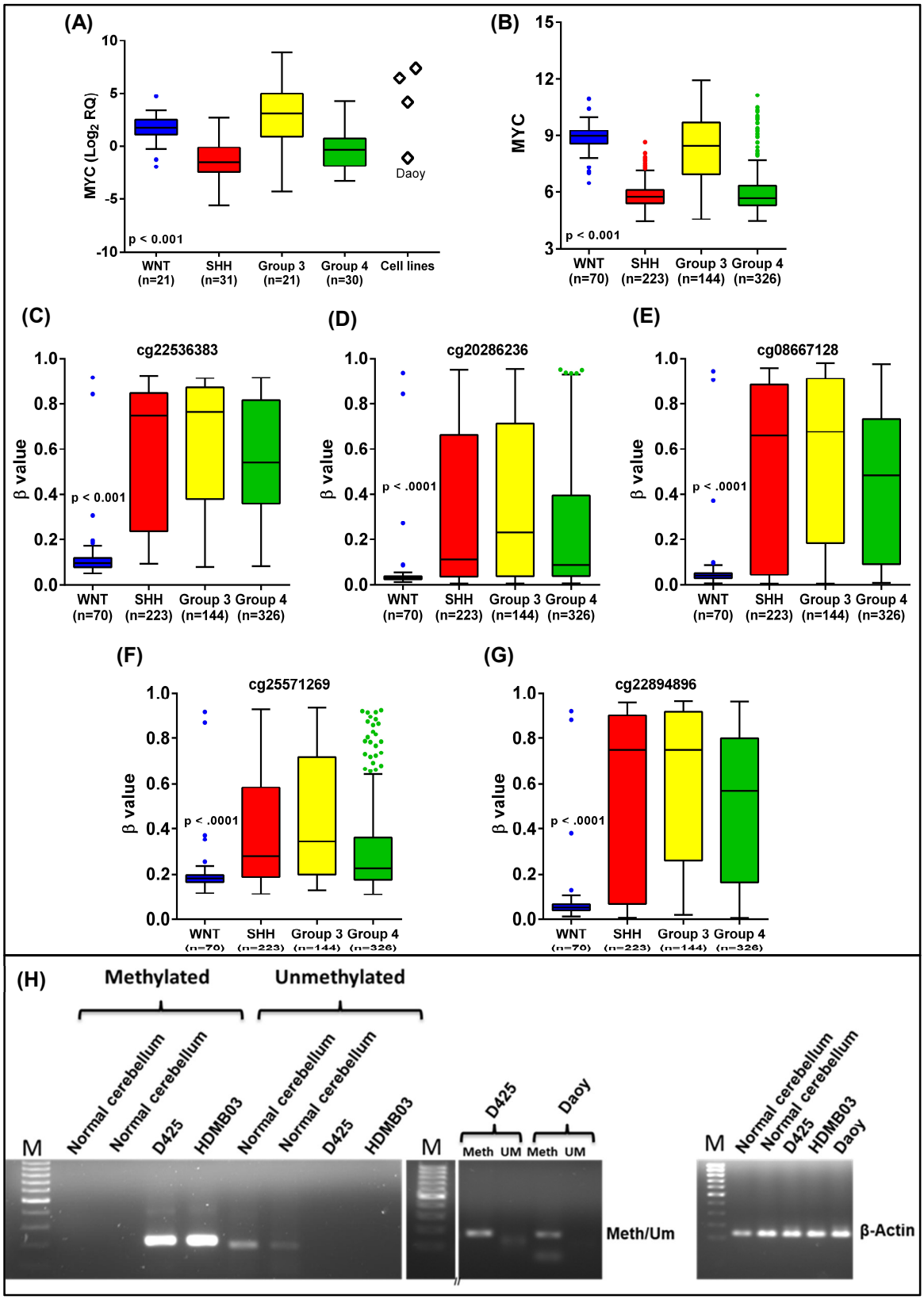

Fig 4.2: Expression of MYC and the methylation status of the miR-193a promoter region in the four molecular subgroups of medulloblastomas.

(**A) and B)** Expression levels of MYC in the four molecular subgroups of medulloblastomas from the Indian cohort and MAGIC cohort, respectively. (**C), (D), (E), (F), and (G)** Box and whisker plots representing the methylation status of multiple CpG residues in the miR-193a promoter region, in the four molecular subgroups of medulloblastomas from the MAGIC cohort. (**H)** MiR-193a promoter CpG methylation status in the medulloblastoma cell lines using two distinct sets of primers (I, II) as studied by the methylation-specific PCR. The presence of PCR amplified product of the expected size (~200 bp) in the PCR reaction using the primers specific for methylated or un-methylated CpG residues indicate methylated or unmethylated CpG residues, respectively in the indicated cell line or in the normal cerebellum.

MYC expression in Daoy cells belonging to SHH subgroup was low and was equivalent to that observed in the SHH medulloblastomas as studied by the real-time RT-PCR assay (Fig. 4.2A). MYC is overexpressed in the WNT and Group 3 medulloblastomas in the microarray expression data for 763 samples of the MAGIC cohort (Fig. 4.2B). MYC was found to induce the miR-193a expression by directly interacting with the E-box sequence in the miR-193a promoter region. However, miR-193a is not expressed in Group 3 medulloblastomas and medulloblastoma cell lines despite having high expression of MYC.

Analysis of the miR-193a genomic locus in the UCSC genome browser shows the presence of the CpG island covering the entire miR-193a primary transcript, including the region upstream of the TSS. A data from recently published Genome-wide methylation profiling study of 763 medulloblastomas [78] was analyzed for the methylation status of the CpG island in the promoter region of miR-193a. The analysis showed methylation of multiple CpG residues in the three non-WNT subgroups of medulloblastomas, as indicated by high β-values in these subgroups. On the other hand, the β-values in the WNT subgroup medulloblastoma are low, indicating the absence of methylation at these CpG residues in WNT subgroup (Fig. 3C, D, E, F, and G)The methylation status of the miR-193a promoter

in the medulloblastoma cell lines was studied by the methylation specific PCR. The CpG island in the miR-193a promoter region was found to be methylated in the Group 3 cell lines D425 and HD-MB03 as well as in the Daoy cell line belonging to the SHH subgroup. Thus, the expression of miR-193a is likely to be repressed by promoter hypermethylation in non-WNT medulloblastomas.

4.1.3. Restoration of miR-193a expression upon treatment with a DNA methylation inhibitor, 5-aza-2'-deoxycytidine

The medulloblastoma cell line D283, D425, HD-MB03, and Daoy were treated with varying concentrations of DNA methylation inhibitor, 5-aza-2'-deoxycytidine. The cell lines D283 and D425 failed to grow in the presence of the lowest dose of 5-aza-2'-deoxycytidine. Therefore, HD-MB03 and Daoy medulloblastoma cells were treated with 100 nM concentration of the DNA methylation inhibitor, 5-aza-2'-deoxycytidine for 5 days. The medium was replenished each day. Total RNA was extracted from the 5-aza-2'-deoxycytidine treated cells after 5 days, and the expression of miR-193a was analyzed using the real-time RT-PCR assay. The expression of *WIF1*, a gene known to be epigenetically repressed in medulloblastoma cell lines, was used as a positive control [179]. The expression levels of *WIF1* increased by 2.5 to 4.0 fold upon treatment with 5-aza-2'-deoxycytidine indicating the efficacy of the treatment. Further, the expression levels of miR-193a also increased by 2.5 to 4.0 fold upon treatment with 5-aza-2'-deoxycytidine compared to the vehicle-treated cells (Fig. 4). Thus, miR-193a appears to be downregulated in non-WNT medulloblastomas and cell lines due to promoter hypermethylation.

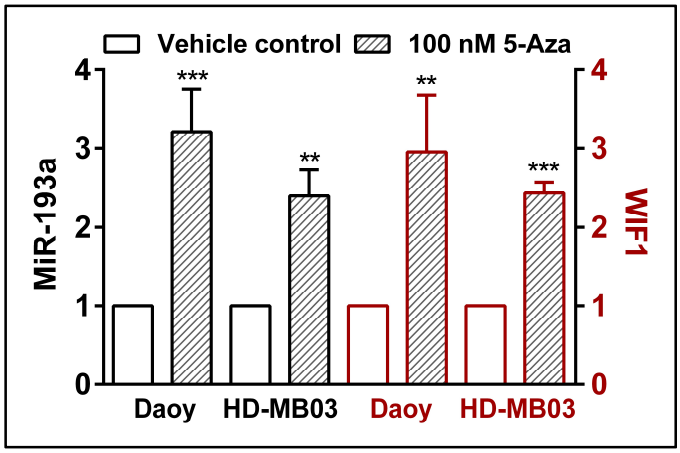

Fig 4.3: Fold change in the expression levels of miR-193a and WIF1 in the 5-aza-2′-deoxycytidine-treated medulloblastoma cells as evaluated by the real-time RT-PCR assay. ** and *** indicate $p < 0.001$ and $p < 0.0001$, respectively.

4.1.4. Establishment of stable polyclonal populations of D283, D425, and HD-MB03 expressing miR-193a in a doxycycline-inducible manner and effect of miR-193a expression on the proliferation of medulloblastoma cells

The Group 3 medulloblastoma cell lines do not express mir-193a. For the stable expression of miR-193a, the genomic region encoding miR-193a (564 bp) was cloned in pTRIPZ doxycycline-inducible lentiviral vector (Ph.D. thesis-Pratibha Boga). Group 3 medulloblastoma cell lines D283, D425, and HD-MB03 were transduced with the lentiviral particles generated using the pTRIPZ-miR-193a construct or the parental pTRIPZ vector Two stable microRNA expressing polyclonal populations (P1 and P2) and an empty vector expressing polyclonal population were selected in the presence of Puromycin. The expression of miR-193a in the stable polyclonal populations of medulloblastoma cell lines was assessed by the real-time RT-PCR assay before and after doxycycline induction for 48 h. MiR-193a was found to be expressed in the doxycycline-induced P1, P2 populations in

the range of RQ 0.5 to 4.5 at levels similar to those in the WNT subgroup tumors (Fig. 4.4A and 4.1A).

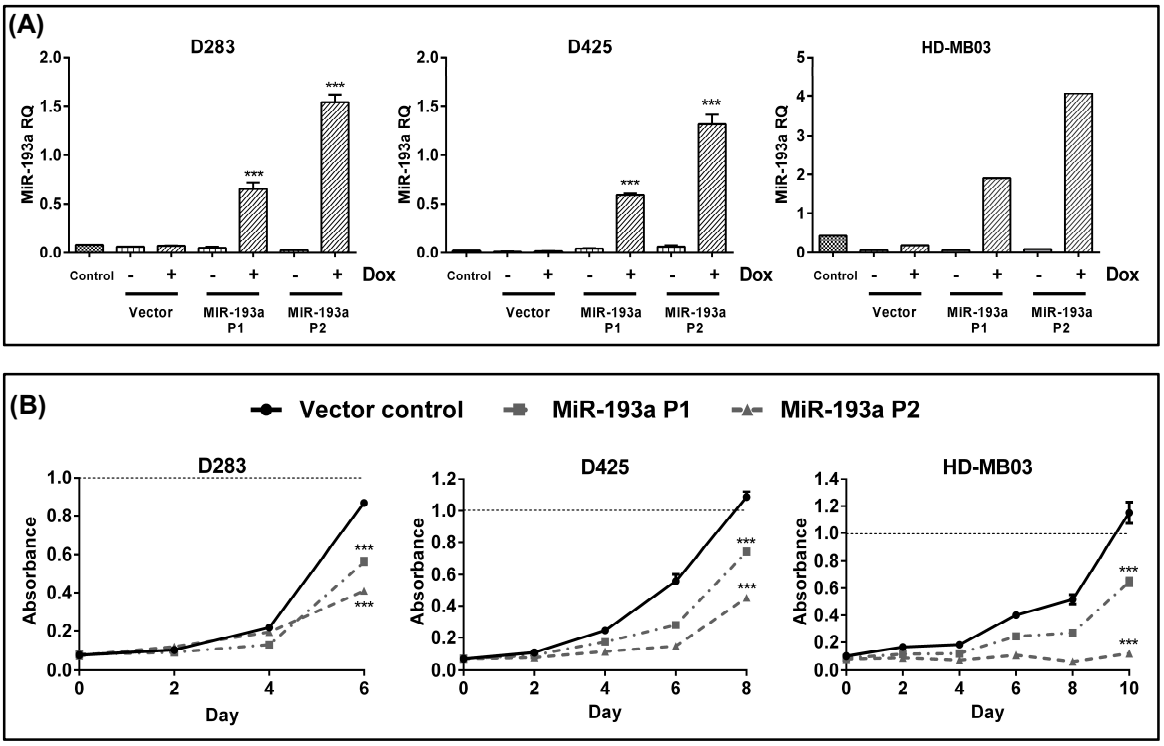

Fig 4.4: Exogenous expression of miR-193a in medulloblastoma cell lines and effect of miR-193a expression on the proliferation of medulloblastoma cells.

(**A)** Bar chart depicting the expression levels of miR-193a in the indicated medulloblastoma cell lines and its established P1 or P2 polyclonal populations stably expressing pTRIPZ-miR-193a construct or the parental pTRIPZ vector before and after doxycycline (Dox) treatment for 48 h. (**B)** Growth curves of the doxycycline-treated vector control or P1, P2 populations of the indicated medulloblastoma cell line as studied by the MTT assay. *** indicates $p < 0.0001$

The effect of miR-193a expression on the proliferation of medulloblastoma cells was studied by the MTT assay. For induction of miR-193a expression P1, P2 polyclonal populations and the vector control population were induced using 4 µg/ml of doxycycline for 48 h. One thousand cells of each population were then seeded in 100 µl of doxycycline containing medium per well in a 96 well plate in triplicates. The growth of the cells was

monitored over a period of 10-12 days. MiR-193a expression inhibited the growth of all the cell lines by 40 to 90 %, depending upon the level of miR-193a expression ($p < 0.001$) (Fig. 4.4B).

4.1.5. Effect of miR-193a expression on the cell cycle profile of medulloblastoma cells

The effect of miR-193a expression on the cell cycle profile of medulloblastoma cells was studied by flow cytometry. The cellular DNA content was evaluated by Propidium iodide staining using flow cytometry after doxycycline induction of miR-193a expression for 96 h. The vector control and P2 polyclonal population of D283 and HD-MB03 medulloblastoma cells were then fixed in chilled 70 % ethanol, followed by staining with Propidium iodide. The cell cycle analysis showed a higher percentage of miR-193a expressing P2 polyclonal populations in the G0/G1 phase of the cell cycle (76 % (± 3.3) of D283, and 67.11 % (± 2.74) of HD-MB03 cell line) as compared to the corresponding vector control population (57.51 % (± 2.25) of D283 and 45 % (± 1.66) of HD-MB03 cell line) indicating the cell cycle arrest in the G0/G1 phase upon miR-193a expression. The analysis also showed 20 to 30 % of miR-193a expressing cells in the sub-G0/G1 fraction, indicating the induction of cell death upon miR-193a expression (Fig. 4.5A and 4.5B). The western blot analysis showed the cleavage of PARP [Poly (ADP-Ribose) Polymerase] upon miR-193a expression, further confirming the apoptotic cell death (Fig. 4.5C). The expression of p16, a CDK4/CDK6 inhibitor, was also found to be increased in medulloblastoma cells upon miR-193a expression, which is consistent with the growth arrest of the cells in the G0/G1 phase of the cell cycle (Fig.4.5D).

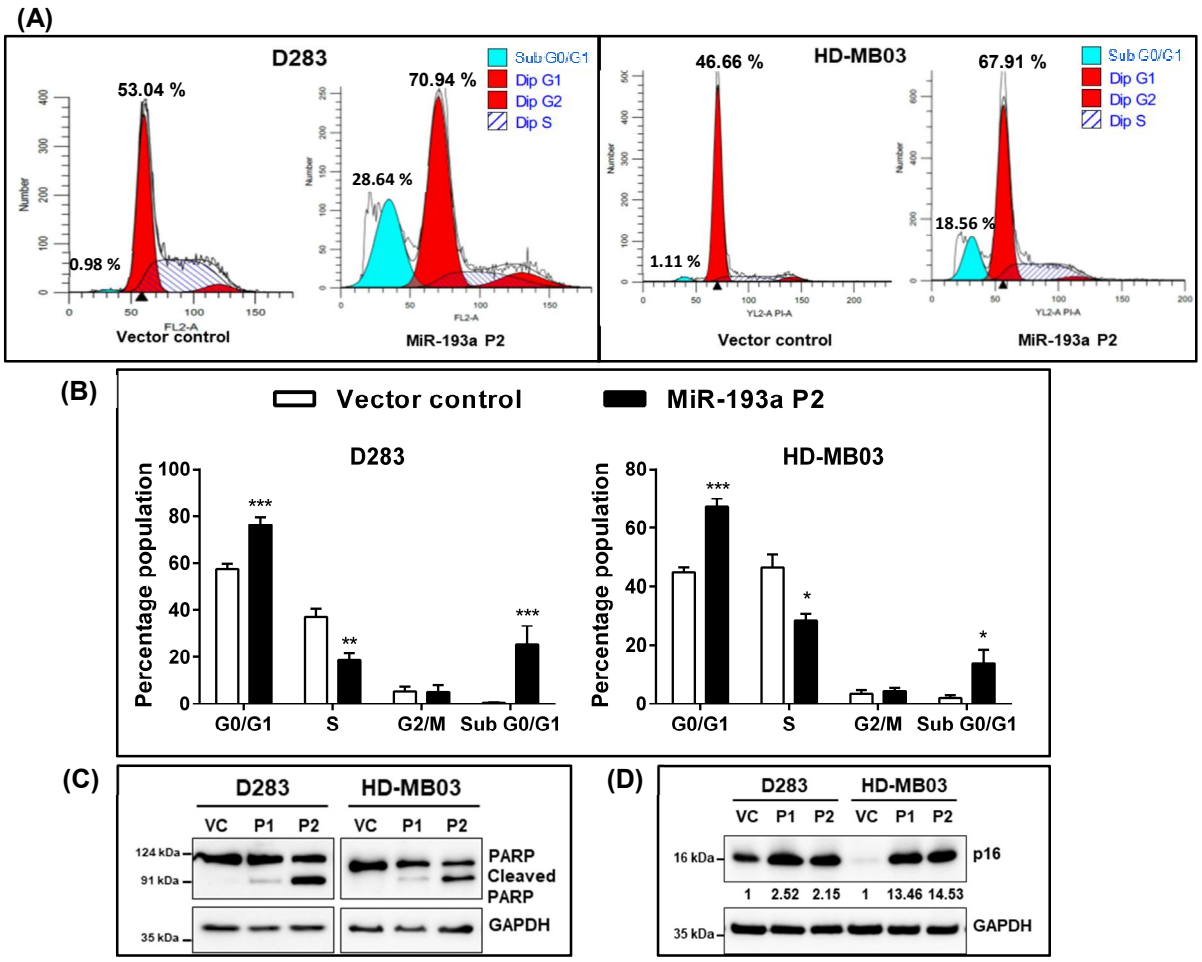

Fig 4.5: Effect of miR-193a expression on the cell cycle profile of D283 and HD-MB03 medulloblastoma cells.

(A) Cell cycle analysis of D283 and HD-MB03 medulloblastoma cells as evaluated by flow cytometry. **(B)** Bar charts depicting the percentage of the cell population of the indicated cell line in each phase of the cell cycle obtained from three independent experiments. **(C) and (D)** Western blot analysis of PARP, a marker of apoptotic cell death, and p16, a CDK4/CDK6 inhibitor in the indicated medulloblastoma cells. GAPDH was used as a loading control. VC: vector control. ***, ** and * indicate $p < 0.0001$, $p < 0.001$ and $p < 0.01$, respectively

4.1.6. Effect of miR-193a expression on the radiation sensitivity of medulloblastoma cells

Medulloblastoma cell lines D283 and HD-MB03 grow in a semi-adherent to non-adherent manner. Hence, the effect of miR-193a expression on the radiation sensitivity of medulloblastoma cells was studied by the MTT assay. For the radiation sensitivity estimation by the MTT assay, vector control cells, and the P1, P2 population cells were treated with doxycycline for 48 h, 2500 cells were seeded in triplicate per well in a 96 well plate. After seeding, the cells were irradiated using a telecobalt machine at a dose ranging from 2 Gy to 6 Gy. The cell growth was monitored for six days. The radiation sensitivity of D283 and HD-MB03 cells was found to be increased by 2.34 to 3.3 fold and 1.7 to 2.8 fold, respectively, upon miR-193a expression as evaluated based on the reduction in the D_0 dose of radiation (Fig. 4.6A and 4.6B). D_0 dose of radiation is the dose at which the surviving fraction of the cells is reduced to 37 %.

4.1.7. Effect of miR-193a expression on the anchorage-independent growth potential of medulloblastoma cells.

A soft agar colony formation assay was performed to assess the effect of miR-193a expression on the anchorage-independent growth of medulloblastoma cells. One thousand cells of the vector control or P1, P2 polyclonal populations of medulloblastoma cells were seeded with and without 48 h doxycycline treatment. The cells were seeded in 0.4 % agarose over a basal layer of 1 % agarose in the medium supplemented with 10 % FBS. The colonies containing at least 20 cells were counted from each plate after 10-15 days of incubation. MiR-193a expression inhibited the anchorage-independent growth potential of medulloblastoma cells by 40-70 % ($p \leq 0.001$).

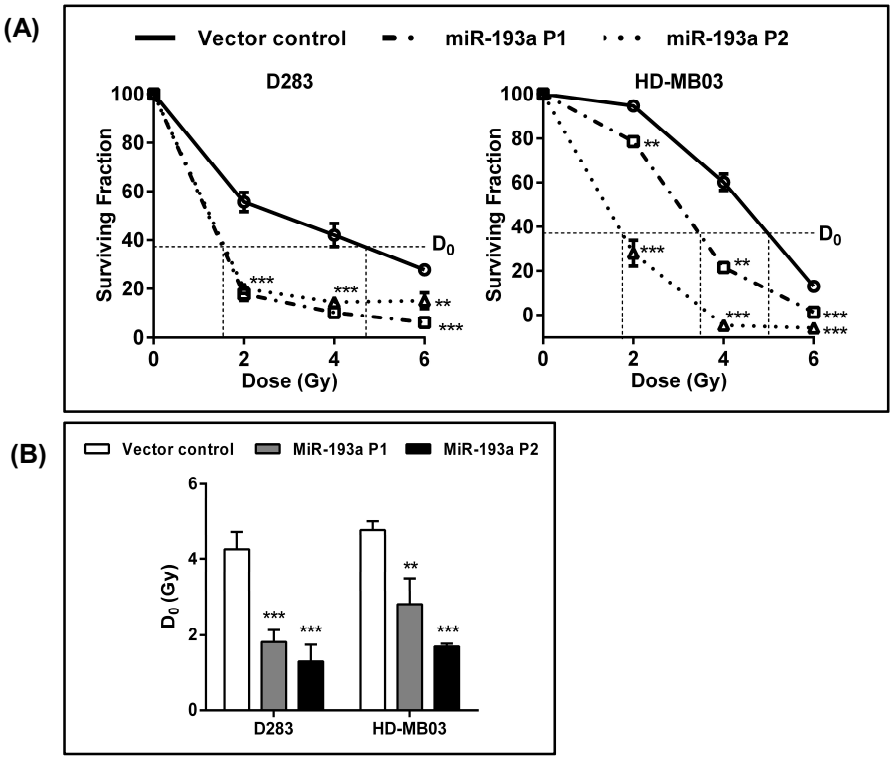

Fig 4.6: Effect of miR-193a expression on the radiation sensitivity of medulloblastoma cells studied by the MTT assay.

(A) Y-axis shows the surviving fraction of the indicated medulloblastoma cells upon irradiation at a dose ranging from 2 Gy to 6 Gy. **(B)** Y-axis shows the D0 dose of the indicated medulloblastoma cells evaluated from three independent radiation sensitivity experiments. **, *** and ns indicate $p < 0.001$, $p < 0.0001$, respectively. VC: Vector control

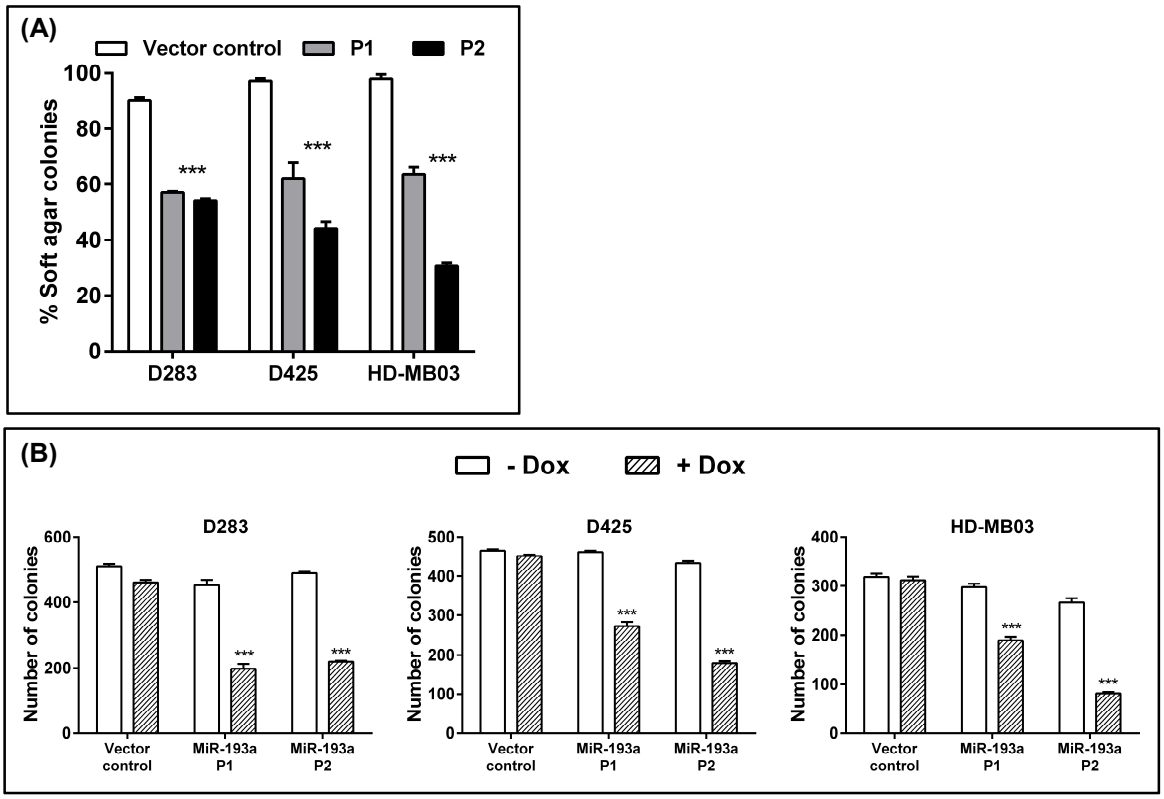

Fig 4.7: Effect of miR-193a expression on the anchorage-independent growth of medulloblastoma cells.

(A) Y-axis shows the soft agar colony formation of doxycycline-treated population as a percentage of the untreated population of the indicated cell line. **(B)** Y-axis shows the number of soft agar colonies of indicated cell populations with and without doxycycline treatment. *** indicates $p < 0.0001$

4.1.8. Effect of miR-193a expression on *in vivo* tumorigenic potential of medulloblastoma cells

The effect of miR-193a expression on *in vivo* tumorigenic potential of medulloblastoma cells was studied using the orthotopic xenograft model. MiR-193a expressing or vector control populations of HD-MB03 cells were engineered to express the firefly luciferase gene. The cells were stereotactically injected into the cerebellum of the NOD/SCID mice after 48 h of doxycycline treatment *in vitro*. In order to maintain the expression of miR-193a throughout the duration of the experiment, the animals were fed 1 g / l of doxycycline in a 5 % sucrose solution. The tumor growth was monitored by *in vivo* bioluminescence imaging at an interval of 7 days. The *in vivo* bioluminescence imaging showed a 200-fold to 800-fold decrease in the average radiance of tumors derived from the miR-193a expressing cells on Day 20/21 (Fig. 4.8A, 4.8B, and 4.8D). The Kaplan Meier survival analysis was performed to assess the survival advantage conferred by miR-193a to the tumor-bearing mice. The Log Rank test was used to determine the statistical significance of the survival curves. The mice injected with miR-193a expressing cells survived 8-10 days longer compared to 20-22 days survival of the mice injected with the vector control cells, indicating a ~30 % increase in the survival of the tumor-bearing mice upon miR-93a expression (Fig. 4.8C).

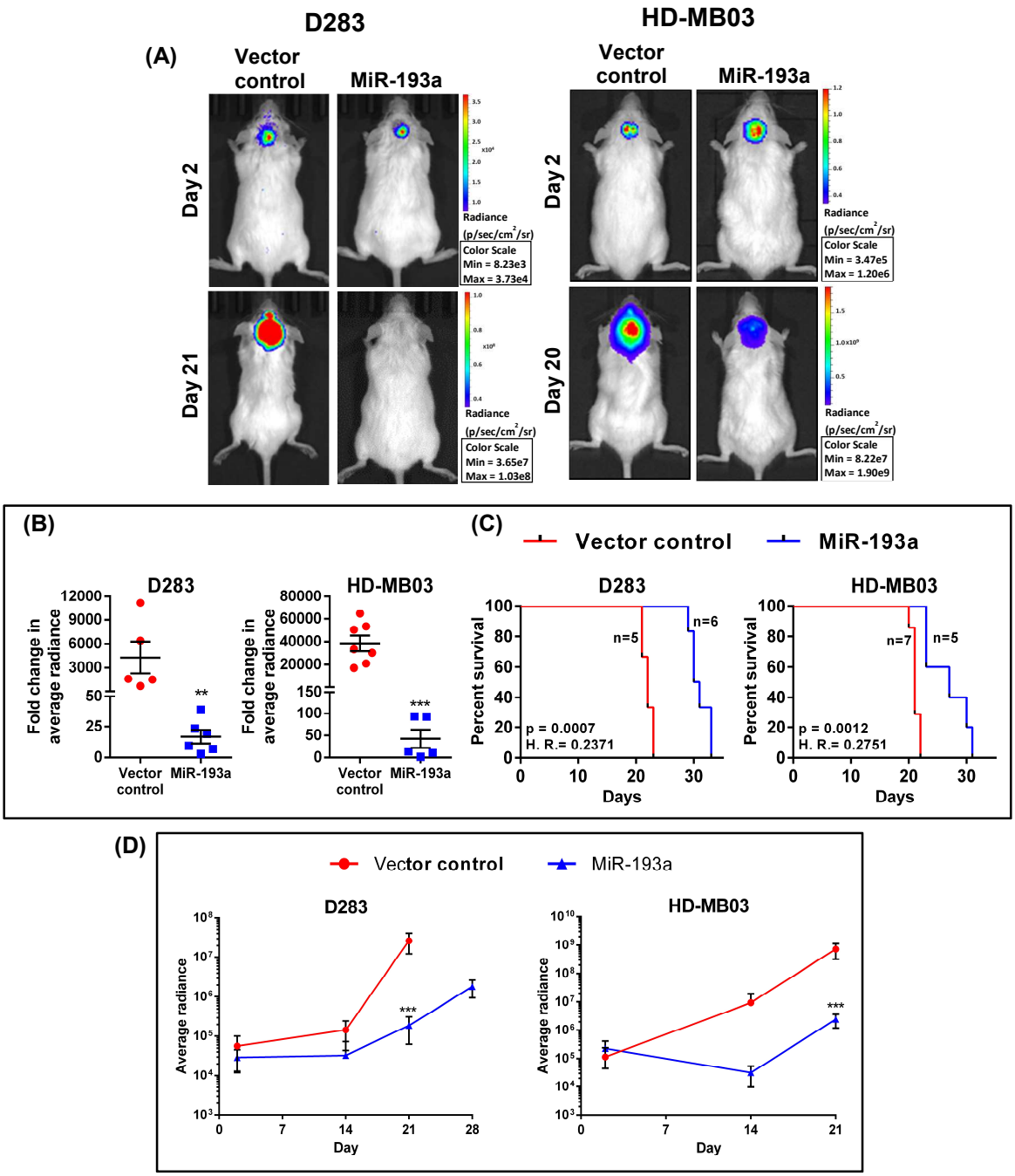

Fig 4.8: Effect of miR-193a expression on the tumorigenic potential of medulloblastoma cells.

(A) Bioluminescence images of the tumor-bearing mice orthotopically injected in the cerebellum with firefly luciferase-tagged vector control or miR-193a expressing populations of the indicated cell line on day 2 and day 21 post-injection. **(B)** Scatter plots depicting the fold change in the average radiance of the tumors on day 21 compared to that on day 2 on the Y-axis for the indicated cell lines. **(C)** Kaplan Meier survival analysis comparing the survival of the mice injected with vector control or miR-193a expressing

medulloblastoma cells of the indicated cell line. H.R. = Hazard Ratio **(D)** Y-axis depicts the average radiance of the orthotopic tumors derived from the vector control or miR-193a expressing populations of D283, HD-MB03 cells at the indicated time points. **, *** indicate $p < 0.001$, $p < 0.0001$ respectively.

4.1.9. Transcriptome analysis of HD-MB03 medulloblastoma expressing miR-193a and identification of direct target genes of miR-193a

The molecular mechanism underlying the tumor-suppressive effect of miR-193a expression was studied by performing the RNA-Seq analysis of the parental, vector control, and miR-193a expressing HD-MB03 medulloblastoma cells. The genes significantly differentially expressed (fold change ≥ 1.5 or ≤ -1.5, Bonferroni adjusted p-value < 0.05) upon miR-193a expression in HD-MB03 cells were identified using the DESeq software in the R Bioconductor environment. Seven hundred and three genes were found to be significantly ($p_{adj} < 0.05$) differentially expressed upon miR-193a expression in the HD-MB03 cells. The gene set enrichment analysis using the microRNA motif database showed 1.67 fold enrichment of validated and putative target genes among the genes significantly downregulated upon miR-193a expression. The validated miR-193a targets included *KMT2A*, *ING5*, and *MCL1* [20-22] and putative miR-193a targets included *DCAF7*, *STMN1*, *MAX*, and *MAP3K3* (Fig. 4.9A).

MiR-193a binding sites in the 3'UTR of the genes *DCAF7*, *STMN1*, *MAX*, and *MAP3K3* were identified using the TargetScan software (www.targetscan.org). The 3'UTR of *DCAF7* harbors two miR-193a binding sites (one 8-mer and one 7-mer-m8), whereas the 3'UTR of *STMN1*, *MAX,* and *MAP3K3* harbor one miR-193a binding site each. The binding sites in the 3'UTR of *DCAF7*, *STMN,1,* and *MAX* have percentile context scores between 95-99 % identifying these genes as probable miR-193a targets. On the other hand,

the percentile context score for the miR-193a binding site in the 3'UTR of the MAP3K3 gene is only 38 %. The 3'UTRs of the putative miR-193a target genes and known target genes *ERBB4* and *KMT2A* were PCR amplified and cloned downstream of the luciferase cDNA in the reporter vector [16, 22]. Upon co-transfection of the luciferase reporter construct and miR-193a expression construct into the HEK293FT cells, the reporter activity decreased by 40 to 70 % in the case of known miR-193a targets *ERBB4*, *KMT2A*, and putative targets *MAX*, *STMN1*, and *DCAF7* but not in the case of *MAP3K3* (Fig. 4.9B). Alterations in the miR-193a binding site created by the site-directed mutagenesis in the 3'UTRs of *MAX*, *STMN1*, and *DCAF7* abrogated the reduction in the luciferase activity, thereby confirming these genes as the direct targets of miR-193a (Fig. 4.9B and 4.9C). The real-time RT-PCR analysis also showed a reduction in the expression levels of target genes *KMT2A*, *DCAF7*, and *STMN1* in HD-MB03 and D283 cells upon miR-193a expression (Fig. 4.9D). MiR-193a expression decreased the protein levels of known targets *CCND1*, *MCL1*, and the novel target *MAX* in the medulloblastoma cells, as validated by the western blot analysis (Fig. 4.9E).

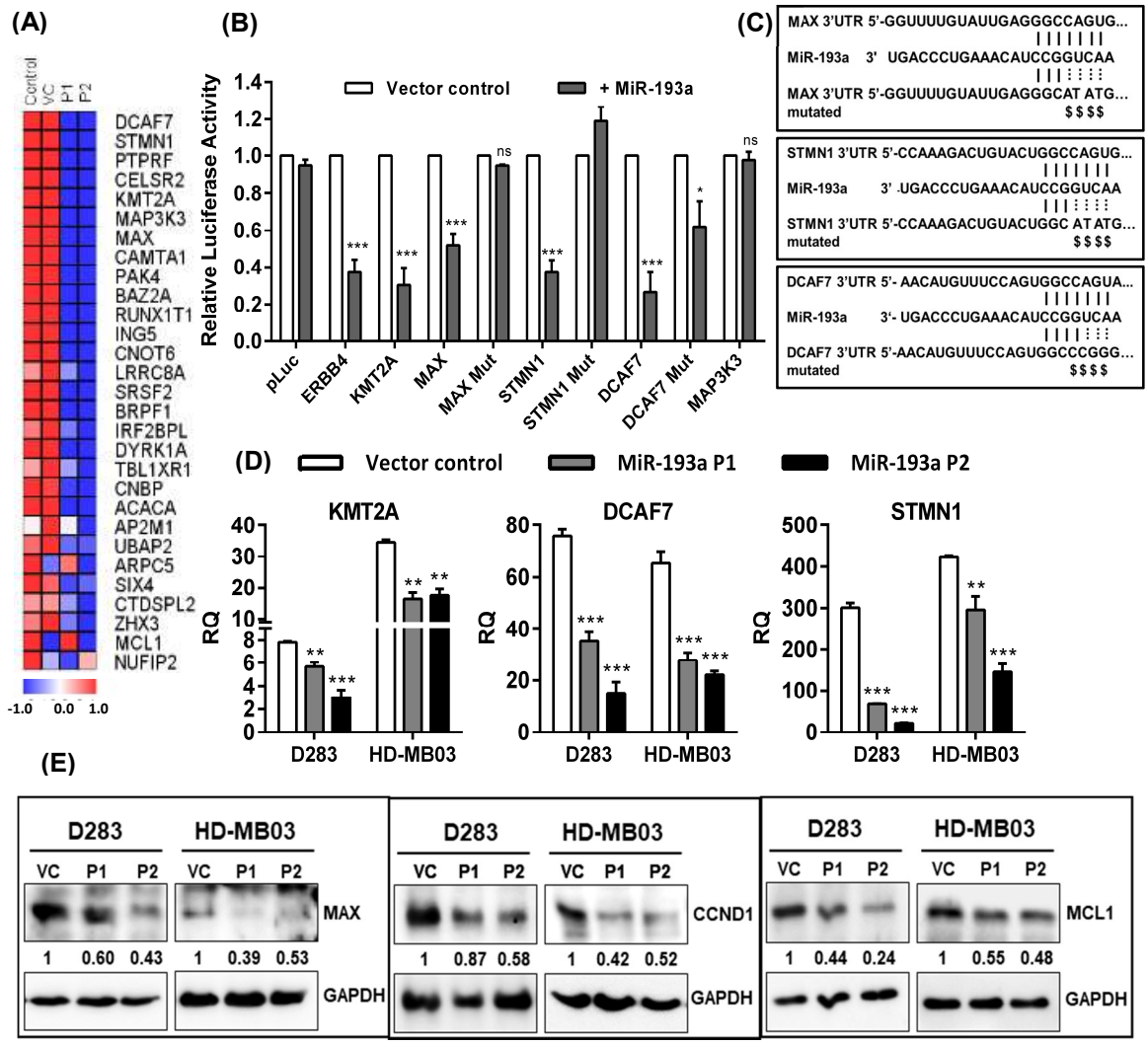

Fig 4.9: Identification of miR-193a targets by the RNA-seq analysis and validation of the targets by the luciferase reporter assay, real-time RT-PCR assay, and western blotting.

(A) Heatmap of the genes significantly differentially expressed upon miR-193a expression in HD-MB03 cells showing the enrichment of the miR-193a target genes (C-Parental cells, VC-vector control, P1/P2-polyclonal populations of HD-MB03 cells expressing miR-193a). **(B)** Y-axis depicts the relative activity of the luciferase reporter of the 3′UTR construct of the indicated gene before and after miR-193a expression (Mut: Mutant 3′UTR construct). **(C)** The sequence of the miR-193a binding sites in the 3'UTR region of the indicated target genes and the mutations created in the miR-193a binding site by the site-directed mutagenesis in the 3′UTR constructs. The altered nucleotides are indicated by the $ symbols. **(D)** Real-time RT-PCR analysis of the indicated miR-193a target genes in the doxycycline-treated polyclonal populations of HD-MB03 or D283 cells expressing miR-193a and an empty pTRIPZ vector as a control (RQ-relative quantity). **(E)** Western blot analysis of the miR-193a target genes MAX, CCND1, and MCL1 in the doxycycline-

treated polyclonal populations of the medulloblastoma cells expressing miR-193a and an empty pTRIPZ vector as a control. The GAPDH expression served as a loading control. The numbers below each blot indicate the fold change in the protein levels of the indicated gene in the P1, P2 polyclonal populations compared to the vector control after normalization using the expression of the loading control. *, **, *** and ns indicate $p < 0.01$, $p < 0.001$, $p < 0.0001$ and non-significant, respectively.

4.1.10. MiR-193a expression brought about widespread repression of gene expression with the decrease in the global levels of histone marks of active chromatin

The protein-protein interaction network analysis of the genes significantly downregulated upon miR-193a expression in the HD-MB03 cells was carried out using the ClueGo, a Cytoscape plugin software (https://cytoscape.org/). The interaction network was analyzed for the enrichment of biological pathways from the KEGG and the Reactome databases. The interaction network analysis of the 459 genes downregulated (log_2 fold change = 0.8; padj < 0.05) upon miR-193a expression showed significant enrichment (padj < 0.01) of several pathways, including the cell cycle regulation, DNA replication/DNA synthesis, chromatin remodeling, NOTCH signaling, WNT signaling, and the translation machinery (Fig. 4.10A). MiR-193a downregulated the expression of cell cycle regulation and proliferation-related genes like *CCND1*, *CCND2*, *CDK2,* and *E2F1*, of which *CCND1* and *E2F1* are known targets of miR-193a. The DNA polymerase genes like *POLD1*, *POLD2, POLE,* and the components of replisome complex like *CDC45*, minichromosome maintenance complex genes *MCM2*, *MCM5, MCM7* were also downregulated upon miR-193a expression. The downregulation of these genes could lead to the inhibition of DNA replication and DNA repair. Therefore, the downregulation of these genes is consistent with the growth inhibition of medulloblastoma cells upon miR-193a expression. The

downregulation of genes involved in the NOTCH signaling like *NOTCH1*, *JAG1*, *PLXND1,* and the genes involved in the WNT signaling like *TCF7L1*, *LRP5*, *DVL1*, and *TLE3* suggests inhibition of the WNT and NOTCH signaling pathways upon miR-193a expression. MiR-193a expression also resulted in a reduction in the expression of several genes belonging to the chromatin organization. The genes belonging to the SWI/SNF remodeling complex, histone encoding genes, and histone modifier genes were downregulated upon miR-193a expression. The SWI/SNF complex genes included *ARID1A*, *ARID1B*, *SMARCB1*, *SMARCD3*, and *SMARCC2*, while the histone encoding genes included *HIST1H4E*, *HIST1H2BD*, and *H3F3B*. The histone modifier genes included known miR-193a target *KMT2A*, as well as *KMT2D*, and *KAT5* (Fig. 11A). *KMT2A*, a SET1/MLL family protein, is a part of multiprotein complex that incorporates the trimethylation mark at the 4^{th} lysine residue of histone H3 (H3K4me3) [22]. Therefore, the effect of miR-193a expression on global H3K4me3 in medulloblastoma cell lines was studied by the western blot analysis. MiR-193a expression decreased the total levels of H3K4me3 and H3K27ac (Histone H3 acetyl K27), which are marks of active gene expression, by 55 to 78 %. On the other hand, the total levels of H3K27me3 (Histone H3

trimethyl K27), an epigenetic mark of repression of gene expression, increased by 1.66 to 2 fold upon miR-193a expression (Fig. 4.10B).

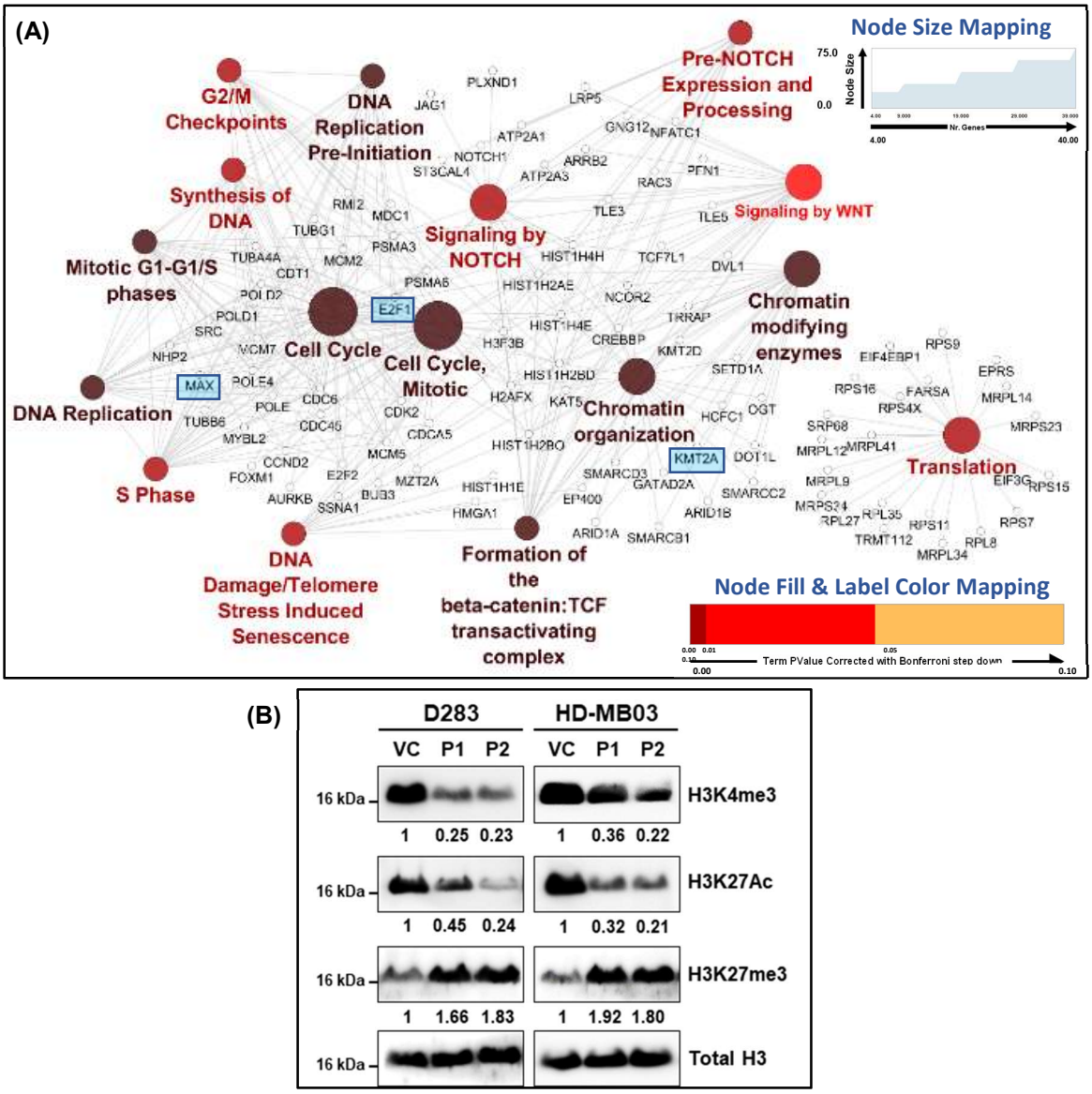

Fig 4.10: Protein interaction network analysis of genes significantlly downregulated upon miR-193a expression in HD-MB03meduloblastoma cells.

(A) Protein-protein interaction network analysis of the pathways significantly enriched in the genes downregulated upon miR-193a expression. MiR-193a target genes *E2F1*, *MAX*, and *KMT2A* are highlighted in the interaction network. The color intensity of the node circle and the node title indicate the statistical significance of the enrichment of the pathway. The size of the node corresponds to the number of interacting genes. **(B)** Western blot analysis of the expression levels of the core histone marks H3K4me3, H3K27ac, and

H3K27me3 in the vector control (VC) and miR-193a expressing polyclonal populations (P1, P2) of the medulloblastoma cells. The numbers below each band indicate the fold change in the expression levels of the histone mark in the P1, P2 populations expressing miR-193a as compared to the vector control cells after normalization using the total histone H3 levels as the loading control.

4.1.11. Destabilization of MYC upon miR-193a expression

MAX is the obligate heterodimerization partner of MYC, required for the transcriptional activity of *MYC*. *MYC* was found to induce the expression of miR-193a. On the other hand, *MAX* was identified as a novel target of miR-193a. Thus, miR-193a mediated downregulation of *MAX* could inhibit the transcriptional activity of the MYC oncoprotein as MAX is the obligate heterodimerization partner of MYC. A recently published study has shown that loss of MAX destabilizes MYC and inhibits *MYC* driven lymphomagenesis [23]. MYC is a transcription factor with a high turnover rate with a half-life of 15-30 min depending upon the cell type. Therefore, the effect of downregulation of *MAX* on the stability of MYC oncoprotein was investigated. Cycloheximide treatment completely inhibits protein synthesis in a cell, thus enables the study of the stability of a given protein. Doxycycline-induced vector control or miR-193a expressing HD-MB03 cells were treated with 50 µg /ml of cycloheximide, and the protein lysates were made at an interval of 30 min. The western blot analysis of the lysates showed decreased expression of MAX in miR-193a expressing cells as compared to vector control cells (Fig. 4.11). Upon blockade of the protein synthesis, the half-life of MYC was found to be reduced by 7-8 min in miR-193a expressing HD-MB03 cells compared to the vector control cells, indicating the destabilization of MYC protein (Fig. 4.11A and 4.11B). To further confirm the destabilization of MYC caused by miR-193a mediated downregulation of MAX, the doxycycline-treated vector control and miR-193a expressing polyclonal population of

medulloblastoma cells were treated with MG-132 (a proteasomal inhibitor) for 6 h. The MG-132 treatment to miR-193a expressing and vector control population showed less accumulation of MYC in miR-193a expressing cells compared to vector control cells further confirming the destabilization of MYC upon miR-193a-mediated downregulation of MAX (Fig. 4.11C). Thus, the expression of miR-193a destabilizes the MYC protein in *MYC* amplified Group 3 medulloblastoma cells.

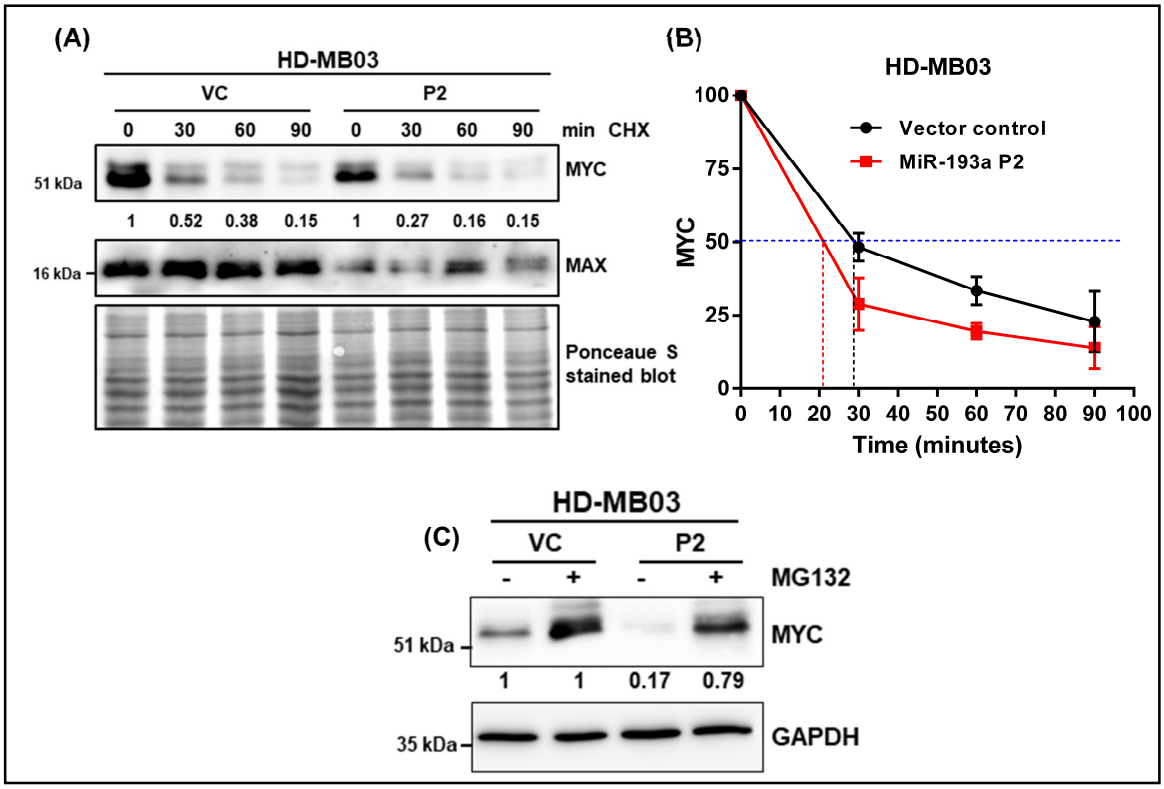

Fig 4.11: Effect of miR-193a expression on the expression levels of MYC in HD-MB03 cells.

(A) Western blot analysis of MYC and MAX in the doxycycline-induced medulloblastoma cells after treatment with 50 µg/ml of cycloheximide at indicated time intervals. **(B)** Y-axis denotes the normalized MYC expression level in the doxycycline-induced medulloblastoma cells based on three independent experiments. The MYC expression was normalized to the total amount of proteins in the respective lane determined by the densitometric analysis of the Ponceau S-stained blot. **(C)** Western blot analysis of MYC in the medulloblastoma cells after treatment with MG132, a proteasomal inhibitor. The GAPDH expression served as a loading control. The numbers below each blot indicate the

fold change in the protein levels of the indicated gene in the P1, P2 polyclonal populations compared to the vector control (VC) after normalization to the expression of the loading control.

4.2. Discussion

4.2.1. Role of miR-193a in medulloblastoma biology

Medulloblastoma is not a single tumor type but consists of four distinct molecular subgroups WNT, SHH, Group 3, and Group 4. These four subgroups differ in their expression profiles, genetic alterations, and clinical characteristics [2, 180]. Among the four subgroups, the WNT subgroup has the best long-term survival rate of over 90 %, whereas Group 3 performs quite poorly with the five-year survival rate of ~50 %. MicroRNA expression profiling of medulloblastomas has revealed the subgroup-specific expression of microRNAs [9]. WNT subgroup medulloblastomas have the most distinctive microRNA expression profile with overexpression of several microRNAs. MiR-193a was identified as one of the most WNT subgroup-specific microRNAs. The WNT subgroup restricted expression of miR-193a was confirmed by a real-time RT-PCR assay in an Indian cohort of 103 medulloblastomas [151]. In the present study, the expression of miR-193a was analyzed in an independent larger western cohort consisting of 763 medulloblastomas, which further validated its WNT subgroup-specific expression.

4.2.2. MiR-193a expression is upregulated by MYC and is suppressed by DNA promoter methylation in non-WNT subgroup medulloblastomas

MYC, an oncogenic target of the canonical WNT signaling, is overexpressed in WNT subgroup medulloblastomas. In the present study, MYC was found to induce miR-193a

promoter activity. Furthermore, enforced expression of MYC in HEK293FT cells resulted in 1.7 fold - 2.0 fold induction of miR-193a expression. Therefore, the MYC transcription factor appears to upregulate the expression of miR-193a in WNT subgroup medulloblastomas. Earlier, expression of another WNT subgroup-specific microRNA, miR-148a was also shown to be regulated by the MYC transcription factor (Ph. D. thesis- Kedar Yogi). Thus, the activated WNT signaling appears to upregulate the expression of these two WNT subgroup-specific microRNAs in a MYC-dependent manner.

MYC is also overexpressed in almost all Group 3 medulloblastomas at levels comparable to those seen in the WNT subgroup tumors [2, 78]. 10-17 % Group 3 tumors overexpress MYC due to the amplification of the MYC locus, which is also a marker of poor prognosis in this subgroup. Medulloblastoma cell lines have been established from MYC-amplified or MYC overexpressing Group 3 tumors [160, 178]. However, miR-193a is neither expressed in Group 3 medulloblastomas nor in Group 3 cell lines despite having high expression of MYC. MiR-193a is located on chromosome 17 at the 17q11.2 locus having a CpG island. The q arm of chromosome 17 is duplicated in 26 % of Group 3 and 80 % of Group 4 tumors [2, 60]. Still, both the subgroups have low miR-193a expression. MiR-193a expression is known to be silenced as a result of promoter hypermethylation in several cancers like breast cancer, NSCLC, AML, ovarian cancer, hepatocellular carcinoma and oral squamous cell carcinoma (Table 4.1). In the present study, several CpG residues in the miR-193a promoter region were found to be methylated in the three non-WNT subgroups in 763 medulloblastomas from the MAGIC cohort. The miR-193a CpG island was also found to be methylated in the non-WNT medulloblastoma cell lines, as analyzed by the methylation-specific PCR. Furthermore, miR-193a expression could be restored in

SHH and Group 3 cell lines upon treatment with the 5'-Aza-2'-deoxycytidine, a DNA methylation inhibitor, indicating the repression of miR-193a expression by DNA methylation. Thus, the expression of miR-193a appears to be induced by MYC in the WNT subgroup medulloblastomas and silenced in the non-WNT medulloblastoma subgroups due to promoter hypermethylation.

4.2.3. Restoration of miR-193a expression is tumor-suppressive in Group 3 medulloblastoma cell lines and is associated with widespread downregulation of gene expression

Restoration of miR-193a expression in MYC overexpressing/amplified Group 3 medulloblastoma cell lines inhibited proliferation, anchorage-independent growth, and tumorigenic potential. It also increased the radiation sensitivity of the medulloblastoma cells. The miR-193a expression arrested the cells in the G0/G1 phase of the cell cycle and induced apoptosis, albeit to a limited extent. Thus, miR-193a appears to play a tumor-suppressive role in medulloblastoma pathogenesis by inhibiting the growth and malignant behavior of medulloblastoma cells. These findings are consistent with the tumor-suppressive role of miR-193a in several other cancers like breast cancer, NSCLC, AML, ovarian cancer, hepatocellular carcinoma and oral squamous cell carcinoma (Table 4.1). The expression of miR-193a in Group 3 medulloblastomas cells resulted in the downregulation of several hundred genes. The gene set enrichment analysis showed significant enrichment of several validated and putative miR-193a target genes like *STMN1*, *DCAF7*, *MAP3K3*, *KMT2A*, *E2F1*, *ING5*, *MAX*, *CCND1*, and *MCL1* among the genes downregulated upon miR-193a expression [176, 177]. Among these genes, *STMN1* and *DCAF7* were identified as the novel direct targets of miR-193a. Stathmin 1 (*STMN1*)

gene encodes a 17 kDa protein that plays a crucial role in microtubule dynamics, thereby affecting the cell cycle. The inhibition of *STMN1* in cancer cells is known to induce apoptosis and cause cell cycle arrest [181, 182]. Another target gene, *DCAF7*, also known as WDR68 or HAN11, encodes a WD-40 repeat-containing protein. *DCAF7* acts as a scaffold protein, which facilitates protein-protein interactions, thereby allowing the formation of large functional protein complexes [183-185]. *DCAF7* is known to interact with the ERCC1-XPF complex through XPF and is required for maintaining cellular levels of the ERCC1-XPF endonuclease complex, which is involved in DNA repair [184, 186]. Thus, the decrease in the *DCAF7* levels may impair the DNA repair activity, thereby contribute to the miR-193a mediated increase in the radiation sensitivity of Group 3 medulloblastoma cells. *DCAF7* is also known to promote myogenesis by mediating the phosphorylation of RNA pol II [187]. *CCND1* and *MCL1* are the known miR-193a targets, which were downregulated in medulloblastoma cells upon miR-193a expression. Cyclin D1 (CCND1), along with its partners, CDK4 and CDK6, governs the G1/S transition of cells during the cell cycle [188]. MCL1 is a BCL2-family anti-apoptotic protein, which is known to be often overexpressed in cancer cells. The depletion of MCL1 in cancer cells has been shown to induce apoptosis, and increases chemo-radiation sensitivity [189]. *MCL1* deficiency has also been shown to inhibit DNA DSB repair and the re-initiation of the stalled replication forks, thereby increasing the radiation sensitivity [190]. Hence, miR-193a mediated downregulation of *DACF7*, *STMN1*, *CCND1,* and *MCL1* in Group 3 medulloblastoma cells is likely to contribute to the tumor-suppressive effect of miR-193a by inhibiting proliferation, inducing apoptosis, and increasing radiation sensitivity.

Cancer cells are characterized by higher expression of the DNA repair pathway genes to efficiently tackle the replicative stress arising due to the increased proliferation rate. MiR-193a expression also downregulated genes involved in DNA replication like *POLD1*, *POLD2,* and *POLE,* indicating inhibition of DNA replication. Along with their central role in DNA replication, these proteins also play a role in DNA repair [191]. Furthermore, several genes involved in DNA replisome complex like *CDC45*, minichromosome maintenance proteins *MCM2*, *MCM5,* and *MCM7* were downregulated upon miR-193a expression. These MCM proteins, along with the other MCM family members, form hetero-hexamers that act as a scaffold for recruiting proteins involved in bidirectional DNA replication at the origin of replication. Cancer cells exhibit high expression of the MCM proteins to cope up with the replication stress [192]. Therefore, the decrease in the levels of the MCM proteins upon miR-193a expression may contribute to apoptosis induction in medulloblastoma cells. The MCM proteins are also required for the checkpoint execution in response to the radiation-induced DNA damage [193]. *CDC45*, another component of the replisome complex, is known to interact with the MCM7 protein directly and is involved in the loading of DNA polymerase and PCNA onto the chromatin [194]. The downregulation of CDC45, upon miR-193a expression, can lead to the inhibition of DNA synthesis. Therefore, the downregulation of DNA polymerases and the proteins involved in the DNA replisome complex could contribute to the decreased proliferation, apoptosis induction, and increased radiation sensitivity of the Group 3 medulloblastoma cells upon miR-193a expression.

The genes downregulated upon miR-193a expression in medulloblastoma cells also included several chromatin modifier genes indicating remodeling of the chromatin upon

miR-193a expression. *KMT2A*, a SET1/MLL family protein, is responsible for the incorporation of trimethylation marks at the 4th lysine residue of the histone H3 [195]. These marks are usually present at the actively transcribed regions at the promoter and enhancer sites. *KMT2A* has been recently demonstrated as a miR-193a target gene [196]. MiR-193a expression decreased the global H3K4me3 marks along with the reduction in H3K27ac, a mark of active transcription, and simultaneously increased the levels of H3K27me3, a mark of inactive chromatin. However, the widespread repression of gene expression observed upon miR-193a expression is unlikely to be the result of the decrease in *KMT2A* levels alone.

4.2.4. The interplay of miR-193a, MAX, and MYC

The MYC family of transcription factors comprises *MYC*, *MYCN* (N-MYC), and *MYCL* genes [197]. The expression of *MYC* transcription factors is upregulated upon various mitogenic signals like serum stimulus, growth factor signaling, WNT signaling, and SHH signaling [86, 197]. The activation of MYC transcription factors drives multiple cellular processes like cell proliferation, apoptosis, metabolic reprogramming, stem cell renewal, and differentiation. The targets of *MYC* include the genes involved in cell cycle regulation, nucleotide metabolism, ribosome biogenesis, and cellular metabolism [86, 94, 197]. In the present study, MYC associated factor X (MAX), a bHLH leucine zipper transcription factor, was identified as a novel target of miR-193a. MAX is an obligate heterodimerization partner of MYC, required for its transcriptional activity. Unlike MYC, MAX can form homodimers and heterodimers with MYCN, MYCL, and MXD/MGA/MNT family proteins. The MXD/MGA/MNT family of proteins is known to antagonize the pro-proliferative activity of MYC [198, 199].

Apart from direct targets of MYC transcription factor, high MYC expression in cancer cells is known to result in higher occupancy of MYC at the promoters of actively transcribed genes [85]. Thus, MYC not only upregulates its target genes but also upregulates all genes transcribed in the cells, thereby further stimulating cell growth and survival. MYC, therefore, is a highly potent oncogene.

In the present study, MYC was found to induce the expression of miR-193a, whereas MAX was identified as a direct target of miR-193a. The miR-193a mediated downregulation of MAX could inhibit the transcriptional activity of MYC as MAX is obligatory for MYC activity. Deletion or loss of MAX has been shown to abrogate MYC-driven lymphomagenesis by destabilizing the MYC oncoprotein [200]. MiR-193a decreased the expression of MAX in the MYC amplified/overexpressing Group 3 medulloblastoma by directly targeting it. Concurrently, the expression of MYC also decreased upon miR-193a expression. The half-life of MYC protein was found to decrease upon miR-193a expression, indicating the destabilization of MYC in medulloblastoma cells. MAX has also been reported to repress the expression of miR-193a by directly interacting with the miR-193a promoter [10]. Therefore, miR-193a and MAX appear to negatively regulate each other's expression, thereby modulating the activity of the MYC transcription factor family.

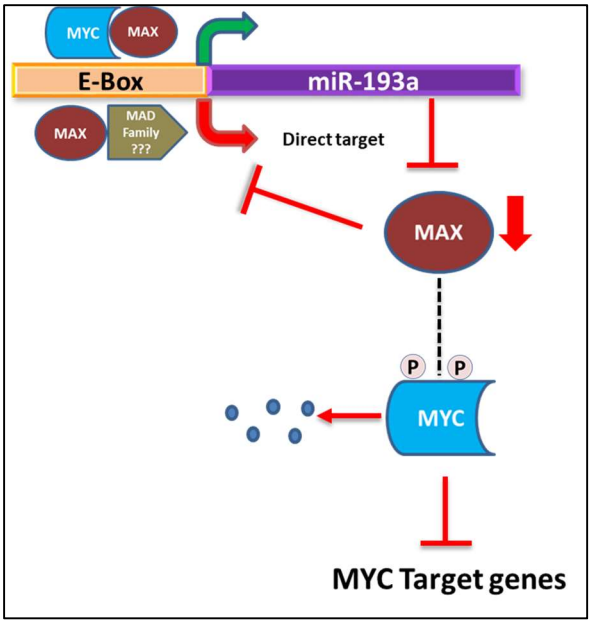

Fig 4.12 : A schematic representation of the role of miR-193a in regulating the activity of MYC transcription factor.

4.2.5. Role of miR-193a in medulloblastoma pathogenesis

The canonical WNT signaling pathway is constitutively activated in the WNT subgroup medulloblastomas due to the activating mutations in the *CTNNB1* gene encoding beta-catenin in over 90 % tumors or inactivating mutations in the *AXIN1*, *APC,* or *CDH1* gene in the remaining tumors [2, 39]. The canonical WNT signaling pathway is known to bring about the epithelial-mesenchymal transition, stem cell self-renewal, and immune evasion [201, 202]. All these characteristics are known to be associated with aggressive cancers. However, WNT subgroup medulloblastomas have an excellent long-term survival of over 95 %. MYC was found to induce miR-193a by binding to its consensus binding site in the miR-193a promoter region. MYC is the target of the canonical WNT signaling [201, 202]. MiR-193a expression, thus, appears to be upregulated by the constitutively active WNT signaling in WNT subgroup medulloblastomas. In turn, miR-193a appears to control

MYC's transcriptional activity, thereby regulating the effect of WNT signaling on cell growth. Thus, miR-193a could keep the oncogenic activity of MYC under check in the WNT subgroup medulloblastomas. On the other hand, Group 3 medulloblastomas lack miR-193a expression unleashing the full potential of MYC's oncogenic activity. Thus, miR-193a is likely to contribute to the excellent survival of the WNT subgroup medulloblastomas by keeping the oncogenic activity of MYC under control and by targeting several other known oncogenic targets like *STMN1*, *KRAS*, *MCL1*. On the other hand, the silencing of the miR-193a gene in Group 3 and SHH subgroup tumors, which overexpress MYC and MYCN, respectively, is likely to contribute to the pathogenesis of these tumors.

4.2.6. Therapeutic potential of miR-193a

The deregulation of microRNAs can lead to a change in gene expression, which alters an array of biological processes and can contribute to various pathological conditions including cancer.

MiR-193a expression is reported to be silenced in several cancers by various mechanisms like downregulation mediated by transcription factors, epigenetic silencing by DNA hypermethylation, and modulation of the microRNA activity by competing endogenous RNAs. *Illiopolus* et al. have shown that the expression of miR-193a is suppressed during the cellular transformation by transcription factors MAX and RXRα in two independent isogenic models of cellular transformation [10]. In AML, the fusion transcriptional regulator AML1-ETO was shown to bind to the miR-193a promoter and downregulate miR-193a expression by promoting DNA methylation via recruitment of HDAC and DNMTs [19]. MiR-193a is known to be downregulated in breast cancer, ovarian cancer,

NSCLC, hepatocellular carcinoma, and oral squamous cell carcinoma due to promoter hypermethylation [19, 203-206]. Thus, DNA hypermethylation appears to be the most common mechanism involved in the downregulation of miR-193a in various cancer types. In the past decade, the role of long non-coding RNAs (lncRNAs) has been characterized for their ability to modulate microRNA function. These lncRNAs do so by competing with the endogenous microRNA targets for microRNA binding, thereby decreasing the effect of the microRNAs on their targets. Therefore, the lncRNAs are referred as competing endogenous RNAs (ceRNAs) or microRNA sponges [207]. The lncRNA-UCA1 and linc00152 were shown to dysregulate the miR-193a function in NSCLC and hepatocellular carcinoma, gastric cancer, respectively, thereby favoring the malignant phenotype by upregulting the expression of miR-193a targets ERBB4, CCND1, and MCL1 [207-210]. The multiple mechanisms for downregulation of miR-193a at transcriptional or post-transcriptional levels strongly indicate a tumor-suppresive role of miR-193a in various cancers. Furthermore, the restoration of miR-193a expression has been shown to suppress cell growth, tumorigenic potential and, invasion potential of several types of cancer cells, including both hematopoietic and solid cancers (Table 4.1). MiR-193a targets include proliferation stimulators like cyclin D1, E2F6, growth factor receptor, and signaling proteins like ERBB4, KRAS, KIT, S6K2, and GRB7. MiR-193a targets also include genes like PLAU, MCL1, STMN1, and DCAF7, which are involved in cell migration/invasion, apoptosis control, cell-cycle regulation, and DNA repair, respectively. Thus, miR-193a appears to target several oncogenes responsible for regulating malignant phentotypes in a wide variety of cancers. The tumor-suppresive role of miR-193a in the pathogenesis of

multiple cancer types makes miR-193a a strong potential candidate for the treatment of cancer.

Table 4.1: Table depicting the role of miR-193a in various cancers, the mechanism of regulation of its expression, the gene targets of miR-193a in the indicated cancers, and cancer-related phenotypes modulated by miR-193a.

Tumor type	Expression status	Mechanism of regulation of expression	Target genes	Affected cancer related phenotype	Ref
Breast cancer,	Down	MAX and RXRα	KRAS, PLAU	Inhibition of cell growth, tumorigenicity, invasion potential	[10]
Acute myeloid leukemia (AML)	Down	DNA methylation mediated by AML-ETO fusion protein	ETO, KIT, CCND1, HDAC3, MDM2, DNMT3A	-	[19]
Non-small cell lung cancer (NSCLC)	Down	DNA methylation	KRAS, ERBB4, S6K2	Inhibition of cell growth, tumorigenicity	[211, 212]
Breast cancer, Ovarian cancer	Down	DNA methylation	GRB7	Inhibition of cell growth, tumorigenicity, invasion potential	[203, 206]
Pancreatic cancer	Down	-	CCND1	Proliferation inhibition	[213, 214]
Hepatocelluar carcinoma	Down	-	CCND1	Proliferation inhibition, induction of apoptosis	[215]
Acute myeloid leukemia	Down	DNA methylation	KIT	Proliferation inhibition	[216]

Oral squamous cell carcinoma	Down	DNA methylation	E2F6	Proliferation inhibition	[204]
Hepatocelluar carcinoma	Down	DNA methylation	E2F1, SRSF2	Proliferation inhibition, induction of apoptosis	[205]
Bladder cancer	Down	-	ING5, SRSF2, HIC2, PLAU, PSEN1	Proliferation inhibition, reversal of chemo-resistance	[217, 218]
Malignant pleural mesothelioma	Down	-	MCL1	Tumorigenicity inhibition, induction of apoptosis	[219]
Hepatocellular carcinoma	Down	ceRNA (LINC00152)	CCND1		[209]
Gastric cancer	Down	ceRNA (LINC00152)	MCL1	Inhibition of proliferation, tumorigenicity	[208]
Non-small cell lung cancer	Down	ceRNA (LncRNA-UCA1)	ERBB4	Inhibition of proliferation, tumorigenicity	[210]

In this study, miR-193a was found to target MAX and thereby repress activity MYC, one of the most potent oncogenes. MYC is overexpressed in about 50 % of all cancers and has been implicated in their pathogenesis. It does so by regulating critical cellular processes like cell proliferation, cell growth, apoptosis, stem cell renewal, differentiation via upregulation of its target genes. Moreover, in cancer cells having high expression of MYC, MYC accumulates in the promoter regions of actively transcribed genes and brings about their transcriptional amplification. In fact, the MYC overexpressing tumors are thought to be addicted to MYC, wherein a partial or complete inhibition of its activity leads to the

tumor regression accompanied by proliferation inhibition, induction of apoptosis, cellular differentiation or senescence, and even remodeling of the tumor microenvironment and suppression of angiogenesis [94]. This makes MYC an important target for cancer therapy. However, targeting MYC is challenging. It is difficult to design small molecule inhibitors to suppress MYC, MYC being a transcription factor that lacks specific activation sites, a strategy adopted against kinases. Secondly, it is localized in the nuclear compartment, thus inhibiting MYC using antibodies is technically difficult [82]. Alternative strategies include deregulation of MYC expression by RNA interference or inhibition of its dimerization with MAX using a small molecular inhibitor [220].

In the present study, miR-193a expression in MYC overexpressing Group 3 medulloblastoma cells not only targeted several proliferation-related genes like *CCND1*, *E2F1*, *STMN*1, anti-apoptotic gene MCL1, DNA repair genes, chromatin modifier gene *KMT2A*, but also downregulated expression of *MYC* resulting in widespread repression of gene expression. Thus, miR-193a inhibited the malignant properties of MYC overexpressing medulloblastoma cells by decreasing the transcriptional activity of MYC. Therefore, miR-193a holds a therapeutic potential for the treatment of highly aggressive Group 3 medulloblastoma and possibly several other MYC overexpressing cancers.

Chapter 5

To study the molecular mechanism underlying the effect of the miR-204 expression on medulloblastoma cell behavior.

5. Objective 2- Results and Discussion

5.1. Results

MiR-204 is one of the microRNAs that are differentially expressed across the four molecular subgroups. Its expression is high in all the WNT subgroup tumors. Almost all SHH subgroup, 60 % Group 3 and 15 % Group 4 medulloblastomas have low miR-204 expression as compared to the normal cerebellar tissues (Fig. 5.1) [11]. The expression of miR-204 was found to correlate with overall survival in Group 3/Group 4 medulloblastomas wherein lower expression levels of miR-204 identified a highly aggressive subset of these tumors (Ph.D. thesis, Raikamal Paul). Restoration of miR-204 expression inhibited the anchorage-independent growth and invasion potential of medulloblastoma cells. In the present study, the effect of restoration of expression of miR-204 on the tumorigenic potential of group 3 cell lines was studied, and the molecular mechanism underlying the tumor-suppressive effect of miR-204 expression was delineated.

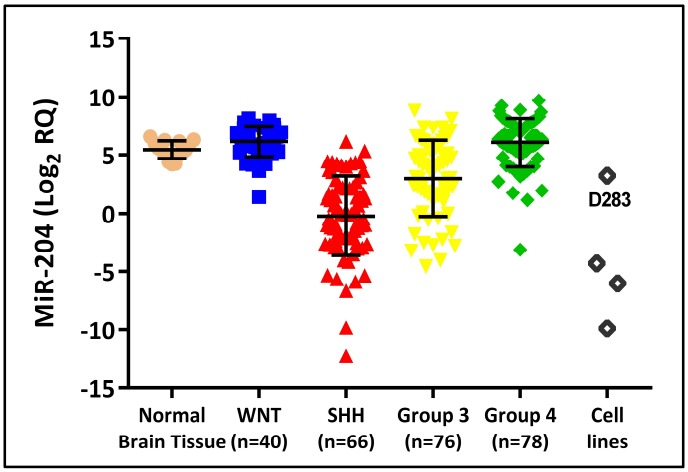

Fig 5.1: MiR-204 expression in normal cerebellar tissues, four molecular subgroups of medulloblastomas (n = 260), and medulloblastoma cell lines analyzed by the real-time RT-PCR assay.

5.1.1. *TRPM3/MIR204* promoter methylation analysis and upregulation of miR-204 expression upon treatment with HDAC inhibitors

MiR-204 is a located within the 6th intron of the host gene *TRPM3* and is transcribed along with the *TRPM3* gene at chromosome 9q21.12-q21.13. About 47 % of SHH medulloblastomas harbor loss of q arm of chromosome 9 [2]. However, miR-204 is downregulated in almost all SHH medulloblastomas. Loss of chromosome 9 is not frequent in Group 3 / Group 4 medulloblastomas with less than 20 % and 5 % loss of chromosome 9q arm in Group 3, Group 4 tumors, respectively. Downregulation of miR-204 expression has also been reported to occur due to promoter methylation [221, 222]. Therefore, the methylation status of the CpG island at the *TRPM3*/*MIR204* promoter locus was analyzed from the genome-wide methylation study of 763 medulloblastomas from the MAGIC cohort [78]. The analysis showed that the *TRPM3* promoter is not methylated in any of the medulloblastoma subgroups as indicated by lower β-values at the CpG residue (Fig. 5.2A). Moreover, the locus was not found to be methylated in the medulloblastoma cell lines as studied by the bisulphite sequencing (Ph. Thesis-Pooja Panwalkar). Therefore, the cells were treated with the HDAC inhibitors Sodium valproate and Trichostatin A. The treatment of medulloblastoma cell lines D283, D425, and HD-MB03 with the HDAC inhibitors resulted in 2 to 4 fold increase in expression levels of miR-204 (Fig. 5.2B) accompanied by the increase in the global histone acetylation as judged by studying the status of H3K9 acetylation mark by the western blotting (Fig. 5.2C).

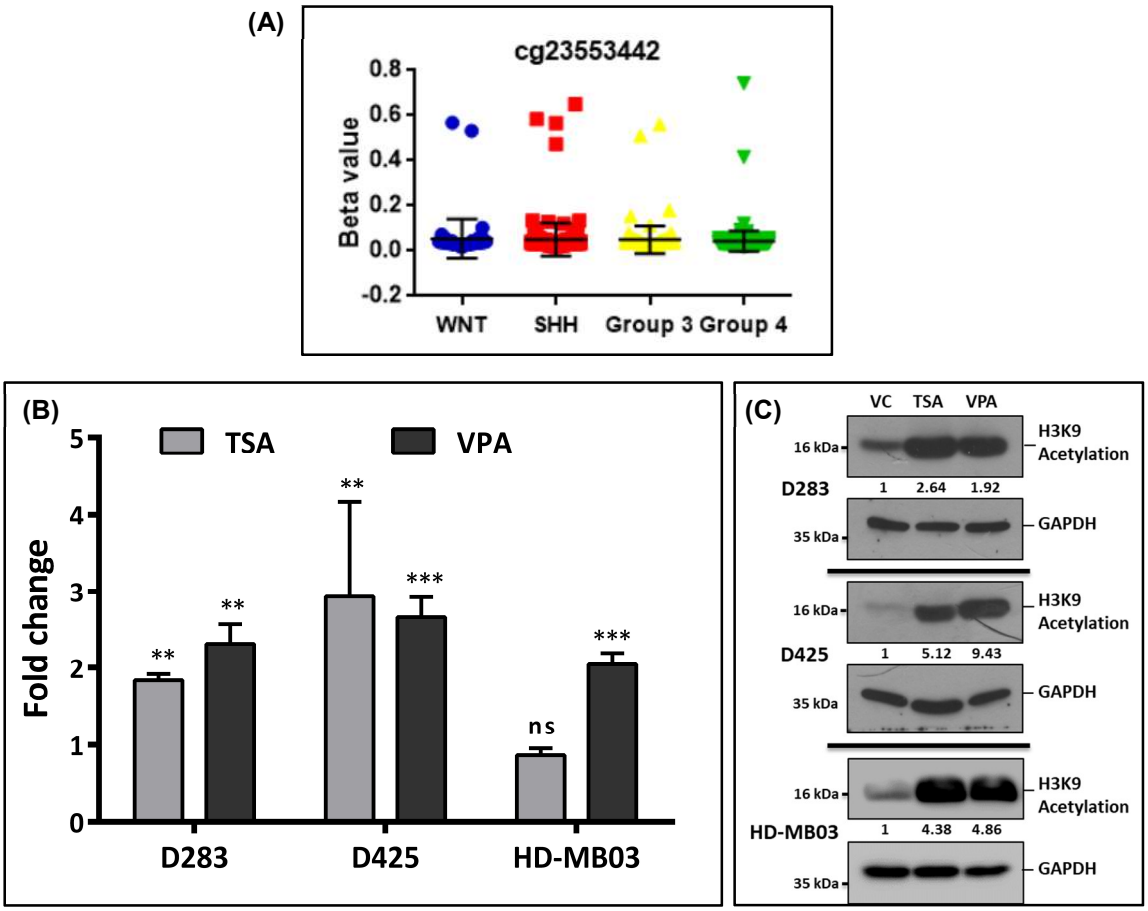

Fig 5.2: TRPM3 methylation status and restoration of miR-204 expression upon treatment of medulloblastoma cells with HDAC inhibitors.

(A) Scatter plot depicting the CpG methylation status of the CpG residue within the *TRPM3* promoter region. **(B)** Y-axis depicts the fold change in the miR-204 expression upon treatment of the medulloblastoma cells with the HDAC inhibitors, sodium valproate or Trichostatin A compared to those treated with the vehicle control DMSO. **(C)** Western blot analysis of the H3K9 acetylation status in the medulloblastoma cells upon treatment with the HDAC inhibitors. The numbers below the blots indicate the fold change in the expression levels of H3K9 acetylation upon HDAC inhibitor treatment (VC-vehicle control, TSA-Trichostatin A, VPA-Sodium valproate). **, *** and ns indicate $p < 0.001$, $p < 0.0001$ and non-significant, respectively.

5.1.2. Effect of miR-204 expression on *in vivo* tumorigenic potential of medulloblastoma cells

The restoration of miR-204 expression in Group 3 medulloblastoma cell lines D283, D425, D341, and HD-MB03 resulted in the reduction in their anchorage-independent growth and invasion potential (Ph. D. Thesis-Raikamal Paul). Hence, the effect of miR-204 expression on the tumorigenic potential of D283, D341, and HD-MB03 cells was studied using an *in vivo* orthotopic xenograft model. The vector control and miR-204 expressing populations of medulloblastoma cells engineered to express firefly luciferase were injected in the cerebellum of NOD/SCID mice using a stereotaxic apparatus. Restoration of miR-204 expression was found to significantly ($p < 0.002$ to 0.0001) decrease the tumorigenicity of all the medulloblastoma cell lines by 8.8 fold - 25 fold as judged by the reduction in the average radiance of the orthotopic tumors evaluated by in vivo bioluminescence imaging (Fig. 5.3A and 5.3B). Furthermore, the survival of the tumor-bearing mice was increased by 26 to 34 % upon miR-204 expression, indicating the tumor-suppressive effect of miR-204 in medulloblastoma (Fig. 5.3C).

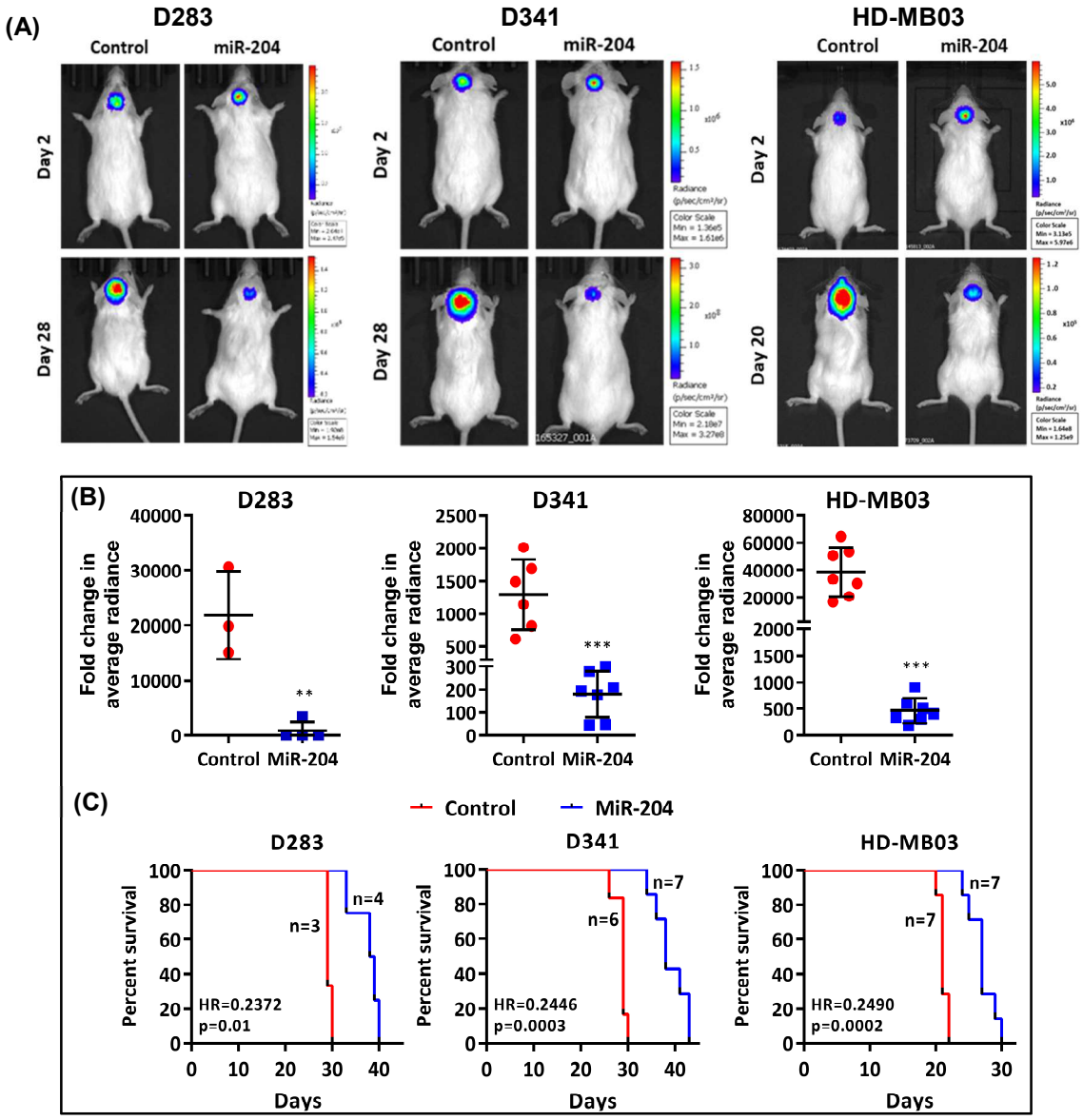

Fig 5.3: Effect of miR-204 expression on the tumorigenic potential of medulloblastoma cells.

(A) Bioluminescence images of the tumor-bearing NOD/SCID mice orthotopically injected in the cerebellum with firefly luciferase tagged vector control or miR-204 expressing populations of the indicated cell line at day 2 and day 21 post-injection. **(B)** Y-axis depicts the fold change in the average radiance on day 21 compared to that on day two. **(C)** Kaplan Meier survival analysis indicating the difference in the survival of the mice injected with the doxycycline-treated vector control cells and miR-204 expressing medulloblastoma cells of the indicated cell line. P1, P2: Medulloblastoma cells expressing miR-204 upon doxycycline treatment.

5.1.3. Transcriptome analysis of HD-MB03 and Daoy medulloblastoma cells expressing miR-204

To study the molecular mechanism underlying the tumor-suppressive role of miR-204 in medulloblastoma cells, the genes differentially expressed upon miR-204 expression were identified by the RNA-seq analysis of HD-MB03 and Daoy medulloblastoma cells. The genes differentially expressed in the polyclonal populations P1, P2 expressing miR-204 compared to the vector control and parental cell line were identified by the DESeq analysis. GSEA analysis using the microRNA target motif database identified significant enrichment of miR-204 target genes among the genes downregulated upon miR-204 expression from both datasets. Known validated targets of miR-204 like *RAB22A*, *M6PR*, *BCL2,* and *AP1S2* were among the top downregulated genes [223] (Fig. 5.4A, 5.4B, and 5.4C).

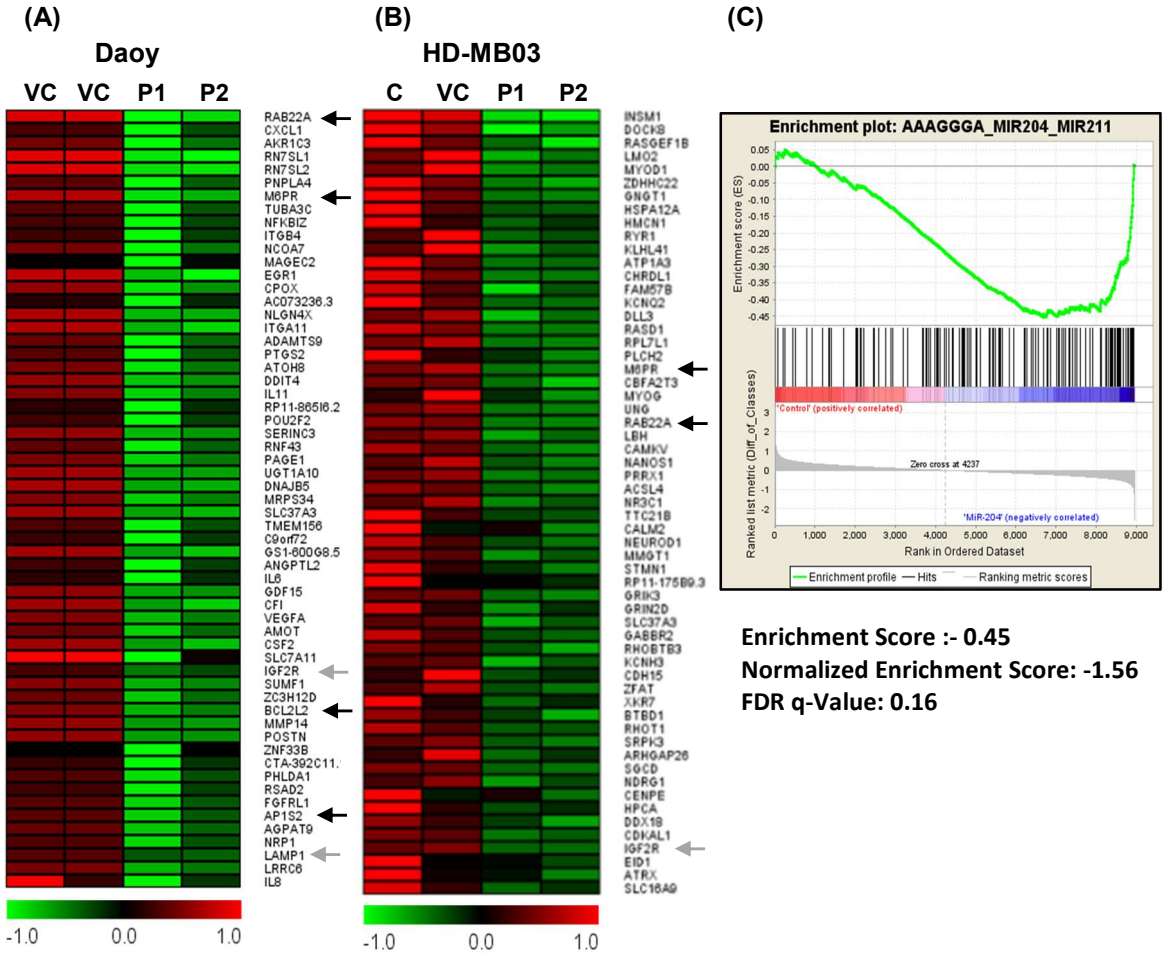

Fig 5.4: Downregulation of miR-204 target genes upon its expression in medulloblastoma cells.

(A) and (B) Heat map of top 60 genes ranked based on the significance of the fold change ($p \leq 0.05$), which were downregulated upon miR-204 expression in Daoy and HD-MB03 cells (C: control parental cells, VC: vector control, P1/P2: miR-204 expressing polyclonal populations). Known validated miR-204 targets *M6PR*, *RAB22A*, *AP1S2* and *BCL2L2* are indicated by black arrows, whereas putative targets *IGF2R* and *LAMP1* are indicated by gray arrows. **(C)** GSEA analysis of the genes downregulated upon miR-204 expression showing the most significant enrichment of the 'miR-204 target gene set' using the microRNA motif database.

5.1.4. Protein-protein interaction network analysis of the genes significantly downregulated upon miR-204 expression

The protein-protein interaction network analysis of the genes significantly downregulated upon miR-204 expression in Daoy cells was performed using the ClueGo plugin in the Cytoscape application. The network shows significant enrichment (padj < 0.01) of several pathways including the lysosome pathway, extracellular matrix organization, degradation of the extracellular matrix, TNF signaling pathway and transcriptional misregulation in cancer (Fig. 5.5). The genes belonging to the lysosome pathway include *IGF2R*, *LAMP1*, *M6PR*, *AP1S2*, *MCOLN1*, *HGSNAT*, *SUMF1*, and *SLC11A2*. The genes involved in the extracellular matrix organization, and degradation of the extracellular matrix included genes belonging to integrin subunits like *ITGA11* and *ITGB4*, genes involved in collagen formation like *COL1A1*, *COL3A1*, *COL5A2*, *COL5A3*, and *NID2,* and several matrix-metalloproteases like *MMP2*, *MMP9*, *MMP14*, *MMP15* and *MMP19* which are known to be involved in the degradation of the extracellular matrix (Fig. 5.5). Among these downregulated genes, *M6PR*, *AP1S2*, *MMP9* and *MMP19* are known direct targets of miR-204 [223-225], whereas genes like *IGF2R*, *LAMP1*, *MCOLN1,* and *HGSNAT* are putative target genes of miR-204.

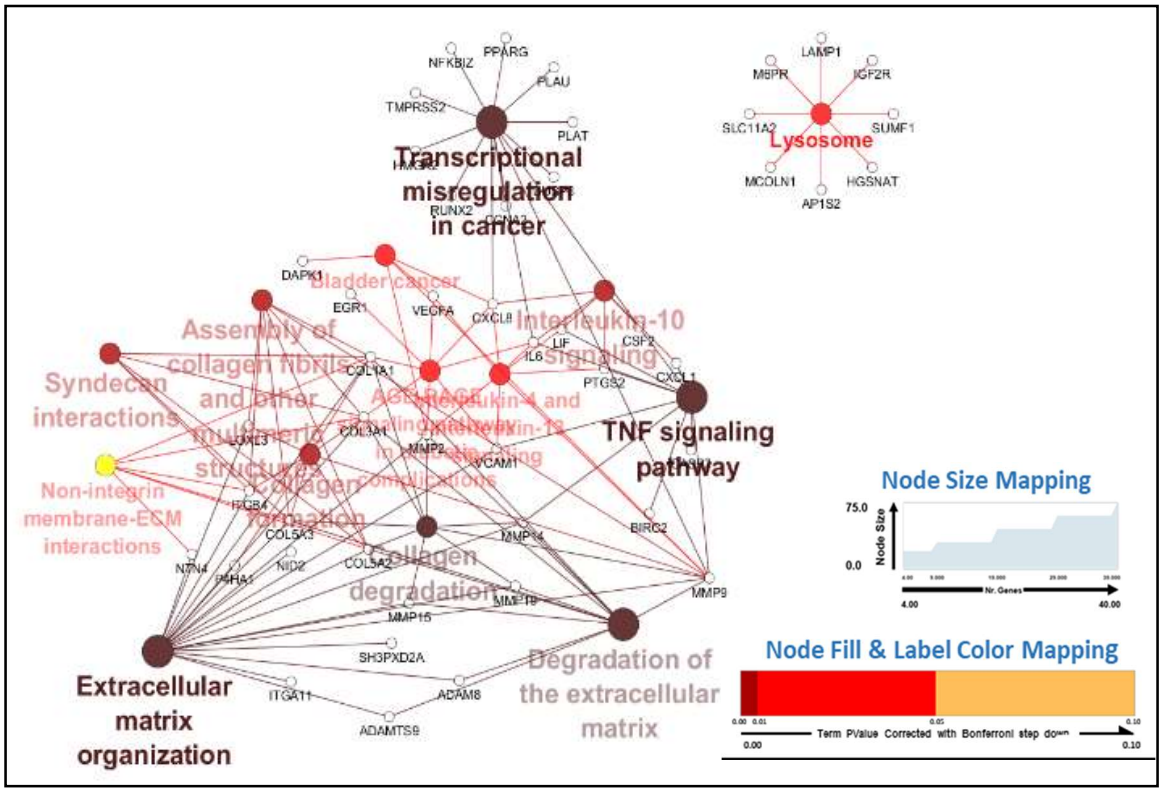

Fig 5.5: Protein interaction network analysis of the pathways significantly enriched in the genes downregulated upon miR-204 expression.

Protein interaction network analysis of the pathways significantly enriched in the genes downregulated upon miR-204 expression in Daoy medulloblastoma cells studied using the ClueGo plugin in the Cytoscape application. The color intensity of the node circle and the node title indicate the statistical significance of the enrichment of the pathway. The size of the node corresponds to the number of interacting genes.

5.1.5. Luciferase reporter assay identified IGF2R and LAMP1 as direct targets of miR-204

IGF2R and *LAMP1* are putative miR-204 target genes, which were downregulated upon miR-204 expression in medulloblastoma cells. TargetScan analysis shows the presence of a single conserved 8-mer miR-204 binding sites in the 3'UTR region of these genes. The percentile context score for the sites was 88 and 94 for IGF2R and LAMP1, respectively

making these genes likely targets of miR-204. To check if *IGF2R* and *LAMP1* are direct target genes of miR-204, the 3'UTR regions of *IGF2R*, *LAMP1*, and the known target *EZR* were cloned downstream of the luciferase cDNA in the pcDNA3.0 vector. The miR-204 sponge luciferase reporter was used as a positive control. Co-transfection of miR-204 sponge luciferase reporter and *EZR* 3'UTR construct along with the miR-204 expression vector in HEK293FT cells showed reduction in the luciferase activity by 30-60 %. The luciferase activity of the *IGF2R* and *LAMP1* 3'UTR constructs decreased by 25-30 %, indicating *IGF2R* and *LAMP1* as direct target genes of miR-204 (Fig. 5.6A). MiR-204-mediated reduction in the luciferase activity was abrogated upon mutating the miR-204 binding site in the 3'UTR of *IGF2R* and *LAMP1,* validating them as direct targets of miR-204 (Fig. 5.6A and 5.6B). The miR-204 targets like *RAB22A*, *M6PR*, *IGF2R* and *LAMP1* were found to be downregulated at RNA level upon miR-204 expression in medulloblastoma cell lines as studied by real-time RT-PCR assay (Fig. 5.6C). Furthermore, downregulation of IGF2R and LAMP1 protein levels upon miR-204 expression in medulloblastoma cell lines was confirmed by the western blotting (Fig. 5.6D).

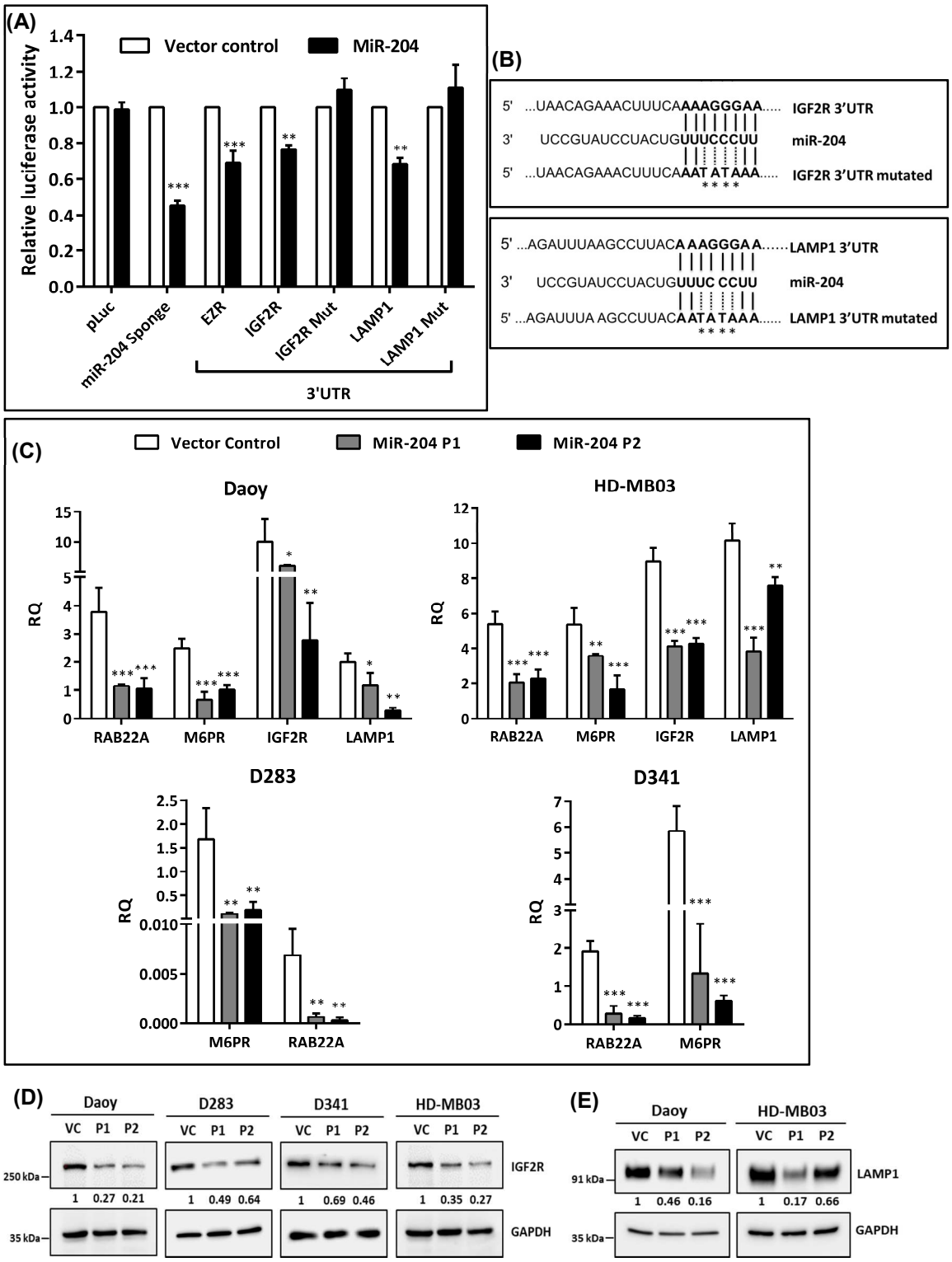

Fig 5.6: Validation of the miR-204 targets by luciferase reporter assay, real-time RT-PCR assay, and western blotting.

(A) Y-axis denotes the relative activity of the luciferase reporter of the 3′UTR construct of the indicated gene before and after miR-204 expression (Mut: Mutant 3′UTR construct).

(B) Mutations introduced in the miR-204 binding site by the site-directed mutagenesis in the 3′UTR constructs of the indicated gene. **(C)** Real-time RT-PCR analysis of the miR-204 target in the doxycycline-treated polyclonal populations of indicated medulloblastoma cells expressing miR-204 or an empty pTRIPZ vector as a control (RQ-relative quantity). **(D)** Western blot analysis of the miR-204 target genes in the doxycycline-treated polyclonal populations of medulloblastoma cells expressing miR-204 or an empty pTRIPZ vector as a control. The GAPDH expression served as a loading control. The numbers below each blot indicate the fold change in the protein levels of the indicated gene in the P1, P2 polyclonal populations compared to the vector control after normalization to the expression of the loading control. *, **, *** and ns indicate $p < 0.01$, $p < 0.001$, $p < 0.0001$ and non-significant, respectively.

5.1.6. Effect of miR-204 expression on the levels of lysosomal proteases in medulloblastoma cells

The lysosomal proteases are synthesized on the rough endoplasmic reticulum, and further transported to cis-face of Golgi apparatus as proenzymes [226, 227]. These proenzymes are post- translationally modified by addition of the Mannose-6-phosphate residue in the cis-Golgi apparatus. The mannose-6-phosphate receptors *M6PR* and *IGF2R* are known to be involved in the trafficking of the lysosomal proteases from the trans-Golgi apparatus to early lysosomal compartments by the clathrin-coated vesicles [29, 30]. In the acidic pH of the lysosomal compartment, these proenzymes are released from the receptors and get matured upon the cleavage of the signal peptide. *M6PR* and *IGF2R* were identified as novel direct target genes of miR-204. Therefore, the levels of lysosomal enzymes Cathepsin B (CTSB) and Cathepsin D (CTSD) in miR-204 expressing medulloblastoma cells was studied by the western blotting. MiR-204 expression resulted in considerable downregulation of the mature form of these lysosomal enzymes in all medulloblastoma cell lines indicating impaired transport of these proteases to the lysosomes (Fig. 5.7). Thus,

the decreased levels of lysosomal enzymes can compromise the activity of the lysosomes. The lysosomes play an important role in the pathway of autophagy. The final steps of autophagy involves the fusion of autophagosomes with the lysosomes after which the cargo inside the autophagosome is degraded by the lysosomal proteases. *SQSTM1*/p62 is an adaptor protein involved in the selective autophagy undergoes lysosomal degradation upon fusion of autophagosome and lysosome. The levels of SQSTM1/p62 were found to be increased upon miR-204 expression in medulloblastoma cells indicating the compromised lysosomal degradation pathway (Fig. 5.7).

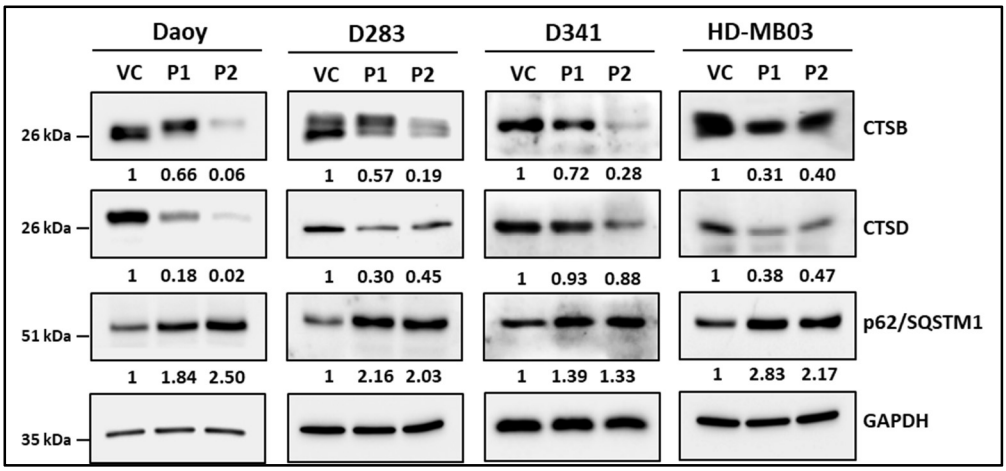

Fig 5.7: Western blot analysis of the lysosomal proteases cathepsin B (CTSB), cathepsin D (CTSD) and p62/SQSTM1.

Western blot analysis of the lysosomal proteases cathepsin B (CTSB), cathepsin D (CTSD) and that of p62/SQSTM1, an autophagy adaptor protein in the doxycycline-treated polyclonal populations of medulloblastoma cells expressing miR-204 or an empty pTRIPZ vector as a control. The GAPDH expression served as a loading control. The numbers below each blot indicate the fold change in the protein levels of the indicated gene in the P1, P2 polyclonal populations compared to the vector control after normalization using the expression levels of the loading control.

5.2. Discussion

MiR-204 is located in the sixth intron of the host gene TRPM3 and is most abundantly expressed in the brain and kidney. *MIR204*/*TRPM3* locus falls within the cancer associated genomic region at 9q21.1–q22.3 that is known to be frequently deleted in various cancers. In a large-scale microRNA profiling study of 4419 human samples consisting of 3312 tumors, 1107 non-malignant tissues corresponding to 51 cancer types, and 50 normal tissues, the miR-204-211 family was found to be the top deleted microRNA family [13]. Therefore, miR-204 appears to have a tumor-suppressive role in cancer. MiR-204 is one of the differentially expressed microRNAs whose expression is high in all the WNT subgroup tumors. The differential expression of miR-204 was further validated in an independent large cohort consisting of 763 medulloblastomas from the MAGIC cohort. Despite the overlap and complexity of genetic alterations present in the Group 3 / Group 4 medulloblastomas, miR-204 expression identifies a subset of these tumors having poor survival in our Indian cohort as well as in an independent western cohort. Thus, miR-204 is a useful marker for risk stratification in medulloblastoma, particularly important in Group 3 and Group 4 medulloblastomas where there is a paucity of good prognostication markers [11].

Almost all SHH subgroup, 60 % Group 3 and 15 % Group 4 medulloblastomas were found to have low miR-204 expression as compared to normal cerebellar tissue [11]. Loss of one copy of 9q is known to occur in 36- 38 % of SHH medulloblastomas, which could contribute to the loss of miR-204 expression [60]. However, miR-204 is downregulated in almost all SHH medulloblastomas. Loss of chromosome 9q occurs in less than 20 % and 5 % of Group 3, Group 4 tumors, respectively [60]. MiR-204 is also known to be

downregulated as a result of promoter hypermethylation [222]. However, the promoter region of miR-204's host gene *TRPM3* was found to be not methylated in the four subgroups of medulloblastomas as analysed from the methylation data of 763 medulloblastomas. Hence, other mechanisms are likely to be involved in the regulation of miR-204 expression in medulloblastomas. The treatment of HDAC inhibitors has been reported to inhibt the growth of Group 3 medulloblastoma cell lines (ref). In the present study, the treatment of Group 3 medulloblastoma cell lines with HDAC inhibitors Trichostatin A or Sodium valproate resulted in moderate upregulation of miR-204 levels. This suggests histone deacetylation playing a role in the downregulation of miR-204 expression. Since almost all SHH subgroup medulloblastomas do not express miR-204, SHH signaling may play a role in the repression of miR-204 expression. HDAC inhibitors could inhibit growth of medulloblastoma cells by upregulating miR-204 expression and hence could have therapeutic potential in the treatment of medulloblastomas.

Earlier studies in our lab have shown that restoration of miR-204 expression inhibits anchorage-independent growth and invasion potential of medulloblastoma cells (Ph.D. Theses-Pooja Panwalkar and Raikamal Paul). MiR-204 expression was found to inhibit autophagy in medulloblastoma cells [11]. In the present study, miR-204 expression inhibited tumorigenic potential of Group 3 cell lines and prolonged the survival of the tumor bearing mice indicating the tumor-suppressive role of miR-204 in medulloblastoma. The gene expression profiling of medulloblastoma cells showed significant downregulation of several genes upon miR-204 expression. The gene set enrichment analysis using the microRNA motif database showed significant enrichment of the miR-204 target genes among the downregulated genes. MiR-204 expression brought

downregulation of several genes involved in the extracellular matrix organization and degradation. The integrin subunit gene *ITGA11,* which encodes integrin subunit α11, forms a cell surface collagen receptor by dimerizing with β1 subunit, which is involved in cell migration, and collagen reorganization [228]. ITGB4, another integrin subunit downregulated upon miR-204 expression codes for integrin β4 receptor protein. The silencing of *ITGB4* has been shown to inhibit cell proliferation, clonogenic potential, and cell invasiveness in hepatocellular carcinoma [229]. Integrins are connecting links between the cytoskeleton and the extracellular matrix (ECM), which help to detect changes in the cellular microenvironment enabling cells to react accordingly. These are involved in the regulation process of cell proliferation, differentiation, migration, tumor invasion, and metastasis [230, 231]. The matrix metalloproteinases (MMPs) regulate the epithelial-mesenchymal transition and are involved in the process of cell migration and invasion [232, 233]. Several MMP genes like *MMP2*, *MMP9*, *MMP14*, *MMP15* and *MMP19* were observed to be downregulated upon miR-204 expression, of which, *MMP15* is a putative target gene of miR-204 whereas *MMP9* is known validated target of miR-204. The downregulation of *MMP9* by miR-204 has been shown to reduce the migration and invasion potential of melanoma cells [224]. Thus, the downregulation of these genes is consistent with the inhibition of invasion and tumorigenic potential of medulloblastoma cells upon miR-204 expression.

The genes *IGF2R*, *M6PR*, *AP1S2,* and *LAMP1* were also found to be downregulated upon miR-204 expression in medulloblastoma cells. These genes are involved in lysosomal pathway. In the present work, *IGF2R* and *LAMP1* were identified as novel direct target genes of miR-204, whereas *M6PR* and *AP1S2* are known validated targets of miR-204

[223]. The lysosomes are membrane-bound cell organelles functioning as a digestive system for the cells. These are involved in the management of cellular waste from within the cytoplasm and degradation of materials taken inside the cells through endocytosis. The process of degradation is undertaken by an array of lytic enzymes capable of degrading variety of biomolecules, which are active in the low pH of the lysosomes. These lysosomal proteases are synthesized on the rough endoplasmic reticulum, and then transported to cis-face of Golgi apparatus as proenzymes. These proenzymes are post-translationally modified by an addition of the Mannose-6-phosphate tag in the cis-Golgi. Both cation-dependent and cation-independent mannose-6-phosphate receptors i.e. *M6PR* and *IGF2R,* respectively are known to be involved in trafficking of lysosomal proteases from the trans-Golgi apparatus to early lysosomal compartments through clathrin-coated vesicles [227, 234]. In the acidic pH of the lysosomal compartment, these proenzymes are released from the receptors and get matured by the cleavage of the signal peptide. *AP1S2* is a validated miR-204 target gene and was also downregulated upon miR-204 expression in medulloblastoma cells. AP1S2 encodes Adaptor related protein 1 complex subunit sigma 2 protein. It is the part of AP1 heterotetrameric complex located at the trans-golgi face and is involved in sorting of the cargo in the clathrin coated vesicles which are further directed to endosomal and lysosomal compartments [235]. The Mannose-6-phosphate receptors loaded with the lysosomal proenzymes are sorted to the clathrin-coated vesicles by the AP1 complex consisting of *AP1S2* [236]. As *IGF2R*, *M6PR* and *AP1S2* which are involved in the trafficking of the lysosomal proteases are downregulated upon miR-204 expression in medulloblastoma cells, in this study, the effect of miR-204 expression on the levels of lysosomal enzymes Cathepsin B (*CTSB*) and Cathepsin D (*CTSD*) in medulloblastoma

cells was studied by western blotting. MiR-204 expression resulted in considerable downregulation of the mature form of these lysosomal enzymes in all medulloblastoma cell lines indicating impaired transport of these proteases to the lysosomes. SQSTM1/p62, an adaptor protein involved in the autophagy is known to undergo lysosomal degradation upon fusion of autophagosome and lysosome [237, 238]. The levels of SQSTM1/p62 were found to be increased upon miR-204 expression in medulloblastoma cells, indicating the compromised lysosomal degradation.

LAMP1 was identified as another novel direct target gene of miR-204. LAMP1 and LAMP2 constitute about 50 % of the total membrane proteins of lysosomes. *LAMP1* is known to be involved in lysosomal biogenesis, maintaining lysosomal membrane integrity and interaction of lysosomes with other vesicular compartments within the cells [239, 240]. Therefore, downregulation of LAMP1 can contribute to the compromised lysosomal function. Lysosomal degradation pathway plays a major role in autophagy [241, 242]. Thus, compromised lysosomal function mediated by downregulation of mannose-6-phosphate receptors (*M6PR* and *IGF* and *LAMP1* can contribute to the inhibition of autophagy upon miR-204 expression in medulloblastoma cells. Furthermore, LAMP1 is expressed at higher levels on the surface of the cancer cells having high metastatic potential [243-245]. The higher expression of LMAP1 was found to positively correlate with the higher metastatic ability of cancer cells [240]. Thus, the downregulation of LAMP1 by miR-204 is consistent with the lower incidence of metastasis of Group 3/Group 4 medulloblastomas having higher miR-204 expression [11].

In summary, restoration of miR-204 expression exhibited a tumor-suppressive effects in MYC overexpressing/amplified Group 3 medulloblastoma cells. MiR-204 expression

resulted in downregulation of the genes involved in the lysosomal degradation pathway and extracellular matrix organization and degradation. IGF2R and LAMP1 were identified as direct novel target genes of miR-204. The downregulation of these genes is consistent with the inhibition of invasion potential and autophagy upon miR-204 expression in medulloblastoma cells. The treatment of medulloblastoma cells with HDAC inhibitors resulted in modest upregulation of miR-204 levels in Group 3 medulloblastoma cells suggesting a possible role of HDAC inhibitors in the treatment of medulloblastomas.

Chapter 6

6. Summary and Conclusions

WNT subgroup medulloblastomas have excellent survival among the four molecular subgroups of medulloblastomas. The molecular mechanism underlying this high survival rate of the WNT subgroup is largely not understood. WNT subgroup has the most distinctive microRNA profile, which could play a crucial role in its biology. The functional role of two WNT subgroup microRNAs, miR-193a and miR-204, was studied in detail. The molecular mechanism underlying the WNT subgroup enriched expression of the two microRNAs was investigated. The microRNA was expressed in a doxycycline-inducible manner in established medulloblastoma cell lines. The effect of restoration of microRNA expression on the growth and malignant characteristics of medulloblastoma cells was investigated by studying their anchorage-independent growth, invasion potential, and tumorigenicity. The underlying molecular mechanism was deciphered by transcriptome sequencing and by identifying direct targets of the microRNAs.

The salient findings of the present study are as follows.

6.1. MiR-193a

- The expression of miR-193a is restricted to the WNT subgroup medulloblastomas, as analyzed in two independent cohorts of molecularly classified medulloblastomas.
- The miR-193a expression is upregulated by MYC, a downstream target of WNT signaling. Therefore, the expression of miR-193a in the WNT subgroup medulloblastomas appears to be upregulated by the constitutively activated WNT signaling pathway.
- The CpG island in the miR-193a promoter region was found to be hypermethylated in the three non-WNT subgroups of medulloblastomas. The expression of miR-193a could be restored upon the treatment of medulloblastoma cell lines with a DNA methylation

inhibitor, 5-aza-2'-deoxycytidine. Thus, miR-193a expression appears to be downregulated in non-WNT medulloblastomas due to promoter hypermethylation.

- Restoration of miR-193a expression in MYC amplified/overexpressing Group 3 medulloblastoma cells inhibited their growth, tumorigenic potential, and increased their sensitivity to radiation, indicating a tumor-suppressive role of miR-193a in medulloblastoma pathogenesis.
- *MAX*, *DCAF7*, and *STMN1* were identified as novel targets of miR-193a that are likely to contribute to its tumor-suppressive effect.
- MAX is an obligate heterodimerization partner of MYC required for the transcriptional activity of MYC. The expression of miR-193a in MYC overexpressing/amplified Group 3 medulloblastoma cells resulted in the downregulation of MAX and destabilization of MYC as indicated by the reduction in the half-life of MYC. Thus, miR-193a appears to act as a feedback inhibitor of the MYC signaling.

- MAX has been reported to suppress the expression of miR-193a by directly interacting with the miR-193a promoter [10]. Therefore, miR-193a and MAX appear to negatively regulate each other's expression, thereby modulating the activity of the MYC transcription factor family.
- MiR-193a expression in the medulloblastoma cells brought about widespread repression of gene expression that included genes involved in the WNT signaling, NOTCH signaling, cell cycle regulators, DNA replication as well as chromatin organization and modification. The miR-193a mediated widespread repression of gene expression was found to be accompanied by a substantial decrease in the global levels of H3K4me3,

H3K27ac, the histone marks of active chromatin, and an increase in H3K27me3, a mark of repressed chromatin, indicating genome-wide chromatin remodeling.

- In cancer cells having high MYC expression, MYC accumulates at the promoters of actively transcribed genes bringing about their transcriptional amplification. Therefore, miR-193a mediated inhibition of MYC activity is likely to contribute to the widespread repression of gene expression in Group 3 medulloblastoma cells.
- MiR-193a expression led to a tumor-suppressive effect in MYC overexpressing Group 3 cells mediated by a decrease in the activity of MYC and reduction in the levels of several oncogenic targets and global epigenomic repression of gene expression. Hence miR-193a has a therapeutic potential in MYC overexpressing aggressive Group 3 medulloblastomas.

6.2. MiR-204

- MiR-204 is differentially expressed in the four molecular subgroups of medulloblastomas. However, the miR-204 promoter region was not found to be hypermethylated in medulloblastoma tumor tissues MiR-204 expression could be partially restored in medulloblastoma cells upon treatment with HDAC inhibitors.
- Restoration of miR-204 inhibited tumorigenicity of Group 3 medulloblastoma cell lines, with an increase in the survival duration of the tumor-bearing mice by 25-34 %. This indicates the tumor-suppressive effect of miR-204 in medulloblastomas, which is consistent with its role in several other cancers.
- The transcriptome analysis of miR-204 expressing cells has identified downregulation of several known validated target genes of miR-204 like RAB22A, M6PR, AP1S2, and EZR.

- IGF2R and LAMP1, which were downregulated upon miR-204 expression were identified as novel target genes of miR-204.
- The protein-protein interaction network analysis of the genes significantly downregulated upon miR-204 expression identified downregulation of several genes involved in the extracellular matrix organization and degradation. The downregulation of these genes is consistent with the inhibition of tumorigenicity and invasion potential of medulloblastoma cells upon miR-204 expression.
- Lysosomal degradation pathway is one of the major pathways identified to be affected by miR-204 expression in medulloblastoma cells as indicated by downregulation of key genes involved in this pathway which includes IGF2R, M6PR, LAMP1, and AP1S2.
- IGF2R, M6PR, and AP1S2 are known to be involved in the transportation of lysosomal proteases from the trans-Golgi network to the lysosomal compartment. MiR-204 expression significantly reduced the levels of mature lysosomal proteases cathepsin B and cathepsin D in medulloblastoma cells.
- The miR-204 expression increased the levels of SQSTM1/p62, an adaptor protein involved in the pathway of autophagy, which gets degraded by lysosomal activity upon fusion of autophagosomes with lysosomes. This suggests the reduction in the lysosomal degradation and autophagy pathway upon miR-204 expression medulloblastoma cells.
- The expression miR-204 in medulloblastoma cells brings about inhibition of autophagy (Ph.D. thesis, Raikamal Paul). Lysosomal degradation pathway is known to play a pivotal role in autophagy. Hence, downregulation of key genes involved in the lysosomal pathway accompanied by reduced levels of lysosomal proteases are likely to contribute to autophagy inhibition upon miR-204 expression,

- Autophagy inhibition upon ATG5 knockdown in medulloblastoma cells led to inhibition of their invasion potential (Ph. D. thesis, Raikamal Paul) [156]. Therefore, the inhibition of the autophagy-lysosomal degradation pathway is likely to contribute to the decrease in the invasion potential of medulloblastoma cells upon miR-204 expression.
- Upregulation of miR-204 expression upon treatment with HDAC inhibitors, although modest, suggests a role of these inhibitors in the treatment of medulloblastomas.

6.3. Contribution of microRNAs in excellent survival rates of WNT subgroup medulloblastomas

The WNT subgroup tumors have the most distinctive microRNA expression profile with overexpression of several microRNAs, including miR-193a, miR-204, miR-148a, miR-224 [9, 151]. Previously in our lab, miR-204 and miR-148a have been shown to inhibit the anchorage-independent growth, tumorigenicity, and invasion potential of medulloblastoma cells. Interestingly, miR-148a was also found to be induced by MYC (Ph.D. thesis, Kedar Yogi). The tumor-suppressive activity of miR-148a in medulloblastoma cells was found to be contributed by a reduction in the levels of its direct target NRP1, a co-receptor of several growth factors including VEGF, EGF, PDGF, TGF-β1, and HGF. MiR-204 is another microRNA overexpressed in the WNT subgroup and downregulated in almost all SHH and several Group 3 and Group 4 tumors. The higher expression of miR-204 correlates with the better overall survival in Group 3/Group 4 medulloblastomas. Restoration of miR-204 expression inhibited anchorage-independent growth, invasion potential, tumorigenicity and increased the radiation sensitivity of medulloblastoma cells (Ph. D. Thesis- Raikamal Paul) accompanied by inhibition of autophagy indicating a tumor-suppressive role of miR-204 in medulloblastoma pathogenesis [11]. Exogenous expression of miR-224 was found

to inhibit growth and increase the radiation sensitivity of medulloblastoma cells. MiR-224 was also reported to be downregulated in glioma tumor tissues and cell lines and its expression was shown to increase the radiation sensitivity of glioma cells by targeting API5 [246]. Therefore, the higher expression of several tumor-suppressive microRNAs is likely to contribute to the excellent survival of WNT subgroup medulloblastomas by decreasing the malignant potential and increasing response to radiation therapy.

6.4. MicroRNAs: the evolving therapeutic agents

Despite the tremendous progress in understanding the cancer biology, there is a paucity of effective therapies due to inadequate targeting of the oncogenic pathways, the emergence of drug resistance, and drug-induced toxicity [247, 248]. Cancer is caused by multiple genetic alterations. Targeting a single oncogene, therefore, has limited efficacy both due to lack of complete dependence of cancer cells on a single alteration and due to the development of resistance. Each microRNA targets multiple genes in a biologically relevant manner. MicroRNAs are evolutionarily conserved natural endogenous small RNAs that cells use for controlling cellular mechanisms like proliferation, stem cell maintenance, differentiation. MicroRNAs, therefore, offer a novel natural therapeutic modality for cancer treatment. Numerous studies have proved the oncogenic and tumor-suppressive role of microRNAs in cancer [8, 248]. The microRNAs can be used for the treatment provided they are exclusively tumor-suppressive or oncogenic. Although microRNA-based drugs have not yet entered the clinics, the safety of microRNA-based therapeutics has been demonstrated in several phase I clinical trials [249, 250]. Restoration of tumor suppressor microRNA expression or inhibition of oncomiR function is the current strategy for the microRNA-based therapeutics for the treatment of cancer. MiR-34 is a

validated tumor-suppressor microRNA known to target over 30 oncogenes involved in various cellular pathways in multiple tumor types. MiR-16 mimic, encapsulated in bacterially derived minicells conjugated to anti-EGFR antibody, has entered phase II clinical trial for the treatment of lung cancer cells having a high expression of EGFR [250, 251]. Several clinical trials are ongoing like the miR-10b inhibitor in glioblastoma and miR-155 inhibitor in T-cell lymphoma. These trials using formulations of the lock nucleic acids for the inhibition of microRNAs have yielded promising results [252]. Rapid advances are being made in designing and optimizing various approaches for targeted microRNA delivery that include use of liposomes, nanoparticles, exosomes, as well as viral vectors like adeno-associated vectors [253, 254]. In the case of brain tumors, the blood-brain barrier also needs to be overcome. Non-invasive focused ultrasound treatment that disrupts the blood-brain barrier in a targeted area is one of the potential approaches for targeted delivery into brain tumors [255]. In the present study, the tumor-suppressive role of miR-193a and miR-204 was experimentally demonstrated in highly aggressive MYC overexpressing Group 3 medulloblastoma cell lines, making them promising molecules for the treatment of medulloblastomas. The therapeutic efficacy and safety of these microRNAs in combination with other treatment modalities like radiation therapy could be evaluated in patient-derived xenograft models by delivering these microRNAs systemically or by directly injecting into the tumor.

6.5. Significance of the study

- Both miR-193a and miR-204 are WNT subgroup enriched microRNAs, which exhibited a significant tumor-suppressive effect in MYC overexpressing/amplified Group

3 medulloblastoma cells. Thus, both microRNAs hold a therapeutic potential in the treatment of the highly aggressive Group 3 medulloblastomas.

- The WNT subgroup has an excellent long-term survival of over 90 %, even though WNT signaling is expected to impart a highly malignant nature to the tumors. MiR-193a and miR-204, two microRNAs expressed in the WNT subgroup were found to be tumor-suppressive in medulloblastoma cells. MiR-193a was found to decrease the activity of MYC, a crucial downstream target of WNT signaling. MiR-193a increases the radiation sensitivity of medulloblastoma cells. MiR-204 was found to inhibit invasion potential of medulloblastoma cells by inhibiting autophagy-lysosomal degradation pathway. Thus, the microRNAs are likely to contribute to the better overall survival of the WNT subgroup medulloblastomas.
- MYC is overexpressed in more than 50 % of malignancies and is a known marker of poor prognosis [82]. MiR-193a, on the other hand, was shown to destabilize MYC by downregulation of MAX. Thus, miR-193a is likely to be a promising therapeutic microRNA for other MYC overexpressing malignancies as well.

6.6. Future directions

- The tumor-suppressive effect of miR-193a and miR-204 on the highly aggressive MYC overexpressing/amplified Group 3 medulloblastoma cell lines suggests the therapeutic potential of the two microRNAs in the treatment of Group 3 medulloblastomas. The therapeutic efficacy of these microRNAs either alone or in combination, could be evaluated in pre-clinical models, including PDX models and transgenic mouse models of medulloblastomas. The microRNAs can be delivered as lipid encapsulated mimics, using adenoviral vectors or encapsulated in exosomes.

- MiR-204 expression is downregulated in almost all SHH subgroup medulloblastomas. The role of miR-204 in the pathogenesis of SHH subgroup tumors and possibly on the SHH signaling pathway could be explored using SHH medulloblastoma cell lines, PDX models, and transgenic mouse models of SHH subgroup medulloblastomas. MiR-204 may have therapeutic potential in the treatment of SHH subgroup medulloblastomas as well.

7. Bibliography

1. Ostrom, Q. T.Gittleman, H.Fulop, J.Liu, M.*, et al.* (2015) CBTRUS Statistical Report: Primary Brain and Central Nervous System Tumors Diagnosed in the United States in 2008-2012, *Neuro-oncology.* **17 Suppl 4**, iv1-iv62.

2. Northcott, P. A.Robinson, G. W.Kratz, C. P.Mabbott, D. J.*, et al.* (2019) Medulloblastoma, *Nature reviews Disease primers.* **5**, 11.

3. Taylor, M. D.Northcott, P. A.Korshunov, A.Remke, M.*, et al.* (2012) Molecular subgroups of medulloblastoma: the current consensus, *Acta neuropathologica.* **123**, 465-72.

4. Kool, M.Korshunov, A.Remke, M.Jones, D. T.*, et al.* (2012) Molecular subgroups of medulloblastoma: an international meta-analysis of transcriptome, genetic aberrations, and clinical data of WNT, SHH, Group 3, and Group 4 medulloblastomas, *Acta neuropathologica.* **123**, 473-84.

5. Bartel, D. P. (2004) MicroRNAs: genomics, biogenesis, mechanism, and function, *Cell.* **116**, 281-97.

6. Bartel, D. P. (2009) MicroRNAs: target recognition and regulatory functions, *Cell.* **136**, 215-33.

7. Garzon, R.Calin, G. A. & Croce, C. M. (2009) MicroRNAs in Cancer, *Annual Review of Medicine.* **60**, 167-179.

8. Garzon, R.Fabbri, M.Cimmino, A.Calin, G. A.*, et al.* (2006) MicroRNA expression and function in cancer, *Trends in molecular medicine.* **12**, 580-7.

9. Gokhale, A.Kunder, R.Goel, A.Sarin, R.*, et al.* (2010) Distinctive microRNA signature of medulloblastomas associated with the WNT signaling pathway, *Journal of cancer research and therapeutics.* **6**, 521-9.

10. Iliopoulos, D.Rotem, A. & Struhl, K. (2011) Inhibition of miR-193a expression by Max and RXRalpha activates K-Ras and PLAU to mediate distinct aspects of cellular transformation, *Cancer research.* **71**, 5144-53.

11. Bharambe, H. S.Paul, R.Panwalkar, P.Jalali, R.*, et al.* (2019) Downregulation of miR-204 expression defines a highly aggressive subset of Group 3/Group 4 medulloblastomas, *Acta neuropathologica communications.* **7**, 52.

12. Lee, Y.Yang, X.Huang, Y.Fan, H.*, et al.* (2010) Network modeling identifies molecular functions targeted by miR-204 to suppress head and neck tumor metastasis, *PLoS computational biology.* **6**, e1000730.

13. Volinia, S.Galasso, M.Costinean, S.Tagliavini, L.*, et al.* (2010) Reprogramming of miRNA networks in cancer and leukemia, *Genome research.* **20**, 589-99.

14. Bailey, P. & Cushing, H. (1925) Medulloblastoma cerebelli: A common type of midcerebellar gliom of childhood., *Archives of Neurology & Psychiatry.* **14**, 192-224.

15. Hart, M. N. & Earle, K. M. (1973) Primitive neuroectodermal tumors of the brain in children, *Cancer.* **32**, 890-7.

16. Rorke, L. B. (1983) The cerebellar medulloblastoma and its relationship to primitive neuroectodermal tumors, *J Neuropathol Exp Neurol.* **42**, 1-15.

17. Pomeroy, S. L.Tamayo, P.Gaasenbeek, M.Sturla, L. M.*, et al.* (2002) Prediction of central nervous system embryonal tumour outcome based on gene expression, *Nature.* **415**, 436-42.

18. Jozwiak, J.Sontowska, I.Bikowska, B.Grajkowska, W.*, et al.* (2011) Favourable prognosis in medulloblastoma with extensive nodularity is associated with mitogen-activated protein kinase upregulation, *Folia neuropathologica.* **49**, 257-61.

19. Massimino, M.Antonelli, M.Gandola, L.Miceli, R.*, et al.* (2013) Histological variants of medulloblastoma are the most powerful clinical prognostic indicators, *Pediatric blood & cancer.* **60**, 210-6.

20. Crawford, J. R.MacDonald, T. J. & Packer, R. J. (2007) Medulloblastoma in childhood: new biological advances, *The Lancet Neurology.* **6**, 1073-85.

21. Rossi, A.Caracciolo, V.Russo, G.Reiss, K.*, et al.* (2008) Medulloblastoma: from molecular pathology to therapy, *Clinical cancer research : an official journal of the American Association for Cancer Research.* **14**, 971-6.

22. Smoll, N. R. & Drummond, K. J. (2012) The incidence of medulloblastomas and primitive neurectodermal tumours in adults and children, *Journal of clinical neuroscience : official journal of the Neurosurgical Society of Australasia.* **19**, 1541-4.

23. Edward, P. & Prados, M. D. (2003) Adult Medulloblastomas in *Holland-Frei Cancer Medicine* (Kufe, D. W., Pollock, R. E. & Weichselbaum, R. R., eds), BC Decker, Hamilton (ON).

24. Lassaletta, A. & Ramaswamy, V. (2016) Medulloblastoma in adults: they're not just big kids, *Neuro-oncology.* **18**, 895-7.

25. Giordana, M. T.Schiffer, P.Lanotte, M.Girardi, P.*, et al.* (1999) Epidemiology of adult medulloblastoma, *International journal of cancer.* **80**, 689-92.

26. Louis, D. N.Ohgaki, H.Wiestler, O. D.Cavenee, W. K.*, et al.* (2007) The 2007 WHO classification of tumours of the central nervous system, *Acta neuropathologica.* **114**, 97-109.

27. Cushing, H. (1930) Experiences with the Cerebellar Medulloblastomas: A criticl review, *Acta Pathologica Microbiologica Scandinavica*.

28. Rutka, J. T. & Hoffman, H. J. (1996) Medulloblastoma: a historical perspective and overview, *Journal of neuro-oncology.* **29**, 1-7.

29. Ingraham, F. D.Bailey, O. T. & Barker, W. F. (1948) Medulloblastoma cerebelli; diagnosis, treatment and survivals, with a report of 56 cases, *The New England journal of medicine.* **238**, 171-4.

30. Paterson, E. & Farr, R. F. (1953) Cerebellar medulloblastoma: treatment by irradiation of the whole central nervous system, *Acta radiologica.* **39**, 323-36.

31. Dennis, M.Spiegler, B. J.Hetherington, C. R. & Greenberg, M. L. (1996) Neuropsychological sequelae of the treatment of children with medulloblastoma, *Journal of neuro-oncology.* **29**, 91-101.

32. Packer, R. J.Goldwein, J.Nicholson, H. S.Vezina, L. G.*, et al.* (1999) Treatment of children with medulloblastomas with reduced-dose craniospinal radiation therapy and adjuvant chemotherapy: A Children's Cancer Group Study, *Journal of clinical oncology : official journal of the American Society of Clinical Oncology.* **17**, 2127-36.

33. de Bont, J. M.Packer, R. J.Michiels, E. M.den Boer, M. L.*, et al.* (2008) Biological background of pediatric medulloblastoma and ependymoma: a review from a translational research perspective, *Neuro-oncology.* **10**, 1040-60.

34. Doussouki, M. E.Gajjar, A. & Chamdine, O. (2019) Molecular genetics of medulloblastoma in children: diagnostic, therapeutic and prognostic implications, *FUTURE NEUROLOGY.* **14**.

35. Pfister, S.Remke, M.Benner, A.Mendrzyk, F.*, et al.* (2009) Outcome prediction in pediatric medulloblastoma based on DNA copy-number aberrations of chromosomes 6q and 17q and the MYC and MYCN loci, *Journal of clinical oncology : official journal of the American Society of Clinical Oncology.* **27**, 1627-36.

36. Roussel, M. F. & Hatten, M. E. (2011) Cerebellum development and medulloblastoma, *Current topics in developmental biology.* **94**, 235-82.

37. Cowan, R.Hoban, P.Kelsey, A.Birch, J. M.*, et al.* (1997) The gene for the naevoid basal cell carcinoma syndrome acts as a tumour-suppressor gene in medulloblastoma, *British journal of cancer.* **76**, 141-5.

38. Hamilton, S. R.Liu, B.Parsons, R. E.Papadopoulos, N.*, et al.* (1995) The molecular basis of Turcot's syndrome, *The New England journal of medicine.* **332**, 839-47.

39. Northcott, P. A.Buchhalter, I.Morrissy, A. S.Hovestadt, V.*, et al.* (2017) The whole-genome landscape of medulloblastoma subtypes, *Nature.* **547**, 311-317.

40. Nusslein-Volhard, C. & Wieschaus, E. (1980) Mutations affecting segment number and polarity in Drosophila, *Nature.* **287**, 795-801.

41. Choudhry, Z.Rikani, A. A.Choudhry, A. M.Tariq, S.*, et al.* (2014) Sonic hedgehog signalling pathway: a complex network, *Annals of neurosciences.* **21**, 28-31.

42. Ahn, S. & Joyner, A. L. (2005) In vivo analysis of quiescent adult neural stem cells responding to Sonic hedgehog, *Nature.* **437**, 894-7.

43. Bhardwaj, G.Murdoch, B.Wu, D.Baker, D. P.*, et al.* (2001) Sonic hedgehog induces the proliferation of primitive human hematopoietic cells via BMP regulation, *Nature immunology.* **2**, 172-80.

44. Liu, S.Dontu, G.Mantle, I. D.Patel, S.*, et al.* (2006) Hedgehog signaling and Bmi-1 regulate self-renewal of normal and malignant human mammary stem cells, *Cancer research.* **66**, 6063-71.

45. Mabbott, D. J.Spiegler, B. J.Greenberg, M. L.Rutka, J. T.*, et al.* (2005) Serial evaluation of academic and behavioral outcome after treatment with cranial radiation in childhood, *Journal of clinical oncology : official journal of the American Society of Clinical Oncology.* **23**, 2256-63.

46. Wechsler-Reya, R. J. & Scott, M. P. (1999) Control of neuronal precursor proliferation in the cerebellum by Sonic Hedgehog, *Neuron.* **22**, 103-14.

47. Archer, T. C.Weeraratne, S. D. & Pomeroy, S. L. (2012) Hedgehog-GLI pathway in medulloblastoma, *Journal of clinical oncology : official journal of the American Society of Clinical Oncology.* **30**, 2154-6.

48. Goodrich, L. V.Milenkovic, L.Higgins, K. M. & Scott, M. P. (1997) Altered neural cell fates and medulloblastoma in mouse patched mutants, *Science.* **277**, 1109-13.

49. Hatton, B. A.Villavicencio, E. H.Tsuchiya, K. D.Pritchard, J. I.*, et al.* (2008) The Smo/Smo model: hedgehog-induced medulloblastoma with 90 % incidence and leptomeningeal spread, *Cancer research.* **68**, 1768-76.

50. Low, J. A. & de Sauvage, F. J. (2010) Clinical experience with Hedgehog pathway inhibitors, *Journal of clinical oncology : official journal of the American Society of Clinical Oncology.* **28**, 5321-6.

51. Nusse, R. & Varmus, H. (2012) Three decades of Wnts: a personal perspective on how a scientific field developed, *The EMBO journal.* **31**, 2670-84.

52. Clevers, H. & Nusse, R. (2012) Wnt/beta-catenin signaling and disease, *Cell.* **149**, 1192-205.

53. Hart, M.Concordet, J. P.Lassot, I.Albert, I.*, et al.* (1999) The F-box protein beta-TrCP associates with phosphorylated beta-catenin and regulates its activity in the cell, *Current biology : CB.* **9**, 207-10.

54. Komiya, Y. & Habas, R. (2008) Wnt signal transduction pathways, *Organogenesis.* **4**, 68-75.

55. Thompson, M. C.Fuller, C.Hogg, T. L.Dalton, J.*, et al.* (2006) Genomics identifies medulloblastoma subgroups that are enriched for specific genetic alterations, *Journal of clinical oncology : official journal of the American Society of Clinical Oncology.* **24**, 1924-31.

56. Kool, M.Koster, J.Bunt, J.Hasselt, N. E.*, et al.* (2008) Integrated genomics identifies five medulloblastoma subtypes with distinct genetic profiles, pathway signatures and clinicopathological features, *PloS one.* **3**, e3088.

57. Northcott, P. A.Korshunov, A.Witt, H.Hielscher, T.*, et al.* (2011) Medulloblastoma comprises four distinct molecular variants, *Journal of clinical oncology : official journal of the American Society of Clinical Oncology.* **29**, 1408-14.

58. Cho, Y. J.Tsherniak, A.Tamayo, P.Santagata, S.*, et al.* (2011) Integrative genomic analysis of medulloblastoma identifies a molecular subgroup that drives poor clinical outcome, *Journal of clinical oncology : official journal of the American Society of Clinical Oncology.* **29**, 1424-30.

59. Ramaswamy, V.Remke, M.Bouffet, E.Faria, C. C.*, et al.* (2013) Recurrence patterns across medulloblastoma subgroups: an integrated clinical and molecular analysis, *The Lancet Oncology.* **14**, 1200-7.

60. Northcott, P. A.Shih, D. J.Peacock, J.Garzia, L.*, et al.* (2012) Subgroup-specific structural variation across 1,000 medulloblastoma genomes, *Nature.* **488**, 49-56.

61. Gibson, P.Tong, Y.Robinson, G.Thompson, M. C.*, et al.* (2010) Subtypes of medulloblastoma have distinct developmental origins, *Nature.* **468**, 1095-9.

62. Louis, D. N.Perry, A.Reifenberger, G.von Deimling, A.*, et al.* (2016) The 2016 World Health Organization Classification of Tumors of the Central Nervous System: a summary, *Acta neuropathologica.* **131**, 803-20.

63. Wetmore, C.Eberhart, D. E. & Curran, T. (2001) Loss of p53 but not ARF accelerates medulloblastoma in mice heterozygous for patched, *Cancer research.* **61**, 513-6.

64. Dey, J.Ditzler, S.Knoblaugh, S. E.Hatton, B. A.*, et al.* (2012) A distinct Smoothened mutation causes severe cerebellar developmental defects and medulloblastoma in a novel transgenic mouse model, *Molecular and cellular biology.* **32**, 4104-15.

65. Lee, Y.Kawagoe, R.Sasai, K.Li, Y.*, et al.* (2007) Loss of suppressor-of-fused function promotes tumorigenesis, *Oncogene.* **26**, 6442-7.

66. Schuller, U.Heine, V. M.Mao, J.Kho, A. T.*, et al.* (2008) Acquisition of granule neuron precursor identity is a critical determinant of progenitor cell competence to form Shh-induced medulloblastoma, *Cancer cell.* **14**, 123-34.

67. Yang, Z. J.Ellis, T.Markant, S. L.Read, T. A.*, et al.* (2008) Medulloblastoma can be initiated by deletion of Patched in lineage-restricted progenitors or stem cells, *Cancer cell.* **14**, 135-45.

68. Swartling, F. J.Savov, V.Persson, A. I.Chen, J.*, et al.* (2012) Distinct neural stem cell populations give rise to disparate brain tumors in response to N-MYC, *Cancer cell.* **21**, 601-13.

69. Bai, R. Y.Staedtke, V.Lidov, H. G.Eberhart, C. G.*, et al.* (2012) OTX2 represses myogenic and neuronal differentiation in medulloblastoma cells, *Cancer research.* **72**, 5988-6001.

70. Boulay, G.Awad, M. E.Riggi, N.Archer, T. C.*, et al.* (2017) OTX2 Activity at Distal Regulatory Elements Shapes the Chromatin Landscape of Group 3 Medulloblastoma, *Cancer discovery.* **7**, 288-301.

71. Bunt, J.Hasselt, N. A.Zwijnenburg, D. A.Koster, J.*, et al.* (2013) OTX2 sustains a bivalent-like state of OTX2-bound promoters in medulloblastoma by maintaining their H3K27me3 levels, *Acta neuropathologica.* **125**, 385-94.

72. Bunt, J.Hasselt, N. E.Zwijnenburg, D. A.Hamdi, M.*, et al.* (2012) OTX2 directly activates cell cycle genes and inhibits differentiation in medulloblastoma cells, *International journal of cancer.* **131**, E21-32.

73. Pan, E.Pellarin, M.Holmes, E.Smirnov, I.*, et al.* (2005) Isochromosome 17q is a negative prognostic factor in poor-risk childhood medulloblastoma patients, *Clinical cancer research : an official journal of the American Association for Cancer Research.* **11**, 4733-40.

74. Adamson, D. C.Shi, Q.Wortham, M.Northcott, P. A.*, et al.* (2010) OTX2 is critical for the maintenance and progression of Shh-independent medulloblastomas, *Cancer research.* **70**, 181-91.

75. Northcott, P. A.Lee, C.Zichner, T.Stutz, A. M.*, et al.* (2014) Enhancer hijacking activates GFI1 family oncogenes in medulloblastoma, *Nature.* **511**, 428-34.

76. Cook Sangar, M. L.Genovesi, L. A.Nakamoto, M. W.Davis, M. J.*, et al.* (2017) Inhibition of CDK4/6 by Palbociclib Significantly Extends Survival in Medulloblastoma Patient-Derived Xenograft Mouse Models, *Clinical cancer research : an official journal of the American Association for Cancer Research.* **23**, 5802-5813.

77. Faria, C. C.Agnihotri, S.Mack, S. C.Golbourn, B. J.*, et al.* (2015) Identification of alsterpaullone as a novel small molecule inhibitor to target group 3 medulloblastoma, *Oncotarget.* **6**, 21718-29.

78. Cavalli, F. M. G.Remke, M.Rampasek, L.Peacock, J.*, et al.* (2017) Intertumoral Heterogeneity within Medulloblastoma Subgroups, *Cancer cell.* **31**, 737-754 e6.

79. Schwalbe, E. C.Lindsey, J. C.Nakjang, S.Crosier, S.*, et al.* (2017) Novel molecular subgroups for clinical classification and outcome prediction in childhood medulloblastoma: a cohort study, *The Lancet Oncology.* **18**, 958-971.

80. Sharma, T.Schwalbe, E. C.Williamson, D.Sill, M.*, et al.* (2019) Second-generation molecular subgrouping of medulloblastoma: an international meta-analysis of Group 3 and Group 4 subtypes, *Acta neuropathologica.* **138**, 309-326.

81. Roussel, M.Saule, S.Lagrou, C.Rommens, C.*, et al.* (1979) Three new types of viral oncogene of cellular origin specific for haematopoietic cell transformation, *Nature.* **281**, 452-5.

82. Chen, H.Liu, H. & Qing, G. (2018) Targeting oncogenic Myc as a strategy for cancer treatment, *Signal transduction and targeted therapy.* **3**, 5.

83. G.C., P. (1997) Myc Structure and Function in *Oncogenes as Transcriptional Regulators Progress in Gene Expression* (M., Y. & J., G., eds), Springer, Birkhäuser, Basel.

84. Adhikary, S. & Eilers, M. (2005) Transcriptional regulation and transformation by Myc proteins, *Nature reviews Molecular cell biology.* **6**, 635-45.

85. Lin, C. Y.Loven, J.Rahl, P. B.Paranal, R. M.*, et al.* (2012) Transcriptional amplification in tumor cells with elevated c-Myc, *Cell.* **151**, 56-67.

86. Dang, C. V. (1999) c-Myc target genes involved in cell growth, apoptosis, and metabolism, *Molecular and cellular biology.* **19**, 1-11.

87. Roussel, M. F. & Robinson, G. W. (2013) Role of MYC in Medulloblastoma, *Cold Spring Harbor perspectives in medicine.* **3**.

88. Oliver, T. G.Grasfeder, L. L.Carroll, A. L.Kaiser, C.*, et al.* (2003) Transcriptional profiling of the Sonic hedgehog response: a critical role for N-myc in proliferation of neuronal precursors, *Proceedings of the National Academy of Sciences of the United States of America.* **100**, 7331-6.

89. Thomas, W. D.Chen, J.Gao, Y. R.Cheung, B.*, et al.* (2009) Patched1 deletion increases N-Myc protein stability as a mechanism of medulloblastoma initiation and progression, *Oncogene.* **28**, 1605-15.

90. Ayrault, O.Zindy, F.Rehg, J.Sherr, C. J.*, et al.* (2009) Two tumor suppressors, p27Kip1 and patched-1, collaborate to prevent medulloblastoma, *Molecular cancer research : MCR.* **7**, 33-40.

91. Kessler, J. D.Hasegawa, H.Brun, S. N.Emmenegger, B. A.*, et al.* (2009) N-myc alters the fate of preneoplastic cells in a mouse model of medulloblastoma, *Genes & development.* **23**, 157-70.

92. Kawauchi, D.Robinson, G.Uziel, T.Gibson, P.*, et al.* (2012) A mouse model of the most aggressive subgroup of human medulloblastoma, *Cancer cell.* **21**, 168-80.

93. Pei, Y.Moore, C. E.Wang, J.Tewari, A. K.*, et al.* (2012) An animal model of MYC-driven medulloblastoma, *Cancer cell.* **21**, 155-67.

94. Gabay, M.Li, Y. & Felsher, D. W. (2014) MYC activation is a hallmark of cancer initiation and maintenance, *Cold Spring Harbor perspectives in medicine.* **4**.

95. Zhukova, N.Ramaswamy, V.Remke, M.Pfaff, E.*, et al.* (2013) Subgroup-specific prognostic implications of TP53 mutation in medulloblastoma, *Journal of clinical oncology : official journal of the American Society of Clinical Oncology.* **31**, 2927-35.

96. Swartling, F. J.Grimmer, M. R.Hackett, C. S.Northcott, P. A.*, et al.* (2010) Pleiotropic role for MYCN in medulloblastoma, *Genes & development.* **24**, 1059-72.

97. Friedman, R. C.Farh, K. K.Burge, C. B. & Bartel, D. P. (2009) Most mammalian mRNAs are conserved targets of microRNAs, *Genome research.* **19**, 92-105.

98. He, L. & Hannon, G. J. (2004) MicroRNAs: small RNAs with a big role in gene regulation, *Nature Reviews Genetics.* **5**, 522.

99. Peng, Y. & Croce, C. M. (2016) The role of MicroRNAs in human cancer, *Signal transduction and targeted therapy.* **1**, 15004.

100. Esquela-Kerscher, A. & Slack, F. J. (2006) Oncomirs - microRNAs with a role in cancer, *Nature reviews Cancer.* **6**, 259-69.

101. Baskerville, S. & Bartel, D. P. (2005) Microarray profiling of microRNAs reveals frequent coexpression with neighboring miRNAs and host genes, *Rna.* **11**, 241-7.

102. Mundade, R.Ozer, H. G.Wei, H.Prabhu, L.*, et al.* (2014) Role of ChIP-seq in the discovery of transcription factor binding sites, differential gene regulation mechanism, epigenetic marks and beyond, *Cell cycle.* **13**, 2847-52.

103. Schanen, B. C. & Li, X. (2011) Transcriptional regulation of mammalian miRNA genes, *Genomics.* **97**, 1-6.

104. Borchert, G. M.Lanier, W. & Davidson, B. L. (2006) RNA polymerase III transcribes human microRNAs, *Nature structural & molecular biology.* **13**, 1097-101.

105. Bhattacharyya, M.Das, M. & Bandyopadhyay, S. (2012) miRT: a database of validated transcription start sites of human microRNAs, *Genomics, proteomics & bioinformatics.* **10**, 310-6.

106. de Rie, D.Abugessaisa, I.Alam, T.Arner, E.*, et al.* (2017) An integrated expression atlas of miRNAs and their promoters in human and mouse, *Nature biotechnology.* **35**, 872-878.

107. Georgakilas, G.Vlachos, I. S.Paraskevopoulou, M. D.Yang, P.*, et al.* (2014) microTSS: accurate microRNA transcription start site identification reveals a significant number of divergent pri-miRNAs, *Nature communications.* **5**, 5700.

108. Godnic, I.Zorc, M.Jevsinek Skok, D.Calin, G. A.*, et al.* (2013) Genome-wide and species-wide in silico screening for intragenic MicroRNAs in human, mouse and chicken, *PloS one.* **8**, e65165.

109. Kunej, T.Godnic, I.Ferdin, J.Horvat, S.*, et al.* (2011) Epigenetic regulation of microRNAs in cancer: an integrated review of literature, *Mutation research.* **717**, 77-84.

110. Saito, Y.Liang, G.Egger, G.Friedman, J. M.*, et al.* (2006) Specific activation of microRNA-127 with downregulation of the proto-oncogene BCL6 by chromatin-modifying drugs in human cancer cells, *Cancer cell.* **9**, 435-43.

111. Rountree, M. R.Bachman, K. E.Herman, J. G. & Baylin, S. B. (2001) DNA methylation, chromatin inheritance, and cancer, *Oncogene.* **20**, 3156-65.

112. Baer, C.Claus, R. & Plass, C. (2013) Genome-wide epigenetic regulation of miRNAs in cancer, *Cancer research.* **73**, 473-7.

113. O'Brien, J.Hayder, H.Zayed, Y. & Peng, C. (2018) Overview of MicroRNA Biogenesis, Mechanisms of Actions, and Circulation, *Frontiers in Endocrinology.* **9**.

114. Altuvia, Y.Landgraf, P.Lithwick, G.Elefant, N.*, et al.* (2005) Clustering and conservation patterns of human microRNAs, *Nucleic acids research.* **33**, 2697-706.

115. Cullen, B. R. (2004) Derivation and function of small interfering RNAs and microRNAs, *Virus research.* **102**, 3-9.

116. Denli, A. M.Tops, B. B.Plasterk, R. H.Ketting, R. F.*, et al.* (2004) Processing of primary microRNAs by the Microprocessor complex, *Nature.* **432**, 231-5.

117. Zeng, Y.Yi, R. & Cullen, B. R. (2005) Recognition and cleavage of primary microRNA precursors by the nuclear processing enzyme Drosha, *The EMBO journal.* **24**, 138-48.

118. Okada, C.Yamashita, E.Lee, S. J.Shibata, S.*, et al.* (2009) A high-resolution structure of the pre-microRNA nuclear export machinery, *Science.* **326**, 1275-9.

119. Zhang, H.Kolb, F. A.Jaskiewicz, L.Westhof, E.*, et al.* (2004) Single processing center models for human Dicer and bacterial RNase III, *Cell.* **118**, 57-68.

120. Czech, B. & Hannon, G. J. (2011) Small RNA sorting: matchmaking for Argonautes, *Nature reviews Genetics.* **12**, 19-31.

121. Kawamata, T. & Tomari, Y. (2010) Making RISC, *Trends in biochemical sciences.* **35**, 368-76.

122. Chiang, H. R.Schoenfeld, L. W.Ruby, J. G.Auyeung, V. C.*, et al.* (2010) Mammalian microRNAs: experimental evaluation of novel and previously annotated genes, *Genes & development.* **24**, 992-1009.

123. Jo, M. H.Shin, S.Jung, S. R.Kim, E.*, et al.* (2015) Human Argonaute 2 Has Diverse Reaction Pathways on Target RNAs, *Molecular cell.* **59**, 117-24.

124. Jonas, S. & Izaurralde, E. (2015) Towards a molecular understanding of microRNA-mediated gene silencing, *Nature reviews Genetics.* **16**, 421-33.

125. Lee, R. C.Feinbaum, R. L. & Ambros, V. (1993) The C. elegans heterochronic gene lin-4 encodes small RNAs with antisense complementarity to lin-14, *Cell.* **75**, 843-54.

126. Lal, A.Navarro, F.Maher, C. A.Maliszewski, L. E.*, et al.* (2009) miR-24 Inhibits cell proliferation by targeting E2F2, MYC, and other cell-cycle genes via binding to "seedless" 3'UTR microRNA recognition elements, *Molecular cell.* **35**, 610-25.

127. Shin, C.Nam, J. W.Farh, K. K.Chiang, H. R.*, et al.* (2010) Expanding the microRNA targeting code: functional sites with centered pairing, *Molecular cell.* **38**, 789-802.

128. Witkos, T. M.Koscianska, E. & Krzyzosiak, W. J. (2011) Practical Aspects of microRNA Target Prediction, *Current molecular medicine.* **11**, 93-109.

129. Alexiou, P.Maragkakis, M.Papadopoulos, G. L.Reczko, M.*, et al.* (2009) Lost in translation: an assessment and perspective for computational microRNA target identification, *Bioinformatics.* **25**, 3049-55.

130. Martinez-Sanchez, A. & Murphy, C. L. (2013) MicroRNA Target Identification-Experimental Approaches, *Biology.* **2**, 189-205.

131. Agarwal, V.Bell, G. W.Nam, J. W. & Bartel, D. P. (2015) Predicting effective microRNA target sites in mammalian mRNAs, *eLife.* **4**.

132. Leva, G. D.Garofalo, M. & Croce, C. M. (2014) MicroRNAs in Cancer, *Annual Review of Pathology: Mechanisms of Disease.* **9**, 287-314.

133. Calin, G. A.Dumitru, C. D.Shimizu, M.Bichi, R.*, et al.* (2002) Frequent deletions and down-regulation of micro- RNA genes miR15 and miR16 at 13q14 in chronic lymphocytic leukemia, *Proceedings of the National Academy of Sciences of the United States of America.* **99**, 15524-9.

134. Cimmino, A.Calin, G. A.Fabbri, M.Iorio, M. V.*, et al.* (2005) miR-15 and miR-16 induce apoptosis by targeting BCL2, *Proceedings of the National Academy of Sciences of the United States of America.* **102**, 13944-9.

135. Kumar, M. S.Erkeland, S. J.Pester, R. E.Chen, C. Y.*, et al.* (2008) Suppression of non-small cell lung tumor development by the let-7 microRNA family, *Proceedings of the National Academy of Sciences of the United States of America.* **105**, 3903-8.

136. Kasinski, A. L.Kelnar, K.Stahlhut, C.Orellana, E.*, et al.* (2015) A combinatorial microRNA therapeutics approach to suppressing non-small cell lung cancer, *Oncogene.* **34**, 3547-55.

137. Kasinski, A. L. & Slack, F. J. (2012) miRNA-34 prevents cancer initiation and progression in a therapeutically resistant K-ras and p53-induced mouse model of lung adenocarcinoma, *Cancer research.* **72**, 5576-87.

138. Costinean, S.Zanesi, N.Pekarsky, Y.Tili, E.*, et al.* (2006) Pre-B cell proliferation and lymphoblastic leukemia/high-grade lymphoma in E(mu)-miR155 transgenic mice, *Proceedings of the National Academy of Sciences of the United States of America.* **103**, 7024-9.

139. Eis, P. S.Tam, W.Sun, L.Chadburn, A.*, et al.* (2005) Accumulation of miR-155 and BIC RNA in human B cell lymphomas, *Proceedings of the National Academy of Sciences of the United States of America.* **102**, 3627-32.

140. Mattiske, S.Suetani, R. J.Neilsen, P. M. & Callen, D. F. (2012) The oncogenic role of miR-155 in breast cancer, *Cancer epidemiology, biomarkers & prevention : a publication of the American Association for Cancer Research, cosponsored by the American Society of Preventive Oncology.* **21**, 1236-43.

141. Murphy, B. L.Obad, S.Bihannic, L.Ayrault, O.*, et al.* (2013) Silencing of the miR-17~92 cluster family inhibits medulloblastoma progression, *Cancer research.* **73**, 7068-78.

142. Northcott, P. A.Fernandez, L. A.Hagan, J. P.Ellison, D. W.*, et al.* (2009) The miR-17/92 polycistron is up-regulated in sonic hedgehog-driven medulloblastomas and induced by N-myc in sonic hedgehog-treated cerebellar neural precursors, *Cancer research.* **69**, 3249-55.

143. Babar, I. A.Cheng, C. J.Booth, C. J.Liang, X.*, et al.* (2012) Nanoparticle-based therapy in an in vivo microRNA-155 (miR-155)-dependent mouse model of lymphoma, *Proceedings of the National Academy of Sciences of the United States of America.* **109**, E1695-704.

144. Hatley, M. E.Patrick, D. M.Garcia, M. R.Richardson, J. A.*, et al.* (2010) Modulation of K-Ras-dependent lung tumorigenesis by MicroRNA-21, *Cancer cell.* **18**, 282-93.

145. Medina, P. P.Nolde, M. & Slack, F. J. (2010) OncomiR addiction in an in vivo model of microRNA-21-induced pre-B-cell lymphoma, *Nature.* **467**, 86-90.

146. He, L.Thomson, J. M.Hemann, M. T.Hernando-Monge, E.*, et al.* (2005) A microRNA polycistron as a potential human oncogene, *Nature.* **435**, 828-33.

147. Cortez, M. A.Bueso-Ramos, C.Ferdin, J.Lopez-Berestein, G.*, et al.* (2011) MicroRNAs in body fluids--the mix of hormones and biomarkers, *Nature reviews Clinical oncology.* **8**, 467-77.

148. Pierson, J.Hostager, B.Fan, R. & Vibhakar, R. (2008) Regulation of cyclin dependent kinase 6 by microRNA 124 in medulloblastoma, *Journal of neuro-oncology.* **90**, 1-7.

149. Li, K. K.Pang, J. C.Ching, A. K.Wong, C. K.*, et al.* (2009) miR-124 is frequently down-regulated in medulloblastoma and is a negative regulator of SLC16A1, *Human pathology.* **40**, 1234-43.

150. Ferretti, E.De Smaele, E.Po, A.Di Marcotullio, L.*, et al.* (2009) MicroRNA profiling in human medulloblastoma, *International journal of cancer.* **124**, 568-77.

151. Kunder, R.Jalali, R.Sridhar, E.Moiyadi, A.*, et al.* (2013) Real-time PCR assay based on the differential expression of microRNAs and protein-coding genes for molecular classification of formalin-fixed paraffin embedded medulloblastomas, *Neuro-oncology.* **15**, 1644-51.

152. Fuziwara, C. S. & Kimura, E. T. (2015) Insights into Regulation of the miR-17-92 Cluster of miRNAs in Cancer, *Frontiers in Medicine.* **2**.

153. Yogi, K.Sridhar, E.Goel, N.Jalali, R.*, et al.* (2015) MiR-148a, a microRNA upregulated in the WNT subgroup tumors, inhibits invasion and tumorigenic potential of medulloblastoma cells by targeting Neuropilin 1, *Oncoscience.* **2**, 334-48.

154. Singh, S. V.Dakhole, A. N.Deogharkar, A.Kazi, S.*, et al.* (2017) Restoration of miR-30a expression inhibits growth, tumorigenicity of medulloblastoma cells accompanied by autophagy inhibition, *Biochemical and biophysical research communications.* **491**, 946-952.

155. Panwalkar, P.Moiyadi, A.Goel, A.Shetty, P.*, et al.* (2015) MiR-206, a Cerebellum Enriched miRNA Is Downregulated in All Medulloblastoma Subgroups and Its Overexpression Is Necessary for Growth Inhibition of Medulloblastoma Cells, *Journal of molecular neuroscience : MN.* **56**, 673-80.

156. Paul, R.Bharambe, H. & Shirsat, N. V. (2020) Autophagy inhibition impairs the invasion potential of medulloblastoma cells, *Molecular biology reports.* **47**, 5673-5680.

157. Joshi, P.Katsushima, K.Zhou, R.Meoded, A.*, et al.* (2019) The therapeutic and diagnostic potential of regulatory noncoding RNAs in medulloblastoma, *Neuro-Oncology Advances.* **1**.

158. Laneve, P. & Caffarelli, E. (2020) The Non-coding Side of Medulloblastoma, *Frontiers in cell and developmental biology.* **8**, 275.

159. Vidal, D. O.Marques, M. M.Lopes, L. F. & Reis, R. M. (2013) The role of microRNAs in medulloblastoma, *Pediatric hematology and oncology.* **30**, 367-78.

160. Milde, T.Lodrini, M.Savelyeva, L.Korshunov, A.*, et al.* (2012) HD-MB03 is a novel Group 3 medulloblastoma model demonstrating sensitivity to histone deacetylase inhibitor treatment, *Journal of neuro-oncology.* **110**, 335-48.

161. Strober, W. (2015) Trypan Blue Exclusion Test of Cell Viability, *Current protocols in immunology.* **111**, A3 B 1-A3 B 3.

162. Reid, Y.Storts, D.Riss, T. & Minor, L. (2004) Authentication of Human Cell Lines by STR DNA Profiling Analysis in *Assay Guidance Manual* (Sittampalam, G. S., Grossman, A., Brimacombe, K., Arkin, M., Auld, D., Austin, C. P., Baell, J., Bejcek, B., Caaveiro, J. M. M., Chung, T. D. Y., Coussens, N. P., Dahlin, J. L., Devanaryan, V., Foley, T. L., Glicksman, M., Hall, M. D., Haas, J. V., Hoare, S. R. J., Inglese, J., Iversen, P. W., Kahl, S. D., Kales, S. C., Kirshner, S., Lal-Nag, M., Li, Z., McGee, J., McManus, O., Riss, T., Saradjian, P., Trask, O. J., Jr., Weidner, J. R., Wildey, M. J., Xia, M. & Xu, X., eds), Bethesda (MD).

163. Uphoff, C. C. & Drexler, H. G. (2005) Detection of mycoplasma contaminations, *Methods in molecular biology.* **290**, 13-23.

164. Young, L.Sung, J.Stacey, G. & Masters, J. R. (2010) Detection of Mycoplasma in cell cultures, *Nature protocols.* **5**, 929-34.

165. Chomczynski, P. & Sacchi, N. (1987) Single-step method of RNA isolation by acid guanidinium thiocyanate-phenol-chloroform extraction, *Analytical biochemistry.* **162**, 156-9.

166. Chen, C.Ridzon, D. A.Broomer, A. J.Zhou, Z.*, et al.* (2005) Real-time quantification of microRNAs by stem-loop RT-PCR, *Nucleic acids research.* **33**, e179.

167. Varkonyi-Gasic, E.Wu, R.Wood, M.Walton, E. F.*, et al.* (2007) Protocol: a highly sensitive RT-PCR method for detection and quantification of microRNAs, *Plant methods.* **3**, 12.

168. Mosmann, T. (1983) Rapid colorimetric assay for cellular growth and survival: application to proliferation and cytotoxicity assays, *Journal of immunological methods.* **65**, 55-63.

169. Beyzadeoglu, M.Ozyigit, G. & Ebruli, C. (2010) *Basic radiation oncology*, 1st edn, Springer-Verlag, Berlin Heidelberg.

170. Allen, P. & Davies, D. (2007) *Flow Cytometry-Principles and Applications*, Humana Press.

171. Riccardi, C. & Nicoletti, I. (2006) Analysis of apoptosis by propidium iodide staining and flow cytometry, *Nature protocols.* **1**, 1458-61.

172. Lee, Y. H.Andersen, J. B.Song, H. T.Judge, A. D.*, et al.* (2010) Definition of ubiquitination modulator COP1 as a novel therapeutic target in human hepatocellular carcinoma, *Cancer research.* **70**, 8264-9.

173. Miyoshi, H.Blomer, U.Takahashi, M.Gage, F. H.*, et al.* (1998) Development of a self-inactivating lentivirus vector, *Journal of virology.* **72**, 8150-7.

174. Frankiln, K. & Paxinos, G. *The Mouse Brain in Stereotaxic Coordinates, Compact 3rd Edition*, 3rd Edition edn, Academic Press.

175. Bindea, G.Mlecnik, B.Hackl, H.Charoentong, P.*, et al.* (2009) ClueGO: a Cytoscape plug-in to decipher functionally grouped gene ontology and pathway annotation networks, *Bioinformatics.* **25**, 1091-3.

176. Grossi, I.Salvi, A.Abeni, E.Marchina, E.*, et al.* (2017) Biological Function of MicroRNA193a-3p in Health and Disease, *International journal of genomics.* **2017**, 5913195.

177. Mamoori, A.Gopalan, V. & Lam, A. K. (2018) Role of miR-193a in Cancer: Complexity and Factors Control the Pattern of its Expression, *Current cancer drug targets.* **18**, 618-628.

178. Ivanov, D. P.Coyle, B.Walker, D. A. & Grabowska, A. M. (2016) In vitro models of medulloblastoma: Choosing the right tool for the job, *Journal of biotechnology.* **236**, 10-25.

179. Vibhakar, R.Foltz, G.Yoon, J. G.Field, L.*, et al.* (2007) Dickkopf-1 is an epigenetically silenced candidate tumor suppressor gene in medulloblastoma, *Neuro-oncology.* **9**, 135-44.

180. Northcott, P. A.Korshunov, A.Pfister, S. M. & Taylor, M. D. (2012) The clinical implications of medulloblastoma subgroups, *Nat Rev Neurol.* **8**, 340-51.

181. Alli, E.Yang, J. M. & Hait, W. N. (2007) Silencing of stathmin induces tumor-suppressor function in breast cancer cell lines harboring mutant p53, *Oncogene.* **26**, 1003-12.

182. Kang, W.Tong, J. H.Chan, A. W.Lung, R. W.*, et al.* (2012) Stathmin1 plays oncogenic role and is a target of microRNA-223 in gastric cancer, *PloS one.* **7**, e33919.

183. Glenewinkel, F.Cohen, M. J.King, C. R.Kaspar, S.*, et al.* (2016) The adaptor protein DCAF7 mediates the interaction of the adenovirus E1A oncoprotein with the protein kinases DYRK1A and HIPK2, *Scientific reports.* **6**, 28241.

184. Kawara, H.Akahori, R.Wakasugi, M.Sancar, A.*, et al.* (2019) DCAF7 is required for maintaining the cellular levels of ERCC1-XPF and nucleotide excision repair, *Biochemical and biophysical research communications.* **519**, 204-210.

185. Yousefelahiyeh, M.Xu, J.Alvarado, E.Yu, Y.*, et al.* (2018) DCAF7/WDR68 is required for normal levels of DYRK1A and DYRK1B, *PloS one.* **13**, e0207779.

186. Scharer, O. D. (2013) Nucleotide excision repair in eukaryotes, *Cold Spring Harbor perspectives in biology.* **5**, a012609.

187. Yu, D.Cattoglio, C.Xue, Y. & Zhou, Q. (2019) A complex between DYRK1A and DCAF7 phosphorylates the C-terminal domain of RNA polymerase II to promote myogenesis, *Nucleic acids research.* **47**, 4462-4475.

188. Matsushime, H.Ewen, M. E.Strom, D. K.Kato, J. Y.*, et al.* (1992) Identification and properties of an atypical catalytic subunit (p34PSK-J3/cdk4) for mammalian D type G1 cyclins, *Cell.* **71**, 323-34.

189. Xiang, W.Yang, C. Y. & Bai, L. (2018) MCL-1 inhibition in cancer treatment, *OncoTargets and therapy.* **11**, 7301-7314.

190. Mattoo, A. R.Pandita, R. K.Chakraborty, S.Charaka, V.*, et al.* (2017) MCL-1 Depletion Impairs DNA Double-Strand Break Repair and Reinitiation of Stalled DNA Replication Forks, *Molecular and cellular biology.* **37**.

191. Nicolas, E.Golemis, E. A. & Arora, S. (2016) POLD1: Central mediator of DNA replication and repair, and implication in cancer and other pathologies, *Gene.* **590**, 128-41.

192. Neves, H. & Kwok, H. F. (2017) In sickness and in health: The many roles of the minichromosome maintenance proteins, *Biochimica et biophysica acta Reviews on cancer.* **1868**, 295-308.

193. Cortez, D.Glick, G. & Elledge, S. J. (2004) Minichromosome maintenance proteins are direct targets of the ATM and ATR checkpoint kinases, *Proceedings of the National Academy of Sciences of the United States of America.* **101**, 10078-83.

194. Mimura, S.Masuda, T.Matsui, T. & Takisawa, H. (2000) Central role for cdc45 in establishing an initiation complex of DNA replication in Xenopus egg extracts, *Genes to cells : devoted to molecular & cellular mechanisms.* **5**, 439-52.

195. Li, Y.Han, J.Zhang, Y.Cao, F.*, et al.* (2016) Structural basis for activity regulation of MLL family methyltransferases, *Nature.* **530**, 447-52.

196. Sengupta, D.Deb, M.Kar, S.Parbin, S.*, et al.* (2019) miR-193a targets MLL1 mRNA and drastically decreases MLL1 protein production: Ectopic expression of the miRNA aberrantly lowers H3K4me3 content of the chromatin and hampers cell proliferation and viability, *Gene.* **705**, 22-35.

197. Dang, C. V. (2012) MYC on the path to cancer, *Cell.* **149**, 22-35.

198. Amati, B. & Land, H. (1994) Myc-Max-Mad: a transcription factor network controlling cell cycle progression, differentiation and death, *Current opinion in genetics & development.* **4**, 102-8.

199. Grandori, C.Cowley, S. M.James, L. P. & Eisenman, R. N. (2000) The Myc/Max/Mad network and the transcriptional control of cell behavior, *Annual review of cell and developmental biology.* **16**, 653-99.

200. Mathsyaraja, H.Freie, B.Cheng, P. F.Babaeva, E.*, et al.* (2019) Max deletion destabilizes MYC protein and abrogates Emicro-Myc lymphomagenesis, *Genes & development.* **33**, 1252-1264.

201. Polakis, P. (2012) Wnt signaling in cancer, *Cold Spring Harbor perspectives in biology.* **4**.

202. Zhan, T.Rindtorff, N. & Boutros, M. (2017) Wnt signaling in cancer, *Oncogene.* **36**, 1461-1473.

203. Chen, K.Liu, M. X.Mak, C. S.Yung, M. M.*, et al.* (2018) Methylation-associated silencing of miR-193a-3p promotes ovarian cancer aggressiveness by targeting GRB7 and MAPK/ERK pathways, *Theranostics.* **8**, 423-436.

204. Kozaki, K.Imoto, I.Mogi, S.Omura, K.*, et al.* (2008) Exploration of tumor-suppressive microRNAs silenced by DNA hypermethylation in oral cancer, *Cancer research.* **68**, 2094-105.

205. Ma, K.He, Y.Zhang, H.Fei, Q.*, et al.* (2012) DNA methylation-regulated miR-193a-3p dictates resistance of hepatocellular carcinoma to 5-fluorouracil via repression of SRSF2 expression, *The Journal of biological chemistry.* **287**, 5639-49.

206. Tang, Y.Yang, S.Wang, M.Liu, D.*, et al.* (2019) Epigenetically altered miR193a3p promotes HER2 positive breast cancer aggressiveness by targeting GRB7, *International journal of molecular medicine.* **43**, 2352-2360.

207. Lopez-Urrutia, E.Bustamante Montes, L. P.Ladron de Guevara Cervantes, D.Perez-Plasencia, C.*, et al.* (2019) Crosstalk Between Long Non-coding RNAs, Micro-RNAs and mRNAs: Deciphering Molecular Mechanisms of Master Regulators in Cancer, *Frontiers in oncology.* **9**, 669.

208. Huang, Y.Luo, H.Li, F.Yang, Y., *et al.* (2018) LINC00152 down-regulated miR-193a-3p to enhance MCL1 expression and promote gastric cancer cells proliferation, *Bioscience reports.* **38**.

209. Ma, P.Wang, H.Sun, J.Liu, H., *et al.* (2018) LINC00152 promotes cell cycle progression in hepatocellular carcinoma via miR-193a/b-3p/CCND1 axis, *Cell cycle.* **17**, 974-984.

210. Nie, W.Ge, H. J.Yang, X. Q.Sun, X., *et al.* (2016) LncRNA-UCA1 exerts oncogenic functions in non-small cell lung cancer by targeting miR-193a-3p, *Cancer letters.* **371**, 99-106.

211. Fan, Q.Hu, X.Zhang, H.Wang, S., *et al.* (2017) MiR-193a-3p is an Important Tumour Suppressor in Lung Cancer and Directly Targets KRAS, *Cellular physiology and biochemistry : international journal of experimental cellular physiology, biochemistry, and pharmacology.* **44**, 1311-1324.

212. Yu, T.Li, J.Yan, M.Liu, L., *et al.* (2015) MicroRNA-193a-3p and -5p suppress the metastasis of human non-small-cell lung cancer by downregulating the ERBB4/PIK3R3/mTOR/S6K2 signaling pathway, *Oncogene.* **34**, 413-23.

213. Chen, Z. M.Yu, Q.Chen, G.Tang, R. X., *et al.* (2019) MiR-193a-3p inhibits pancreatic ductal adenocarcinoma cell proliferation by targeting CCND1, *Cancer management and research.* **11**, 4825-4837.

214. Liu, Y.Xu, X.Xu, X.Li, S., *et al.* (2017) MicroRNA-193a-3p inhibits cell proliferation in prostate cancer by targeting cyclin D1, *Oncology letters.* **14**, 5121-5128.

215. Wang, S. S.Huang, Z. G.Wu, H. Y.He, R. Q., *et al.* (2020) Downregulation of miR-193a-3p is involved in the pathogenesis of hepatocellular carcinoma by targeting CCND1, *PeerJ.* **8**, e8409.

216. Gao, X. N.Lin, J.Li, Y. H.Gao, L., *et al.* (2011) MicroRNA-193a represses c-kit expression and functions as a methylation-silenced tumor suppressor in acute myeloid leukemia, *Oncogene.* **30**, 3416-28.

217. Li, Y.Deng, H.Lv, L.Zhang, C., *et al.* (2015) The miR-193a-3p-regulated ING5 gene activates the DNA damage response pathway and inhibits multi-chemoresistance in bladder cancer, *Oncotarget.* **6**, 10195-206.

218. Deng, H.Lv, L.Li, Y.Zhang, C., *et al.* (2015) The miR-193a-3p regulated PSEN1 gene suppresses the multi-chemoresistance of bladder cancer, *Biochimica et biophysica acta.* **1852**, 520-8.

219. Williams, M.Kirschner, M. B.Cheng, Y. Y.Hanh, J., *et al.* (2015) miR-193a-3p is a potential tumor suppressor in malignant pleural mesothelioma, *Oncotarget.* **6**, 23480-95.

220. Lu, X.Vogt, P. K.Boger, D. L. & Lunec, J. (2008) Disruption of the MYC transcriptional function by a small-molecule antagonist of MYC/MAX dimerization, *Oncology reports.* **19**, 825-30.

221. Xia, F.Wang, W.Jiang, B.Chen, Y.*, et al.* (2019) DNA methylation-mediated silencing of miR-204 is a potential prognostic marker for papillary thyroid carcinoma, *Cancer management and research.* **11**, 1249-1262.

222. Ying, Z.Li, Y.Wu, J.Zhu, X.*, et al.* (2013) Loss of miR-204 expression enhances glioma migration and stem cell-like phenotype, *Cancer research.* **73**, 990-9.

223. Li, G.Luna, C.Qiu, J.Epstein, D. L.*, et al.* (2011) Role of miR-204 in the regulation of apoptosis, endoplasmic reticulum stress response, and inflammation in human trabecular meshwork cells, *Investigative ophthalmology & visual science.* **52**, 2999-3007.

224. Luan, W.Qian, Y.Ni, X.Bu, X.*, et al.* (2017) miR-204-5p acts as a tumor suppressor by targeting matrix metalloproteinases-9 and B-cell lymphoma-2 in malignant melanoma, *OncoTargets and therapy.* **10**, 1237-1246.

225. Yu, Y.Wang, L.Liu, T. & Guan, H. (2015) MicroRNA-204 suppresses trophoblast-like cell invasion by targeting matrix metalloproteinase-9, *Biochemical and biophysical research communications.* **463**, 285-91.

226. Luzio, J. P.Hackmann, Y.Dieckmann, N. M. & Griffiths, G. M. (2014) The biogenesis of lysosomes and lysosome-related organelles, *Cold Spring Harbor perspectives in biology.* **6**, a016840.

227. Luzio, J. P.Pryor, P. R. & Bright, N. A. (2007) Lysosomes: fusion and function, *Nature reviews Molecular cell biology.* **8**, 622-32.

228. Tiger, C. F.Fougerousse, F.Grundstrom, G.Velling, T.*, et al.* (2001) alpha11beta1 integrin is a receptor for interstitial collagens involved in cell migration and collagen reorganization on mesenchymal nonmuscle cells, *Developmental biology.* **237**, 116-29.

229. Li, X. L.Liu, L.Li, D. D.He, Y. P.*, et al.* (2017) Integrin beta4 promotes cell invasion and epithelial-mesenchymal transition through the modulation of Slug expression in hepatocellular carcinoma, *Scientific reports.* **7**, 40464.

230. Bianconi, D.Unseld, M. & Prager, G. W. (2016) Integrins in the Spotlight of Cancer, *International journal of molecular sciences.* **17**.

231. Ginsberg, M. H. (2014) Integrin activation, *BMB reports.* **47**, 655-9.

232. Cathcart, J.Pulkoski-Gross, A. & Cao, J. (2015) Targeting Matrix Metalloproteinases in Cancer: Bringing New Life to Old Ideas, *Genes & diseases.* **2**, 26-34.

233. Gialeli, C.Theocharis, A. D. & Karamanos, N. K. (2011) Roles of matrix metalloproteinases in cancer progression and their pharmacological targeting, *The FEBS journal.* **278**, 16-27.

234. Brown, W. J.Goodhouse, J. & Farquhar, M. G. (1986) Mannose-6-phosphate receptors for lysosomal enzymes cycle between the Golgi complex and endosomes, *The Journal of cell biology.* **103**, 1235-47.

235. Park, S. Y. & Guo, X. (2014) Adaptor protein complexes and intracellular transport, *Bioscience reports.* **34**.

236. Klumperman, J.Kuliawat, R.Griffith, J. M.Geuze, H. J.*, et al.* (1998) Mannose 6-phosphate receptors are sorted from immature secretory granules via adaptor protein AP-1, clathrin, and syntaxin 6-positive vesicles, *The Journal of cell biology.* **141**, 359-71.

237. Glick, D.Barth, S. & Macleod, K. F. (2010) Autophagy: cellular and molecular mechanisms, *The Journal of pathology.* **221**, 3-12.

238. Sanchez-Martin, P. & Komatsu, M. (2018) p62/SQSTM1 - steering the cell through health and disease, *Journal of cell science.* **131**.

239. Eskelinen, E. L. (2006) Roles of LAMP-1 and LAMP-2 in lysosome biogenesis and autophagy, *Molecular aspects of medicine.* **27**, 495-502.

240. Andrejewski, N.Punnonen, E. L.Guhde, G.Tanaka, Y.*, et al.* (1999) Normal lysosomal morphology and function in LAMP-1-deficient mice, *The Journal of biological chemistry.* **274**, 12692-701.

241. Mizushima, N. (2007) Autophagy: process and function, *Genes & development.* **21**, 2861-73.

242. Ryter, S. W.Bhatia, D. & Choi, M. E. (2019) Autophagy: A Lysosome-Dependent Process with Implications in Cellular Redox Homeostasis and Human Disease, *Antioxidants & redox signaling.* **30**, 138-159.

243. Agarwal, A. K.Srinivasan, N.Godbole, R.More, S. K.*, et al.* (2015) Role of tumor cell surface lysosome-associated membrane protein-1 (LAMP1) and its associated carbohydrates in lung metastasis, *Journal of cancer research and clinical oncology.* **141**, 1563-74.

244. Jensen, S. S.Aaberg-Jessen, C.Christensen, K. G. & Kristensen, B. (2013) Expression of the lysosomal-associated membrane protein-1 (LAMP-1) in astrocytomas, *International journal of clinical and experimental pathology.* **6**, 1294-305.

245. Sarafian, V.Jadot, M.Foidart, J. M.Letesson, J. J.*, et al.* (1998) Expression of Lamp-1 and Lamp-2 and their interactions with galectin-3 in human tumor cells, *International journal of cancer.* **75**, 105-11.

246. Upraity, S.Kazi, S.Padul, V. & Shirsat, N. V. (2014) MiR-224 expression increases radiation sensitivity of glioblastoma cells, *Biochemical and biophysical research communications.* **448**, 225-30.

247. Bader, A. G.Brown, D.Stoudemire, J. & Lammers, P. (2011) Developing therapeutic microRNAs for cancer, *Gene therapy.* **18**, 1121-6.

248. Kasinski, A. L. & Slack, F. J. (2011) Epigenetics and genetics. MicroRNAs en route to the clinic: progress in validating and targeting microRNAs for cancer therapy, *Nature reviews Cancer.* **11**, 849-64.

249. van der Ree, M. H.van der Meer, A. J.de Bruijne, J.Maan, R.*, et al.* (2014) Long-term safety and efficacy of microRNA-targeted therapy in chronic hepatitis C patients, *Antiviral research.* **111**, 53-9.

250. van Zandwijk, N.Pavlakis, N.Kao, S. C.Linton, A.*, et al.* (2017) Safety and activity of microRNA-loaded minicells in patients with recurrent malignant pleural mesothelioma: a first-in-man, phase 1, open-label, dose-escalation study, *The Lancet Oncology.* **18**, 1386-1396.

251. Viteri, S. & Rosell, R. (2018) An innovative mesothelioma treatment based on miR-16 mimic loaded EGFR targeted minicells (TargomiRs), *Translational lung cancer research.* **7**, S1-S4.

252. Hanna, J.Hossain, G. S. & Kocerha, J. (2019) The Potential for microRNA Therapeutics and Clinical Research, *Frontiers in Genetics.* **10**.

253. Fernandez-Pineiro, I.Badiola, I. & Sanchez, A. (2017) Nanocarriers for microRNA delivery in cancer medicine, *Biotechnology advances.* **35**, 350-360.

254. Xie, J.Burt, D. R. & Gao, G. (2015) Adeno-associated virus-mediated microRNA delivery and therapeutics, *Seminars in liver disease.* **35**, 81-8.

255. Dong, X. (2018) Current Strategies for Brain Drug Delivery, *Theranostics.* **8**, 1481-1493.

List of abbreviations

AML: Acute Myeloid Leukemia

AP: Anterio-posterior

ATCC: American Type Culture Collection

ATP: Adinosine tri-phosphate

AT/RT: Atypical Teratoid and Rhabdoid Tumor

BBS: BES Buffered Saline

BES: N, N-Bis (2-hydroxyethyl)-2-aminoethanesulfonic acid

bHLH: Basic Helix-Loop-Helix

bp: Base pairs

cDNA: Complementary DNA

ceRNA: Competing Endogenous Ribonucleic acid

CGNPs: Cerebellar Granule Neural Precursors

CHX: Cycloheximide

CLL: Chronic Lymphocytic Leukemia

CNS: Central Nervous System

DLBCL: Diffuse Large B-cell Lymphoma

DMEM: Dulbecco's Modified Eagle Medium

DMEM/F12: Dulbecco's Modified Eagle Medium:Nutrient Mixture F12

DMSO: Dimethyl sulfoxide

DTT: Dithiothretol

DV: Dorso-ventral

EGTA: Ethylene glycol-bis (β-aminoethyl ether)-N,N,N′,N′-tetra acetic acid

FBS: Fetal Bovine Serum

GEO: Gene Expression Omnibus

Gly-Gly: Glycine-Glycine

gDNA: Genomic DNA

GO: Gene Ontology

GSEA: Gene Set Enrichment Analysis

H3K9ac: Acetyl Histone H3 at Lysine 9

H3K27ac: Acetyl Histone H3 at Lysine 27

H3K4me3: Tri-methyl Histone H3 at Lysine 4

H3K27me3: Tri-methyl Histone H3 at Lysine 27

HDAC: Histone Deacetylase

I.U.: International Units

kDa: Kilodaltons

KEGG: Kyoto Encyclopedia of Genes and Genomes

LC/A: Large cell/Anaplastic

LNA: Locked Nucleic Acid

LncRNA: Long Non-coding Ribonucleic acid

MAGIC: Medulloblastoma Advanced Genomics International Consortium

MAPK: Mitogen Activated Protein Kinase

MBEN: Medulloblastoma with Extensive Nodularity

miRISC: MicroRNA Induced Silencing Complex

MRE: MicroRNA Response Element

MRI: Magnetic Resonance Imaging

NOD/SCID: Nonobese Diabetic/Severe Combined Immunodeficiency

NSCLC: Non-Small Cell Lung Cancer

ncRNA: Non-coding Ribonucleic acid

PBS: Phosphate Buffered Saline

PCR: Polymerase Chain Reaction

PI3K: Phosphatidylinositol-3-kinase

PNET: Primitive Neuroectodermal Tumors

ROI: Region of Interest

RQ: Relative Quantity

RT: Room Temperature

RT-PCR: Reverse Transcription-Polymerase Chain Reaction

RTK: Receptor Tyrosine Kinase

SCLC: Small Cell Lung Cancer

SCNAs: Somatic Copy Number Alterations

SHH: Sonic Hedgehog

SNV: Somatic Nucleotide Variant

STR: Short Tandem Repeat

SWI/SNF: Switch/Sucrose Non-Fermenting

TU: Transducing Units

TSS: Transcription Start Site

WNT: Wingless and Int-1

VC: Vector Control/Vehicle Control

THESIS HIGHLIGHTS

Name of the student: Harish Shrikrishna Bharambe **Enrolment No.:**LIFE09201404008

Name of the CI/OCC: Dr. Neelam V. Shirsat **Date of viva voce**: 09/03/2021

Discipline: Life Sciences **Sub Discipline:** Cancer Biology

Thesis Title: Molecular mechanism underlying the effect of miRNA expression on medulloblastoma cell behavior

Role of miR-193a in medulloblastoma biology: Medulloblastoma consist of four distinct molecular subgroups: WNT, SHH, Group 3 and Group 4. WNT subgroup medulloblastomas have an excellent survival of over 90 % and are characterized by distinct microRNA expression profile. The expression of miR-193a, a WNT subgroup specific microRNA is regulated by MYC, a potent oncogenic target of canonical WNT signalling. MiR-193a is not expressed in non-WNT medulloblastoma subgroups and Group 3 medulloblastoma cell lines as a result of promoter hypermethylation. Restoration of miR-193a expression in MYC amplified Group 3 medulloblastoma cell lines inhibited proliferation, anchorage independence, tumorigenic potential and increased radiation sensitivity of medulloblastoma cells indicating its tumor-suppressive role in medulloblastoma. Restoration of miR-193a expression resulted in downregulation of genes involved in multiple cellular pathways suggesting a widespread repression of gene expression. MiR-193a mediated downregulation of MAX was found to destabilize the MYC oncoprotein. Thus, miR-193a mediated decrease in the activity of MYC is likely to contribute to the miR-193a mediated widespread repression of gene expression in the MYC overexpressing Group 3 medulloblastoma cells. In cancer cells having high MYC expression, MYC brings about transcriptional amplification of all active genes apart from the induction of its target genes. MiR-193a, on the other hand, brought about global repression of gene expression. Therefore, miR-193a has therapeutic potential in the treatment of not only Group 3 medulloblastomas but also for other MYC overexpressing aggressive cancers as well.

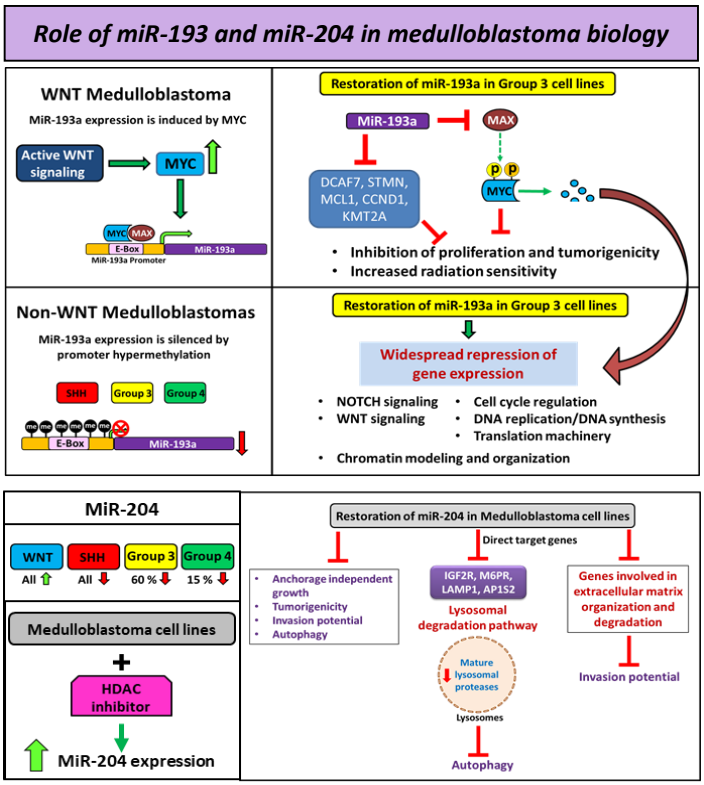

Role of miR-204 in medulloblastoma biology: Restoration of miR-204 expression inhibited the tumorigenic properties of medulloblastoma cell lines indicating the tumor suppressive role of miR-204 in medulloblastomas. MiR-204 expression in medulloblastoma cell lines resulted in downregulation of several genes involved in extracellular matrix organization/degradation and lysosomal pathway. IGF2R and LAMP1 were identified as novel miR-204 targets. MiR-204 was found to decrease expression levels of mature lysosomal proteases cathepsin D and cathepsin B, thereby affecting lysosomal degradation pathway. MiR-204 expression also resulted in inhibition of autophagy that is known to be dependent on the lysosomal degradation pathway. Moreover, the treatment with HDAC inhibitors resulted in upregulation of miR-204 expression in medulloblastoma cells, suggesting therapeutic role for these inhibitors in the treatment of medulloblastomas.